Direct Preparation of Alpha-Calcium Sulfate Hemihydrate from Sulfuric Acid

by

Yuanbing Ling

Department of Mining, Metals, and Materials Engineering
McGill University, Montreal
December 2003

A thesis submitted to McGill University in partial fulfillment
of the requirements of the degree of
Doctor of Philosophy

Library and
Archives Canada

Published Heritage
Branch

395 Wellington Street
Ottawa ON K1A 0N4
Canada

Bibliothèque et
Archives Canada

Direction du
Patrimoine de l'édition

395, rue Wellington
Ottawa ON K1A 0N4
Canada

Your file Votre référence
ISBN: 0-612-98307-2
Our file Notre référence
ISBN: 0-612-98307-2

NOTICE:
The author has granted a non-exclusive license allowing Library and Archives Canada to reproduce, publish, archive, preserve, conserve, communicate to the public by telecommunication or on the Internet, loan, distribute and sell theses worldwide, for commercial or non-commercial purposes, in microform, paper, electronic and/or any other formats.

The author retains copyright ownership and moral rights in this thesis. Neither the thesis nor substantial extracts from it may be printed or otherwise reproduced without the author's permission.

AVIS:
L'auteur a accordé une licence non exclusive permettant à la Bibliothèque et Archives Canada de reproduire, publier, archiver, sauvegarder, conserver, transmettre au public par télécommunication ou par l'Internet, prêter, distribuer et vendre des thèses partout dans le monde, à des fins commerciales ou autres, sur support microforme, papier, électronique et/ou autres formats.

L'auteur conserve la propriété du droit d'auteur et des droits moraux qui protège cette thèse. Ni la thèse ni des extraits substantiels de celle-ci ne doivent être imprimés ou autrement reproduits sans son autorisation.

In compliance with the Canadian Privacy Act some supporting forms may have been removed from this thesis.

While these forms may be included in the document page count, their removal does not represent any loss of content from the thesis.

Conformément à la loi canadienne sur la protection de la vie privée, quelques formulaires secondaires ont été enlevés de cette thèse.

Bien que ces formulaires aient inclus dans la pagination, il n'y aura aucun contenu manquant.

Canada

To my family

For their love

The more I read the papers,
the less I comprehend.
---Ira Gershwin

Abstract

In this work, the crystallization of α-calcium sulfate hemihydrate in sulfuric acid solution and the correlation between its properties and preparation conditions by reaction of sulfuric acid with lime (CaO) have been thoroughly investigated. The research involved the study of conversion-dissolution of calcium sulfate dihydrate in H_2SO_4 solution, the measurement of solubilities, thermo-dynamic calculations and the preparation of α-$CaSO_4 \cdot 0.5\ H_2O$ via different methods of reactive mixing of H_2SO_4 and CaO. It was found that the calcium sulfate solids can saturate the sulfuric acid solutions in only 5 minutes. The solubility of calcium sulfate hemihydrate in 0-3.0M H_2SO_4 solution at 100°C was experimentally determined and thermodynamic calculations with the aid of FactSage and OLI have led to establishment of the phase diagram for the $CaSO_4$–H_2SO_4–H_2O system. An operating window has been determined in terms of H_2SO_4 concentration, temperature and time within which α-hemihydrate can be produced by reaction of lime with H_2SO_4. This window is defined as 0.6-1.1M H_2SO_4 (steady-state concentrations), 98-105°C and 1 hour retention time. Dihydrate was found to form as intermediate phase quickly converting to hemihydrate. The kinetics of conversion depends on the acidity level.

For the standard preparation procedure of adding lime into hot sulfuric acid, α-hemihydrate grows in the **c**-axis direction much more rapidly than in other directions ending in the form of fine needle crystals. Also, independent of the shape of the seed particles, the resultant crystals of hemihydrate are needle-shaped, which suggests a "dissolution-recrystallization" mechanism. Upon prolonged equilibration in their acid-preparation solution hemihydrate needle-shape crystals become fibrous and eventually convert to anhydrite. It is believed that uptake of SO_4^{2-} instead of Ca^{2+} is the rate-determining step in the hemihydrate crystallization process. The hot SO_4^{2-}-rich environment rendered most of the additives (particularly organic) tried ineffective. Trivalent cations such as Fe^{3+} and Al^{3+}, are the only ones found to modify the crystal morphology from needle-shape to small "grain" type morphology.

Slow addition of H_2SO_4 solution to slaked lime – reverse procedure was found to favor the production of α-hemihydrate with column-shaped as opposed to needle-shaped crystal morphology within otherwise the same operating window, 0.6-1.1M H_2SO_4. Preliminary assessment of the properties of the α-hemihydrate materials synthesized in this work showed them to compare satisfactorily with other materials produced by conversion of dihydrate to hemihydrate.

Résumé

Dans le présent travail, la cristallisation du sulfate de calcium hémihydrate α dans des solutions d'acide sulfurique et la corrélation entre les propriétés du matériau synthétisé et les conditions de préparation par réaction d'acide sulfurique (H_2SO_4) et de chaux (CaO) ont été investiguées en détail. La recherche a impliqué l'étude de la conversion/dissolution du sulfate de calcium dihydrate dans des solutions de H_2SO_4, des mesures de solubilité, des calculs thermodynamiques et la préparation de $CaSO_4{\cdot}0.5H_2O$ α en utilisant diverses méthodes de mélange réactif de H_2SO_4 et de CaO. Il a été découvert que les sulfates de calcium solides peuvent saturer les solutions d'acide sulfurique en seulement cinq minutes. La solubilité du sulfate de calcium hémihydrate dans des solutions à 0-3 M H_2SO_4 et à 100°C a été déterminée expérimentalement et des calculs thermodynamiques réalisés à l'aide de FactSage et OLI ont permis la construction du diagramme de phase du système $CaSO_4$-H_2SO_4-H_2O. Une fenêtre d'opération a été déterminée en termes de concentration de H_2SO_4, de température et de temps à l'intérieur de laquelle l'hémihydrate α peut être produit par réaction de chaux et de H_2SO_4. Cette fenêtre est définie par 0.6-1.1 M H_2SO_4 (concentrations en régime permanent), 98-105°C et 1 heure de temps de rétention. Il a été observé que le dihydrate est formé en tant que phase intermédiaire et est rapidement converti en hémihydrate. La cinétique de conversion dépend du niveau d'acidité.

Il a été découvert que, lors de la préparation d'hémihydrate α selon la procédure standard consistant à ajouter de la chaux à de l'acide sulfurique chaud, les cristaux formés croissent dans la direction de l'axe **c** beaucoup plus rapidement que dans les autres directions leur donnant ainsi une forme aciculaire. Également, indépendamment de la forme des particules utilisées comme germes, les cristaux d'hémihydrate produits ont une forme aciculaire, suggérant un mécanisme de «dissolution-recristallisation». Après un temps d'équilibration prolongé dans leur solution de préparation acide, les cristaux aciculaires d'hémihydrate deviennent fibreux et se convertissent éventuellement en anhydrite. L'incorporation de SO_4^{2-} au lieu de Ca^{2+} semble être l'étape déterminant le taux du processus de cristallisation de l'hémihydrate. L'environnement chaud et riche en sulfates a rendu la majorité des additifs testés (particulièrement les additifs organiques) inefficaces. Les cations trivalents tels que Fe^{3+} et Al^{3+} sont les seuls parmi les additifs testés qui modifient la morphologie des cristaux la faisant passer de type aciculaire à type petits «grains».

Il a également été découvert que, à l'intérieur de la même fenêtre d'opération (0.6-1.1 M H_2SO_4), l'addition lente de solutions de H_2SO_4 au lait de chaux (procédure inverse) favorise la production d'hémihydrate α colonnaire par opposition à la morphologie cristalline aciculaire obtenue par la procédure standard. Une évaluation préliminaire des propriétés de l'hémihydrate α produit dans ce travail a démontré que les matériaux synthétisés se comparent de façon satisfaisante aux autres matériaux produits par conversion de dihydrate à hémihydrate.

Acknowledgements

I would, first of all, like to say "Sorry" to Professor G. P. Demopoulos, my supervisor (and teacher), simply because there were many occasions that I should say "Thank you" but I never did. Professor Demopoulos' beckoning across the Pacific Ocean, which, at the first place, gave me the chance to enjoy the beauty of Mount Royal and St. Lawrence River; his assistance, which has made it possible for my wife and daughter to join me after one-and-half-year's separation; his guidance, which has enlightened me on many hidden aspects of the research work; … all of these, have never be forgotten. "***Bona fide***" gratitude is buried in the depth of my heart.

I would like also to thank Dr. John College from BPB Company in USA and SICOWA-ProMineral in Germany for providing free samples of alpha hemihydrate and Dr. Ian Swanson from the Neutron Beam Laboratory of National Research Council Canada for instructive discussions on structure identification and XRD data indexing.

I also wish to extend the gratitude to many people who have offered their technical support, Monique Riendeau for XRD, Helen Campbell for SEM, Edward Siliauskas for ICP, Lijun Feng for DSC, Glenn Poirier for microprobe analysis, Dr. Zhen Fang for diamond anvil cell and IR microscopy, Ronald Sheppard for mechanical testing. Thanks are also due to the administrative staff of the Department, Carol Rousseau, Norma Procyshyn, Barbara Hanley who have presented many times "***confirmation***" of my "***status***" "***To Who It May Concern***".

As a member of the McGill Hydrometallurgy Research Group, I am grateful to everyone for standing side by side with me. Marie-Claude Bluteau translated the abstract into French. Dr. Yongfeng Jia proof-read chapters 6 and 7. Georgiana Moldoveneau, is always ready to help me to load the samples into the chamber of an old SEM machine (I'm still somehow scared to do that job). Cinziana Sist, generously leaves her plants in the office, which relaxed my mind from the lonely writing.

Natural Sciences and Engineering Research Council of Canada (NSERC) and Noranda Technology Centre (NTC) are acknowledged for the financial support of this work. Particularly I would like to express my sincere thanks to Dr. Dimitrios Filippou for his generous help, from retouching the conference paper to providing technical equipment for testing.

Finally, I'd like to mention my family. My parents, as peasants from a remote village in China, supported me unconditionally until I finished my bachelor degree. I know how hard they have struggled, and I know how much they have sacrificed. They are always silently "watching" me no matter where I am. And my daughter, Siliang, at whom, I, as a father, didn't have a single glance until she was thirteen-month old, is always "sitting" behind me whenever I drive, is always alongside with me on the way to McGill or back home no matter it is sunny, or windy or snowy or rainy, and, yes, always there to energize me to cheer up, to be a strong "Daddy". Another person I am particularly indebted to is Qiuxia, my wife, who, has, and will accompany me to go through all the ups and downs. With my study expected to come to completion this year or early next year, she gave me another "*little*" gift, baby Cindy with birthday of January 24, who has already "*graduated from the high-chair*" (quote from Bernadette, educator of the baby class at McGill's daycare).

This thesis is dedicated to my family for their love.

December 2003
Montreal

Contents

Appendices

List of Figures

List of Tables

List of Symbols

a, b, c	parameters for unit cell of crystal: three vectors (a, b, c) that form the edges of a parallelepiped
A, B, C and D	fitting constants
AH	calcium sulfate anhydrite
α, α_0	activities of the dissolved solute and of the pure solute in equilibrium with a macroscopic crystal respectively
α_{H_2O}	activity of H_2O
anhydrite	calcium sulfate anhydrite
ASTM	American Society for Testing and Materials
C_p	heat capacity [J mol^{-1} K^{-1}]
DH	calcium sulfate dihydrate
dihydrate	calcium sulfate dihydrate
hemihydrate	calcium sulfate hemihydrate
HH	calcium sulfate hemihydrate
I_h, I_g and I_s	additional integration constants
$K1$	the first dissociation constant of H_2SO_4
$K2$	the second dissociation constant of H_2SO_4
K_{sp}	solubility product constant
m	molality [mol (kg H_2O)$^{-1}$]
M	molarity [mol L^{-1}]
mw	molecular weight
n	number of water molecules in formula unit of $CaSO_4 \bullet n\ H_2O$, $0<n<1$
P	total pressure [Pa], [atm] or [psi]
P_{H_2O}	partial water vapor pressure [Pa], [atm] or [psi]
r	the radius of the cation corresponding to the solid state
R	universal gas constant, 8.314 [J mol^{-1}K^{-1}]
RH	relative humidity [%]
rpm	revolutions per minute

R-squared	goodness of fit, or coefficient of determination, the proportion of variation in the dependent variables that has been explained or accounted for by the regression equation, the value may vary from zero to one.
R value	R_{wp}, ***R-weighted pattern value,*** calculated from the differences between each individual point of the observed and calculated powder diffraction patterns, a good indicator of the progress of the refinements. Values of R_{wp} reported for refined structures are often in the range 5 - 15 %.
S	supersaturation value, defined by that ratio of α / α_0
S_{cr}	critical supersaturation value, (when reached) signifying the onset of nucleation of crystal. $S_{cr,secondary}$, $S_{cr,heterogeneous}$, $S_{cr,homogeneous}$ represent respectively the critical supersaturation values for secondary nucleation, heterogeneous nucleation and homogeneous nucleation.
Sol_{CaSO4}	solubility of calcium sulfate [g L^{-1}], [m] or [wt%]
T	temperature [^{o}C] or [K]
wt%	weight percentage
Z	coordination number in the unit cell

Greek letters

α, β, γ	parameters for unit cell of crystal: the angles between the vectors (α, the angle between b and c; β, the angle between a and c; γ, the angle between a and b).
$\gamma_{Ca^{2+}}$	activity coefficient of Ca^{2+} ion
$\gamma_{SO_4^{2-}}$	activity coefficient of SO_4^{2-} ion
μ^{0}	chemical potential under standard conditions [V]
$\mu_{AH,\,l}$	chemical potential of anhydrite in solution [V]
$\mu_{AH,\,s}$	chemical potential of hemihydrate corresponding to solid state [V]
$\mu_{DH,\,l}$	chemical potential of dihydrate in solution [V]
$\mu_{DH,\,s}$	chemical potential of dihydrate corresponding to solid state [V]

$\mu_{HH,l}$	chemical potential of hemihydrate in solution [V]
$\mu_{HH,s}$	chemical potential of hemihydrate corresponding to solid state [V]
Ψ	charge of the cation

Other symbols

ΔG	Gibbs free energy [$J\ mol^{-1}$]
ΔH	enthalpy [$J\ mol^{-1}$]
ΔS	entropy [$J\ K^{-1}\ mol^{-1}$]

Chapter 1

Introduction

1.1 Background

Gypsum plaster has been used for many years on a large scale in the building and pottery trades as well as in dentistry. The historical importance of the material can be gauged by several facts: according to Desch[1], the setting of gypsum plaster was first investigated by Lavoisier in 1768 in *l'analyse du Gypse* and Le Chatelier who proposed for the first time a mechanism for the setting of gypsum plaster in his doctoral thesis in 1887. Investigation on various calcium sulfates and their relationships was first done by vant'Hoff and his associates in 1903[2][1].

Despite some controversy, it is generally agreed that: the principal phases that occur in the $CaSO_4$-H_2O system are $CaSO_4{\cdot}2H_2O$ (gypsum), hemihydrate ($CaSO_4{\cdot}0.5H_2O$), γ-$CaSO_4$ (soluble anhydrite), $CaSO_4$ (insoluble anhydrite or β-$CaSO_4$) and a high-temperature form of anhydrite, α-anhydrite. Of the abovementioned phases, the hemihydrate and γ-$CaSO_4$ can exist only metastably.

Hemihydrate may exist in two phases, i.e., α- and β-forms. The industrial production and use of hemihydrate began more than one hundred years ago. But it was its β-form, also called Plaster of Paris that was used.

The most characteristic property of α-hemihydrate is the development of extremely high early and final strengths in pastes, mortars, concrete, dental materials, etc., which make it totally different from the well known traditional β-form. Alpha-hemihydrate has been known as an excellent building material, but always too expensive for large volume applications. In recent years, however, α-hemihydrate has gained more

---

[1] Actually as retrieved by SciFinder[3] in the databank of the *Chemical Abstracts*, it can only be dated back to 1906, *Researches on Plaster of Paris* by de Forcrand[4].

acceptance in modern building materials, molding, special binder systems, dental materials and some other innovative applications due to the better workability and higher strength values. Most of the α- hemihydrate used in North America has been imported from Germany [5].

1.2 Present technologies for preparation of α-hemihydrate

(i) Autoclaving method

$$CaSO_4{\bullet}2H_2O \rightarrow CaSO_4{\bullet}0.5H_2O + 1.5H_2O \tag{1-1}$$

In this most common method, α-hemihydrate is obtained by autoclave calcination of gypsum at a steam pressure of about 20 ~ 40 psi (1.36~2.72 kg/cm^2), about 130~150°C, for four to six hours. The specific operating parameters vary slightly. According to Singh and Rai[6], complete hemihydrate conversion was achieved on autoclaving at 25.7 psi (1.75kg/cm^2) steam pressure for 7 hours or at 36 psi (2.45 kg/cm^2) for 4-6 hours. The most successful current industrial practice is the SICOWA-ProMineral autoclaving process in Germany [7].

(ii) Oxidation method

$$2CaSO_3+H_2O+O_2(g) \rightarrow 2CaSO_4{\bullet}0.5H_2O \tag{1-2}$$

Gaseous SO_2[8] is reacted with CaO-H_2SO_4 slurry which is subsequently pressure-oxidized into α-hemihydrate in pressurized oxidation vessel at around 100~145°C and super-atmospheric pressure of about 20~60 psi (1.36~4.08 kg/cm^2).

(iii) Hydro-chemical methods

There are some other methods reported in the literature. Most of them are described in patents which apparently have not resulted in industrial applications [9-15]. In most of these methods, calcium sulfate dihydrate is converted to α-hemihydrate by curing it in concentrated inorganic salt solutions. In some of those methods the use of sulfuric acid (as opposed to phosphoric acid in the majority of them) at the boiling point has been reported. The Czech method patented in 1973 [16] differs from the other ones as it refers to production of α-hemihydrate from waste liquors containing sulfuric acid and sulfate salts (most important of which was $Fe_2(SO_4)_3$, in some cases, up to 50 g/L $Fe_2(SO_4)_3$) by neutralization with lime or limestone.

Overall it may be stated that the two commercially-proven technologies (the autoclaving and oxidation methods) are on one hand energy-intensive while on the other hand the alternative methods (third group) have not attracted commercial interest nor have been thoroughly investigated.

1.3 Thesis objectives

The research reported in this thesis is driven by the need of finding new application-uses for the surplus sulfuric acid produced by the non-ferrous metallurgical industry. One such potential application is the low cost production of high value α-hemihydrate building material directly from sulfuric acid (i.e. without the prior production of dihydrate) by reaction with lime (or limestone).

The primary objectives of this Ph.D research thesis are (a) determine the conditions under which α-hemihydrate may be produced directly by reaction of H_2SO_4 solution with lime; (b) study the fundamentals of crystallization of α-hemihydrate in sulfuric acid-lime-water system and (c) correlate the structure and properties of α-hemihydrate to its preparation conditions. The overall goal is to develop a novel, direct and cost-effective method for preparation of α-hemihydrate from sulfuric acid and if possible under atmospheric as opposed to elevated pressure conditions. The project in particular aims to:

(i) theoretically establish the phase diagram for $CaSO_4$-H_2SO_4-H_2O system;

(ii) define the region of operating conditions (such as temperature, H_2SO_4 concentration, lime/acid ratio, seeding, etc.) that favour the formation of alpha-hemihydrate;

(iii) investigate various factors that influence the formation of α-hemihydrate such as order of adding the reactants (different procedures to initiate the reaction), inorganic and organic additives, retention time, agitation, seeding, recycling, supersaturation control, etc.;

(iv) study and interpret the crystallization phenomena governing the process by characterizing in detail the product (final and intermediate phases) and monitoring the progress of the reaction; and

(v) determine the physical properties (such as normal consistency, setting time, compressive strength, etc.) of the laboratory-produced alpha-hemihydrate materials following ASTM standard procedures (ASTM 472-93).

1.4 About the organization of the thesis

The thesis is divided into 8 chapters. In chapter 2, Literature Survey, an extensive review about the intermediate calcium sulfate subhydrate phases in the $CaSO_4$-H_2O system, analysis methods employed in the investigation and current technologies for the preparation of α-hemihydrate is presented. In chapter 3, the methods of preparation, characterization techniques and procedures for sample treatment are described. In chapter 4, the phase diagram for the $CaSO_4$-H_2SO_4-H_2O is first described on the basis of thermodynamic calculations with the aid of OLI software [17] and FactSage [18]. In the same chapter the solubility of alpha-hemihydrate in sulfuric acid is determined in order to be used in the following work. In chapter 5, the transformation of calcium sulfate dihydrate and hemihydrate materials in aqueous sulfuric acid is investigated. And also, supersaturation-control tests have been carried out for better understanding of the crystallization/precipitation mechanism involved in the reactions between lime and sulfuric acid. In chapters 6 and 7, different procedures for producing α-hemihydrate are investigated. The operating window for reacting lime with sulfuric acid solution is then determined followed by the investigation of the effects of lime/acid ratio, inorganic and organic additives, seeding and recycling. In particular, dry lime versus slaked lime is compared. Also in chapter 7, testing results of some laboratory-made or commercial α-hemihydrate materials following the ASTM standard procedures are presented. Finally, the chapter of Synopsis summarizes the main findings of the work and states the originality and contributions made to knowledge along with a brief outline for possible future work.

References

[1] Desch, C. H., The mechanism of the setting process in plaster and cement, Trans. Faraday Soc., 14, 1-7(1919).

[2] van't Hoff, J. H., Armstrong, E. F., Himichen, W., Weigert, F. and Just, G., Gips und Anhydrite, Z. Phys. Chem., 45, 257 (1903) (in German).

[3] SciFinder search engine, http://www.SciFinder.com.

[4] de Forcrand, R., Researches on Plaster of Paris, Bull. Soc. Chim., 35, 781-790 (1906) (in French).

[5] Kwasny-Echterhagen, R., Schlieper, H., Kirchen, G., Morgenroth, H. and Wiesgickl, G., Alpha-Hemihydrate - a high value building material made from FGD gypsum, experiences concerning processing, product development and market applications, FGD and Synthetic Gypsum, International Conference, 5th, Toronto, May 11-14, [Proceedings], Process Research ORTECH Inc.: Mississauga, Ontario, Canada, 8, 1-15(1997).

[6] Singh, M. and Rai, M., Autoclaved gypsum plaster from selenite and by-product phosphogypsum, J. Chem. Tech. Biotechnol., 43, 1-12(1988).

[7] Engert, H.J. and Koslowski, T., New gypsum binder Alpha 2000, ZKG International, 51(4), 229-237 (1998).

[8] College, J.W., Sulfur dioxide removal from sulfur dioxide-containing hot gaseous streams under formation of α-hemihydrate gypsum, USA Patent, US 5,312,609 (1994).

[9] Wirsching, F., The production of α-hemihydrate gypsum plaster from byproduct gypsum in salt solutions, Zement-Kalk-Gips, 15, 439-441(1962) (in German).

[10] Miyazaki, H., Preparation of α-hemihydrate from gypsum produced as a by-product in sea salt manufacturing, Gypsum & Lime, 95, 186-193 (1968) (in Japanese).

[11] Kudo, Y., Preparation of α-calcium sulfate hemihydrate, Japan Patent, JP 01,014,112(1989) (in Japanese).

[12] Yamada, T., Mizutani, C. and Nagai, S., Gypsum as a by-product of phosphoric acid production (VII), Dehydration and hydration in mineral acids, Gypsum & Lime, 85, 198-202(1966) (in Japanese).

[13] Robinson, M.C., Kirk, D.W. and Hummel, R.L., Manufacture of hydrogen or electric power and calcium sulfate hemihydrate from calcium sulfite, International Patent, WO 9,118,131(1991).

[14] Zürz, A., Odler, I., Thiemann, F. and Berghöfer, K., Autoclave-free formation of α-hemihydrate gypsum, Journal of American Ceramics Society, 74(5), 1117-1124(1991).

[15] Hina, A. and Nancollas, G.H., Alpha calcium sulfate hemihydrate and a method of making alpha calcium sulfate hemihydrate, International Patent, WO 0,179,116(2001).

[16] Rihanek, S., Alpha-calcium sulfate hemihydrate from acidic waste, Czech. Patent, CS 150,396 (1973) (in Czech).

[17] http://www.olisystems.com.

[18] http://www.FactSage.com.

Chapter 2

Literature Survey

2.1 Introduction

In this chapter, an extensive review of the literature is presented starting with background information about the $CaSO_4$-H_2O system.

2.2 The $CaSO_4$-H_2O system

As mentioned before, the principal phases that occur in the $CaSO_4$-H_2O system are $CaSO_4 \cdot 2H_2O$ (gypsum, dihydrate), hemihydrate ($CaSO_4 \cdot 0.5H_2O$), γ-$CaSO_4$ (soluble anhydrite or anhydrite III), $CaSO_4$ (insoluble anhydrite, β-$CaSO_4$ or anhydrite II) and a high-temperature form[1] of anhydrite, α-anhydrite (or anhydrite I). To avoid confusion[2], the German style, namely anhydrite I, II and III, was followed in this review.

In the $CaSO_4$-H_2O system, the structures of calcium sulfate dihydrate ($CaSO_4 \bullet 2H_2O$) and of anhydrite II (β-$CaSO_4$) are well established. The dihydrate is monoclinic with unit cell parameters (refer to Figure 2.1 for unit cell definition of different systems): $a=5.68Å$, $b=15.18Å$, $c=6.29Å$, $\beta=113^\circ 50'$, $Z=4$ and space group *A2/a* [5]; and anhydrite II (β-$CaSO_4$) is orthorhombic, unit cell: $a=6.99Å$, $b=7.00Å$, $c=6.24Å$, $Z=4$ and space group *Amma* [6].

---

[1] According to Lehmann [1], the transition temperature from anhydrite II (β-$CaSO_4$) to anhydrite I (α-anhydrite) is around 1193°C.

[2] The terms, high-temperature α-anhydrite, insoluble anhydrite β-$CaSO_4$ and soluble anhydrite γ-$CaSO_4$ are really confusing here. In the German and Japanese literature [2-4], these anhydrite phases are referred to as anhydrite I, anhydrite II and anhydrite III respectively to avoid confusion. Particularly, it has to be stressed that, the naming of α- and β-hemihydrates has no crystallographic relation with α-anhydrite and β-anhydrite.

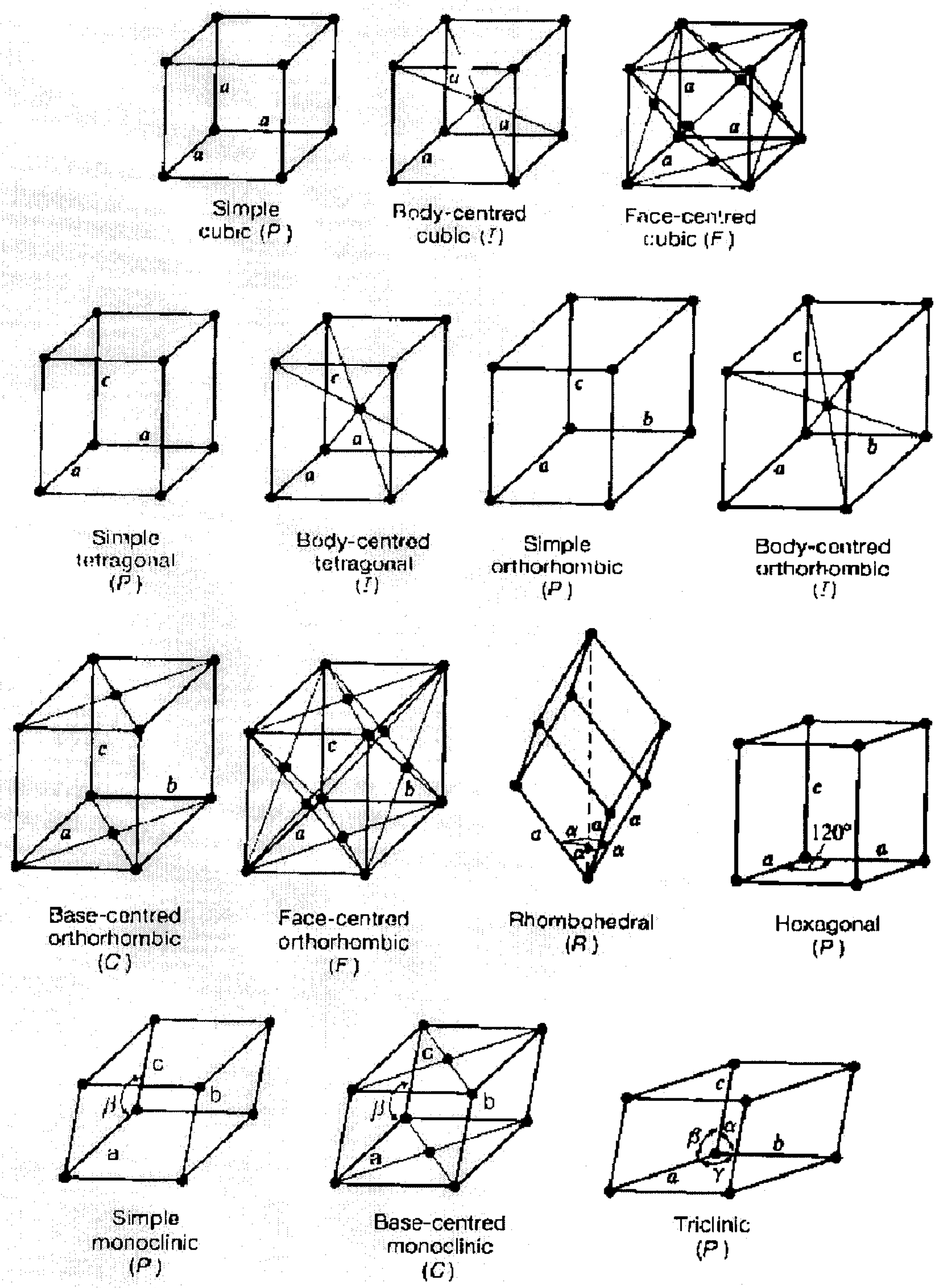

Figure 2.1: Schematic illustration of the space-filling parallelepipeds (after Hammond [7])

Calcium sulfate subhydrate and anhydrite III (γ-$CaSO_4$) are the low temperature dehydration products of dihydrate. Subhydrate, which occurs in nature as hemihydrate, the mineral bassanite (same with Plaster of Paris), is a very important raw material especially in the building industry.

Deer et al. [8] gave a good review of the literature prior to 1960. But the latest edition of the book [9] and some other handbooks [10] avoided to include definite descriptions about the intermediate phases between $CaSO_4 \bullet 2H_2O$ and anhydrite II (β-$CaSO_4$) in the $CaSO_4$-H_2O system due to controversy surrounding these phases.

Generally speaking, it is widely accepted that:

(1) There exist subhydrate(s), $CaSO_4 \bullet nH_2O$ with $0<n<1$ (this term is considered to be more accurate than the term hemihydrate) and anhydrite III (γ-$CaSO_4$) lying between the low temperature stable form, $CaSO_4 \bullet 2H_2O$ and the moderate temperature stable form, anhydrite II (β-$CaSO_4$);

(2) Calcium sulfate dihydrate decomposes thermally as a function of temperature in equilibrium with the ambient water vapor pressure to subhydrate, $CaSO_4 \bullet nH_2O$ with $0<n<1$, then to anhydrite III (γ-$CaSO_4$), and finally to anhydrite II (β-$CaSO_4$);

(3) There are some similarities in the crystal structures between anhydrite III (γ-$CaSO_4$) and subhydrate. In other words, they are structurally connected. The mutual transition between these two phases can readily take place. Hydration of anhydrite III to subhydrate (hemihydrate) occurs very rapidly by a "quasi-zeolitic" reaction which can occur in the presence of water vapor alone, and which, generally believed, does not involve re-crystallization. It is possible to formulate a qualitative model of subhydrate based on the refinement of the anhydrite III (γ-$CaSO_4$) structure; and

(4) There are some uncertainties as far as the structures of anhydrite III (γ-$CaSO_4$) and subhydrate(s) are concerned.

2.3 Controversy over the structure of subhydrate

In Table 2.1 most of the unit cells reported for subhydrate, $CaSO_4 \cdot nH_2O$ ($0<n<1$), are listed. Various n values have been reported in literature such as 0.15 [11], 0.17 (1/6) [12], 0.48 [13], 0.5 [14-16], 0.52 [13], 0.6 [17-20], 0.62 [21], 0.67 (2/3) [21-25], 0.74 [2] and 0.8 [26-27].

The pioneering major contributions to the crystallography of these phases were made by Gallitelli [28], Flörke [29] and Gay [30]. Gallitelli (1933) was the first to propose a structural model for hemihydrate based on single-crystal X-ray data. On the basis of Weissenberg methods, he determined that the structure was characterized by pseudo-trigonal channels which house the water molecules. He also reported that the structure was only slightly distorted from trigonal symmetry and approximated it in terms of space group $P3_121$(refer to Table 2.1). Flörke (1952) expanded upon the work of Gallitelli and suggested from optical data that hemihydrate has two polymorphs depending on the crystallization temperature: hexagonal above 318K(45°C) and orthorhombic below 318K(45°C)(refer to Table 2.1). The orthorhombic form twinned on (001), resulting in pseudo-trigonal symmetry. Flörke's orthorhombic structure was similar to Gallitelli's C2 structure but with water located at (0,0,0) and (0,0,1/3) rather than at (0,0,1/6) and (0,0,1/2). But Gay (1965) rejected this interpretation. On the basis of optical techniques and high-temperature X-ray (Weissenberg) methods, Gay suggested a monoclinic I-centered structure(refer to Table 2.1). He concluded that hemihydrate was multiply-twinned on a fine scale and consisted of monoclinic sub-crystals which differed in the orientation but had their **c** crystallographic axes parallel to the 3-fold axis of pseudo-symmetry and that hemihydrate didn't exhibit the polymorphs suggested by Flörke. Gay also noticed that the symmetry of the crystal structure was confounded by the inter-growth of a substructure of lower symmetry and that the soluble anhydrite (anhydrite III) and hemihydrate structures were closely related. Teimurov et al. [31] proposed a structural model for hemihydrate based on the steric details of the gypsum structure [32] and the mechanism of its dehydration [33].

Table 2.1: Unit cells proposed for subhydrate $CaSO_4 \bullet n\ H_2O$ ($0 < n < 1$)

Investigators	System	Space Group	*a*(Å)	*b*(Å)	*c*(Å)	*β* / *γ* $(^0)$	*Z*	Notes
Gallitelli [28]	Monoclinic	C121	11.94	6.83	12.70	ß= 90.60	12	
	Pseudo-trigonal	$P3_121$	6.83		12.70			approximation to C2 cell
Caspari [14]	Trigonal		6.82		6.24			no difference between hemihydrate and soluble anhydrite
Flöke [29]	Trigonal	$P3_221$	6.86		12.70	a=ß=90 γ=120	6	T> 318K(45°C)
	Orthorhombic	C222	6.8	11.5	12.7			T< 318K(45°C)
Gay [30]	Monoclinic		6.85	11.88	12.60	$\gamma \approx 90$		
Davis [12]			6.469	6.815	7.148		4	n=1/ 6, stable in pressure(<500bar)
Gardet [11]	Hexagonal		6.97		6.27		3	n=0.15
Bushuev [34]	Hexagonal	$P6_122$	6.97		12.76		6	n=0.5 α-modification
	Hexagonal	$P6_122$	13.96		12.75		24	n=0.5 β-modification
Bushuev [22]	Hexagonal	$P3_121$	6.977		12.617		6	n=0.5
	Monoclinic	I2	12.028	38.022	6.927	γ= 90.21	36	n=0.67
Frik [13]	Orthorhombic		12.061	6.933	12.670			n=0.48, relative humidity <5%,
	Hexagonal		13.865		12.718			n=0.52, relative humidity ~40%,
Bushuev [23, 24]	Hexagonal	$P3_121$	6.977		12.617		6	n=0.5
	Monoclinic	I2	12.028	12.674	6.927	γ=90.21	12	n=0.67 (hydrothermal $CaSO_4 \bullet 2H_2O+H_2O$)
Abriel [26]	Trigonal	$P3_121$	6.968		6.410		3	n=0.8
Lager [15]	Monoclinic	I2	12.062	12.660	6.930	γ≈90		n=0.5 dehydration of $CaSO_4 \bullet 2D_2O$
Kuzel [21]	Monoclinic	I2	12.027	6.931	12.692	ß=90.18		n=0.5 $P_{H2O}/P=0.35$, T=295K(22°C)
	Trigonal		13.861		12.739			n=2/3 $P_{H2O}/P=0.76$
Abriel [2]								n=0.74, high local H_2O pressure
Bezou [17]	Monoclinic	I121	12.677	6.928	12.033	ß=90.26		n=0.5
	Orthorhombic	I222	12.377	6.303	12.007			n=0.6
Bezou [19]	Monoclinic	I2	12.019	6.930	12.670	ß=90.23		n=0.5
	Monoclinic	C2	11.999	6.925	6.377	ß=90.00		n=0.6
Abriel [27]	Trigonal	$P3_121$	6.937		6.345		3	n=0.5
Bezou [20]	Monoclinic	I121	12.032	6.927	12.671	ß=90.27	12	n=0.5
	Monoclinic	I121	11.985	6.929	12.750	ß=90	12	n=0.6
Ostrowski [16]	Trigonal		6.83		12.71	α=ß=90 γ=120	6	n=0.5 prepared in presence of succinic acid
Badens [35]	Monoclinic		12.019	6.930	12.670	ß=90.23	12	n=0.5 water vapor pressure 900Pa

Notes: (1) In most of the quotes, the original units are preserved.

(2) Some results from the same investigators are listed for contrast.

(3) Absent data for unit cells are unavailable in the original sources.

Bushuev and his co-workers presented different arguments. In their earlier work[34], they assigned slightly different hexagonal $P6_122$ space groups for α- and β-modifications of hemihydrate for both of which they used the formula of $CaSO_4 \bullet 0.5H_2O$. Their specimens were prepared with van't Hoff's method [36] (by boiling gypsum in 15% NaCl solution or from nitric acid solutions at 50-60°C). Later, Bushuev and his co-workers revised [22-25] their models on the basis of their high temperature Guinier X-ray powder experiments and concluded that α- and β-forms corresponded to monoclinic $CaSO_4 \bullet 0.67H_2O$ or $CaSO_4 \bullet n_1H_2O$ (where water content $0.5 < n_1 \leq 0.67$) and hexagonal $CaSO_4 \bullet 0.5H_2O$ or $CaSO_4 \bullet n_2H_2O$ (where water content $0 < n_2 \leq 0.5$) respectively. The α-form (corresponding to $CaSO_4 \bullet 0.67H_2O$) sample was prepared by slowly dehydrating gypsum dihydrate in closed stainless steel autoclave with solid and water ratio 1:10 and temperature range 107-200°C (best around 120°C) for 24 hours. Bushuev [25] further proposed the following phase transformation scheme for calcium sulfate in the presence of water vapor at atmospheric pressure:

$$\mathrm{DH} \xrightleftharpoons{40\,^{\circ}\mathrm{C}} \alpha\text{-HH} \xrightleftharpoons{73\text{-}79\,^{\circ}\mathrm{C}} \beta\text{-HH} \xrightleftharpoons{180\,^{\circ}\mathrm{C}} \gamma\text{-}CaSO_4 \xrightleftharpoons{300\,^{\circ}\mathrm{C}} \beta\text{-}CaSO_4 \xrightleftharpoons{1200\,^{\circ}\mathrm{C}} \alpha\text{-}CaSO_4 \quad (2\text{-}1)$$

Alpha-form ($CaSO_4 \bullet 0.67H_2O$) converted to β-form ($CaSO_4 \bullet 0.5H_2O$) at around 80°C or so. Kuzel and Hauner [21] also supported the topotactic reaction:

$$CaSO_4 \bullet 4/6H_2O \rightleftharpoons CaSO_4 \bullet 3/6H_2O \rightleftharpoons \gamma\text{-}CaSO_4 \qquad (2\text{-}2)$$

upon dehydration/re-hydration.

Bushuev's monoclinic $CaSO_4 \bullet 0.67H_2O$ symmetry was strongly supported by recent investigators, especially Rinaudo et al. [37][3]. JCPDS-International Centre for Diffraction Data has cards 33-0617 and later version 47-0964 (refer to Table 2.2) for this monoclinic $CaSO_4 \bullet 0.67H_2O$ symmetry based on the work of Rinaudo et al. [37] and Bushuev et al. [24].

---

[3] Rinaudo et al.[37] observed that experimentally determined water loss (7.8 wt%) slightly deviated from the theoretical value (8.1 wt%).

Table 2.2: Unit cells for subhydrate $CaSO_4 \bullet n\, H_2O$ $(0 < n < 1)$

in the databank of JCPDS-International Centre for Diffraction Data

JCPDS Card No.	System	Space Group	a(Å)	b(Å)	c(Å)	β / γ (°)	Z	Notes
01-0999	Hexagonal		6.76		6.34		3	n=0.5 Plaster of Paris [38] Deleted
02-0134								n=0.15 Deleted
02-0135								n=0.19 Deleted
02-0651								n=0.34 Deleted
02-0653								n=0.48 Deleted
02-0654								n=0.02 Deleted
02-0667	Hexagonal		6.76		6.24		3	n=0.5 Plaster of Paris [39] Deleted
02-0675	Hexagonal	P $\bar{3}$m1	6.76		6.24		3	n=0.5 Plaster of Paris Deleted
03-0083								n=0.5 Deleted
14-0453	Hexagonal		6.931		6.344		3	n=0.5 β-form Replaced by 24-1068
21-0167	Orthorhombic		6.47	6.82	7.15		4	n=x uncertain formula [12]
23-0128	Hexagonal		6.978		6.277		3	n=0.15 Gardet [11] To replace 2-0134
24-1067	Monoclinic		6.851	11.866	12.584		6	n=0.5 Gay [30]
24-1068	Hexagonal	P $\bar{3}$m1	6.947		6.342		3	n=0.5 Flöke [29]
33-0310	Orthorhombic		12.031	12.695	6.934		12	n=0.5 Deleted by 41-0224
36-0617	Monoclinic	I2	12.67	6.927	12.028		12	n=0.67 Bushuev [24] Replaced by 41-0224
41-0224	Monoclinic	I2	12.028	6.932	12.691		12	n=0.5 (Kuzel and Hauner [21])
41-0225	Hexagonal	$P3_221$	13.862		12.739			n=0.62 (Kuzel and Hauner[21])
43-0605	**Hexagonal**		**13.862**		**12.739**			**n=0.6(Kuzel and Hauner [21]) α-form**
45-0848	**Hexagonal**	**$P6_122$**	**13.96**		**12.75**		**24**	**n=0.5 (Bushuev [34]) β-form**
47-0964	Monoclinic	I	12.67	6.927	12.028			n=0.67(Rinaudo [37] & Bushuev [24])
76-2312	Hexagonal	$P3_221$	6.968		6.41		3	n=0.8(JCPDS calculation & Abriel [26])
80-1235	Monoclinic	I2	12.019	6.930	12.670	β=90.24	12	n=0.5 (JCPDS calculation & Bezou [19])
80-1236	Monoclinic	C2	11.999	6.925	6.377	β=90.00	6	n=0.6
81-1848	Hexagonal	$P3_121$	6.937		6.345		3	n=0.5 (JCPDS calculation & Abriel [27])
81-1849	Monoclinic	I2	12.028	6.931	12.692	β=90.18	12	
83-0438	Monoclinic	I2	12.032	6.927	12.671		12	n=0.5 (JCPDS calculation & Bezou [19])
83-0440								n=0.583 (JCPDS calculation & Bezou[20])
83-0441	Monoclinic	I2	11.984	6.929	12.751		12	

Notes:

(1) Absent data for unit cells are unavailable in the original sources.

(2) The JCPDS α- and β-hemihydrate standards are highlighted in bold.

Interestingly, JCPDS doesn't use this monoclinic structure as α-hemihydrate standard pattern. Instead it adopted a hexagonal $CaSO_4{\bullet}0.6H_2O$ structure (JCPDS card 43-0605) with the same unit cell parameters as the trigonal model proposed by Kuzel and Hauner [21] even though Kuzel and Hauner [21] suggested the formula unit of $CaSO_4{\bullet}4/6H_2O$ (or $CaSO_4{\bullet}0.67H_2O$) rather than $CaSO_4{\bullet}0.6H_2O$. Also, JCPDS adopted one of Bushuev's earliest models [34], hexagonal β-modification $CaSO_4{\bullet}0.5H_2O$, as the standard pattern of β-hemihydrate (JCPDS card 45-0848).

In addition, according to Bushuev et al. [24], $CaSO_4{\bullet}0.67H_2O$ was the limiting composition due to "*steric hindrance*". However, Lager et al. [15] rejected any subhydrates other than $CaSO_4{\bullet}0.5H_2O$ based on their time-of-flight neutron powder diffraction data as well as steric consideration. They found *"it is difficult to imagine"* the trigonal $CaSO_4{\bullet}0.8H_2O$ structure proposed by Abriel [26]. They collected a high-temperature (378K or 105°C) data set for hemihydrate by dehydrating in-situ $CaSO_4{\bullet}2D_2O$ (deuterized dihydrate) for around 8 hours and found that "*the 295 and 378K patterns are almost identical in appearance and neither can be indexed in the cell proposed by Flörke*". It was concluded that the symmetry was lower than hexagonal. Rejection of additional subhydrates was also supported by the proton magnetic resonance (PMR) results from Goto [40] and Saito [41] and the in-situ IR spectroscopic and thermogravimetric study by Putnis et al [42]. It should be noted that most of their experiments were carried out under conditions of negligible water vapor pressure.

It is likely that, additional subhydrates exist under conditions of significant water vapor pressure as demonstrated by recent investigators. Frik and Kuzel [13] suggested that the structure of hemihydrate was dependent on the vapor pressure of H_2O. They recognized two forms of hemihydrate: an orthorhombic phase stable under low relative humidity conditions (RH<5%) and a hexagonal phase (RH about 40%). Bushuev and Borisov [24] concluded that the existence of the two forms was related to the amount of the water in the channels. Their higher water content form (aforementioned hexagonal $CaSO_4{\bullet}0.67H_2O$) was prepared in the autoclave with pressure "*not more than 50000-70000 Pa*" [43]. Kuzel and Hauner's samples were prepared at various H_2O partial pressures: for $P_{H2O}/P = 0.35$ and T=22°C a monoclinic hydrate with "*idealized*" composition $CaSO_4{\bullet}3/6H_2O$ ($CaSO_4{\bullet}0.5H_2O$) was in equilibrium with the environment;

when the H_2O partial pressure was raised to $P_{H2O}/P = 0.76$ a trigonal H_2O-richer hydrate $CaSO_4{\bullet}4/6H_2O$ ($CaSO_4{\bullet}0.67H_2O$) was formed. Based on the results of on-line multi-channel neutron diffraction data, Abriel et al. proposed highly loaded subhydrates under high local H_2O steam pressures, such as $CaSO_4{\bullet}0.74H_2O$ [2], $CaSO_4{\bullet}0.80H_2O$ [26] structures in which, they believed, additional filled water molecules had no bonds to the mainframe matrix (with bonds in the case of $CaSO_4{\bullet}0.5H_2O$) and could be moved more easily. Other important investigators worthy mentioning are Bezou et al. Bezou et al.[17] quantitatively profiled the stability zones of their monoclinic structures $CaSO_4{\bullet}1/2H_2O$ ($CaSO_4{\bullet}0.5H_2O$) and $CaSO_4{\bullet}3/5H_2O$ ($CaSO_4{\bullet}0.6H_2O$) with water vapor pressures (shown in Figure 2.2). The stability diagram also implies that under most normal atmospheric conditions only the hemihydrate form ($CaSO_4{\bullet}0.5H_2O$) could be observed. Clearly Bezou et al.[18] suggested the following reaction scheme:

$$CaSO_4{\bullet}0.5H_2O_{(s)} + 0.1H_2O_{(g)} \rightleftharpoons CaSO_4{\bullet}0.6H_2O_{(s)} \qquad (2\text{-}3)$$

However, they ruled out the existence of $CaSO_4{\bullet}4/5H_2O$ ($CaSO_4{\bullet}0.8H_2O$) proposed by Abriel [26].

So far, various symmetries have been assigned to subhydrate such as monoclinic, orthorhombic, trigonal and hexagonal. Some suggestions or conclusions are even contradicting to each other. Revisiting the assignment processing of the powder diffraction data can make things potentially less confusing. Take for example the indexing of the $CaSO_4{\bullet}0.6H_2O$ pattern from Bezou et al.[20]; first the synchrotron X-ray powder pattern was collected, then the pattern was decomposed with certain programs such as PAWSYN [44]; the results showed that both orthorhombic as well as hexagonal cells gave acceptable agreement between observed and calculated powder patterns: an orthorhombic I-centered cell with *a=12.008, b=6.931,c=12.737 Å* gave a R value[4] 7.6%

---

[4] Typically three R-values are most-frequently-used in the Rietveld method [45] for analysis of powder diffraction data. The original source did not specify which R value was used, most probably, it referred to R_{wp}, ***R-weighted pattern value,*** which is calculated from the differences between each individual point of the observed and calculated powder diffraction patterns. R_{wp}, is an good indicator of the progress of the refinements. Values of R_{wp} are often reported in the range 5 - 15 % for refined structures.

while a hexagonal cell with *a=6.932, c=6.368 Å* gave a R value of 7.8%, which is the most-frequently-encountered situation: i.e., indexing of the diffraction data results in more than one acceptable solutions[5]. The final assignment(s) made by the various researchers in most cases, thus, is semi-quantitative rather than definitive. This is one of the factors that has caused the controversy about the structure(s) of subhydrate(s), and explains why in several instances the same authors have suggested different models.

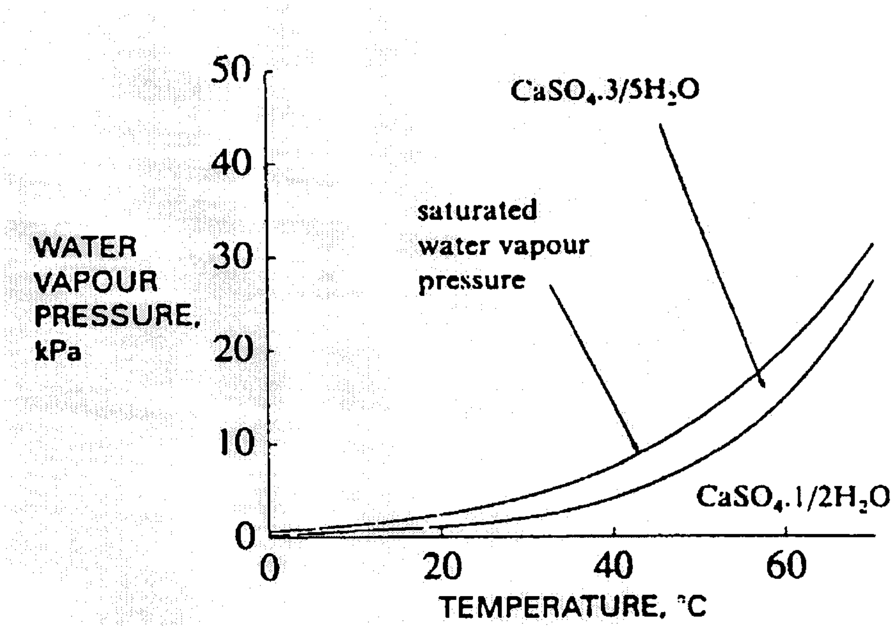

Figure 2.2: Stability zones of calcium sulfate subhydrates versus water vapor pressure (after Bezou et al. [17])

On the other hand, as it can be deduced from the discussion so far, the system is quite complex, and the stability of the possible phases depends on the temperature and the ambient water vapor pressure [47-48] to which the samples are effectively exposed. This explains why in various characterization analyses of gypsum and its related compounds, the operating conditions, the nature of starting material, characteristics of the

---

[5] The author has also tried to use CrysFire [46] to decompose and index the X-ray diffraction data which were obtained in the XRD laboratory of the Department of Mining, Metals & Materials Engineering at McGill University and resulted in similar situation but higher deviations. The determination of symmetry and unit cell parameters is not the focus of this thesis.

equipment, as well as the construction and the material of the equipment, have direct influence on the results [49]. Take synthetic calcium sulfate dihydrate and natural gypsum for examples: it was found that the former was totally decomposed to hemihydrate up to 70°C whereas the TGA curves of the latter began at 62°C and ended at around 190°C[50]. Lager et al. [15] also found that line broadening of the XRD profiles for the hemihydrate sample obtained by dehydration of natural gypsum was considerably less than that for the sample obtained by dehydration of synthetic dihydrate. It is quite possible that the hydration and dehydration mechanism within the tunnel structure is topotactic [51]; under some experimental conditions, the three-dimensional network of the host structure could be partially conserved, which resulted in misleading phenomena, e.g., the lattice of the resultant hemihydrate varied as demonstrated by Badens et al.[35] under very low water vapor pressure (900Pa) and different initial dihydrate crystal sizes (micron-sized or centimeter-sized); or as Saito [41] pointed out, gypsum dehydrated at low temperatures, unlike gypsum dehydrated at higher temperatures, had a dihydrate gypsum pseudo lattice with Ca^{2+} and SO_4^{2-} occupying their original sites; and, consequently, being misinterpreted.

Setting aside all the above controversy, it may be summarized that:

(1) The probable subhydrates have structures with channels where water molecules may be located. All structures in the system $CaSO_4$-H_2O can be interpreted by a model of different packing of chains containing Ca^{2+} and SO_4^{2+} ions (refer to Figure 2.3). According to Abriel et al.[2], in the subhydrate, the tunnel structure of anhydrite III (γ-$CaSO_4$) (Figure 2.3, a, AIII) is filled with water molecules. According to Lager et al.[15], the water molecules occupy two different levels along **b** axis in the channels of a distorted anhydrite III (γ-$CaSO_4$) and the hemihydrate and anhydrite III unit cells can be related by a transformation. Bezou et al.[20] suggested that the water molecules entered the coordination sphere of calcium ions.

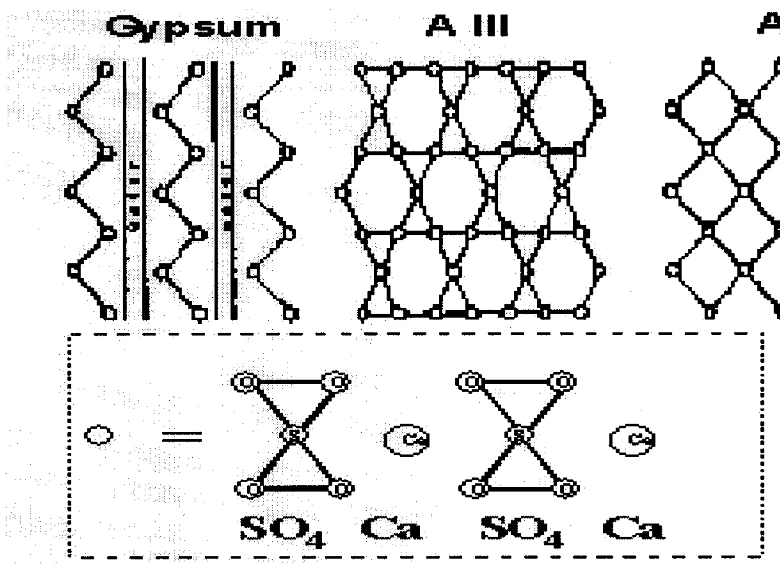

(a) AIII, AII represent anhydrite III and II respectively. The small circle structure represents a chain of alternating Ca^{2+} and SO_4^{2-} perpendicular to plane of paper (after Abriel et al. [2]).

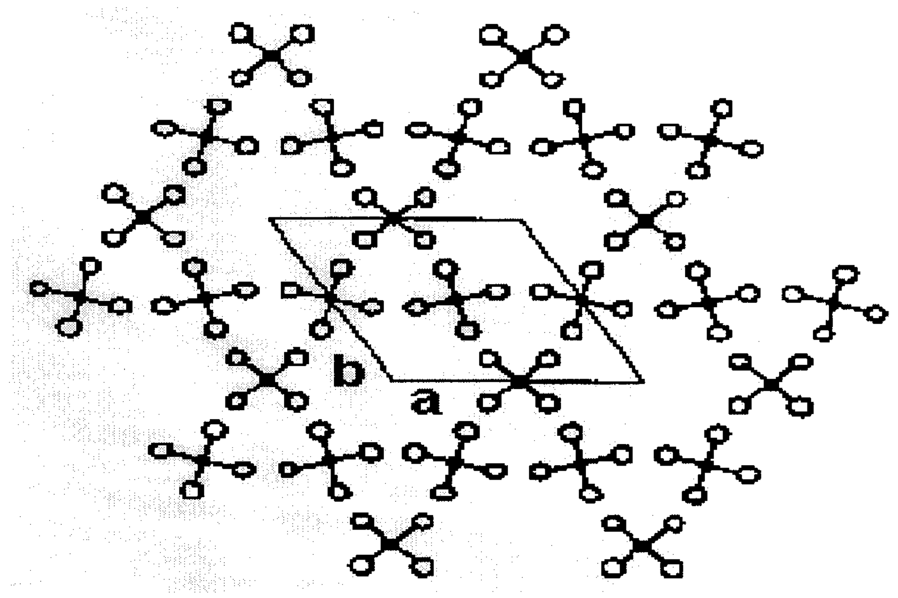

(b) [001] projection of anhydrite III illustrating the channels developed parallel to **c** axis perpendicular to plane of paper (after Lager et al. [15])

Figure 2.3: Schematic illustrations of the structures in $CaSO_4$-H_2O system

(2) The subhydrate with n=1, i.e., a mono-hydrate with completely filled tunnel, is not observed due to "*complete steric hindrance*" (Bushuev's term).

(3) Hemihydrate(with n=0.5) is the most stable phase among the probable intermediate subhydrate phases. Differential thermal and thermo-gravimetric analyses of synthetic and natural gypsum are overall consistent with the dehydration reaction sequence

$$CaSO_4\bullet 2H_2O \rightarrow CaSO_4\bullet 0.5H_2O + 1.50H_2O \quad \text{and}$$

$$CaSO_4\bullet 0.5H_2O \rightarrow \gamma\text{-}CaSO_4+0.5H_2O \qquad (2.4)$$

Slight departures from the stoichiometric composition have been noted: ±0.02 H_2O by Lager [15], and experimental 5.7% versus theoretical 6.2% in case of $CaSO_4\bullet 0.5H_2O$ by Bushuev et al.[25]. Dehydrating dihydrate under various conditions, that is, different temperatures, heating rates, atmospheres, etc. generally produces stoichiometric hemihydrate as determined by weight loss after heating despite the fact that the weight loss measured gravimetrically does not necessarily represent the loss of structural water. According to Abriel et al.[2], from DTA or TGA curves, "*one can only get a signal for the kinetically most stable phase, the hemihydrate, exclusively*".

(4) The relative stability of hemihydrate is ascribed to weak H bonding of H_2O to the SO_4^{2-} group. Guest water molecules occupy one half of all tunnel positions, each of them weakly connected to the framework by $O_3SO\text{-}HOH\text{-}OSO_3$ bonds (2.85-3.03Å, according to Bezou et al. [20]). The point of inflection of the hemihydrate state in corresponding thermogravimetric measurements and some other experimental records indicates the requirements for significant energy level to break the hydrogen bonds to the $CaSO_4$ framework during the course of dehydration.

(5) Additional tunnel positions with no bonds to the matrix are probably filled with water molecules. Uncertainty exists with respect to the number of water molecules in the channels. These guest molecules can be moved more easily in a cooperative migration mechanism using empty sites according to Abriel et al.[2]. According to Bezou et al. [20], two adjacent water molecules in the channels are linked by a strong

hydrogen bond (O-H=1.9Å) in case of $CaSO_4 \bullet 0.6H_2O$, which perhaps provides support for aforementioned cooperative migration mechanism of Abriel et al.[2].

(6) Highly loaded subhydrates other than $CaSO_4 \bullet 0.5H_2O$ structure could exist under high local H_2O vapor pressures or in "*dehydrating solutions*" (Bushuev's term [25]) such as solutions of nitric acid and sodium chloride.

(7) It is clear that JCPDS-International Centre for Diffraction Data has assigned formula unit $CaSO_4 \bullet 0.6H_2O$ to α-hemihydrate and $CaSO_4 \bullet 0.5H_2O$ to β-hemihydrate despite the fact that several investigators consider α-hemihydrate to have the same formula with β-hemihydrate but to be "better-crystallized" than the latter one.

2.4 Analysis and characterization

The techniques employed by various investigators determine, to great extent, how reliable and accurate the acquired data are. Below a brief review of the analysis methods employed in the investigations of the $CaSO_4$-H_2O system is presented.

(1) Thermal analysis

This kind of analysis includes conventional Differential Thermal Analysis (DTA), Differential Thermogravimetric Analysis (DTG), Thermogravimetric Analysis (TGA) and Differential Scanning Calorimetry (DSC). Thermal analysis can provide a macroscopic view of the reaction process on one hand and provide kinetic data that can be used to calculate the empirical activation energy on the other. Those methods have their shortcomings, due to problems such as the possible presence of inter-granular and surface water, or due to the empirical nature of the correlation between rate law and reaction, or finally due to the fact that it averages out the contributions from different mechanisms and cannot be used to determine the phases present. Particularly it is not possible to unambiguously identify absorbed and bound water in the calcium sulfate hydrate system by gravimetric measurements[6]. By TGA, using closed pans with pinholes, the hemihydrate loses weight even at temperatures as low as 50°C [52], from which one can hardly ever discriminate the bond level of water.

On the other hand, DTA and DSC can provide some information about structural differences [53-54], which is going to be elaborated in subsequent section. Measurement of heats of solution as done in 2N hydrochloric acid by Kelley et al.[53] and Fleck et al. [55] can also be included in this category of methods of analysis.

(2) Diffraction Analysis

i. X-ray diffraction

(a) X-ray powder diffraction measurement

Bezou et al. [20] used synchrotron X-ray radiation besides the regular powder diffraction method in order to obtain better resolution.

(b) X ray single-crystal diffraction measurement

Single crystal diffraction patterns sometimes may be important compliment to the powder diffraction pattern. According to Lager et al.[15], it is not possible to decide from X-ray powder diffraction data alone if the symmetry is lower than orthorhombic. The problem with this method is that it is difficult to grow single crystals or the resultant single crystal is not big enough under some certain environment. The traditional way to prepare single crystal of hemihydrate is to follow Caspari's procedure [14], in which dihydrate crystals were dissolved in a concentrated (up to around 60 wt%) nitric acid solution maintained at 353±5K (80±5°C) for a period of several weeks or curing dihydrate in boiling solution of 50 wt% nitric acid [56]. Other alternatives are curing dihydrate in saturated NaCl solution at 337±5 K(64±5°C) for 2 weeks [29][7], or simply in water at around 120°C as performed

---

[6] As warned in the literature, "*Thermogravimetry is not a suitable method for the analysis of the dehydration of gypsum*" (Putnis [42]), "*It is extremely difficult to obtain precise data for structural water in* $CaSO_4{\bullet}0.5H_2O$ *based on weight loss measurements*" (Lager et al.[15]), which explains why no thermogravimetric analysis has been done in this work.

[7] Lager et al.[15] concluded that Na incorporated into the lattice of hemihydrate and the substitution of Na for Ca produced significant changes in the lattice but with no effect on the space group symmetry.

by Bushuev and his co-workers[43] who were able to grow single crystals as large as 10 *mm*.

ii. Neutron diffraction

The position of some molecules in the structure may be easier to detect under neutron radiation. But as Bezou et al. [20] pointed out, for calcium sulfate subhydrates, the background level due to the hydrogen content of the sample is very high. Actually, in the work of Lager et al.[15, 57], deuterized calcium sulfate material was used to reduce the background noise due to hydrogen.

(3) Optical Analysis

i. Infrared spectroscopic analysis (IR)

Different bonds have different kinds of vibrations (such as stretching and bending vibration) under the light in the IR range. Powder IR spectra have been used by several investigators [42, 58-59]. So far, IR has failed to determine *"the existence of hemihydrate with more or less than 0.5* H_2O *per formula unit"* (from Putnis et al.[42]).

ii. Polarizing microscope

Optical data such as morphology, refractive index, birefringence, angle of extinction and the dispersion staining can be used for identification characteristics (Green [60]). It was widely used in phase analysis and was in use long before the discovery of X-rays. These studies generally did not succeed in differentiating the structural properties between α- and β-hemihydrates. On the basis of optical microscopic observations on thin layer, Barriac et al. [61] proposed that liquid water might be the re-crystallization medium of hemihydrate during dehydration of gypsum.

(4) Electron Microscopy

i. Scanning Electron Microscopy(SEM)
ii. Transmission Electron Microscopy(TEM)

The electron microscopic images provide direct information especially for the morphology of the sample (Molony et al.[62]; Yasue et al.[63]).

(5) (Nuclear) Proton Magnetic Resonance

The proton magnetic resonance signal from water in hemihydrate samples has been determined [40-41] (see Figure 2.4). The broad line was obtained from water that is tightly bound in the structure, and the narrower line is from absorbed water that is more mobile. It is rather an effective way to distinguish between absorbed and bound water. Based on the PMR data, the investigators concluded differences between α- and β-hemihydrates were *"merely the results of differences in habit, crystalline size, surface area and lattice perfection"* (from Goto et al. [40]).

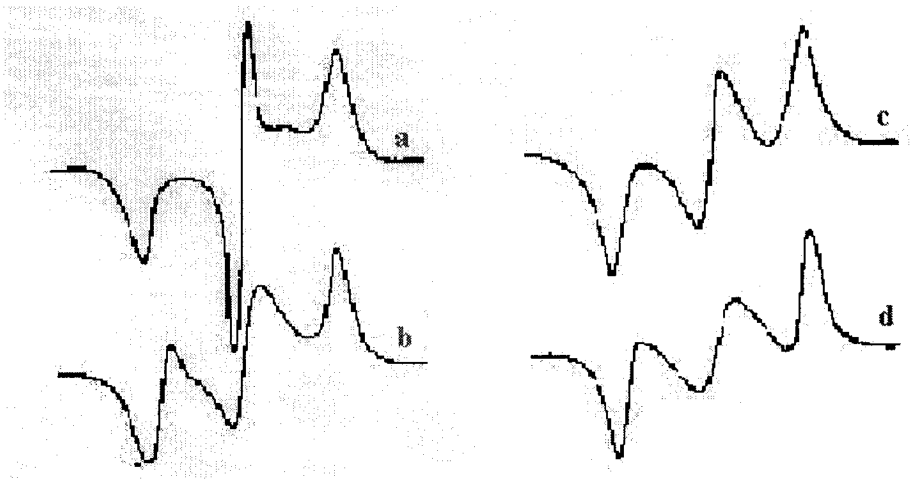

Figure 2.4: Derivative curves of the proton magnetic resonance signal from water in hemihydrate (after Goto et al.[40])

(a) Dry-calcined, 6.6% H_2O; (b)Dry-calcined, 5.8% H_2O;

(c) Autoclave-calcined, 6.4% H_2O; (d) Autoclave-calcined, 6.1% H_2O

(6) Particle size analysis

It includes the analysis of grain size and size distribution.

Generally, combination of two or more methods is employed by the researchers in order to get structural information. In this work, some methods, especially XRD and DSC, were carefully evaluated (this is reported in the following chapter) because of their extensive use to identify various intermediate and final products during the synthetic processing of α-hemihydrate from the sulfuric acid solution. Also, as part of the work, a hydro-thermal diamond anvil cell combined with IR microscopy has also been successfully employed and found to be advantageous for the in-situ tracing down of the ongoing phase transformation in the reacting system [64].

2.5 Differences between α- and β-hemihydrates

It is obvious from the previous discussion that the term "hemihydrate" is not strictly limited to n=0.5 in $CaSO_4 \bullet nH_2O$; but it is equivalent to calcium sulfate subhydrate.

There are two types of hemihydrate known as α and β. The two forms have been originally defined "*thermodynamically*" according to McAdie [56] since they differ "*in thermodynamic properties*" (Kelley et al.[53]) or according to the method of preparation [65-66], not from a standpoint of crystallography or mineralogy. The differences existing between the two phases are:

(a) In terms of preparation

One method of preparing α-hemihydrate is from $CaSO_4 \bullet 2H_2O$ under saturated steam conditions, at a pressure of about 20 psi, about 130°C, for five or six hours, in an autoclave. Different authors have suggested various approaches to the conditions of pressure, temperature, and gypsum lump thickness [67-70]. The other method is the solution process or hydrothermal process, e.g. synthesizing hemihydrate in concentrated nitric acid [14], and or some other salt solution, such as sodium chloride [43, 71-73] or solutions such as $CaCl_2$-H_2SO_4, $Ca(NO_3)_2$-H_2SO_4 [63]. Kojima et al.[3] reported a wet method by adding H_2SO_4 into saturated $CaSO_4$-HNO_3 solution. $NaNO_3$, NH_4Cl, $MgCl_2$, $Al_2(SO_4)_3$, sodium carboxylates, tartrate, succinate, gelatin etc.[74-76] have all been reported to be used as "catalysts" or "modifiers" in the synthesis of α-hemihydrate. Finally as mentioned before, α-hemihydrate may be prepared starting with $SO_2(g)$ material followed by oxidation of resultant $CaSO_3$ in a pressurized vessel [77].

β-hemihydrate on the other hand, is usually prepared by heating gypsum dihydrate under atmospheric conditions or in a vacuum (i.e., in the absence of water or water vapor) at temperature about 150°C (higher or lower, 90°C reported by Khalil and Gad [78]).

(b) In terms of physical properties

The properties include crystallinity, particle size and shape, density, refractive index, specific heat content, solubility, etc. Alpha-hemihydrate is distinguished by its relatively perfect crystal structure, high density, uniform appearance under polarized light, low water requirement for setting; the hydrated form is much stronger than that obtained from β-hemihydrate [79].

(c) In terms of powder diffraction patterns

Morris [80] reported differences in the X-ray reflections from (212) planes and interpreted these due to stacking order defects. But Bensted and Varma [66] contradicted Morris' interpretation by showing that, if the effects of line broadening were considered, and the differences were accounted for as "*due to difference in particle size*", then the X-ray pattern of ground α-hemihydrate was the same as that of β-hemihydrate. Their views were also supported from some more recent investigations [70, 81]. According to Singh and Rai [70], α-hemihydrate showed stronger reflections corresponding to 6.0619, 3.5587 and 3.0557Å but exhibited weaker reflections at other spacings. The two forms of hemihydrate showed no difference regarding the position of the peaks. There was, though, some discrepancy in the peak height which was assigned to the better crystallinity of α-hemihydrate.

(d) In terms of thermal properties

A lot of work has been done in this field, especially by differential thermal analysis. The position of the exothermic peak within the differential thermogram, which is due to the exothermic anhydrite III/II transformation, is claimed to be used as the identification of the hemihydrate forms [55, 82]. It has been reported that in case of β-forms, the exothermic peak occurs at approximately 350°C [8] whereas the peak of α-form is below 250°C immediately following the endotherm. In most early studies (see Figure 2.5), the exotherm typical of α-form is concealed by the endotherm (DTA curves from Lehmann and Holland [83] are exceptions) while the exotherm is very distinct in recent studies (see Figure 2.6).

From the thermal analysis of DTA traces, Lewry and Williamson [81] also found that after grinding the α-hemihydrate, the exotherm typical of α-form shifted from around 225°C to 355°C which is characteristic of β-form. However, Bushuev and Borisov[24] pointed out that, the mechanical grinding of α-form (monoclinic $CaSO_4 \cdot 0.67H_2O$) quite possibly caused local heating of the particles and resulted in conversion to β-form (trigonal $CaSO_4 \cdot 0.5H_2O$), which seems to better explain the observed phenomena.

---

[8] The position of this exothermic peak has been found to vary considerably (about 50°C) depending upon conditions such as the mode of preparation of the samples and heating rate (Goto et al.[40]; Powell[67] and this work too, see chapter 3).

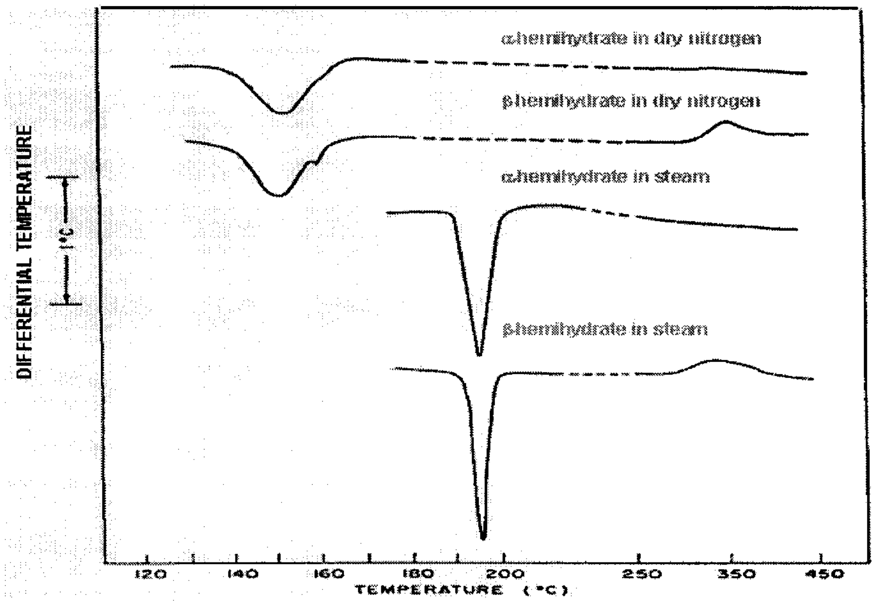

Figure 2.5: Differential thermogram of synthetic hydrates of calcium sulfate under dry nitrogen and steam (after Kuntze [82], Endotherm: Down)

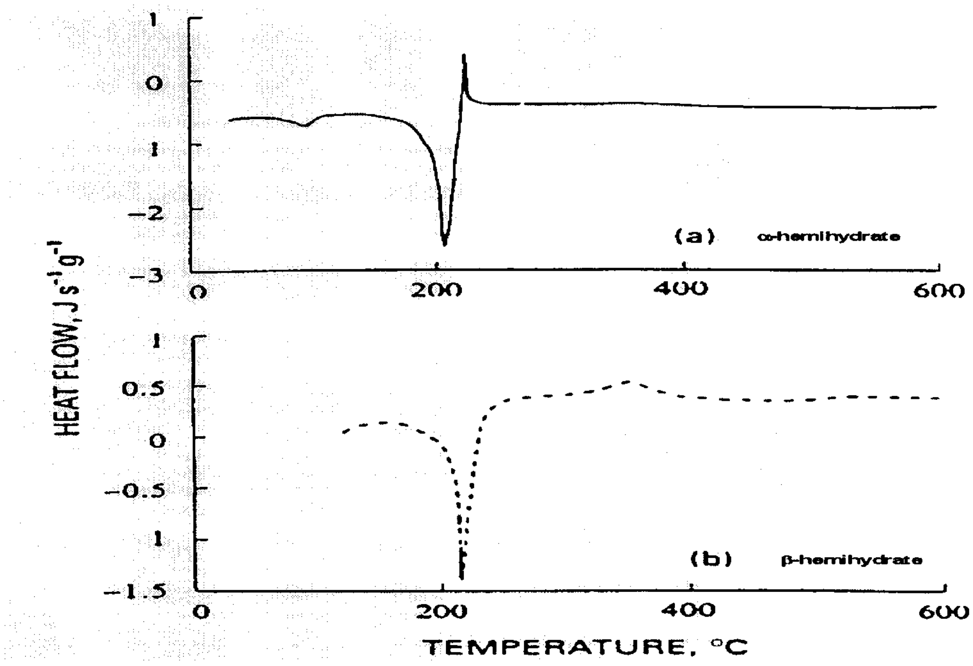

Figure 2.6: DSC traces of α- and β-hemihydrates (after Hand [4], Endotherm: Down)

Since α- and β-hemihydrates have the same crystal structure as supported by many investigators, such as Goto et al.[40], Bensted and Prakash [58], Ridge and Beretka [65], Miyazaki and Takagi [84] and Bensted and Varma [66], the observed differences between the two have to be attributed to other properties such as lattice imperfections, particle size and grain orientation. When the hemihydrate is produced at the atmospheric pressure or vacuum, the water is driven off as steam, which disrupts the crystalline structure resulting in the fragmentation of β-hemihydrate crystals. Dry decomposition leads apparently to a smaller, poorly crystalline, porous product, whereas autoclaving or hydrothermal methods result in larger, dense and well-developed crystals with fewer cracks and pores [81]. *"β forms represent active state of the α-forms."* (from Kuzel and Hauner[9] [21]). The prolongation of setting time in the case of α-plaster is ascribed to the formation of larger crystals of small specific surface area; on the other hand β-hemihydrate has a shorter setting time owing to the increase in the number of effective nuclei for the crystallization of gypsum [70].

But what is the explanation for the remarkably different behaviors upon heating between α- and β-hemihydrates? it seems that no one has given convincing explanation so far, especially if accepted that α- and β-forms have the same structure and only differ in particle size and crystal perfection. According to Lehmann and Holland [83], α-hemihydrate dehydrates to α-anhydrite III and further to anhydrite II while β-hemihydrate dehydrates first to β-anhydrite III and then to anhydrite II. The exotherm typical of α-hemihydrate associates with the conversion of α-anhydrite III to anhydrite II; and the exothermal peak characteristic of β-hemihydrate is related to β-anhydrite III to anhydrite II. A minor endothermic peak is also observed on the DSC trace in Figure 2.6. If accepted that $CaSO_4{\bullet}0.6H_2O$ corresponds to α-hemihydrate and $CaSO_4{\bullet}0.5H_2O$ corresponds to β-hemihydrate, this endotherm could be ascribed to the conversion

$$CaSO_4{\bullet}0.6H_2O_{(s)} \rightleftharpoons CaSO_4{\bullet}0.5H_2O_{(s)} + 0.1H_2O_{(g)} \qquad (2\text{-}5)$$

---

[9] Who proposed $CaSO_4{\bullet}3/6H_2O$ and $CaSO_4{\bullet}4/6H_2O$ structures for calcium sulfate hemihydrates and believed that both structures have α- and β-forms.

2.6 Industrial production and uses of α-hemihydrate

The most characteristic property of α-hemihydrate is the development of extremely high early and final strengths in pastes, mortars, concrete, dental materials [85]. Due to better workability and higher strength values than the conventional β-hemihydrate plaster, α-hemihydrate is considered to have great potential for producing large size panels for walls, bricks, ceiling boards, mortars, chemical construction products, and composites [70]; for the flooring market, i.e. flooring screeds, thin layer systems, cavity floor and false floor systems; and in the area of wall plasters, molding plasters, special binder systems for specialized concrete and other innovative applications [86].

Alpha-hemihydrate is produced industrially by the SICOWA ProMineral autoclaving process in Germany [87] which operates a plant with annual production capacity 240,000 tons. The simplified flow chart is shown in Figure 2.7. The raw material is gypsum sourced from flue-gas-desulphurization (FGD) wastes from coal-fired power generation plants.

Another method of industrial production of α-hemihydrate is the Omega process shown in Figure 2.8 [88]. Sulfur dioxide produced during the combustion of coal is captured in scrubber using a calcium-based alkaline solution. Absorbed sulfur dioxide reacts with lime or limestone and the formed calcium sulfite is thickened and the slurry is pumped to the autoclave where is mixed with some crystal habit modifiers and is oxidized with air; from this slurry, finally, α-hemihydrate is produced under properly controlled temperature and pressure conditions. According to College [88], the Eastroc plant (in USA) officially started up in 1997.

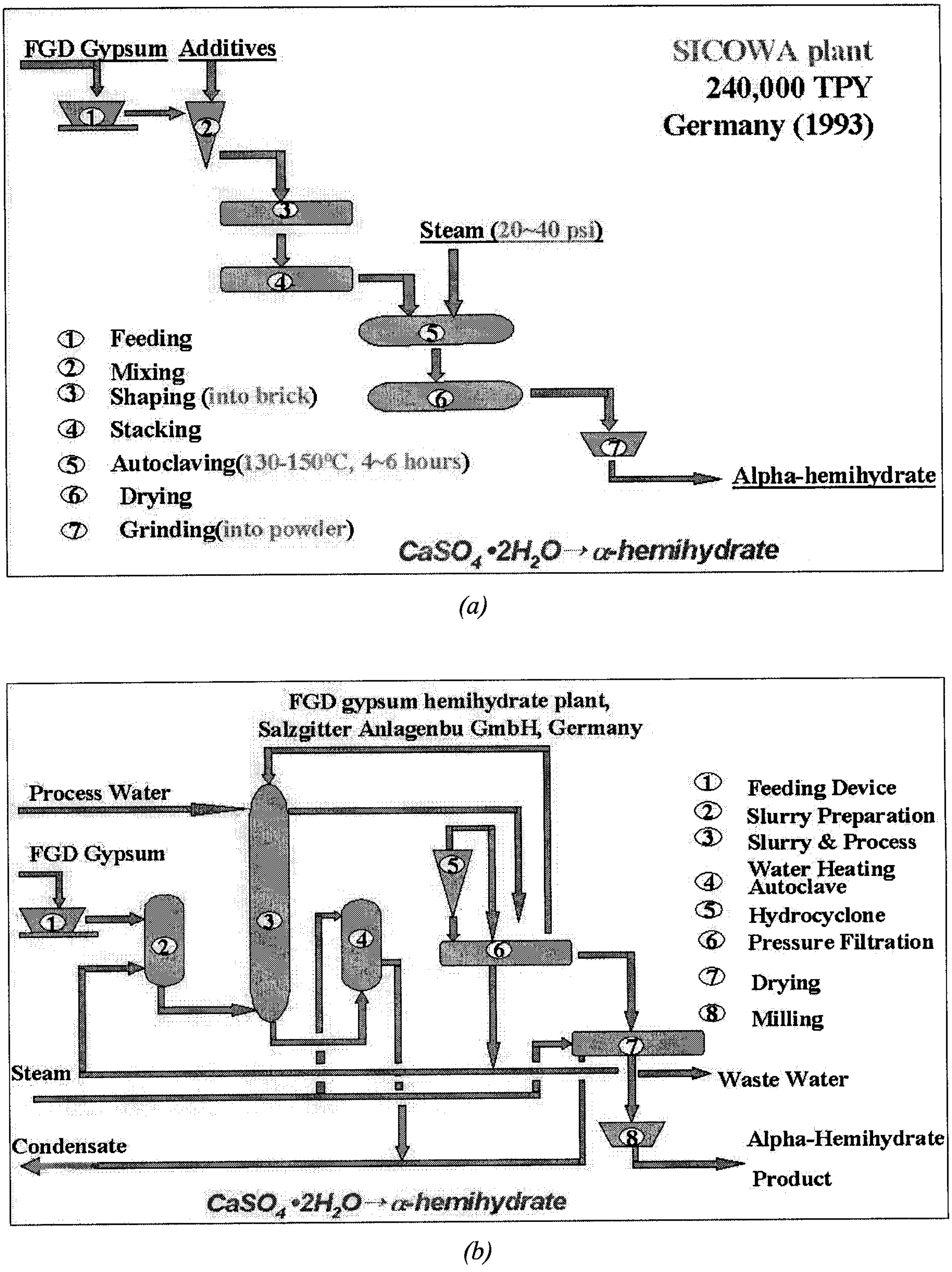

(a)

(b)

Figure 2.7: Simplified flow chart of the autoclaving production process (after Duda and Kloslowski [89])

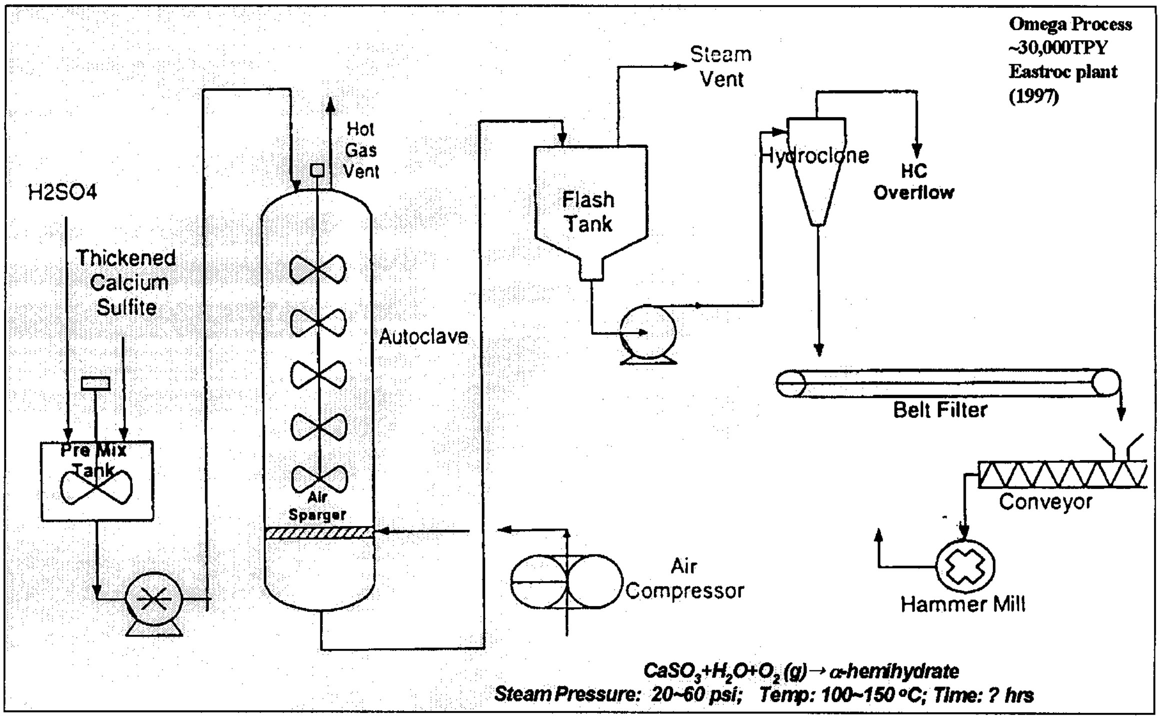

Figure 2.8: Omega process flow diagram (after College [88])

Some other processes are described mostly in forms of patents [90-95], the industrial use of which is unknown.

2.7 Summary

(1) Calcium sulfate subhydrates, $CaSO_4 \cdot nH_2O$ (with $0<n<1$) are intermediate phases between calcium sulfate dihydrate and anhydrite II (β-anhydrite or insoluble anhydrite) in the $CaSO_4$-H_2O system.

(2) The calcium sulfate subhydrates have structures with channels where water molecules may be situated. In the probable calcium sulfate subhydrate phases, monohydrate, i.e. $n=1$, with all the channels filled with water, is unknown due to "*complete steric hindrance*" (Bushuev's term).

(3) Calcium sulfate hemihydrate (with n=0.5) has a relative high stability due to the weak hydrogen bonds formed between the water molecules and the $CaSO_4$ frame.

(4) Additional tunnel positions with no bonds to the framework matrix are probably filled with water molecules. Uncertainty exists with respect to the number of water molecules in the channels.

(5) Highly loaded subhydrates other than $CaSO_4{\bullet}0.5H_2O$ structure could also exist under high local H_2O vapor pressures or in "*dehydrating solutions*" (Bushuev's term) such as solutions of nitric acid and sodium chloride.

(6) The experimental difficulties and the instability of the probable forms of calcium sulfate subhydrate may be the reasons for the introduction of different or even contradicting crystallographic studies in this field. The experimental data are strongly dependent on the analysis methods/techniques employed for the investigation, which have been extensively reviewed.

(7) Alpha and β-calcium sulfate hemihydrates cannot be distinguished from each other on the basis of crystallography or mineralogy. Thermal analysis techniques in particular DSC(or DTA), and from the application point of view physical properties such as water requirement for setting as well as the strength obtained, are used to differentiate between the two forms of hemihydrate.

(8) It seems that no one has given convincing explanation so far, if accepted that α- and β-forms have the same structure but only differ in particle size and crystal perfection, for the remarkably different thermal behavior on DTA/DSC analysis between α- and β-hemihydrates.

(9) It is clear that JCPDS-International Centre for Diffraction Data has assigned formula unit $CaSO_4{\bullet}0.6H_2O$, with hexagonal symmetry, to α-hemihydrate and $CaSO_4{\bullet}0.5H_2O$, also with hexagonal symmetry, to β-hemihydrate despite that

quite a few authors consider α-hemihydrate to be better-crystallized than β-hemihydrate but to have the same formula with the latter, i.e., $CaSO_4 \bullet 0.5H_2O$.

(10) Generally, there are three ways to prepare α-calcium sulfate hemihydrate – using as starting materials calcium sulfate dihydrate (most of the cases) or calcium sulfite. They are: (i) autoclaving process; (ii) oxidation process; and (iii) and hydrothermal (or solution) process. The first two are the only ones practiced on large industrial scale.

References

[1] Lehmann, H., Die Phasenbeziehungen im System $CaSO_4$-H_2O, Tonindustrie-Zeitung und Keramische Rundschau, 91(1), 6-12(1967) (in German).

[2] Abriel, W., Reisdorf, K. and Pannetier, J., Dehydration reactions of gypsum: A neutron and X-ray diffraction study, J. Solid State Chem., 85(1), 23-30(1990).

[3] Kojima, Y., Shibano, K. and Yasue, T., Wet synthesis of α-gypsum hemihydrate from II-anhydrite under atmospheric pressure, Muki Materiaru, 2(255), 84-93(1995) (in Japanese).

[4] Hand, R.J., Calcium sulphate hydrates: a review, British Ceramic Transactions, 96(3), 116-120(1997).

[5] Pedersen, B. F. and Semmingsen, D., Neutron diffraction refinement of the structure of gypsum, $CaSO_4{\bullet}2H_2O$, Acta Crystallographica, Section B: Structural Crystallography and Crystal Chemistry, B38(4), 1074-1077(1982).

[6] Kirfel, A. and Will, G., Charge density in anhydrite, calcium sulfate, from x-ray and neutron diffraction measurements, Acta Crystallographica, Section B: Structural Crystallography and Crystal Chemistry, B36(12), 2881-2890(1980).

[7] Hammond, C., The Basics of Crystallography and Diffraction, 2nd edition, Oxford University Press: New York, NY, USA, 69(2001).

[8] Deer, W. A., Howie, R.A. and Zussnman, J., Gypsum, Rock Forming Minerals, Wiley: New York, NY, USA, 202-218(1962).

[9] Deer, W. A., Howie, R.A. and Zussnman, J., Gypsum, Rock Forming Minerals, Wiley: New York, NY, USA, 612-619(1992).

[10] Hurlbut, C.S. and Sharp, W.E., Dana's Minerals and How to Study Them, 4th ed., John Wiley & Sons Inc.: New York, NY, USA , 22-223, 225-227(1998).

[11] Gardet, J. J., Guilhot, B. and Soustelle, M., Hydrated forms of calcium sulfate, Bull. Soc. Chim. Fr., (10), 3377-3382(1970)(in French).

[12] Davis, B.L. and Walawender, M.J., X-ray observation of chemical and polymorphic equilibria under hydrostatic pressures, J. Phys. Chem. Solids, 29, 1177-1189(1968).

[13] Frik, M. and Kuzel, H. J., Röntgenographische und thermoanalytische Untersuchungen an calciumsulfat-halbhydrat, Fortschritte der Mineralogie, 60, 80-81(1982)(in German).

[14] Caspari, W.A., Calcium Sulfate hemihydrate and the anhydrites, I-Crystallography, Prod. Roy. Soc. London: London, UK, A155, 41-48(1936).

[15] Lager, G.A., Armbruster, T., Rorella, F.J., Jorgensen, J.D. and Hinks, D.G., A crystallographic study of the low-temperature dehydration products of gypsum, $CaSO_4{\bullet}2H_2O$, hemihydrate $CaSO_4{\bullet}0.5H_2O$, and γ-$CaSO_4$, American Mineralogist, 69(9-10), 910-919(1984).

[16] Ostrowski, C., Study of the structure of a-$CaSO_4{\bullet}0.5H_2O$, Cement and Concrete Research, 25(5), 945-947(1995).

[17] Bezou, C., Buisson, L., Mutin, J. C., and Nonat, A., Chemical and radiocrystallographical identification of two subhydrated modifications of calcium sulfate: $CaSO_4{\bullet}0.5H_2O$ and $CaSO_4{\bullet}0.6H_2O$, Comptes Rendus de l'Academie des Sciences, Serie II: Mecanique, Physique, Chimie, Sciences de la Terre et de l'Univers, 311(13), 1493-1498(1990)(in French).

[18] Bezou, C., Mutin, J.C. and Nonat, A., Identification des phases sous-hydratées du sulfate de calcium, J. Chim. Phys., 87(7-8), 1257-1284(1990)(in French).

[19] Bezou, C., Noerlung Christensen, A.; Cox, D., Lehmann, M., Nonat, A., Crystal structures of calcium sulfate hydrates ($CaSO_4{\bullet}0.5H_2O$ and $CaSO_4{\bullet}0.6H_2O$), Comptes Rendus de l'Academie des Sciences, Serie II: Mecanique, Physique, Chimie, Sciences de la Terre et de l'Univers, 312(1),43-48(1991)(in French).

[20] Bezou, C., Nonat, A., Mutin, J.C., Noerlund Christensen, A. and Lehmann, M. S., Investigation of the crystal structure of γ-$CaSO_4$, $CaSO_4{\bullet}0.5H_2O$ and $CaSO_4{\bullet}0.6H_2O$ by powder diffraction methods, J. Solid State Chem., 117(1), 165-176(1995).

[21] Kuzel, H.J. and Hauner, M., Chemical and crystallographic properties of calcium sulfate hemihydrate and anhydite III, Zement-Kalk-Gips, B40(12), 628-632(1987) (in German).

[22] Bushuev, N.N., Structural features of $CaSO_4$ hemihydrate ($CaSO4 \cdot 0.5H_2O$) and calcium sulfate hydrate ($CaSO_4 \cdot 0.67H_2O$), Dokl. Akad. Nauk SSSR, 255(5), 1104-1109(1980) (in Russian).

[23] Bushuev, N.N. and Borisov, V.M., X-ray diffraction investigation of $CaSO_4 \cdot 0.67H_2O$, Russian J. Inorganic Chem., 27(3), 604-609(1982) (English translation).

[24] Bushuev, N.N., Water of crystallization in the $CaSO_4 \cdot 0.67H_2O$ and $CaSO_4 \cdot 0.5H_2O$ structures, Russian J. Inorganic Chem., 27(3), 610-615(1982) (English translation).

[25] Bushuev, N.N., Maslennikov, B.M. and Borisov, V.M., Phase transformations in dehydration of $CaSO_4 \cdot 2H_2O$, Russian J. Inorganic Chem., 28(10), 1404-1407(1983) (English translation).

[26] Abriel, W., Calcium sulfate subhydrate, $CaSO_4 \cdot 0.8H_2O$, Acta Crystallographica, Section C: Crystal Structure Communications, C39(8), 956-958(1983).

[27] Abriel, W., and Nesper, R., Determination of the crystal structure of calcium sulfate hemihydrate by X-ray diffraction and potential-profile calculation, Z. Kristallogr., 205(1), 99-113(1993).

[28] Gallitelli, P., Richerche sul solfato di calcio semidrato sull' anidrite solubie, Periodico Mineral Roma, 4, 1-42(1933) (in Italian).

[29] Flörke, O.W., Kristallographische und Röntgenographische Untersuchungen im system, $CaSO_4$-$CaSO_4 \cdot 2H_2O$, Neues Jahrb. Min., Abh., 84, 189-240(1952) (in German).

[30] Gay, P., Some crystallographic studies in the system $CaSO_4$-$CaSO_4 \cdot 2H_2O$. Part II. The hydrous forms, Mineralogical Magazine, 35, 347-353(1965).

[31] Teimurov, G.S., Mustafaev, N. M., Chiragov, M.I. and Mamedov, K. S., Crystal-chemical characteristics of the conversion of calcium sulfate dihydrate to gypsum hemihydrate, Neorganicheskie Materialy, 15, 1489-1491(1979) (English translation).

[32] Cole, W.E. and Lancucki, C.J., A refinement of the crystal structure of gypsum $CaSO_4 \cdot 2H_2O$, Acta Cryst., Section B, Structural Crystallography and Crystal Chemistry, B30, 921-929(1974).

[33] Weiser, H.B., Milligan, W.O. and Eckholm, W.C., The mechanism of the dehydration of calcium sulfate hemihydrate, J. American Chem. Soc., 58, 1261-1265(1936).

[34] Bushuev, N.N., Frolova, N.G., Nosov, V.N. and Karmyshov, V.F., Characteristic structural features of the α- and β-modifications of $CaSO_4{\bullet}0.5H_2O$, Russian J. Inorganic Chem., 23(12), 1767-1777(1978) (English translation).

[35] Badens, E., Llewellyn, P., Fulconis, J. M., Jourdan, C., Veesler, S., Boistelle, R. and Rouquerol, F., Study of gypsum dehydration by controlled transformation rate thermal analysis (CRTA), J. Solid State Chem., 139(1), 37-44(1998).

[36] van't Hoff, J. H., Armstrong, E. F., Himichen, W., Weigert, F. and Just, G., Gips und Anhydrite, Z. Phys. Chem., 45, 257 (1903) (in German).

[37] Rinaudo, C. and Boistelle, R., Gypsum grown under pressure from dense suspension of $CaSO_4{\bullet}0.67H_2O$, J. Applied Crystallography, 24(2), 129-134(1991).

[38] Hanawalt, J.D., Rinn, H.W. and Frevel, L.K., Chemical analysis by x-ray diffraction. Classification and use of x-ray diffraction patterns, Ind. Eng. Chem., Anal. Ed., 10, 457-512(1938).

[39] Posnjak, E., The system calcium sulfate-water, American J. Science, 35-A, 247-272(1938).

[40] Goto, M., Molony, B., Ridge, M.J. and West, W.G., The forms of calcium sulfate hemihydrate, Australian J. Chem., 19(2), 313-316(1966).

[41] Saito, T., Observation on the process of dehydration and re-hydration of gypsum by means of proton magnetic resonance, Bull. Chem. Soc. Japan, 34, 1454-1457(1961) (in Japanese).

[42] Putnis, A., Winkler, B. and Fernandez-Diaz, L., In situ IR spectroscopic and thermogravimetric study of the dehydration of gypsum, Mineralogical Magazine, 54, 123-128(1990).

[43] Bushuev, N.N., Protasova, V.I., Kharchenko, L., Yu, L., Grankin, A. I., Bochkarev, G. S. and Borisov, V. M., Hydrothermal synthesis of single crystals of calcium sulfate hemihydrate, Zh. Neorg. Khim., 26(10), 2861-2863(1981) (English translation).

[44] Pawley, G.S., Unit cell refinement from powder diffraction scans, J. Applied Crystallography, 14, 357-361(1981).

[45] Reitveld, H.M., Profile refinement method for nuclear and magnetic structures, J. Applied Crystallography, 2, 65-71(1969).

[46] CrysFire Software, http://www.ccp14.ac.uk/tutorial/crys/index.html.

[47] McConnell, J.D.C., Astill, D.M. and Hall, P.L., The pressure dependence of the dehydration of gypsum to bassanite, Mineralogical Magazine, 51, 453-457(1987)

[48] Turk, D.H. and Bounini, L., The effect of sorbed water on the determination of phase composition of $CaSO_4$-H_2O systems by various methods, The chemistry and technology of gypsum, ASTM STP 861, Kuntze, R.A., Ed., American Society for Testing and Materials: Philadelphia, PA, USA, 48-56(1984).

[49] Blazek, A., Thermal Analysis, Van Nostrand Reinhold: New York, NY, USA, 25(1972).

[50] Duval, C., Inorganic Thermogravimetric Analysis, Elsevier: Amsterdam, Netherlands, 152(1953).

[51] Reisdorf, K. and Abriel, W., Reactions in the system calcium sulfate-water and on sodium-polyhalite $Na_2Ca_5(SO_4)_6(H_2O)_3$, Neues Jahrbuch fuer Mineralogie, Abhandlungen, 157(1), 35-46(1987)(in German).

[52] Blaine, R., Dunn, J., Patel, J. and Sills, I., The TGA Hotline, 1, 2(1996).

[53] Kelley, K.K., Southard, J.C. and Anderson, C.F., Thermodynamic properties of gypsum and its dehydration products, U.S. Bur. Mines, Tech. Paper, No 625(1941).

[54] Kuntze, R.A., Differential thermal analysis of calcium sulfate dihydrate, Nature, 193, 772-773(1962).

[55] Fleck, W.E.P., Jones, M.H., Kuntze, R.A. and McAdie, H.G., The differential thermal analysis of natural and synthetic hydrates of calcium sulfate, Canadian J. Chem., 38, 936-943(1960).

[56] McAdie, H.G., The effect of water vapor upon the dehydration of $CaSO_4 \cdot 2H_2O$, Canadian J. Chem., 42, 792-801(1964).

[57] Lager, G.A., Armbruster, T., Rorella, F.J., Jorgensen, J.D. and Hinks, D.G., Neutron powder studies in the system $CaSO_4$-H_2O, Zeitschrift fur Kristallographie, 162, 160-161(1983) (in German).

[58] Bensted, J. and Prakash, S., Investigation of the calcium sulfate-water system by infrared spectroscopy, Nature, 219, 60-61(1968).

[59] Seidl, V., Knop, O. and Falk, M., Infrared studies of water in the crystalline hydrates: $CaSO_4 \bullet 2H_2O$, Canadian J. Chem., 47(8), 1361-1368(1969).

[60] Green, G.W., Gypsum analysis with the polarizing microscope, The Chemistry and technology of gypsum, ASTM STP 861, Kuntze, R.A., Ed., American Society for Testing and Materials: Philadelphia, PA, USA, 22-47(1984).

[61] Barriac, P., Mural, M. and Chevreton, M., Optical microscopic and x-ray crystallographic study of calcium sulfate hemihydrate, Bull. Soc. Fr. Mineral. Cristallogr., 92(3), 284-288(1969) (in French).

[62] Molony, B., Beretka, J. and Ridge, M.J., Observations of the texture of the products of the dehydration of calcium sulfate dihydrate, Australian J. Chem., 24, 449-456(1971).

[63] Yasue, T., Kojima, Y., Kishimoto, Y. and Arai, Y., Preparation of *a*-gypsum hemihydrate and control of its crystal shape under atmospheric pressure, Gypsum & Lime, 239, 230-238(1992) (in Japanese).

[64] Ling, Y., Demopoulos, G. P., Giove, A. and Filippou, D., Technical evaluation and characterization of alpha calcium sulphate materials, Gypsum and Fly Ash 2002, 7th international science and technology conference and short course, Toronto, June 2-4, [Proceeding], Process Research ORTECH Inc.: Mississauga, Ontario, Canada, 6, 1-14(2002).

[65] Ridge, M.J. and Beretka, J., Calcium sulfate hemihydrate and its hydration, Rev. Pure and Applied Chem., 19, 17-44(1969).

[66] Bensted, J. and Varma, S.P., Investigation of the α- and β-forms of calcium sulfate hemihydrate, Cement Technology, March/April, 67-70(1972).

[67] Powell, D.A., Transformation of the α- and β-forms of calcium sulfate hemihydrate into insoluble anhydrite, Nature, 182, 792(1958).

[68] Combe, E.C. and Smith, D.C., Studies on the preparation of calcium sulfate hemihydrate by an autoclave process, J. Applied Chem., 18, 307-312(1968).

[69] Forster, H.J., Production of α-hemihydrate from by-product gypsum, Chemie Ingenieur Technik, 44, 969-972(1972)(in German).

[70] Singh, M. and Rai, M., Autoclaved gypsum plaster from selenite and by-product phosphogypsum, J. Chem. Tech. Biotechnology, 43, 1-12(1988).

[71] Offutt, J.S. and Sekiya, M., Preparation of gypsum plaster by the special hydrothermal method, J. Japan Ceram. Soc. Assocn., 56, 43-47(1947) (in Japanese).

[72] Eipeiltauer, E., Significance of calorimetric measurements for the manufacture and testing of gypsum, Zement-Kalk-Gips, 9, 501-505(1956) (in German).

[73] Powell, D.A., Calcium sulfate hemihydrate prepared in sodium chloride solution, Australian J. Chem., 15, 868-874(1962).

[74] Lee, K.J. and Choi, S.H., Effect of salt on the formation of α-calcium sulfate hemihydrate from by-product gypsum of the phosphoric acid process under hydrothermal conditions, Yongu Pogo – Kungnip Kongop Sihomwon, 37, 164-173(1987) (in Korean).

[75] Lee, K.J. and Lee, K.W., Study of the preparation of α-calcium sulfate hemihydrate under the pressure of water vapor at atmospheric pressure, Yongu Pogo – Kungnip Kongop Sihomwon, 38, 184-188(1988) (in Korean).

[76] Yue, W. and Wang, Z., Investigation on the mechanism of crystal shape modifying agent of α-hemihydrate, Wuhan Gongye Daxue Xuebao, 18(2), 1-4 (1996) (in Chinese).

[77] College, J.W., Sulfur dioxide removal from sulfur dioxide-containing hot gaseous streams under formation of α-hemihydrate gypsum, USA Patent, US 5,312,609 (1994).

[78] Khalil, A.A. and Gad, G.M., Gypsum plasters: I. Preparation of β-hemihydrates, J. Appl. Chem. Biotechnol., 22, 697-701(1972).

[79] Coburn, A., Dudley, E. and Spence, R., Gypsum Plaster: Its Manufacture and Use, Intermediate Technology Publications: London, UK, 48(1989).

[80] Morris, R.J., X-ray diffraction identification of alpha- and beta-forms of calcium sulfate hemihydrate, Nature, 198, 1298-1299(1963).

[81] Lewry, A.J. and Williamson, J., The setting of gypsum plaster, Part I, The hydration of calcium sulfate hemihydrate, J. Mater. Sci., 5279-5284 (1994).

[82] Kuntze, R.A., Effect of water vapor on the formation of $CaSO_4 \cdot 1/2H_2O$ modifications, Canadian J. Chem., 43, 2522-2529(1965).

[83] Lehmann, H. and Holland, H., Processes of transformation of gypsum and its dehydration products by heating, Tonindustrie-Zeitung und Keramische Rundschau, 90(1), 2-20(1966) (in German).

[84] Miyazaki, H. and Takagi, N., Difference between α and β forms of calcium sulfate hemihydrate, Kogyo Kagaku Zasshi, 73(8), 1766-1769(1970) (in Japanese).

[85] Kazimir, J., Strength of hemihydrate plaster, Tonind-Ztg, 91, 22-25(1967) (in German).

[86] Kwasny-Echterhagen, R., Schlieper, H., Kirchen, G., Morgenroth, H. and Wiesgickl, G., Alpha-hemihydrate - a high value building material made from FGD gypsum, experiences concerning processing, product development and market applications, FGD and Synthetic Gypsum, International Conference, 5th, Toronto, May 11-14, [Proceedings], Process Research ORTECH Inc. : Mississauga, Ontario, Canada, 8, 1-15(1997).

[87] Engert, H.J. and Koslowski, T., New gypsum binder Alpha 2000, ZKG International, 51(4), 229-237(1998).

[88] College, J.W., The Omega process, Gypsum 2000, 6th on Natural and FGD Gypsum, International Conference, 6th, Toronto, May 16-19, [Proceeding], Process Research ORTECH Inc.: Mississauga, Ontario, Canada, 25, 1-11(2000).

[89] Duda, A. and Koslowski, T., New Products from FGD Gypsum, VGB Kraftwerkstechnik, 11, 938-943(1991) (in German).

[90] Clementi, F., Achenbach, G. and Alscher, N., Manufacture of α-gypsum from dihydrate-based wastes, the α-hemihydrate, and mortar compositions containing the converted waste, Germany Patent, DE 3,711,367(1988) (in German).

[91] Kudo, Y., Preparation of α-calcium sulfate hemihydrate, Japan Patent, JP 01,014,112(1989) (in Japanese).

[92] Inoe, K. and Onizuka, M., Manufacture of α-type plaster of Paris with uniform particle size, Japan Patent, JP 05,132,344(1993) (in Japanese).

[93] Yoshino, T., Shiraishi, T. and Shinozaki, T., Modification of by-product α-gypsum hemihydrate obtained in wet phosphoric acid manufacture, Japan Patent, JP 08,025,320(1996) (in Japanese).

[94] Hina, A. and Nancollas, G.H., Alpha calcium sulfate hemihydrate and a method of making alpha calcium sulfate hemihydrate, International Patent, WO 0,179,116(2001).

[95] Robinson, M.C., Kirk, D.W. and Hummel, R.L., Manufacture of hydrogen or electric power and calcium sulfate hemihydrate from calcium sulfite, International Patent, WO 9,118,131(1991).

Chapter 3

Experimental Techniques and Characterization Methods

3.1 Introduction

The major experimental components of this work comprised: (i) investigation of dihydrate → hemihydrate transformation, solubility and crystallization - this part of work, which is described in chapter 4, served as foundation for the other parts of research; (ii) investigation of different procedures to initiate the reaction between lime and sulfuric acid - there were two procedures investigated: (1) addition of lime to sulfuric acid solution and (2) addition of sulfuric acid to lime (dry or slaked) described in chapter 6; and (iii) investigation of the role of additives (crystal habit modifiers) and seeding/product recycling – this part of work is described in chapter 7. Specialized experimental methods followed during the conduct of these investigations are described in the respective chapters. In the present chapter some common experimental features are outlined only. Among the features described here are universally-used materials, equipment, analytical and characterization methods, and finally determination of post-reaction treatment procedures.

3.2 Materials

All of the chemicals were of A.C.S. reagent grade. Calcium sulfate dihydrate, $CaSO_4{\bullet}2H_2O$ (Cat. No 10101-41-4), calcium oxide, CaO (Cat. No 1305-78-8), were obtained from A & C American Chemicals; calcium sulfate hemihydrate (Plaster of Paris or β-hemihydrate), $CaSO_4{\bullet}0.5H_2O$ (Cat. No 138-10), sulfuric acid 12N (Cat. No LC25880-3), 2-propanol, $(CH_3)_2CHOH$ (Cat No. A416-20) with assay >99.5% and water < 0.20%, were from Fisher Scientific.

Samples of the α-hemihydrate reagent are not available from chemical vendors, instead they were obtained directly from the gypsum industry, marked as "ProMineral" and "Omega" respectively: (1) "ProMineral" was from ProMineral company in Germany and manufactured with the SICOWA-ProMineral autoclaving process[1]; and (2) "Omega" was produced with the Omega process[2] at Eastroc in the USA - the manufacturing plant is owned by one of the gypsum industry leaders, British Plaster Board (BPB). All the water used in this work was deionized water (except otherwise specified) treated with Cole-Parmer Ion-X-Changer Filter Cartridges. By combining one Universal cartridge (producing water equivalent to single-distilled water) and one Research cartridge (producing water ionically equivalent to triple-distilled water) in series, high quality water with a resisitivity of 15 MΩ-cm or greater (conductivity < 0.1 $\mu S\ cm^{-1}$) was obtained.

3.3 Equipment

Generally, the experiments consisted of three stages: (i) reaction stage; (ii) post-reaction treatment and (iii) characterization of the prepared samples. Here, characterization is viewed as an integrated component of the experimental procedure. Thus, the equipment used for characterization is also included in this part.

Reactor and filtration apparatus

A schematic illustration of the preparation set-up, which consisted of (i) reactor and (ii) filtration and washing unit, is shown in Figure 3.1. The reaction was carried out in a 2L Applikon autoclavable glass reactor under carefully monitored and controlled conditions. Heating was provided with the circulating oil, which was maintained hot with a Cole-Parmer bath and circulator. To avoid corrosion and, consequently, contamination, the agitation unit was redesigned: the shaft was made of glass, and the impeller was made of Teflon. Upon completion of the reaction, the hot slurry was transferred to the filtration/washing unit. The transferring tube (made of Teflon) was preheated to keep the temperature at desired level (e.g., 100±1°C). In some cases, the slurry was poured directly into the filtration/washing unit without pumping. Filtration was done while slurry was hot (temperature was maintained by using a double-walled filter funnel heated with circulating oil). When necessary the temperature of the filtrate was controlled with the aid of heating tape placed around the lower part of filtration conical flask.

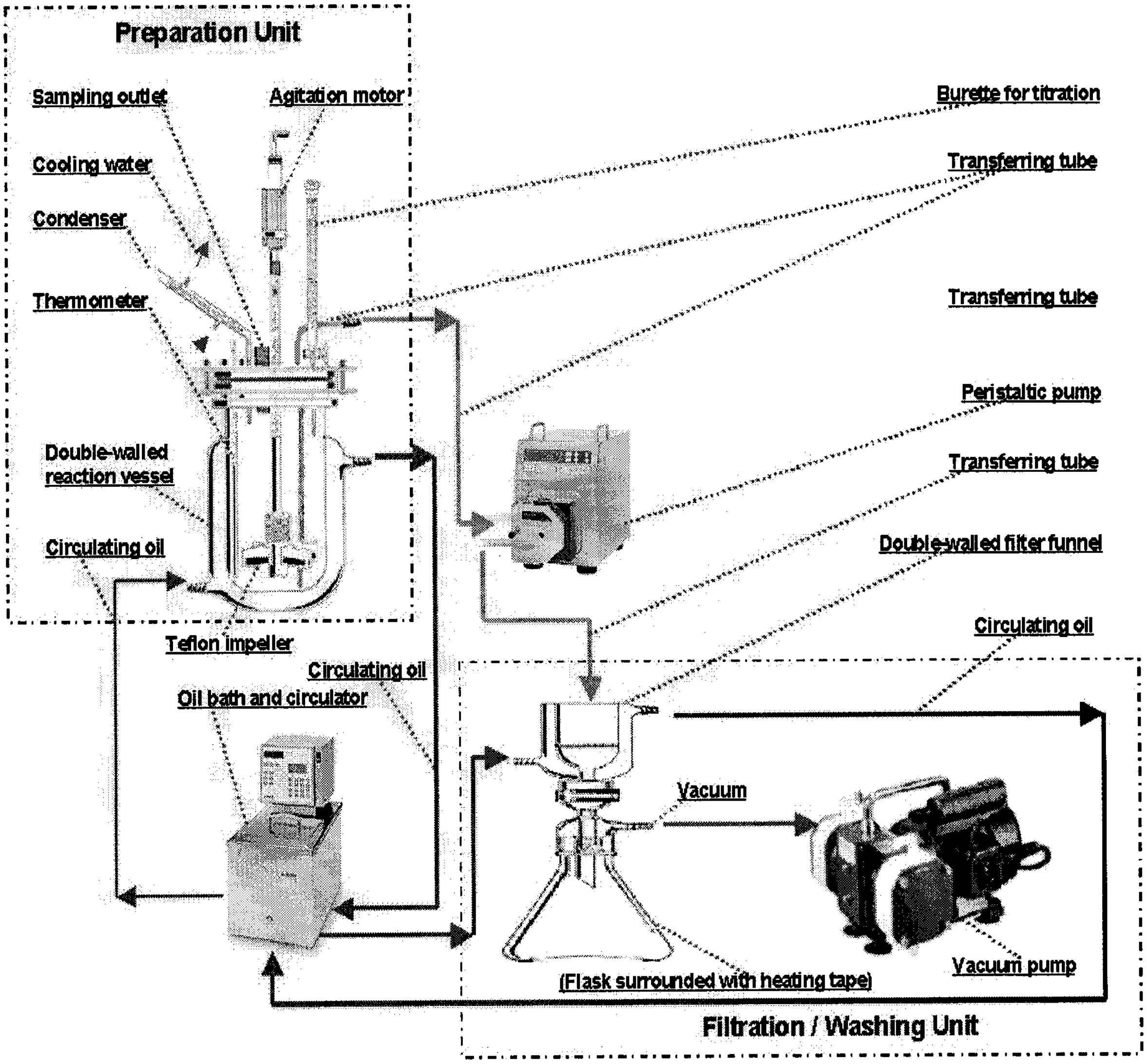

Figure 3.1: Schematic of experimental set-up for preparation of α-hemihydrate consisting of preparation unit (top) and filtration/washing unit(bottom)

Oven

Temperature control is very crucial either for successful preparation or characterization of the experimental samples. The reason is that: the conversion between calcium sulfate hemihydrate and dihydrate can very readily take place in the ordinary working temperature range (from room temperature to around 120°C), thus rendering subsequent characterization totally unreliable. Thus selecting an oven with precise temperature control is crucial. In this work, the Despatch Oven from MagneTek Inc. was used for all of sample drying. Temperature can be controlled with this oven at less than 0.5°C. A separate thermometer was also employed for the sake of accurate reading.

X-ray diffraction analysis

X-ray diffraction analysis (XRD) was performed on a Philips PW1710 X-ray diffractometer with x-ray generator from American Instruments Inc. Normal operating parameters were as following: the X-ray source was Cu-Kα; the scanning was controlled at start angle $2\theta = 10^\circ$, end angle $2\theta = 110^\circ$, step intervals $2\theta = 0.02^\circ$ per 0.5 second. Since, for most of the samples, there are only some trivial peaks beyond $2\theta = 80^\circ$, fast scanning was normally performed in the 2θ range from 10° to 80°. In certain cases, smaller-step continuous scanning was used as well for better resolution/accuracy.

Differential scanning calorimetry

Differential thermal analysis (DTA) is the measurement of the difference in temperature between a sample and a reference as heat is applied to the system. Differential scanning calorimetry (DSC) on the other hand measures independently the rate of heat flow to a sample and a standard that are at the same temperature. Data is taken by monitoring the differential heat flow as a function of temperature. Basically, both DTA and DSC methods are sensitive to endothermic and exothermic processes such as: phase transitions, dehydration, and decomposition, redox, or solid-state reactions. But DSC has the added capability to measure heat capacities. Hence DSC rather than DTA was chosen in this work. DSC analysis was done on a PerkinElmer PYRIS differential scanning calorimeter (analysis work was done in the Polymer Laboratory of the Department of Chemical Engineering at McGill University), which was coupled with high precision Sartorius MC5 micro balance with motorized draft shield and readability of 0.1μg (0.0001 mg).

Scanning electron microscopy

Scanning electron microscopy (SEM) has become an indispensable tool for morphological observation. SEM, in this work, basically was performed on a JEOL-840A SEM, which was equipped with energy dispersive X-ray spectrometer (EDS) and digital imaging system. The samples were exposed to high vacuum. All of the powder samples, in this work, are not electrically conductive. These samples have traditionally required pretreatment, by coating with a conductive film, before SEM examination. Nonconductive samples are subject to a buildup of electrons on the examined surface. This buildup of electrons, or "charging" eventually causes scattering of the incoming electron beam, which interferes with imaging and analysis. The samples were coated in general with carbon, but in certain cases they were coated with gold for better image mapping, analysis of the latter samples was done in the Microanalysis Laboratory of the Department of Earth and Planetary Sciences at McGill University. For most of the morphology analysis, 15.0kV acceleration potential was applied. EDS can provide some quick chemical analysis, which is primarily for qualitative identification of elemental occurrence. The detection capability, however, is poor because the EDS detectors produce poor energy resolutions (around 130eV). It usually has a relative error between 5% and 10%. For chemical analysis beyond the detection limit of EDS, especially when the influence of additives was studied, an electron probe microanalyser (EPMA) was used. The EPMA is designed specifically for X-ray microanalysis using wavelength dispersive spectrometers (WDS). The main advantage of WDS over EDS is that the characteristic peaks are much sharper so that peak overlap is avoided and the chance of loosing trace elements is reduced. It produces better energy resolution between 5 and 20eV. Elements present in concentrations of below 0.10 weight % generally can be detected with relative error ~0.5%, and elements present in smaller concentrations can be measured with somewhat less precision. For certain elements, the sensitivity can go down to the *ppm* level.

3.4 Evaluation of the characterization methods

3.4.1 Use of XRD

As mentioned in the literature review, JCPDS---International Center for Diffraction Data, does have cards for α- and β-hemihydrate, namely, 43-0605 and 45-0848 respectively (shown in Figure 3.2). However, the actual XRD scanning of the commercial or laboratory-made α- and β- hemihydrate powders, results in patterns in which the peaks are in identical positions as shown in Figure 3.3 except that, the intensity of the peaks is higher for α-hemihydrate than for β-hemihydrate. It is clear that XRD alone is not enough to distinguish between α- and β-hemihydrates.

XRD, however, is effective in distinguishing among the various phases of calcium sulfate, i.e., hemihydrate (HH), dihydrate (DH) and anhydrite (AH). Thus XRD was used regularly throughout this work. Since in the experiments described later, dihydrate acts either as starting or intermediate material during the preparation of α-hemihydrate, the detection limits of XRD vis-à-vis hemihydrate and dihydrate have to be determined. To this end, artificial mixtures of hemihydrate (Omega) and dihydrate were prepared according to two groups: In the first group, hemihydrate was the majority phase with dihydrate making 1%DH, 2%DH, 3%DH, 4%DH or 5%DH of the whole mixture. As an example, to prepare, say 1%DH, weighed 1g DH and 99g α-HH (Omega), then mixed in a closed container and shaken with a mechanical shaker for 24 hours followed by 3 hour ultrasonic oscillation. In the second group, dihydrate was the majority phase with hemihydrate making 1%HH, 2%HH, 3%HH, 4%HH or 5%HH of the mixture. The preparation procedure was the same except that, this time, say 1%HH, 99g dihydrate was mixed with 1g α-HH (Omega material).

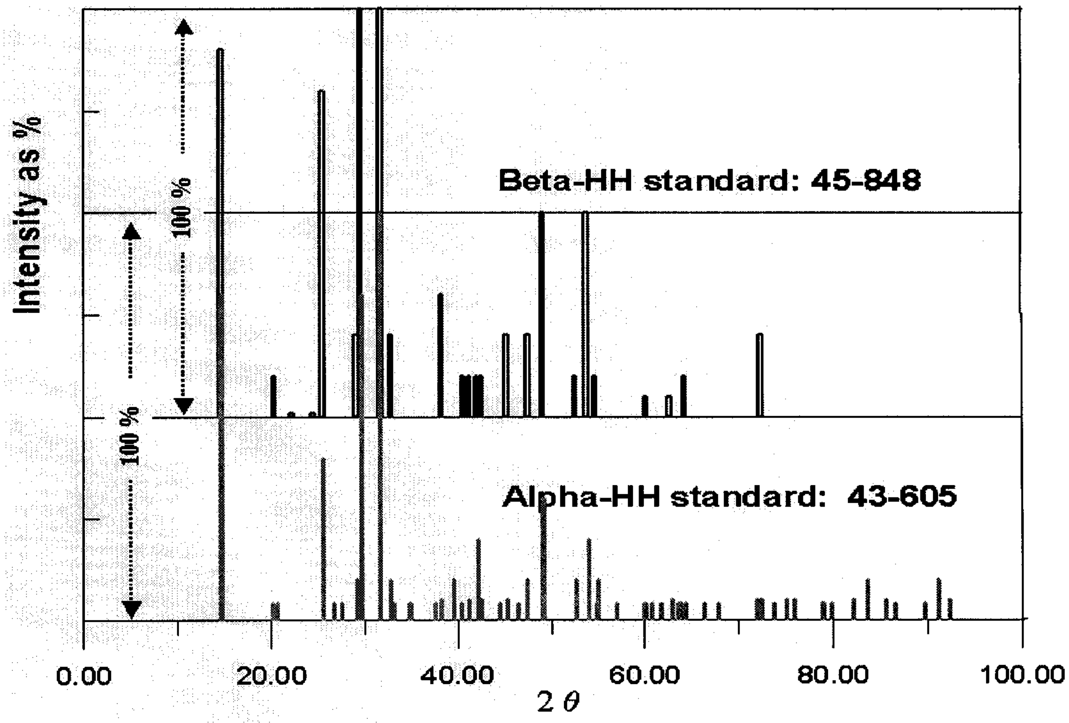

Figure 3.2: XRD standard patterns for α- and β-hemihydrates from JCPDS - International Center for Diffraction Data (the highest peak in each standard pattern referred as 100%)

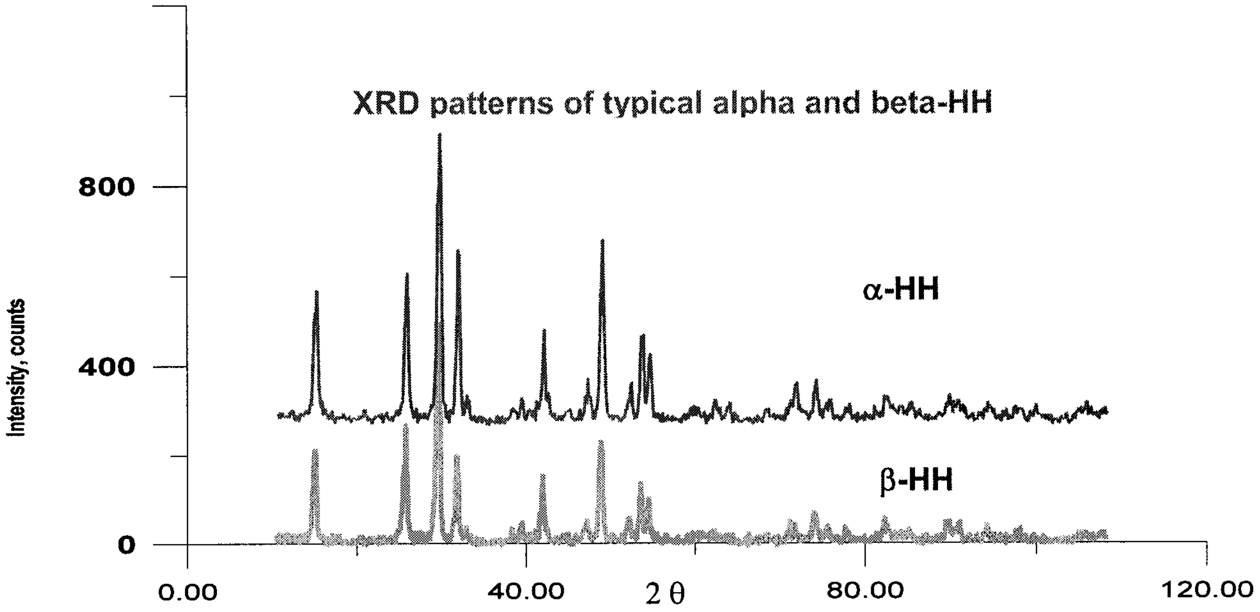

Figure 3.3: Comparison of XRD patterns of typical α- and β-hemihydrates (Sources: α-HH: Omega; and β-HH: Fisher Scientific)

The obtained XRD results are shown in Figures 3.4 and 3.5. The detection limits for both dihydrate and hemihydrate were determined to be about 1 weight %. The actual detection limit could be even a little bit lower, but 1 weight % is an acceptable approximation. Given the fact that the peaks in the 2θ range from 20 to 40 is densely populated or overlapped to each other, even though some peaks at some positions, e.g., 2θ ~32.81 for dihydrate (corresponding to (200) plane), 2θ ~25.6 (corresponding to plane (220)) and 2 θ ~29.7 (corresponding to plane (400)) for hemihydrate are quite pronounced, they are not chosen as the "*characteristic*" peaks; instead, 2θ ~11.57 (corresponding to (020), interplanar distance 7.6 Å) for dihydrate and 2θ ~14.7 (corresponding to (200) plane, interplanar distance 6.0 Å) for hemihydrate are accepted as the "first glance" detection indicator to ascertain the existence of the corresponding calcium sulfate phase, especially at very low percentage content.

3.4.2 Sensitivity of the DSC method

DSC was chosen in this work to distinguish α-hemihydrate from β-hemihydrate. The sensitivity of the DSC method on hemihydrate, however, is not known (this topic has never been reported in the literature, instead, quantitative analysis of the artificial mixtures of α- and β-hemihydrates under high pressure DTA has been done only by Amita et al. [3]), hence a series of tests was done using different amounts of either "pure" α-hemihydrate (Omega), or "pure" β-hemihydrate materials or mixtures of them. Artificial mixtures of α- and β-hemihydrates at 0.1%, 0.25%, 0.5%, 1%, 2%, 3%, 4%, 5% and 6% Beta-HH (they are corresponding to ~0.1, 0.25, 0.5, 0.99, 1.96, 2.91, 3.85, 4.76, 5.66 weight % respectively) [1], were made according to the following procedure: to prepare (say), 5% Beta-HH, 100g Omega was mixed with 5 g β-hemihydrate; the mixture was shaken for 24 hours followed by 3 hours ultrasonic oscillation; and then around 25 mg sample was taken for testing.

---

[1] There is some discrepancy with the method used in the section 3.4.1. Some tests were done more than 2 years ago.

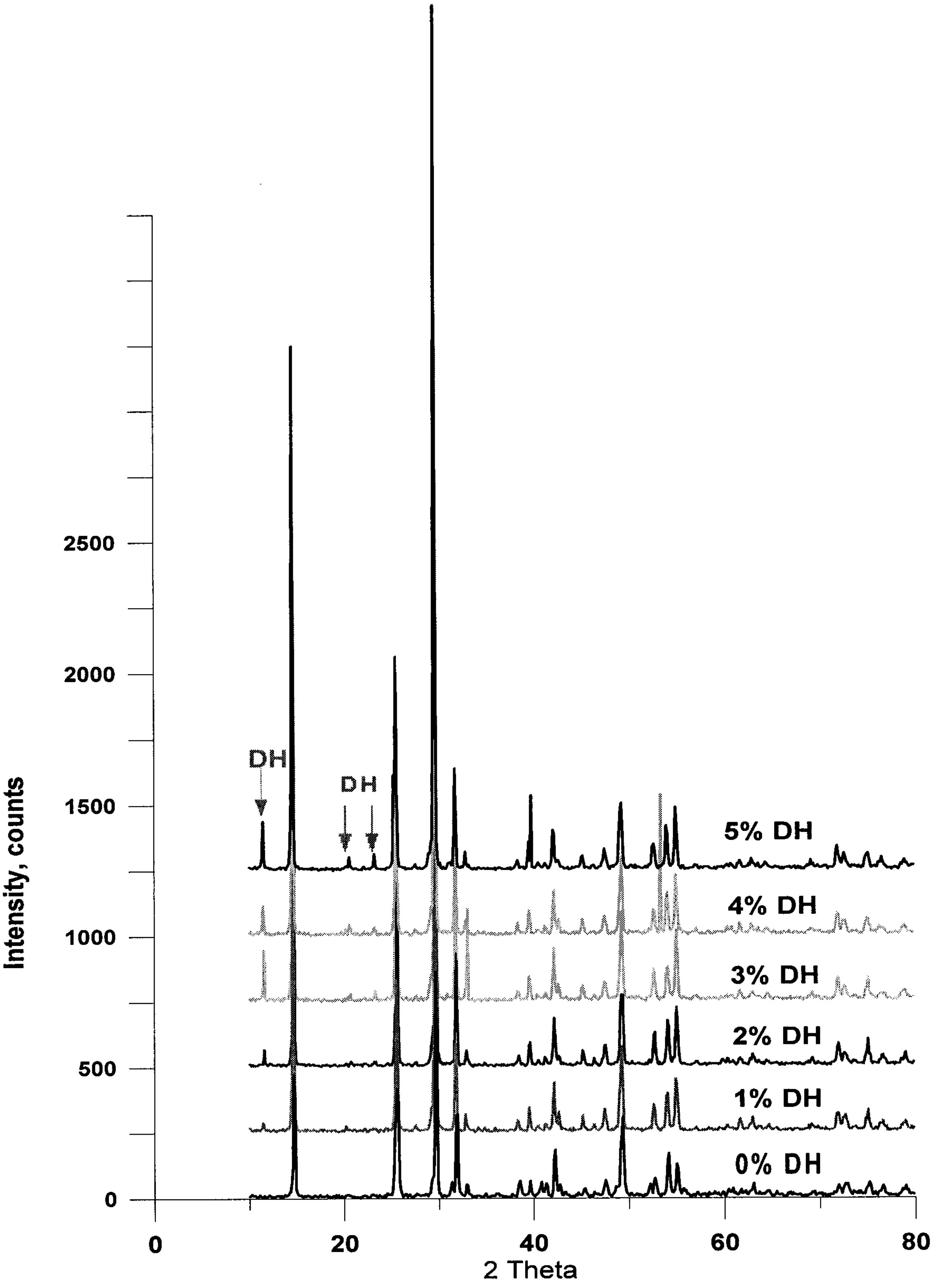

Figure 3.4: Determination of XRD detection limit for dihydrate in hemihydrate

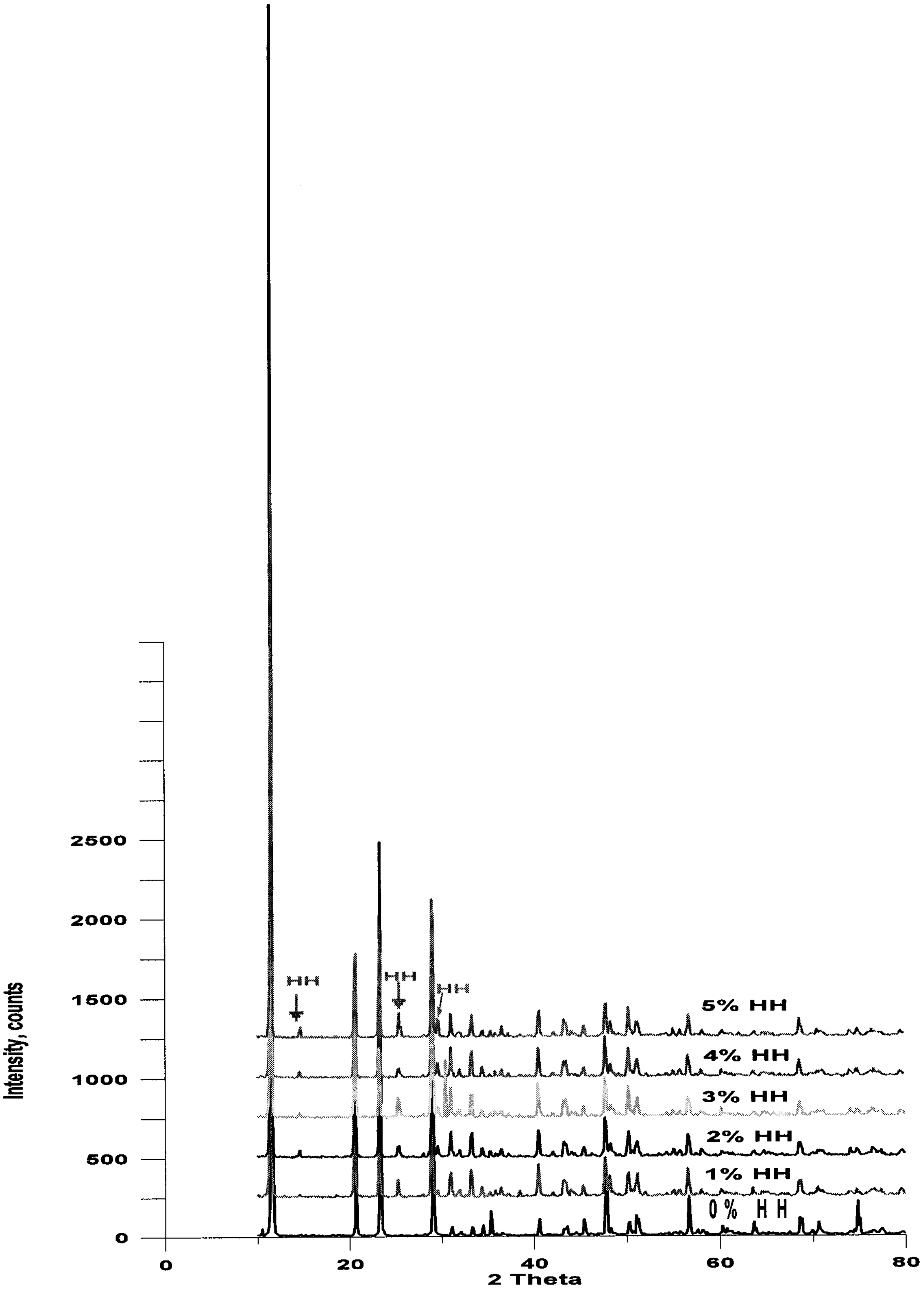

Figure 3.5: Determination of XRD detection limit for hemihydrate in dihydrate

As shown in Figures 3.6 and 3.7 respectively, "pure" α- or β-hemihydrate can be distinguished by the characteristic exothermic peak, around 210°C for the former and around 410°C for the latter (here there is discrepancy with the literature value of around 380°C[4]). It can also be seen that the intensity of thermal signals (after normalization) is strongly related to the weight of the corresponding phase. It is likely that there is a minimum detection weight for α- or β-hemihydrate. Actually, if the sample amount was too little (say 0.01mg), the DSC signal was basically noise. The results for the artificial mixtures are shown in Figure 3.8. With the increase of percentage of the β-hemihydrate in the mixture, the exothermic peak characteristic of α-hemihydrate migrated to higher temperature. The characteristic peak of β-hemihydrate was observed when there was more than 5 weight % β-hemihydrate present (see Figure 3.9). The detection limit may be even higher if a smaller size specimen was used. Hence the 100% purity of α-hemihydrate is rather difficult to ascertain.

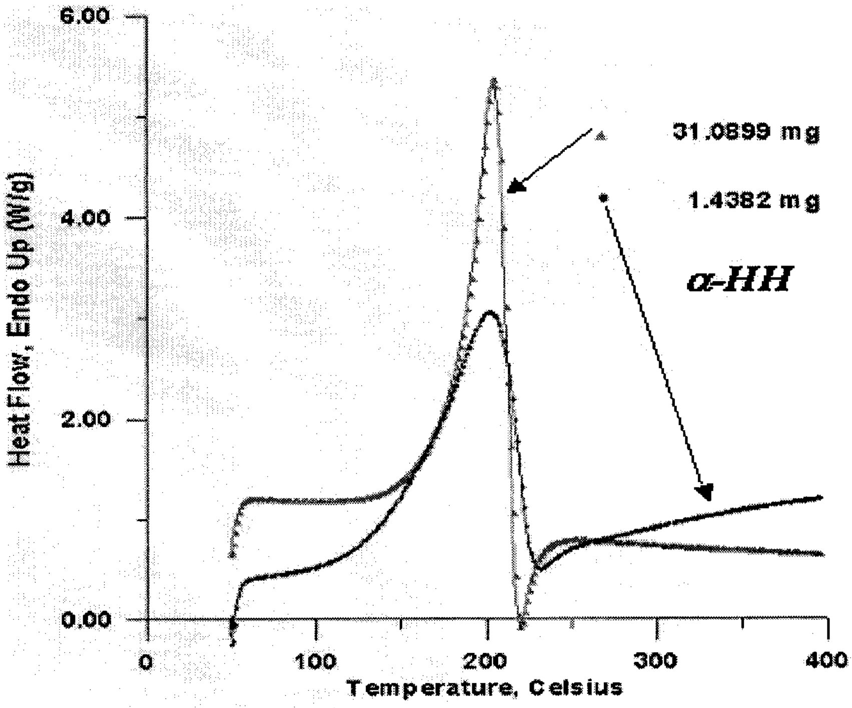

Figure 3.6: DSC traces of "*pure*" α-hemihydrate (Omega)

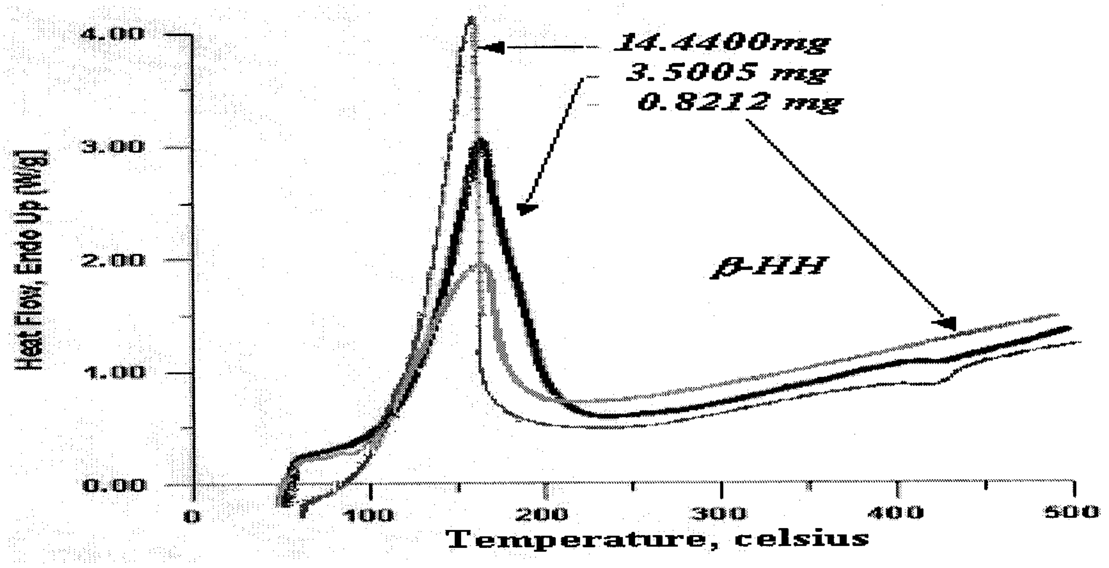

Figure 3.7: DSC traces of "*pure*" β-hemihydrate (Fisher Scientific)

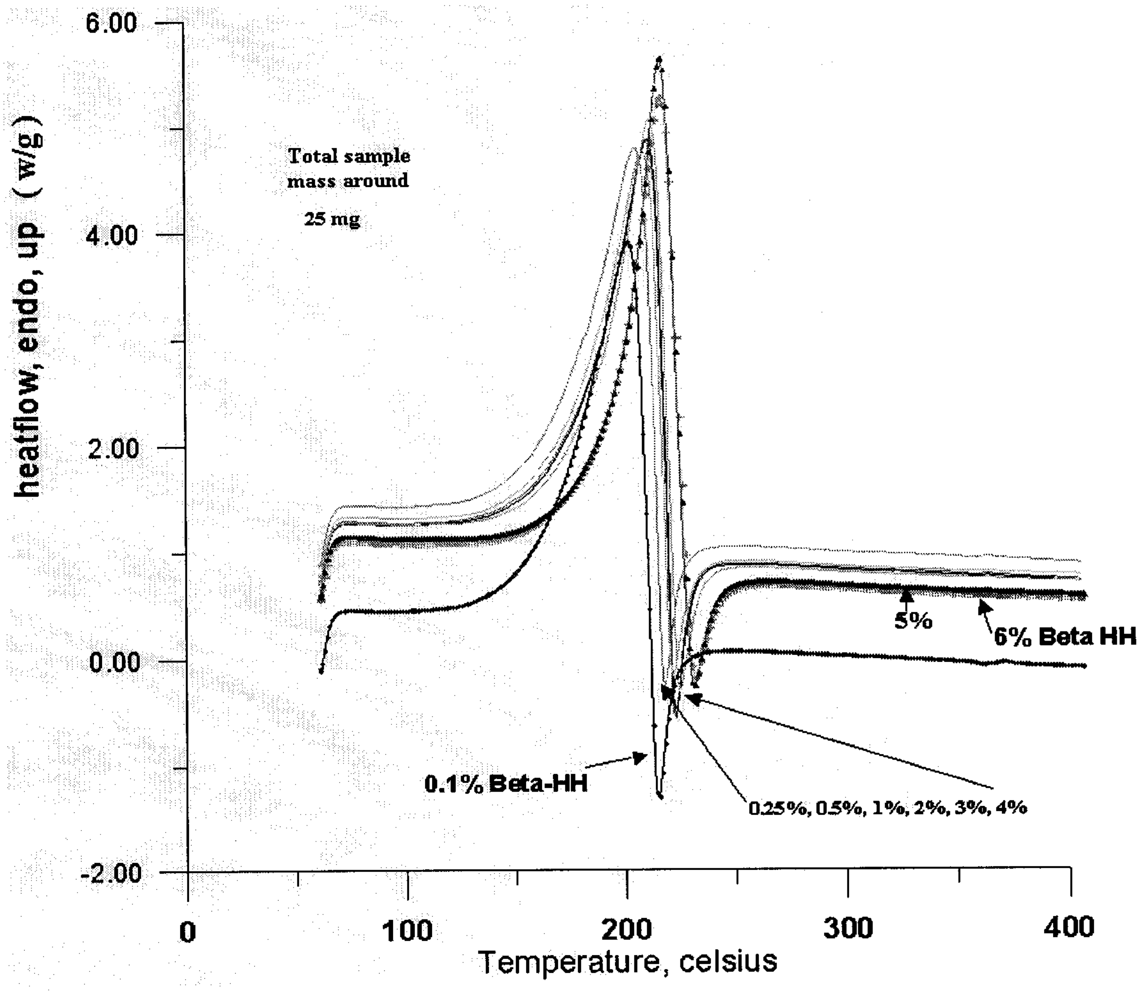

Figure 3.8: DSC traces of artificial mixtures of α- and β-hemihydrates

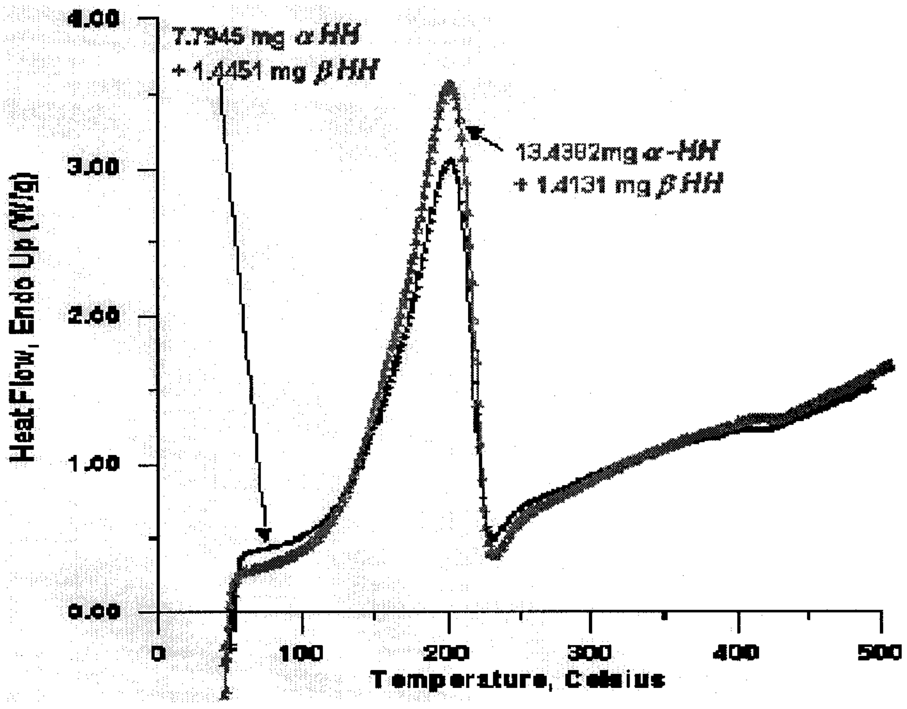

Figure 3.9: DSC traces of artificial mixtures of α- and β-hemihydrates (α- and β-hemihydrates mixed at specific amounts)

3.5 Post-reaction treatment of the produced samples

(i) Drying

Post-reaction treatment of the experimental samples included liquid/solid separation, washing and drying. Atmospheric drying of the calcium sulfate dihydrate in the oven showed that (see Figure 3.10): after 4 hour drying at 65°C, no apparent change was found, but after 10 hours, trace of hemihydrate (confirmed by DSC to be β-hemihydrate) was detected. As the drying temperature increases, the conversion rate from dihydrate to hemihydrate also increases. As it is shown in Figure 3.11, after 4 hour drying at 93°C, there were practically hemihydrate peaks with all dihydrate peaks virtually disappeared. Further tests showed that, at 60°C (it should be carefully controlled so as not to go beyond), even after leaving dihydrate powder in the oven for a week, no hemihydrate peaks were observed.

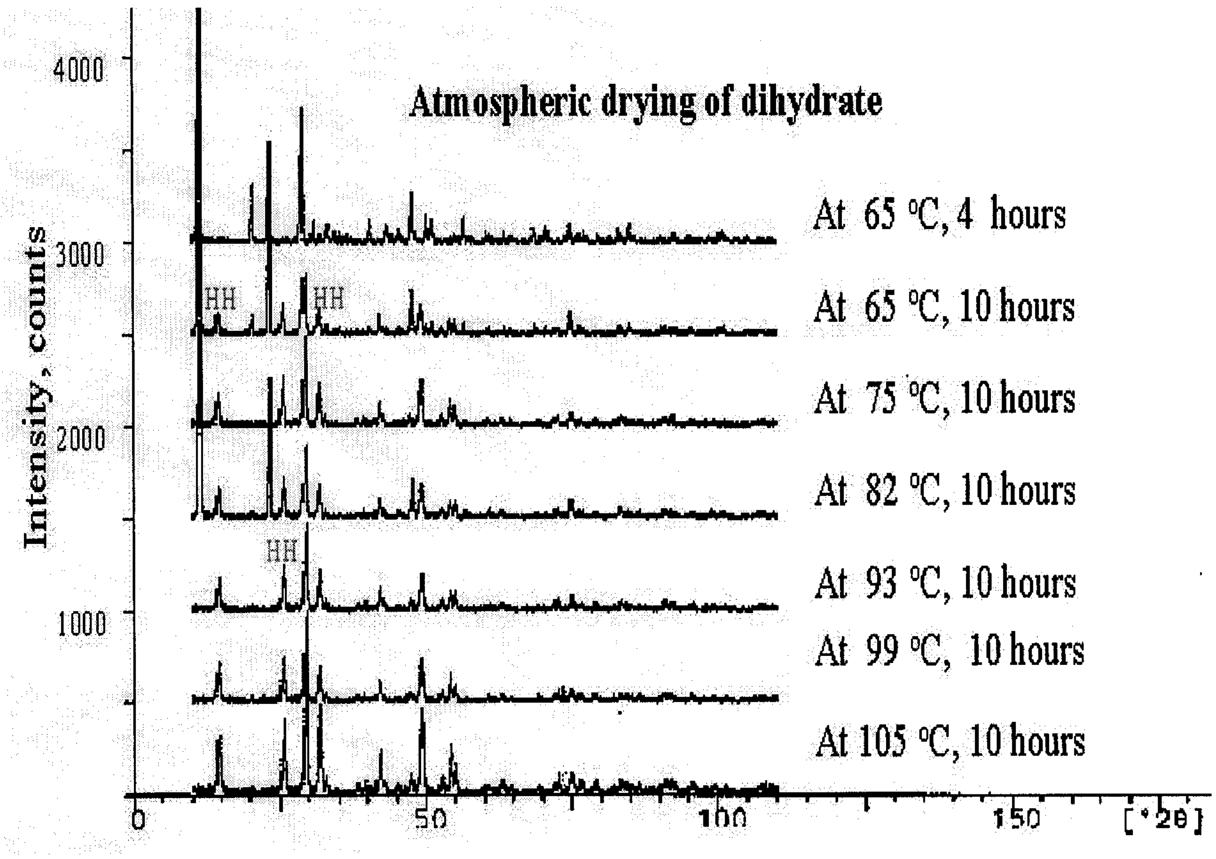

Figure 3.10: Atmospheric drying of calcium sulfate dihydrate at different temperatures and times

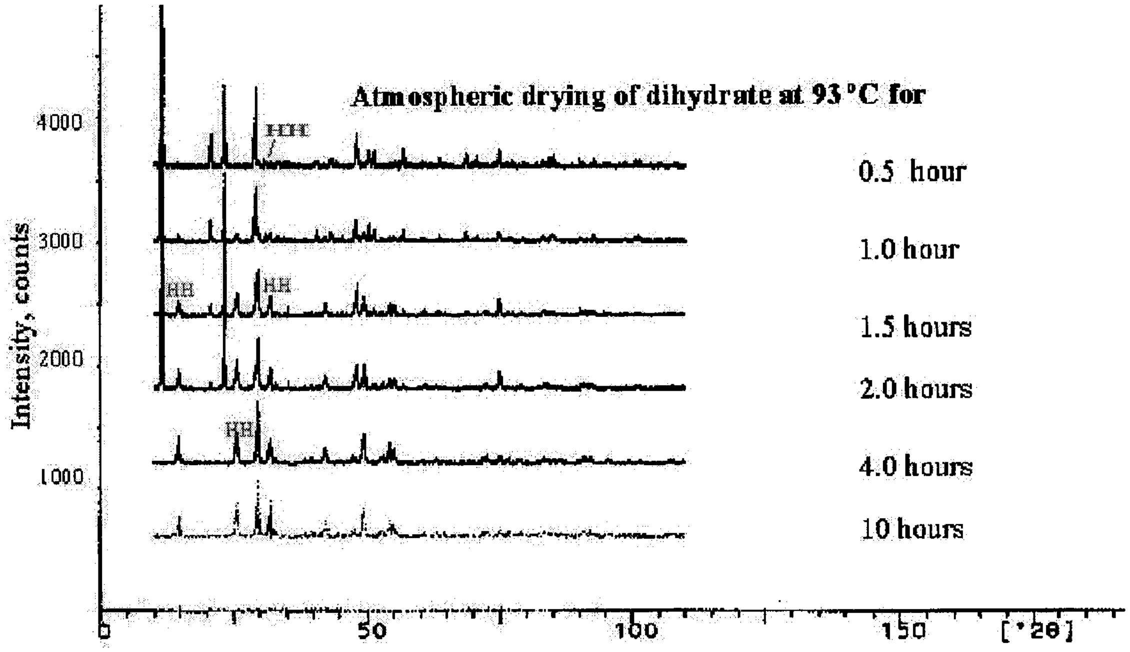

Figure 3.11: Atmospheric drying of calcium sulfate dihydrate at 93°C

The determined stability of dihydrate under atmospheric drying conditions at or below 60°C is experimentally supported by Reisdorf and Abriel [5, 6] who determined with X-ray Guinier device the dehydration reaction of dihydrate to hemihydrate occurs at 62°C (335K as reported) [2]. The author of this thesis here, for the first time, gives thermodynamic explanation by considering with the aid of FactSage[7] the free Gibbs energy change of the reaction:

$$CaSO_4 \bullet 2H_2O(s) \rightleftarrows CaSO_4 \bullet 0.5H_2O(s) + 1.5H_2O(g) \qquad (3\text{-}1)$$

As shown in Figure 3.12, with the decrease of water vapor pressure from 4.000kPa, down through 3.000, 2.500, 2.000, 1.500, 1.000, 0.500kPa to 0.100kPa, the transition temperature between dihydrate and hemihydrate shifts down from around 85°C to around 62°C.

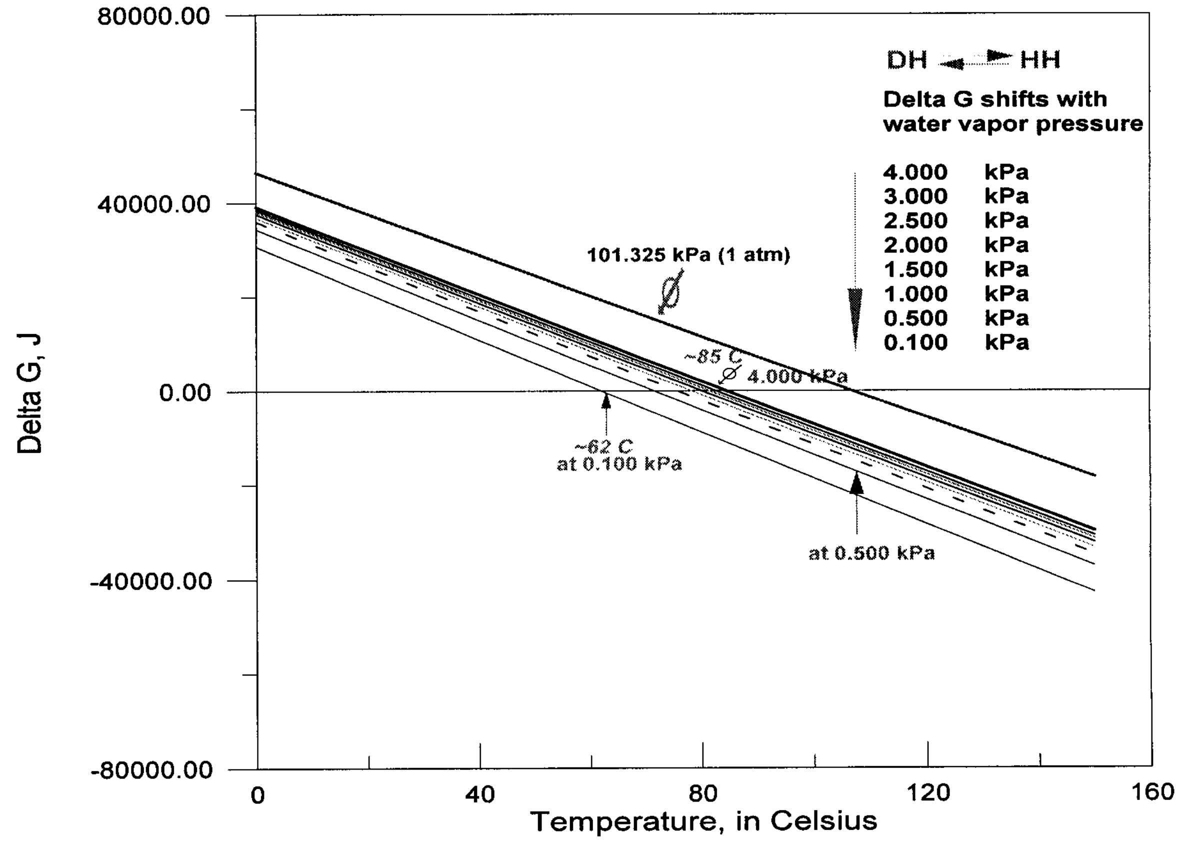

Figure 3.12: Thermodynamic estimation of the transition temperature between dihydrate and hemihydrate in the air with the aid of FactSage 5.0[7]

---

[2] The water vapor condition was not specified in the original source [5, 6].

It should be stated that, atmospheric drying of hemihydrate at higher temperature (65-100°C) for short period of time (less than 7 days) was found not to be a problem. Particularly, α-hemihydrate can be preserved after drying at about 100°C in the oven (typically around 12 hours) as proven by DSC analysis of a number of samples produced in the later part of this work.

From the above investigations, it was determined 59-60°C to be the optimum drying temperature to ensure the preservation of the calcium sulfate dihydrate phase when this was deemed necessary. In routine α-hemihydrate production tests samples were dried at 100°C for around 12 hours,

(ii) Washing and Filtration

There were four alternative methods considered/tested for the washing/filtration of the product. The objective in all these methods is the preservation (i.e., avoidance of alteration) of the phase(s) produced in the reaction environment.

•Method 1 ---Without filtration:

In this method, at the end of reaction, boiling de-ionized water was added into the reaction slurry while keeping heating. Shortly after that, agitation was stopped to allow around 10 minutes for solids settling, and removal of supernatant liquor was done by pump; then, another batch of boiling water (typically 4-6 batches) was added and the procedure was repeated until un-reacted or entrained acid was washed away; completeness of acid (SO_4^{2-}) removal was determined with 0.5 wt% $BaCl_2$ added to wash water. The washed solids were left in the hot reactor at ~100°C until they were completely dried up (around 12 hours).

•Method 2 ---With filtration

In this method, at the end of reaction, the contents of the reactor were pumped into the hot filtration unit. Following separation of solids and filtrate, the solids were washed with boiling water until there was no apparent SO_4^{2-} (again determined with 0.5 wt % $BaCl_2$)[3] detected in wash water. Upon completion of washing wet solids were moved as fast as possible into the pre-heated oven (around 100°C) and left there for around 12 hours. Both methods were determined to be adequate for preserving hemihydrate but not dihydrate. As mentioned earlier, drying of dihydrate at temperature above 60-62°C results in its transformation to hemihydrate. This is a critical issue as it might erroneously lead to the impression that hemihydrate was produced in the reaction vessel. This is indeed what happened with Kostic-Pulek et al. [8] who reported the production of calcium sulfate alpha-hemihydrate in unheated sulfuric acid solutions of 10, 15, 20, 30 or 40wt% content. In reality they had produced dihydrate that was converted to hemihydrate (unknowingly) upon heating their samples at 105°C prior to characterization!

•Method 3 ---With filtration

This method basically is a variant of method 2. After separation of the solid and liquid phases, the solid was first washed with boiling water until there was no apparent SO_4^{2-} left, and then, washed again, with a hydrophilic organic solvent before it was dried in the pre-heated oven (this time around 60°C) for around 12 hours. The purpose of extra organic solvent washing was to remove, as much as possible, the water content in the sample. The ultimate goal was to preserve the co-existing dihydrate and hemihydrate (if any) phases in the sample. Different organics were tried, but 2-propanol was the one that has been chosen as it is viewed favorably in terms of effectiveness and economy. Use of acetone is reported in the literature [9-10], but 2-propanol was found to achieve better results.

•Method 4 ---Without filtration

A quench method plus freeze-drying has been reported for the study of the setting of

---

[3] Typically, for reaction with 500 mL $1.5MH_2SO_4$, the washing water could be around 2-2.5 L depending on the ratio of CaO/H_2SO_4.

dental stone (α-hemihydrate[4]) [11]. At certain time intervals, the ongoing reaction was "*thermally*" stopped by immersing the specimen into liquid nitrogen. Specimens were retained in the liquid nitrogen bath (about -196°C) for at least 10 minutes before they were immediately transferred to a vacuum chamber (~133Pa) where they were kept for around 2 hours to ensure complete removal of water. This method despite its effectiveness was not used in the present work because the used glass reactor could not withstand such temperature change on one hand and on the other because of its impracticability in terms of implementation in industry.

To sum-up, method 3 was used for most of the research activities seeking to produce α-hemihydrate or optimize the reaction conditions; hundreds of tests have proven that both dihydrate and hemihydrate can be preserved very well in cases where both of these phases co-exist. On the other hand, once the operating window for production of α-hemihydrate was defined, the procedure was simplified and method 2 was used instead.

3.6 Sample storage

The low reactivity of hemihydrate powders with atmospheric water vapor is a major advantage for the storage of the final samples in this work. Usually, it was said to be safe at less than 70% RH (relative humidity). But Darvell et al. [12-13] suggested as more reliable criterion, water vapor pressure; they found, at 23°C, water vapor pressure (greater than about 2.3 kPa) to cause rapid reaction. It is coincident that water vapor pressure for 70% RH at 25.6°C = 2.3 kPa. Water vapor pressures for 50% RH at 23°C and 25.6°C are 1.41 kPa and 1.64 kPa respectively. Since the Wong Building (where this work has been undertaken) is under central air conditioning control year around with the RH value in an ordinary lab or office about 33% and temperature about 20°C, it is far below the suggested critical value, no special measurements are needed for storing the prepared samples. Typically, the samples were sealed up in plastic bags. They can stay "stable"

---

[4] Alpha- and β-Hemihydrate products are referred to as dental stone and dental plaster respectively in the dental literature.

under such conditions for years (at least 3 years, from the first preparation of α-hemihydrate till the time this thesis is being prepared).

3.7 Chemical analysis

Sulfuric acid stock solutions were prepared, analyzed and diluted to the concentrations required for the experiments. Free acid was determined by standard acid-base titrations. For accuracy, it was titrated with 0.02N NaOH standard solution and the titration was also monitored by a pH-meter and organic pH indicator, neutral red.

Regular quantitative analyses of elements such as calcium, sulfur, aluminum, etc. were done with Inductively Coupled Plasma - Atomic Emission Spectrometry (**ICP-AES**) [14-15].

References

[1] Engert, H.J. and Koslowski, T., New gypsum binder Alpha 2000, ZKG International, 51(4), 229-237(1998).

[2] College, J.W., Sulfur dioxide removal from sulfur dioxide-containing hot gaseous streams under formation of α-hemihydrate gypsum, USA Patent, US 5,312,609 (1994).

[3] Amita, K., Matsui, H. and Hashizume, G., Quantitative analysis of mixtures of α-$CaSO_4 \bullet 1/2H_2O$ and β-$CaSO_4 \bullet 1/2H_2O$ by high pressure differential thermal analysis, Gypsum & Lime, No. 191, 12-17(1984).

[4] Goto, M., Molony, B., Ridge, M.J. and West, G.W., The forms of calcium sulfate hemihydrate, Australian Journal of Chemistry, 19, 313-16(1966).

[5] Abriel, W., Reisdorf, K. and Pannetier, J., Dehydration reactions of gypsum: a neutron and X-ray diffraction study, Journal of Solid State Chemistry, 85, 23-30 (1990).

[6] Reisdorf, K. and Abriel, W., Reactions in the system $CaSO_4$-H_2O and on Na-polyhalite $Na_2Ca_5(SO_4)_6(H_2O)_3$, Neues Jahrbuch für Mineralogie Abhandlungen, 157(1), 35-46 (1987) (in German).

[7] http://www.FactSage.com

[8] Kostic-pulek, A., Marinkovic, S., Logar, V., Tonec, R. and Popov, S., Production of calcium sulfate alpha-hemihydrate from citro-gypsum in unheated sulfuric acid solution, Ceramics-Sulikaty, 44(3) 104-108(2000) (paper in English).

[9] Melikhov, I.V., Saparin, G.V., Bozhevolnov, V.E., Obyden, S.K. and Kuleshova, O.V., Diagnostics of heterogeneous chemical reactions by cathodolumiscence, Scanning, 13, 358-362(1991).

[10] Sirota, I. S., Dorozhkin, S. V., Kruchnina, M. V. and Melikhov, I. V., Phase transformation and dehydration of calcium sulfate dihydrate in solution studied by SEM, Scanning, 14, 269-275(1992).

[11] Winkler, M. M., Monaghan, P., Gilbert, J. L. and Lautenschlager, E. P., Freeze-drying and scanning electron microscopy of setting dental gypsum, Dental Materials, 11, 226-230(1995).

[12] Torrance, A. and Darvell, B.W., Effect of humidity on calcium sulfate hemihydrate, Australian Dental Journal, 35(3), 230-235(1990).

[13] Chan, T.K.C. and Darvell, B.W., Effect of storage conditions on calcium sulfate hemihydrate-containing products, Dental Materials, 17, 134-141(2001).

[14] Dutrizac, J.E., Calcium sulfate solubilities in simulated zinc processing solutions, Hydrometallurgy, 65, 109-135 (2002).

[15] Martynowicz, E.T.M.J., Witkamp, G.J. and van Rosmalen, G.M., The effect of aluminum fluoride on the formation of calcium sulfate hydrates, Hydrometallurgy, 41(2-3), 171-186(1996).

Chapter 4

Phase Equilibria and Solubilities of Calcium Sulfate Hydrates

4.1 Introduction

In this chapter the $CaSO_4$ - H_2SO_4 - H_2O system is analyzed from a thermodynamic point of view by performing appropriate calculations in an effort to establish a phase diagram depicting the stability or metastability of the various hydrates as a function of temperature and sulfuric acid concentration. Additionally in this chapter, the solubilities of calcium sulfate hydrates in H_2SO_4 - H_2O media are measured and are reported. Such phase diagram and solubility measurements serve then as reference for discussing the experimental findings described in the subsequent chapters.

4.2 Phase equilibria

4.2.1 Thermodynamic basis

For the three major calcium sulfate phases, namely, dihydrate, hemihydrate and anhydrite, the effects of different factors such as solution composition and temperature on their stability can be thermodynamically explained.

Take the following equilibria for consideration:

$$CaSO_4 \bullet 2H_2O(s) \rightleftarrows CaSO_4\,(s) + 2H_2O(l) \qquad (4\text{-}1)$$

$$CaSO_4 \bullet 2H_2O(s) \rightleftarrows CaSO_4 \bullet 0.5H_2O(s) + 1.5H_2O(l) \qquad (4\text{-}2)$$

$$CaSO_4 \bullet 0.5H_2O(s) \rightleftarrows CaSO_4\,(s) + 0.5\,H_2O(l) \qquad (4\text{-}3)$$

$$CaSO_4 \cdot 2H_2O(s) \rightleftharpoons Ca^{2+}(aq) + SO_4^{2-}(aq) + 2H_2O(l) \tag{4-4}$$

$$CaSO_4 \cdot 0.5H_2O(s) \rightleftharpoons Ca^{2+}(aq) + SO_4^{2-}(aq) + 0.5H_2O(l) \tag{4-5}$$

$$CaSO_4\,(s) \rightleftharpoons Ca^{2+}(aq) + SO_4^{2-}(aq) \tag{4-6}$$

One thermodynamic fact is that the heat capacity for each species can be expressed as

$$C_p = A + BT + C/T^2 \tag{4-7}$$

and the corresponding enthalpy as

$$\Delta H = AT + BT^2/2 - C/T + I_h \tag{4-8}$$

hence, the Gibbs free energy and entropy can be expressed as

$$\Delta G = -AT\,\mathrm{In}\,T - BT^2/2 - C/2T + I_h + I_gT \tag{4-9}$$

$$\Delta S = A\,\mathrm{In}\,T + BT - C/2T^2 + I_s \tag{4-10}$$

and for the equilibria (4-4),(4-5) and (4-6), it can be further written as,

$$\mathrm{In}\,K_{sp} = -\Delta G/RT = A\,\mathrm{In}\,T/R + BT/2R + C/2RT^2 - I_h/RT - I_g/R \tag{4-11}$$

where T is temperature in K; A, B and C are constants; I_h, I_g and I_s, are additional integration constants; and K_{sp} is the thermodynamic solubility product, which can be defined as

$$K_{sp,\,DH} = \alpha_{Ca^{2+}}\alpha_{SO_4^{2-}}\,(\alpha_{H_2O})^2, \tag{4-12}$$

$$K_{sp,\,HH} = \alpha_{Ca^{2+}}\alpha_{SO_4^{2-}}\,(\alpha_{H_2O})^{0.5} \tag{4-13}$$

and

$$K_{sp,\,AH} = \alpha_{Ca^{2+}}\alpha_{SO_4^{2-}} \tag{4-14}$$

for dihydrate, hemihydrate and anhydrite respectively.

Generally, for dihydrate and anhydrite, all of the thermodynamic constant values can be found in the literature [1-2]. And for hemihydrate, no complete set of data has been reported. Most commonly-used data can be taken from latest version of "*Selected Values of Chemical Thermodynamic Properties*"[3], "*Thermochemical Properties of Inorganic Substances*"[4] and "*The NBS Tables of Chemical Thermodynamic Properties*"[5]. Relatively completed set of thermal data such as ΔH, ΔS and C_p can also be retrieved from an online databank [6] [1].

---

[1] It is powered by Institute of Process Engineering (formerly Institute of Chemical Metallurgy), Chinese Academy of Sciences, at which the author did his master's degree and worked for approximately two years.

4.2.2 Calculations

Based on above-mentioned information, the transition temperatures for equations (4-1) and (4-2), namely equilibrium between dihydrate and anhydrite, and equilibrium between dihydrate and hemihydrate, can be calculated. Calculations were made with the aid of FactSage [7]. The obtained results are shown in Figure 4.1. As it can be seen, the transition temperature between dihydrate and anhydrite is 55.7°C in pure water (assuming water activity of the water saturated with calcium sulfate to be 1), which is in good agreement with some literature data such as 58±2°C from Hardie[8], 56±3°C from Blount and Dickson[9], 49.5±2.5°C from Innorta et al.[10], 56°C from Langmuir and Melchior [11] and 59.9°C from Raju and Atkinson [1][2]. The transition temperature between dihydrate and hemihydrate was calculated to be 106.6°C, very close to the 104°C value reported by Martynowicz et al.[15].

As for the transition between anhydrite and hemihydrate, the free energy change ΔG is negative in a broad range of temperature (shown also in Figure 4.1), which indicates that equation (4-3) is basically "one-way", hemihydrate → anhydrite, from hemihydrate to anhydrite. No equilibrium between hemihydrate and anhydrite can exist. In other words, anhydrite is thermodynamically always more stable than hemihydrate; hemihydrate can only exist metastably; below 55.7°C, dihydrate is more stable than anhydrite; and above 55.7°C, anhydrite is the stable phase; dihydrate can exist metastably up to 106.6°C, whereas hemihydrate is more metastable than dihydrate above that temperature.

K_{sp} values (in the form $\log K_{sp}$) calculated from ΔG values were also plotted and are shown in the Figure 4.2. For the calculations, the author of this thesis used a mixture of data from the databank of FactSage (version 5.0) [7] and some other sources as mentioned before. The K_{sp} values were calculated using the following simplified equations obtained by fitting[3]:

---

[2] Still there are lower transition temperatures reported such as 42±2°C from Posnjak [12],38-39°C from Partridge and White[13], 42±1°C from Hill[14] and 40°C mentioned in the paper of Martynowicz et al.[15].

[3] The reason for choosing this kind of fitting instead of the "thermodynamic form" as shown in equation (4-11) lies in that, it can be very easily achieved by some user-friendly software such as Microsoft Excel and Grapher from Golden Software.

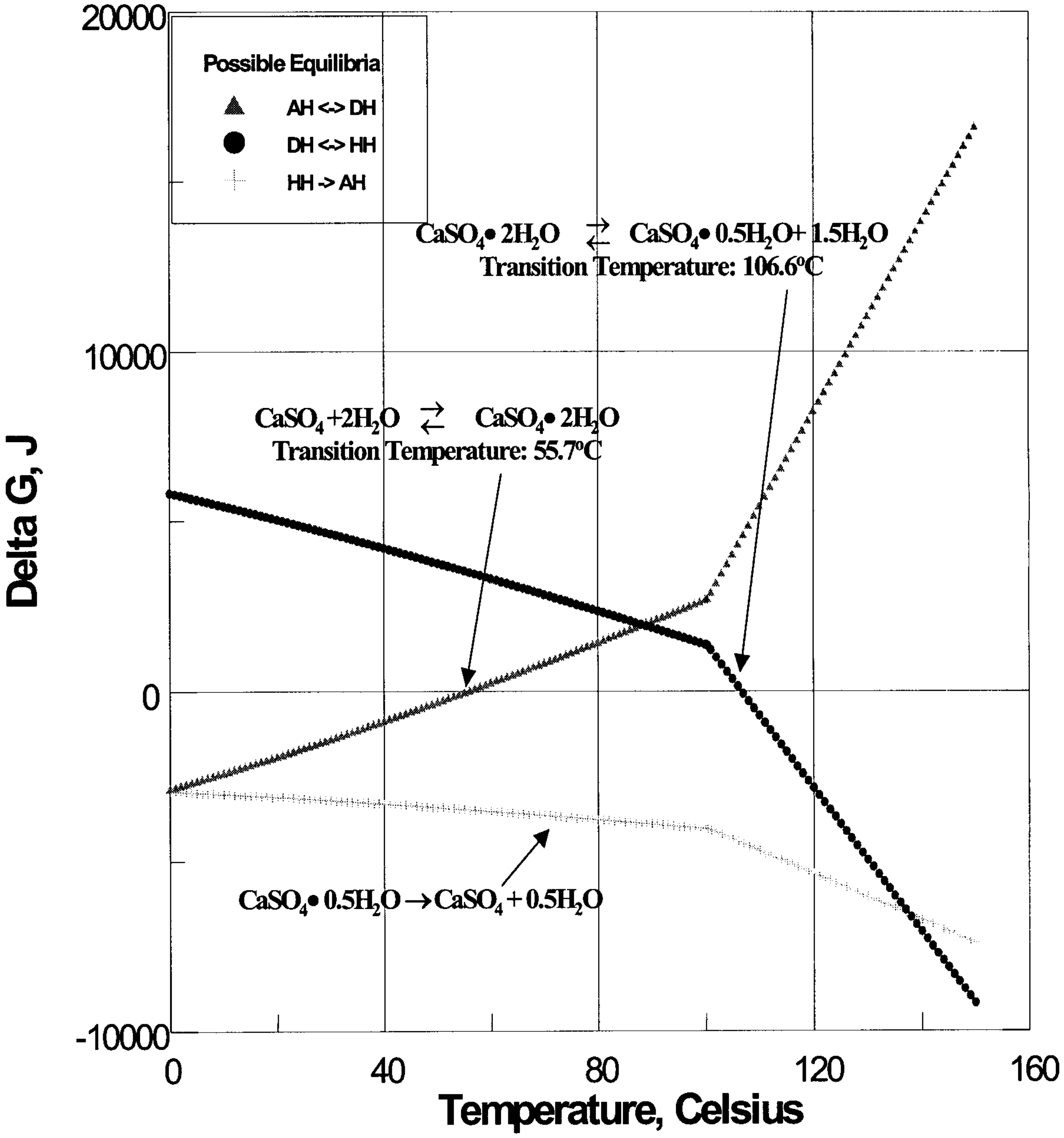

Figure 4.1: Calculated results of free energy change for the possible equilibria among the calcium sulfate phases with the aid of FactSage
(Water activity of the water saturated with calcium sulfate was assumed to be 1.0)

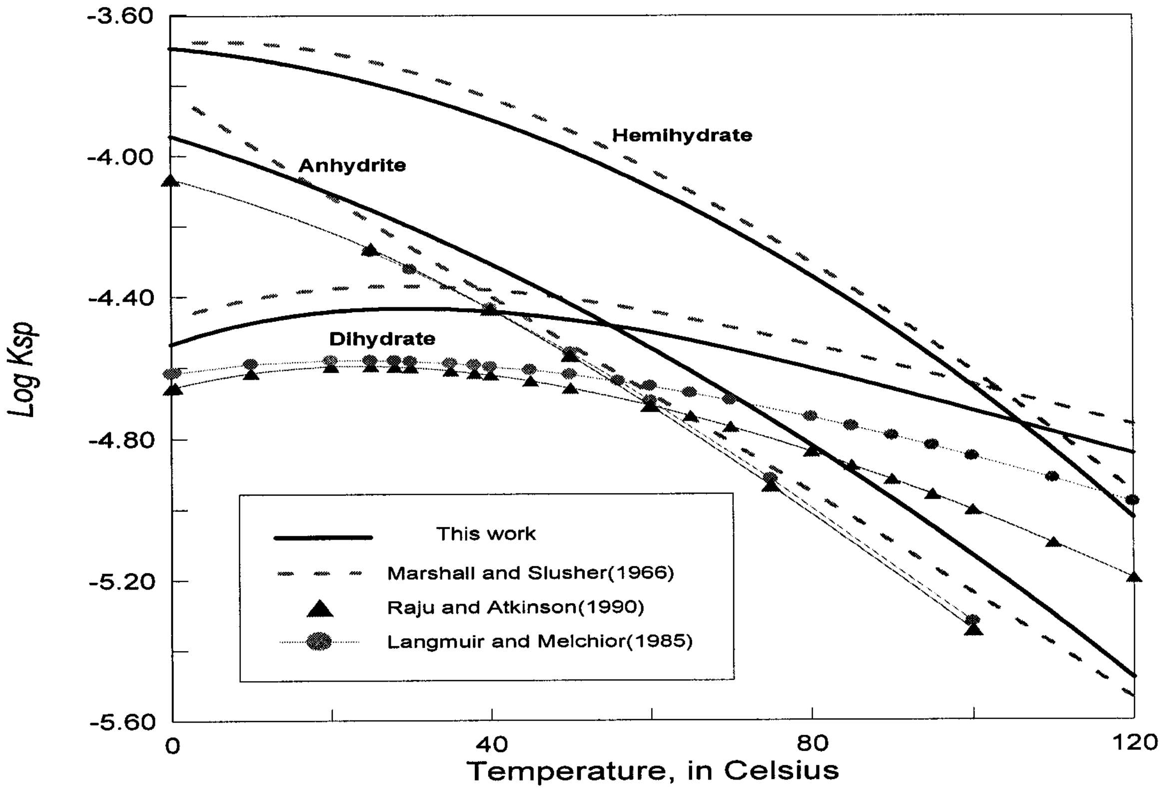

Figure 4.2: Calculated $log\ K_{sp}$ versus temperature

$$Log\ K_{sp,\ DH} = -4.56889 + 0.00262764\ T - 0.00004.05185 \times 10^{-5}\ T^2 \tag{4-15}$$

$$Log\ K_{sp,\ HH} = -3.69526 - 0.00209588\ T - 7.4919 \times 10^{-5}\ T^2 \tag{4-16}$$

$$Log\ K_{sp,\ AH} = -3.94492 - 0.0072334\ T - 4.63984 \times 10^{-5}\ T^2 \tag{4-17}$$

On the same Figure, the K_{sp} values reported by Marshall and Slusher [16], Raju and Atkinson [1] and Langmuir and Meichior [11] are plotted as well for comparison purpose. The agreement of this work's calculations is reasonable with the data from Marshall and Slusher [16], however, discrepancies are seen with the other datasets. The most significant discrepancy is observed with the estimation of the K_{sp} of dihydrate. Given that the K_{sp} from this work lies between the corresponding ones of Marshall and Slusher [16] and Langmuir and Mechior [11], it is deemed overall to be reasonable.

The ultimate goal of this exercise is to deduce a general phase diagram for the $CaSO_4$–H_2SO_4–H_2O system. Since the K_{sp} estimates of Figure 4.2 are deemed reasonable, the author decided to use those data for further deduction.

The chemical potentials of dihydrate, hemihydrate and anhydrite in solution are defined as:

$$\mu_{DH,\,l} = \mu^{0} + RT\,In(\alpha_{Ca^{2+}}\alpha_{SO_4^{2-}}(\alpha_{H_2O})^{2}) \qquad (4\text{-}18)$$

$$\mu_{HH,\,l} = \mu^{0} + RT\,In\,(\alpha_{Ca^{2+}}\alpha_{SO_4^{2-}}\,(\alpha_{H_2O})^{0.5}) \qquad (4\text{-}19)$$

$$\mu_{AH,\,l} = \mu^{0} + RT\,In\,(\alpha_{Ca^{2+}}\alpha_{SO_4^{2-}}) \qquad (4\text{-}20)$$

At the solubility concentration, the chemical potential of the solid, say dihydrate, $\mu_{DH,\,s}$, equals $\mu_{DH,\,l}$; and at the transition point, for the co-equilibrating hemihydrate, the chemical potential of the solid, $\mu_{HH,\,s}$, also equals $\mu_{HH,\,l}$, namely:

$$\begin{cases} \mu_{DH,\,s} = \mu_{DH,\,l} & (4\text{-}21) \\ \mu_{HH,\,s} = \mu_{HH,\,l} & (4\text{-}22) \end{cases}$$

By substitution, it results in:

$$\begin{cases} \mu^{0} + RT\,In(K_{sp,\,DH}) = \mu^{0} + RT\,In(\alpha_{Ca^{2+}}\alpha_{SO_4^{2-}}(\alpha_{H_2O})^{2}) & (4\text{-}23) \\ \mu^{0} + RT\,In(K_{sp,\,HH}) = \mu^{0} + RT\,In(\alpha_{Ca^{2+}}\alpha_{SO_4^{2-}}(\alpha_{H_2O})^{0.5}) & (4\text{-}24) \end{cases}$$

which can be further reduced to:

$$\frac{K_{sp,\,DH}}{K_{sp,\,HH}} = (\alpha_{H_2O})^{1.5} \quad \text{(at the transition point)} \qquad (4\text{-}25)$$

Similar equation can be obtained from the equilibrium between dihydrate and anhydrite,

$$\frac{K_{sp,\,DH}}{K_{sp,\,AH}} = (\alpha_{H_2O})^{2} \quad \text{(at the transition point)} \qquad (4\text{-}26)$$

Equations (4-25) and (4-26) imply that the phase transition temperatures are exclusively determined by the water activity, this is shown graphically in Figure 4.3.

But, water activity is related to the concentration of sulfuric acid under the assumption that the effect of the saturated calcium sulfate on the activity of water is negligible. The dependency of water activity on H_2SO_4 molality as calculated with the aid of OLI StreamAnalyzer [17] is shown in Figure 4.4. By combining the data from Figures 4.3 and 4.4, it was possible to quantitatively establish the phase diagram for the $CaSO_4$–H_2SO_4–H_2O system as shown in Figure 4.5. The stable zones for dihydrate and anhydrite are well defined. The metastable zones for dihydrate and hemihydrate are also clearly bordered. The unstable zone of hemihydrate (and also, the upper bound of the hemihydrate metastable zone) has not been determined due to the lack of data.

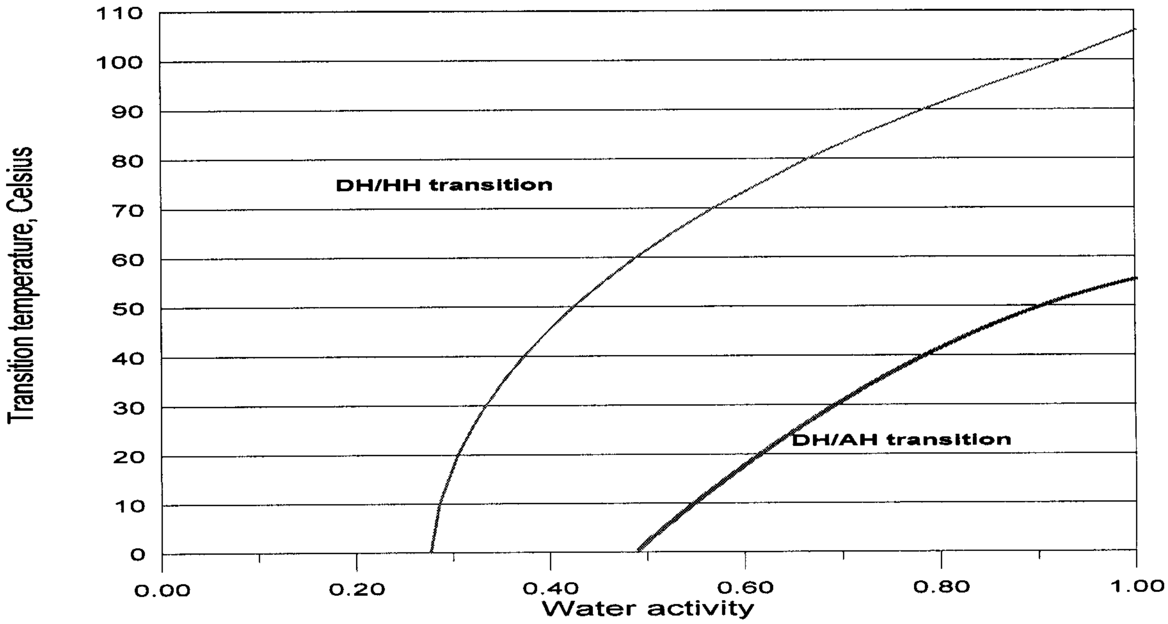

Figure 4.3: Transition temperature as a function of water activity

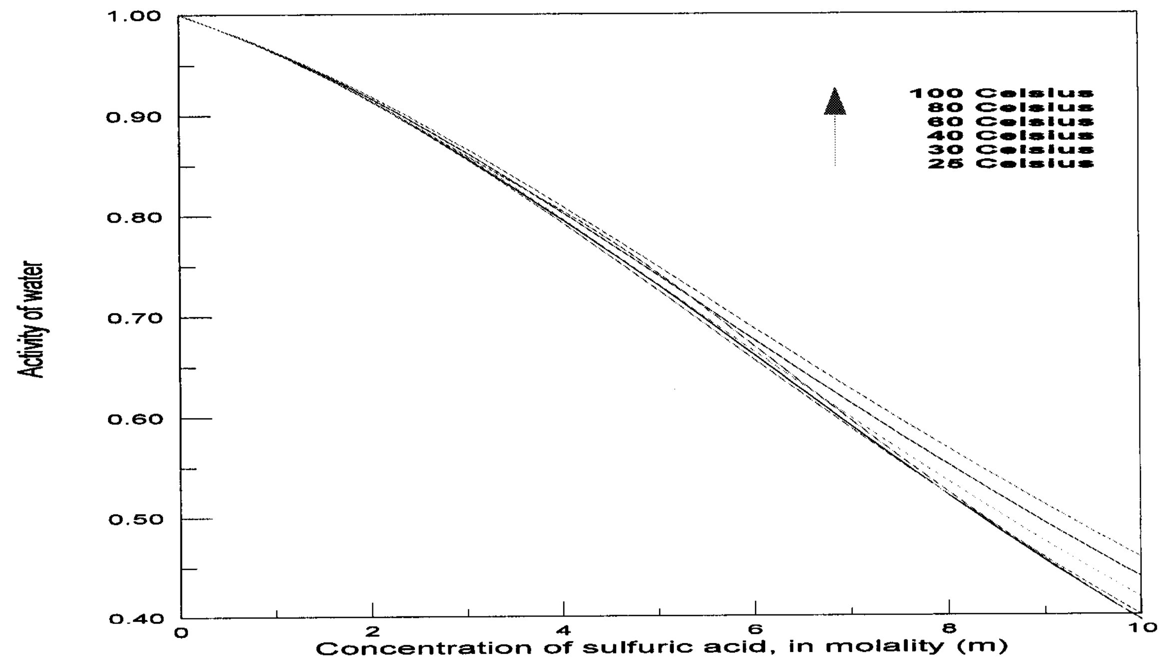

Figure 4.4: Calculated water activities in sulfuric acid solutions with the aid of OLI StreamAnalyzer

(For clarity, only the curves at 25, 30, 40, 60, 80 and 100°C are drawn)

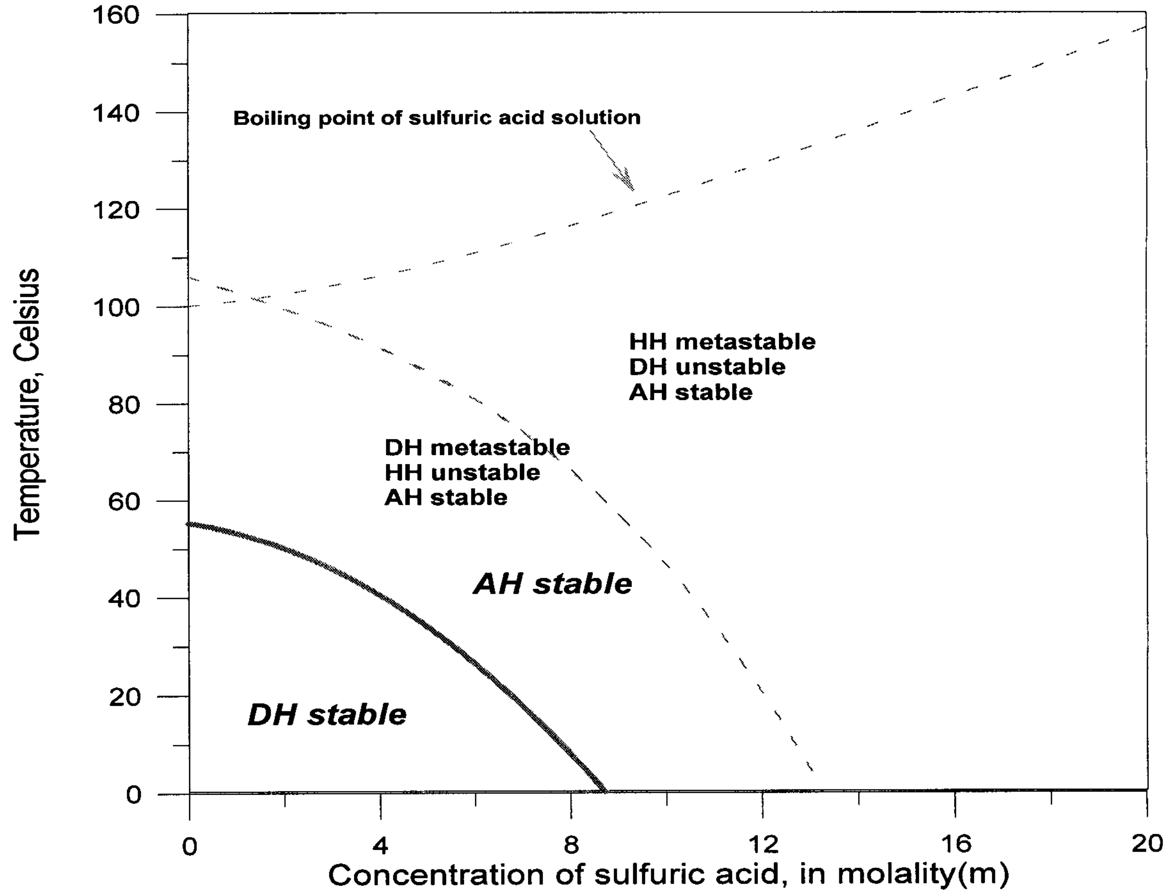

Figure 4.5: Calculated phase diagram for the $CaSO_4$ - H_2SO_4 - H_2O system

Now, the possible reactions between CaO and H_2SO_4 are considered:

$$CaO + H_2SO_4 + H_2O(l) \rightarrow CaSO_4 \cdot 2H_2O(s) \tag{4-27}$$

$$CaO + H_2SO_4 \rightarrow CaSO_4 \cdot 0.5H_2O(s) + 0.5H_2O(l) \tag{4-28}$$

$$CaO + H_2SO_4 \rightarrow CaSO_4(s) + H_2O(l) \tag{4-29}$$

From the calculated free energy change (shown in Figure 4.6), it can be seen that, there is competition among the three reactions (4-27), (4-28) and (4-29). Thus, below 55.7°C, dihydrate is the most stable product; above 55.7°C, anhydrite is the most stable product. In the range 55.7°C to 104.64°C, metastable phase dihydrate is the second stable after anhydrite while, above 104.64°C, hemihydrate assures this position.

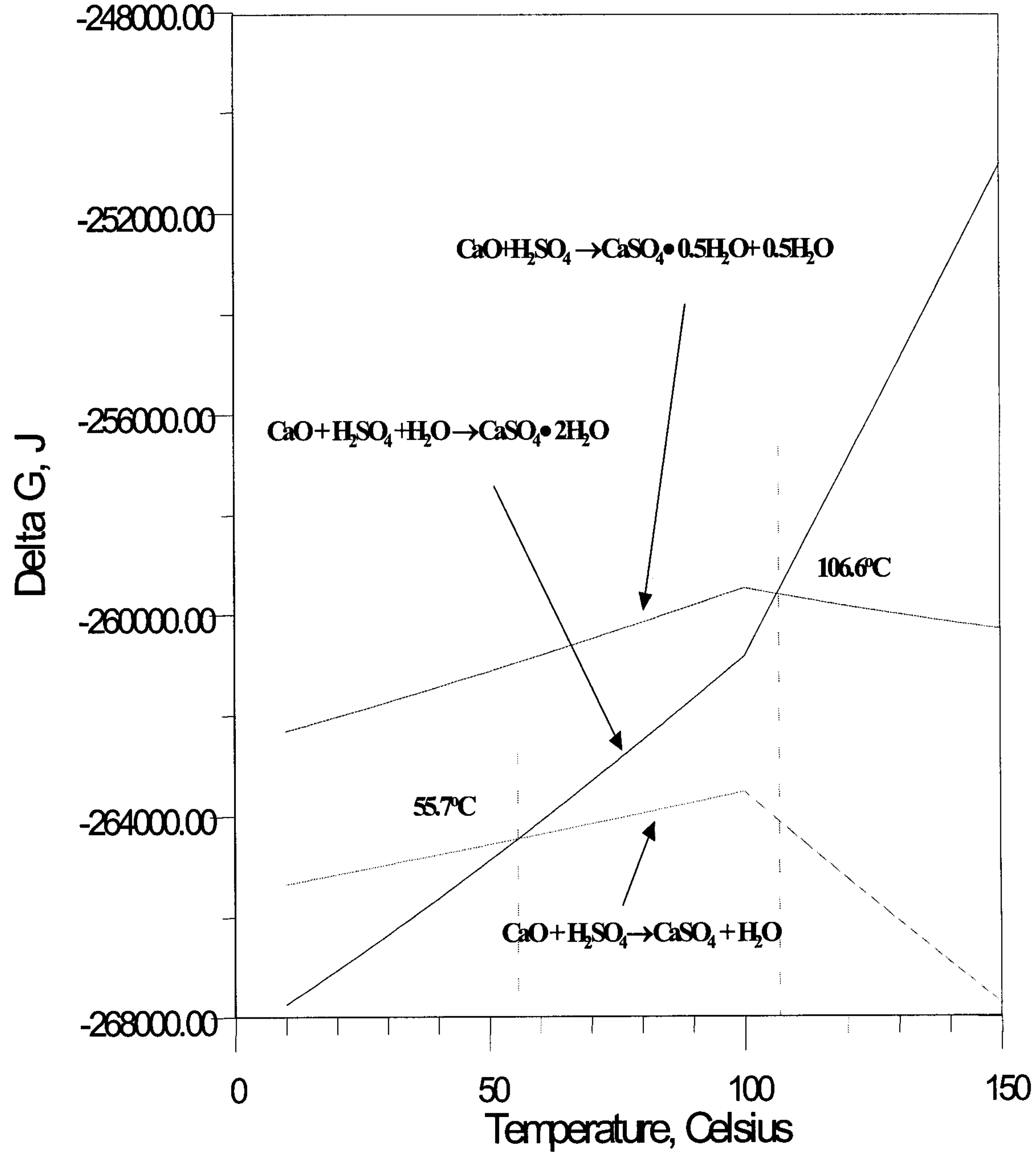

Figure 4.6: Calculated free energy change for the possible reactions between CaO and H_2SO_4 with the aid of FactSage

4.3 Solubilities

4.3.1 Background

For the past half-century, the solubilities of various calcium sulfate phases including, dihydrate, hemihydrate and anhydrite in sulfuric acid have been extensively studied. The solvent solution is either aqueous sulfuric acid, or a mixture of sulfuric acid with nitric acid, phosphoric acid, hydrochloric acid, fluosilicic acid, or salts such as sodium sulfate, calcium chloride, zinc sulfate, etc.; the concentration ranges from 0 to 100 wt%; the temperature spans from 0 to 350°C. Surprisingly, there is no data reported about the solubilities of calcium sulfate phases in the low concentration range (0 to about 4M of H_2SO_4) and at 100°C which is of interest to the present study. A summary of previously published solubility studies is presented in Table 4.1. Wehde and Stichlmair[18] presented a comprehensive "map" of the solubility of calcium sulfate in a wide H_2SO_4 concentration range from 0 to around 90 wt% at various temperatures (see Figure 4.7).

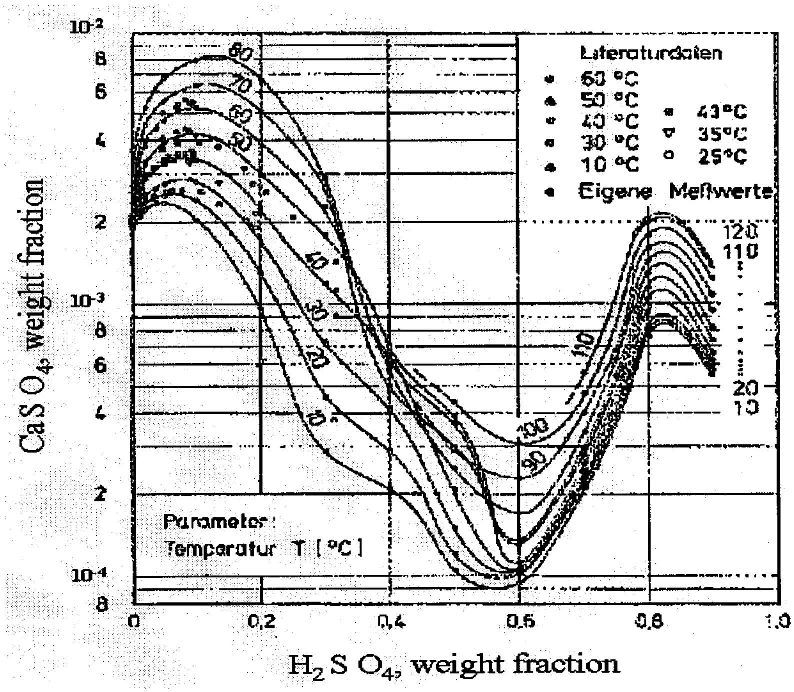

Figure 4.7: Solubility profile of calcium sulfate(s) in H_2SO_4 solutions as a function of temperature (*after Wehde and Stichlmair* [18])

Table 4.1: Review of literature on the solubilities of calcium sulfates in aqueous solution - containing H_2SO_4

Reference	Calcium sulfate(s)	Experimental Conditions
Kleinert et al.[19]		Aqueous system H_2SO_4-Na_2SO_4-$CaSO_4$ at 45, 60 and 80°C
Marshall et al.[20]	DH,AH, HH	DH: 0 - 1.0 m H_2SO_4 at 25, 30, 40, 45, 50, 60°C HH: 0 - 1.0 m H_2SO_4 at 125°C AH: 0 - 1.2 m H_2SO_4 150, 200, 250, 300, 350°C
Augustyn et al. [21]	AH	Aqueous system H_2SO_4-H_2SiF_6-$CaSO_4$ at 0, 20, 50 and 70°C
Zdnaovskii et al.[22-26]	DH,AH, HH	0-40 wt% H_2SO_4 at 25, 50,75,95°C for DH, AH and HH
Ostrovskii et al [27]		100, 98 and 94 wt % H_2SO_4 at 40-80°C
Schaefre et al.[28]	AH	0-10 wt% H_2SO_4 containing 0-40g $NaSO_4$ or $MgSO_4$ at 25°C
Beremzhanov et al.[29-31]	DH, HH	0-10 wt% H_2SO_4 and 0-55 wt % HNO_3 at 25, 40, 50 and 60°C
Zemelman [32]		Aqueous system H_2SO_4-H_3PO_4-$CaSO_4$ at different system
Tsikaeva [33]	AH	65 - 95 wt% H_2SO_4 at 40, 80 and100°C
Dvegubskii et al.[34]		Concentrated H_2SO_4 at 120-180°C
Wehde et al. [18]		0-90 wt% H_2SO_4 at 10-80°C; above 40 wt% H_2SO_4 at 90, 100,110,120°C; and $CaSO_4/FeSO_4/H_2SO_4/H_2O$ system
Khavskii et al. [35]	DH	0-0.255M H_2SO_4 at 25-90°C
Zhang et al. [36]	DH	Aqueous HNO_3 containing $Ca(NO_3)_2$, H_3PO_4, H_2SO_4 at 25°C
Huang et al.[37]	AH	96 wt % H_2SO_4 at 10-200°C
Mutalala, et al. [38]	DH	H_2SO_4 and/or $ZnSO_4$ at 25-60°C
Kojima et al. [39]	HH	HNO_3 with or without 0-1M H_2SO_4 at 100°C
Calmanovici et al. [40]	DH	Mixture of 0-41.4 wt% H_3PO_4 and 0-7.8 wt% H_2SO_4 at 20, 50 and 70°C
Martynowicz et al. [41]	DH, HH	Mixture of H_3PO_4 and H_2SO_4 at 75 and 90°C
Dutrizac [42]	DH	0-0.6M H_2SO_4 at 25-95°C 0.8, 1.2, 1.6, 1.8M H_2SO_4 at 25-90°C, 0.8M to 90°C Mixture of H_2SO_4 with $ZnSO_4$, or $MnSO_4$ or $MgSO_4$

Note:

DH: calcium sulfate dihydrate

HH: calcium sulfate hemihydrate

AH: calcium sulfate anhydrite

M: Molarity m: Molality wt%: weight percent [4]

---

[4] To allow for direct conversion from one set of units (M, m or wt%) to another, Appendix A has been prepared with the aid of OLI [17] – note that the M units in the literature mainly refer to room temperature (sometimes also refer to 25°C), the other units are independent of temperature.

Theoretically, the solubility of calcium sulfates is governed by the equilibrium:

$$CaSO_4 \cdot n\,H_2O(s) \overset{K_{sp}}{\rightleftharpoons} Ca^{2+} + SO_4^{2-} + n\,H_2O \qquad (4.3.1)$$

where K_{sp} is the solubility product, which is given by:

$$K_{sp} = m_{Ca}^{\ 2+}\, m_{SO4}^{\ 2-}\, \gamma_{Ca}^{\ 2+}\, \gamma_{SO4}^{\ 2-}\, (a_{H_2O})^{\,n} \qquad (4.3.2)$$

where $\gamma_{Ca^{2+}}$ and $\gamma_{SO_4^{2-}}$ are the activity coefficients of the respective ions, and a_{H_2O} is the activity of H_2O; $n = 2$, 0.5 or 0 corresponding respectively to dihydrate, hemihydrate and anhydrite.

In sulfuric acid media, equilibrium 4.3.1 is further influenced by the dissociation of H_2SO_4 solution:

$$H_2SO_4 \overset{K1}{\rightleftharpoons} HSO_4^- + H^+ \qquad (4.3.3)$$

$$HSO_4^- \overset{K2}{\rightleftharpoons} SO_4^{2-} + H^+ \qquad (4.3.4)$$

where K_1 and K_2 are the first and second dissociation constants of H_2SO_4 respectively.

At low temperatures (25 to ~60°C), according to Marshall et al. [20] and Zhang et al. [36], H_2SO_4 has a positive effect on the solubility of calcium sulfates in the low concentration range (0 to about 15 wt%). This increase in solubility is attributed to the influence of the second dissociation constant of H_2SO_4 as well as to an increase in ionic strength which results to a decrease in the respective activity coefficients (refer to equation 4.3.2) [20]. With further increase of H_2SO_4 concentration (about 15 wt% to about 50 wt%), the solubility decreases due to a combination of effects, activity coefficient changes and common-ion salting-out; when the concentration of H_2SO_4 goes to very high (about 50 wt% or higher), the solubility increases again due to the formation of $CaSO_4{\cdot}nH_2SO_4$ complexes [27, 33, 37]. Finally, upon temperature elevation, the solubility curves basically follow the same trend with the solubility increasing with temperature [43].

4.3.2 Experimental

Generally, there are two ways to determine the solubility: one is the precipitation method and the other is the dissolution method. The dissolution method is thought to be more reliable simply because it avoids the complications arising from a reactive process as is precipitation. In this work, the dissolution method was used.

The same glass reactor described in section 3.3 was used for this work except that reflux condenser was installed for re-collecting the water vapor. Around 20 grams dihydrate or hemihydrate was introduced into the 500 mL (measured at room temperature) H_2SO_4 solution that was preheated to 25, 75 or 100°C accordingly. The agitation speed was controlled at around 300 rpm. At different temperatures (25 and 100°C), the effect of retention time to allow equilibration was first investigated in 1.5M (1.59 m or 13.485 wt%) H_2SO_4 solution by sampling at different time intervals. When optimum retention time was determined, other concentrations such as 0, 0.1, 0.25, 0.4, 0.5, 0.6, 0.8, 1.0, 1.1, 1.2, 1.3, 1.4, 1.6, 1.8, 2.4, 3.0 and 6.0M were tested. The solids were filtered with cellulosic filter papers from OSMONICS Inc.[5] with porosity of 0.1 micron (Cat. NO E01WP02500). For tests above room temperature, the filtration unit including the filtrate was heated with heating tape. The final analysis of Ca and S was done with ICP-AES. The solubility was expressed as equivalent amount of $CaSO_4$ based on the measured Ca abundance. The density values used to convert among different units such as g/L, M, wt% and m (refer to Appendix A) were calculated with OLI StreamAnalyzer [17], which was pre-calibrated with a few experimental data.

4.3.3 Results and discussion

As shown in Figure 4.8, either starting material, dihydrate or hemihydrate, can saturate the sulfuric acid solution in very short period of time, around 5 minutes[6]. The variation of the measured data is attributed to the experimental errors such as volumetric sampling, dilution and ICP stability.

---

[5] Use of trade names does not constitute a TVA (Temporary Vocational Authorization) endorsement.

[6] This conclusion was also indirectly supported by the work of Sullivan et al. [44], in which they found "*equilibrium*" of hemihydrate in phosphoric acid was established within 3 minutes. In the present work the author avoided using the term "*equilibrium*" since hemihydrate is a metastable phase and the only final stable phase at equilibrium point is anhydrite under such conditions. See thermodynamic analysis presented in section 4.2.

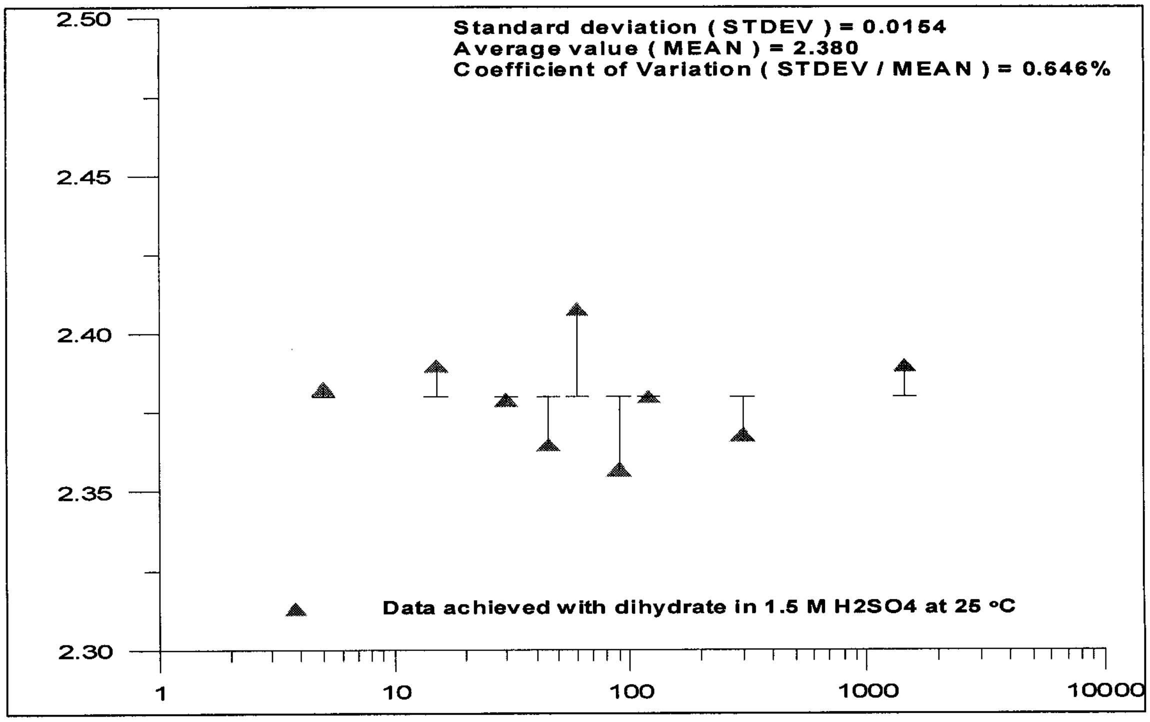

(a) Starting material as dihydrate

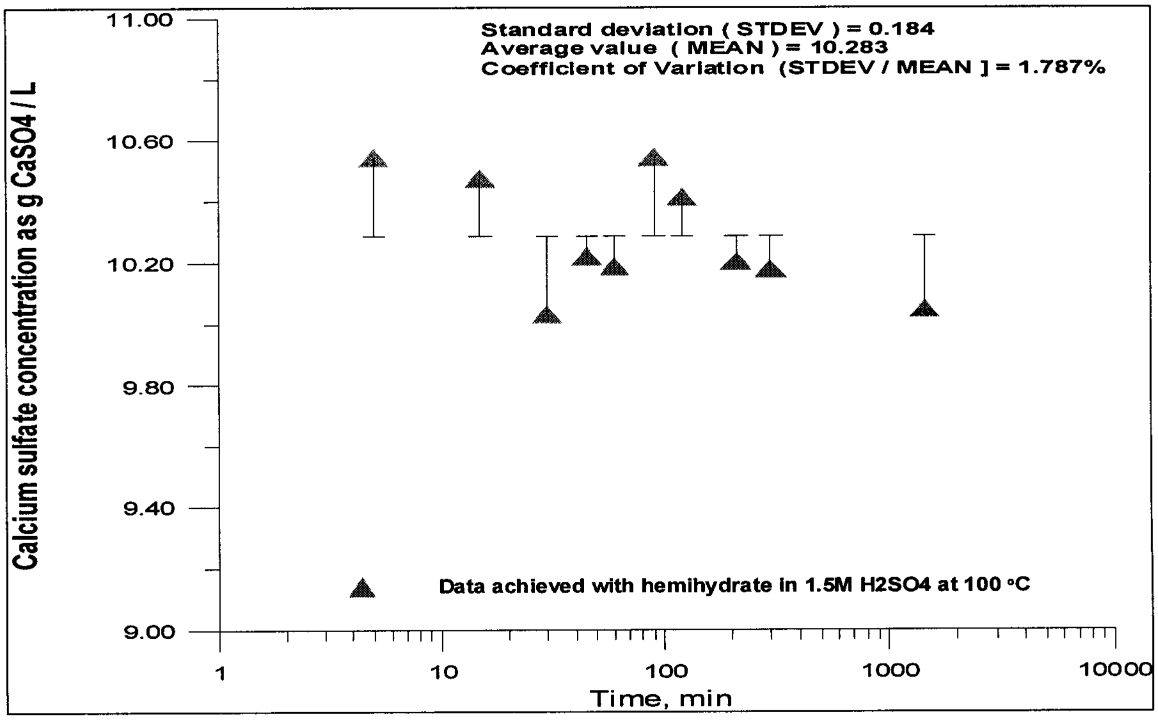

(b) Starting material as hemihydrate

Figure 4.8: The effect of equilibration time on $CaSO_4$ concentration in 1.50M H_2SO_4 at 25 and 100°C

Based on the results of the equilibration time tests, the retention time for the following tests was set at 2 hours with samples taken at 60, 90 and 120 minute. There were 3 replicate measurements which were averaged to get the final solubility value for each H_2SO_4 concentration.

Measurements at 25°C and 70°C were made simply for the purpose of confirmation. As can be seen in Figure 4.9, the data collected in this work exhibit good reproducibility behavior and compare well with published data.

As per findings described in section 4.2, dihydrate was "stable" or "metastable" in the whole H_2SO_4 concentration range tested (0-1.5M) only at 25 and 70°C. At 100°C, dihydrate was "stable" only at zero acidity. All other acid concentrations resulted in conversion of dihydrate to hemihydrate or anhydrite. On the other hand, hemihydrate remained "stable" (within the 2-hour testing time) throughout the acid concentration range tested (0-1.8M) at 100°C. The solubility measurements at 100°C were independent of the starting phase, i.e., dihydrate or hemihydrate (refer to Figure 4.10) simply because as mentioned above dihydrate had converted to hemihydrate or anhydrite (except when no H_2SO_4 was present [7]).

The solubility data (as equivalent $CaSO_4$) of calcium sulfate in sulfuric acid solutions at 100°C is given in Table 4.2 and 4.3; graphical plots are shown as well in Figures 4.11 - 4.13, where solubilities are expressed in respectively g/L, wt% and m[8]. It was found that, in the lower range of H_2SO_4 concentration (0-3.0M), the solubility data could be fitted with a 3rd-degree polynomial:

$$Sol_{CaSO4,\ g/L} = 1.59597M^3 - 10.8168M^2 + 18.5334M + 2.19264 \qquad (4.3.5)$$

With R-squared (goodness of fit, or coefficient of determination) = 0.989466;

In the range of 0-25wt %, the solubility can be expressed as:

---

[7] As far as the solubilities of dihydrate and of hemihydrate in pure water are concerned, there exists some discrepancy with the literature [45] which reported that dihydrate have lower solubility than that of hemihydrate.

[8] It was decided to present solubility data in such way that they are both practical (when expressed in g/L) and consistent with thermodynamics (when expressed in m or wt% units). Such multiple unit representation makes comparison with literature data easier.

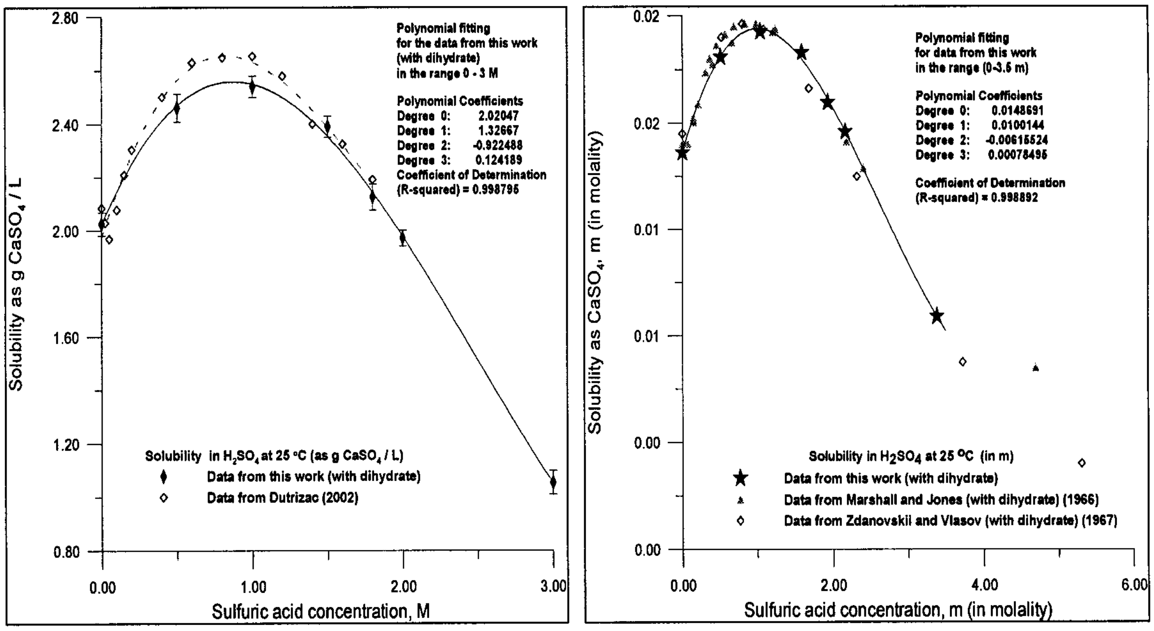

(a) Data measured at 25°C(original as g $CaSO_4$ /L)

(b) Data at 25°C in m

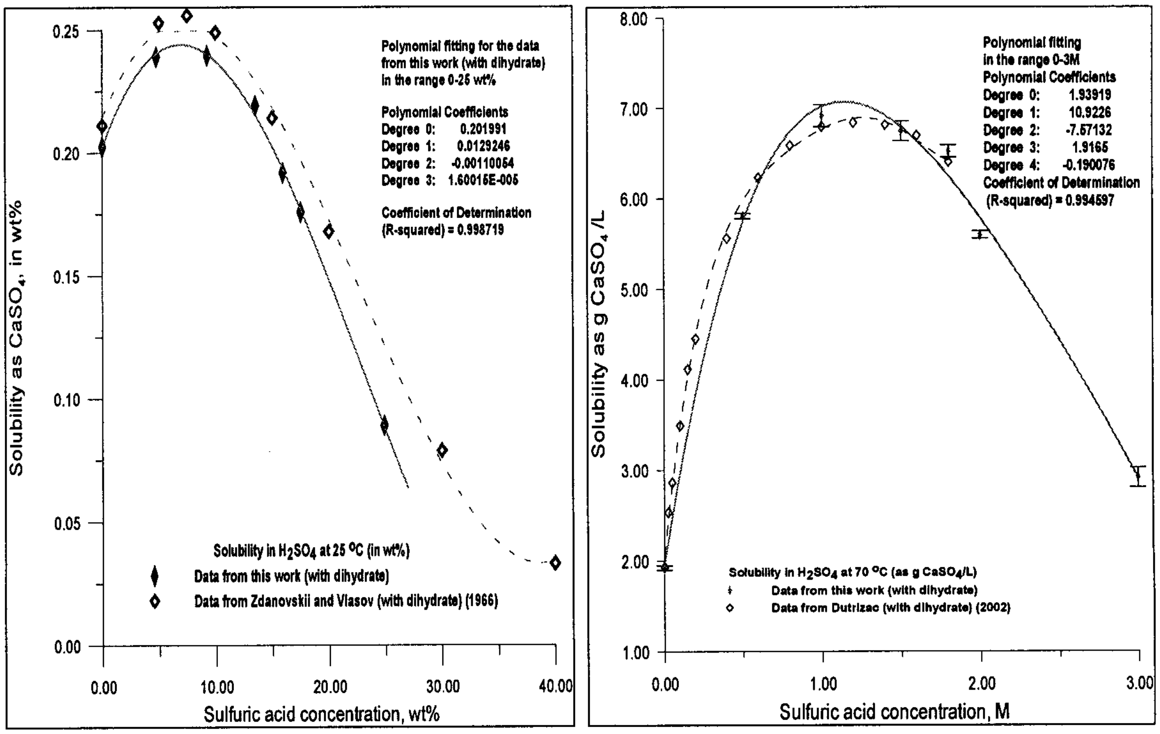

(c) Data at 25°C in wt%

(d) Data measured at 70°C(as g $CaSO_4$ /L)

Figure 4.9: Dihydrate solubility data in H_2SO_4 solutions measured at 25 and 70°C

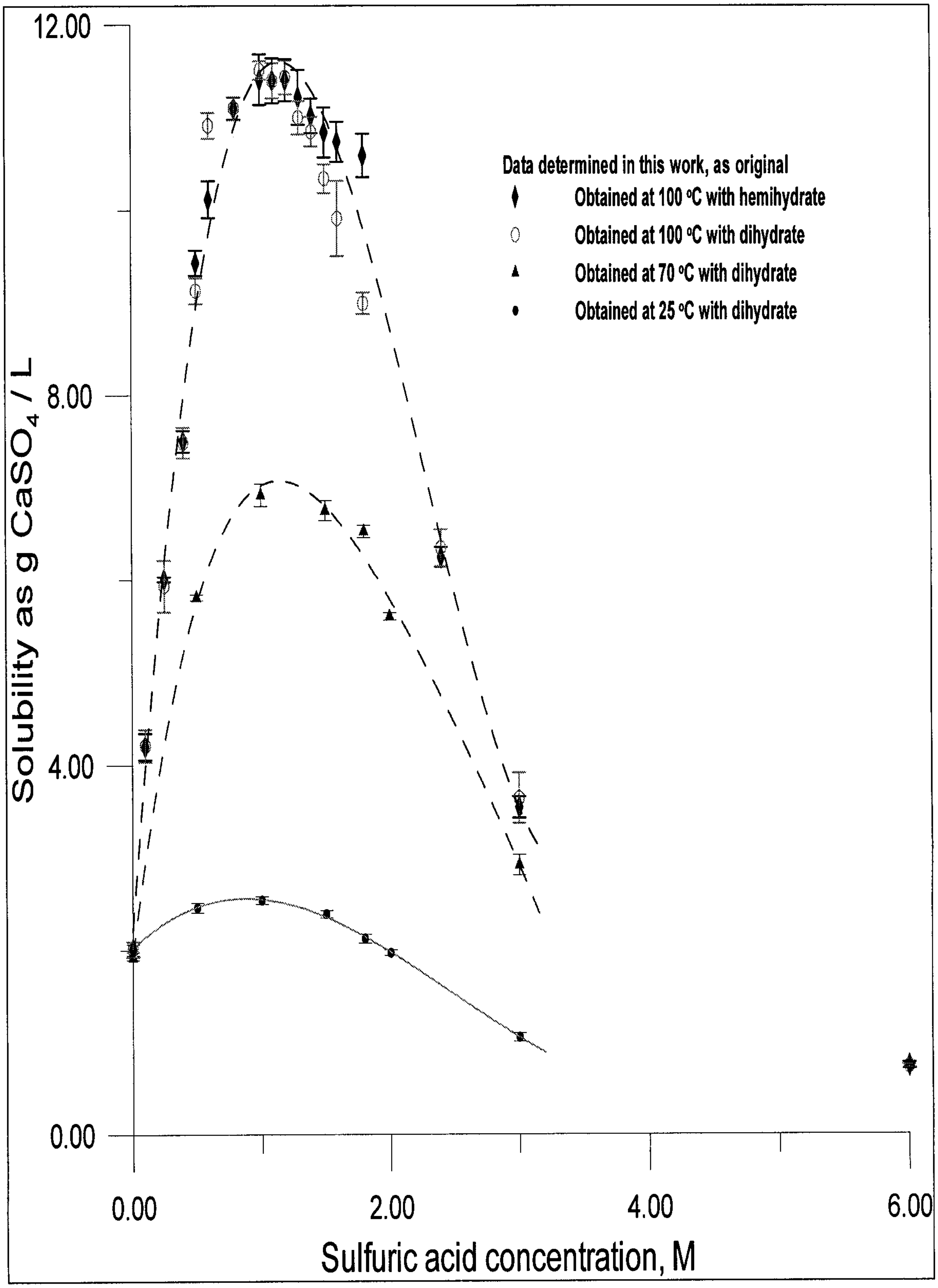

Figure 4.10: $CaSO_4$ solubility in the 0-3.0M H_2SO_4 range as a function of temperature

$$Sol_{CaSO4,\,wt\%}=0.000224189\ wt\%^{3} - 0.0137187\ wt\%^{2} + 0.206176\ wt\% + 0.217479 \quad (4.3.6)$$

With R-squared (goodness of fit, or coefficient of determination) = 0.989092;

In the range of 0-3.5 m, the solubility can be expressed as:

$$Sol_{CaSO4,\,m} = 0.00984176m^{3} - 0.072212m^{2} + 0.135638m + 0.0176073 \quad (4.3.7)$$

With R-squared (goodness of fit, Coefficient of Determination) = 0.988261.

Table 4.2: Solubility of calcium sulfate (added as dihydrate) in sulfuric acid solutions at 100°C

Solution parameters				Solubility as $CaSO_4$ in different units***				Solid phase after 2 hour equilibration (by XRD)
H_2SO_4 molarity (M)*	H_2SO_4 molality (m)	H_2SO_4 (wt%)	Density ** of saturated solution (g/mL)	$CaSO_4$ (g/L)	Standard deviation	$CaSO_4$ (wt%)	$CaSO_4$ (m)	
0.00	0.00	0.00	0.959	2.012	0.082	0.210	0.0154	DH
0.10	0.10	0.98	0.967	4.210	0.173	0.436	0.0323	DH+HH
0.25	0.25	2.42	0.973	5.934	0.279	0.610	0.0459	DH+HH
0.40	0.41	3.83	0.985	7.485	0.165	0.760	0.0581	DH+HH
0.50	0.51	4.76	0.990	9.131	0.139	0.922	0.0712	HH
0.60	0.61	5.68	0.993	10.917	0.139	1.099	0.0857	HH
0.80	0.83	7.49	1.007	11.100	0.125	1.102	0.0876	HH
1.00	1.04	9.25	1.018	11.510	0.098	1.131	0.0916	HH
1.10	1.15	10.12	1.024	11.400	0.191	1.114	0.0911	HH
1.20	1.26	10.97	1.027	11.434	0.182	1.113	0.0919	HH
1.30	1.37	11.82	1.034	11.000	0.180	1.064	0.0887	HH
1.40	1.48	12.66	1.040	10.850	0.157	1.044	0.0879	HH
1.50	1.59	13.49	1.043	10.340	0.156	0.991	0.0842	HH
1.60	1.70	14.30	1.050	9.910	0.408	0.944	0.0810	HH
1.80	1.93	15.91	1.058	8.995	0.116	0.850	0.0743	HH
2.40	2.64	20.54	1.090	6.343	0.199	0.582	0.0538	AH
3.00	3.38	24.87	1.122	3.643	0.274	0.325	0.0318	AH
6.00	7.90	43.64	1.270	0.730	0.018	0.057	0.0075	AH

* Refer to the room temperature (around 20°C).

** Estimated with the aid of OLI.

*** Solubility values are averaged values of the samples at 60, 90 and 120 min.

Table 4.3: Solubility of calcium sulfate (added as hemihydrate) in sulfuric acid solutions at 100°C

Solution parameters				Solubility as $CaSO_4$ in different units***				Solid phase after 2 hour equilibration (by XRD)
H_2SO_4 molarity (M)*	H_2SO_4 molality (m)	H_2SO_4 (wt%)	Density** of saturated solution (g/mL)	$CaSO_4$ (g/L)	Standard deviation	$CaSO_4$ (wt%)	$CaSO_4$ (m)	
0.00	0.00	0.00	0.959	2.012	0.082	0.210	0.0154	HH
0.10	0.10	0.98	0.967	4.200	0.142	0.435	0.0323	HH
0.25	0.25	2.42	0.973	6.006	0.027	0.617	0.0465	HH
0.40	0.41	3.83	0.985	7.500	0.119	0.762	0.0582	HH
0.50	0.51	4.76	0.990	9.431	0.136	0.953	0.0735	HH
0.60	0.61	5.68	0.993	10.117	0.199	1.019	0.0794	HH
0.80	0.83	7.49	1.007	11.100	0.119	1.102	0.0876	HH
1.00	1.04	9.25	1.018	11.410	0.274	1.121	0.0908	HH
1.10	1.15	10.12	1.024	11.400	0.241	1.114	0.0911	HH
1.20	1.26	10.97	1.027	11.405	0.225	1.110	0.0917	HH
1.30	1.37	11.82	1.034	11.220	0.296	1.085	0.0905	HH
1.40	1.48	12.66	1.040	11.020	0.188	1.060	0.0892	HH
1.50	1.59	13.49	1.043	10.840	0.268	1.039	0.0883	HH
1.60	1.70	14.30	1.050	10.740	0.215	1.023	0.0877	HH
1.80	1.93	15.91	1.058	10.590	0.233	1.001	0.0875	HH
2.40	2.64	20.54	1.090	6.243	0.106	0.573	0.0530	AH
3.00	3.38	24.87	1.122	3.543	0.116	0.316	0.0309	AH
6.00	7.90	43.64	1.270	0.740	0.034	0.058	0.0076	AH

* Refer to the room temperature (around 20°C).

** Estimated with the aid of OLI.

*** Solubility data are averaged values of the samples at 60, 90 and 120 min.

Note:

DH: calcium sulfate dihydrate

HH: calcium sulfate hemihydrate

AH: calcium sulfate anhydrite

M: Molarity m: Molality wt%: weight percent

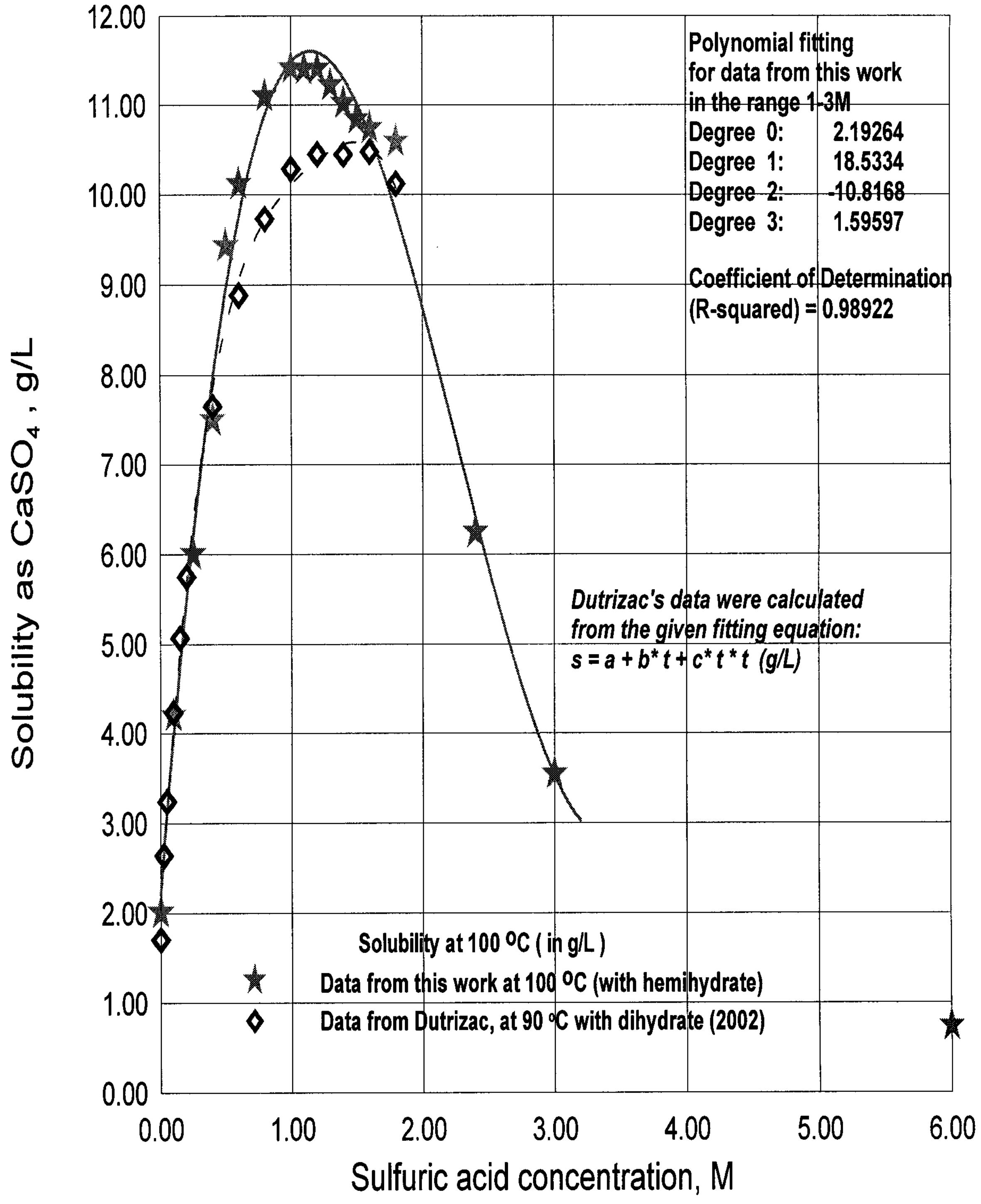

Figure 4.11: Hemihydrate solubility at 100°C in the 0-6.0M H_2SO_4 concentration range (as expressed in g $CaSO_4$ /L)

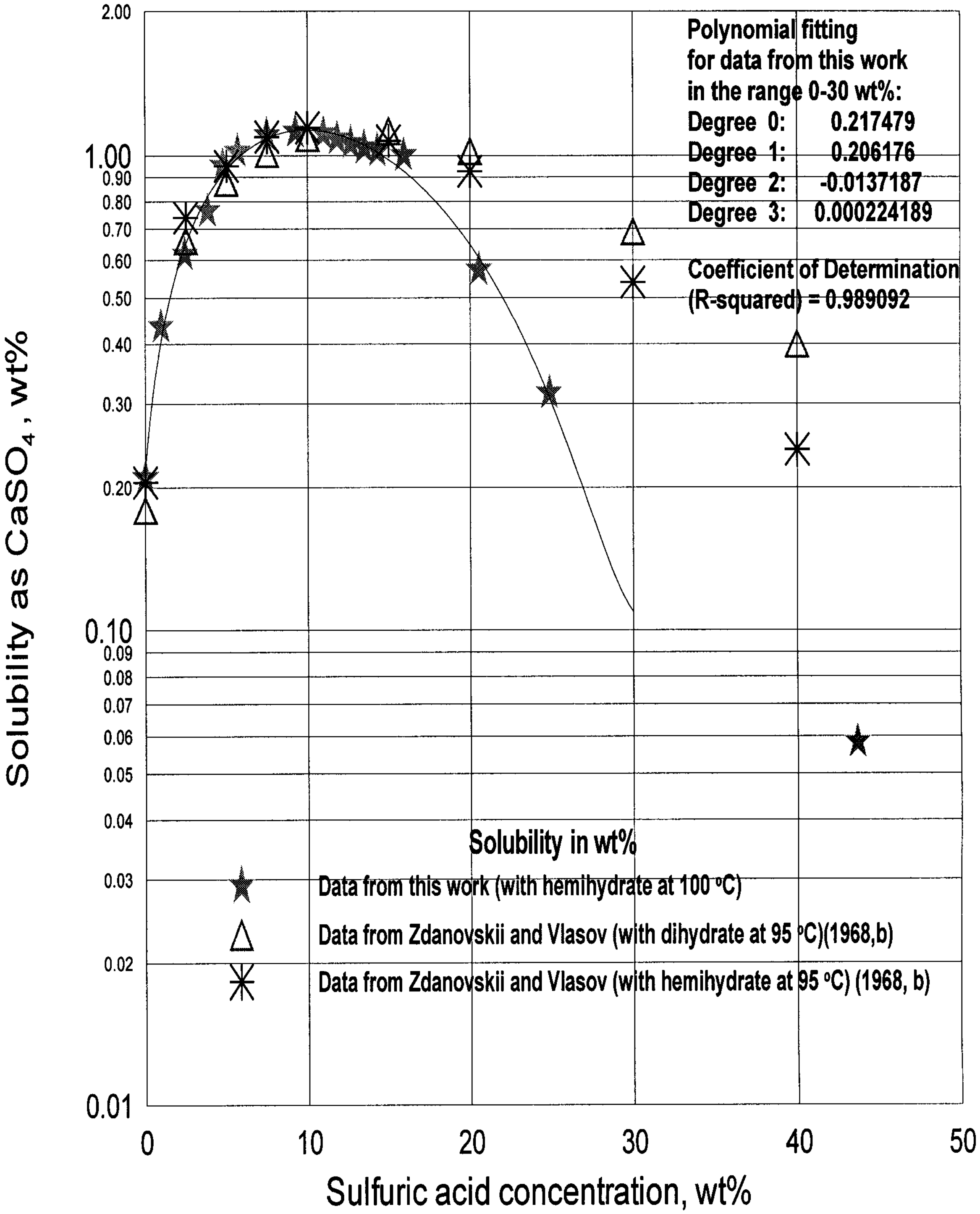

Figure 4.12: Hemihydrate solubility in 0 - 43.5 wt% sulfuric acid solutions at 100°C

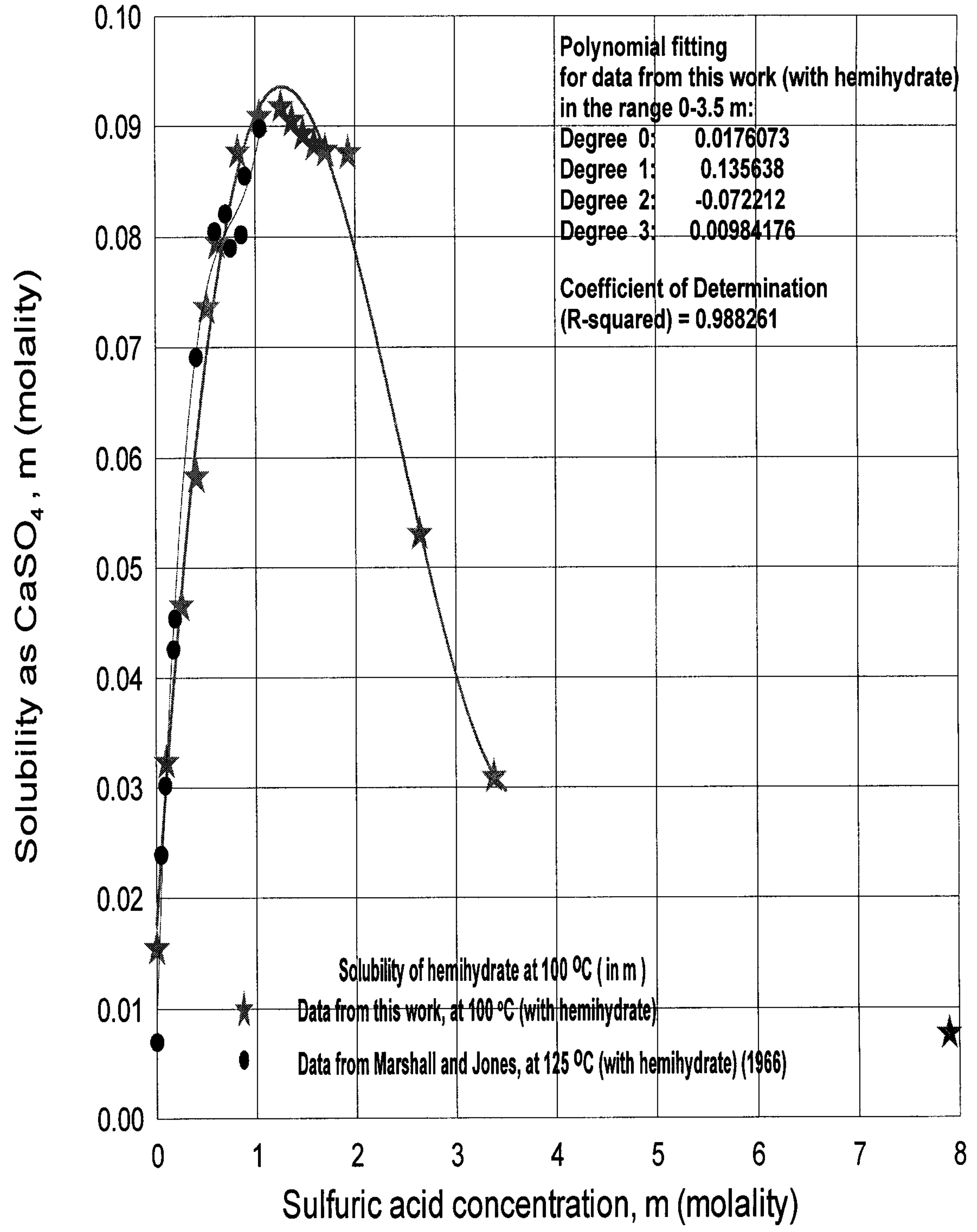

Figure 4.13: Hemihydrate solubility in 0-7.9 m sulfuric acid solutions at 100°C

Unfortunately, there are no literature data for 100°C to compare with data obtained in this work. Wehde and Stichlmair [18] did not provide data tables in their paper; it is almost impossible to extract with accuracy data from their plotted solubility curves (refer to Figure 4.7). Dutrizac [42] listed a series of fitting equations, which permitted to calculate the solubility of calcium sulfate in g $CaSO_4$/L at 90°C. His data are plotted in Figure 4.11. Zdanovskii et al.[23] reported data in terms of wt% for both hemihydrate and dihydrate at 95°C, their data are plotted in Figure 4.12. On the other hand, Marshall and Jones [20] reported the data in terms of m of $CaSO_4$ for hemihydrate at 125°C. These data are plotted in Figure 4.13. It is rather a surprise to see that their data at 125°C are "in very good agreement" with this work's data at 100°C. The reason for this agreement could be found in the later work of Marshall and Jones [46], where it was reported that there is only small change in solubility over the temperature range 125-350°C, this temperature range can be extended now to 100-350°C if the results of this work are included. The effect of temperature in the range 25 to 100°C is better illustrated with the plots of Figure 4.10.

4.4 Conclusions

(1) Based on thermodynamic calculations, it was concluded that, in pure water, the transition temperature between dihydrate and anhydrite is 55.7°C, and the transition temperature between dihydrate and hemihydrate is 106.6°C.

(2) Hemihydrate can only exist metastably; in pure water, below 55.7°C, dihydrate is more stable than anhydrite; and above 55.7°C, anhydrite is the stable phase, dihydrate can exist metastably, and more stable than hemihydrate up to 106.6°C, whereas hemihydrate is more stable than dihydrate above 106.6°C.

(3) The phase transition temperatures, between dihydrate and anhydrite and between dihydrate and hemihydrate, in the aqueous solution are exclusively determined by the water activity.

(4) The water activity was correlated to the concentration of sulfuric acid with the aid of OLI StreamAnalyzer under the assumption that the effect of the saturated calcium sulfate on the activity of water is negligible.

(5) Phase diagram for the $CaSO_4$–H_2SO_4–H_2O system was quantitatively established. The stable zones for dihydrate and anhydrite were well defined. The metastable zones for dihydrate and hemihydrate were also clearly delineated.

(6) For the reactions between CaO and H_2SO_4, below 55.7°C, dihydrate is the most probable product; above 55.7°C, anhydrite is most probable product; in the range 55.7°C to 104.64°C, metastable phase dihydrate is more probable than hemihydrate; and vice versa above 104.64°C.

(7) Independent of the starting material used, i.e., dihydrate or hemihydrate, the sulfuric acid solution was saturated in very short period of time, around 5 minutes.

(8) The solubility of calcium sulfate (more specifically calcium sulfate hemihydrate) in H_2SO_4 solutions with concentration range of 0-3.0M at 100°C was determined for the first time.

(9) The following empirical equations are the solubility of hemihydrate[9] at 100°C in the H_2SO_4 concentration range 0-3.0M or 0-25wt% or 0-3.5m:

$$Sol_{CaSO4,\,g/L} = 1.59597M^3 - 10.8168M^2 + 18.5334M + 2.19264$$

$$Sol_{CaSO4,\,wt\%} = 0.000224189wt\%^3 - 0.0137187wt\%^2 + 0.206176wt\% + 0.217479$$

$$Sol_{CaSO4,\,m} = 0.00984176m^3 - 0.072212m^2 + 0.135638m + 0.0176073.$$

---

[9] The starting material is in the form of hemihydrate. However, the equilibrating phase is anhydrite at the 2-hour testing interval in the H_2SO_4 solutions with concentrations of ~2.0M and above.

References

[1] Raju, K.U.G. and Atkinson, G., The thermodynamics of "scale" mineral solubilities: (3) Calcium sulfate in aqueous NaCl, Journal of Chemical and Engineering data, 35(3), 361-167 (1990).

[2] Barner, H.E. and Scheuerman, R.V., Handbook of Thermochemical Data for Compounds and Aqueous Species, John Wiley & Sons: New York, NY, USA, 37-38, 50, 78(1978).

[3] CRC Handbook of Chemistry and Physics 72nd (1991-92), Selected Values of Chemical Thermodynamic Properties, CRC Press: Cleveland, Ohio, 5-23 (1992) (currently 83rd edition, 2002; refer to http://www.crcpress.com/ or http://www.library.mcgill.ca/psel/database/restricted/crchandbook.htm).

[4] Barin, I., Knacke, O. and Kubaschewski, O., Thermochemical Properties of Inorganic Substances, Springer-Verlag: Berlin, German, 176-177(1973).

[5] Wagman, D. D., Evans, W. H., Parker, V. B., Schumm, R. H., Halow, I., Bailey, S. M., Churney, K. L. and Nuttall, R. L., Journal of Physical and Chemical Reference Data, Vol. 11, Suppl. No. 2: The NBS Tables of Chemical Thermodynamic Properties. Selected Values for Inorganic and C1 and C2 Organic Substances in SI Units, (1982), 392 pp.

[6] Thermal data in online databank, http://gibbs.ipe.ac.cn/sdb/frame_database.htm, or http://gibbs.ipe.ac.cn/ITDB/ITDB.htm.

[7] FactSage software, http://www.FactSage.com.

[8] Hardie, L.A., The gypsum-anhydrite equilibrium at one atmosphere pressure, American Mineralogist, 52(1-2), 171-200(1967).

[9] Blount, C.W. and Dickson, F.W., Gypsum-anhydrite equilibriums in systems calcium sulfate-water and calcium sulfate-sodium chloride-water, American Mineralogist, 58(3-4), 323-331(1973).

[10] Innorta, G., Rabbi, E. and Tomadin, L., The gypsum-anhydrite equilibrium by solubility measurements, Geochimica et Cosmochimica Acta, 44(12), 1931-1936 (1980).

[11] Langmuir, D. and Melchior, D., The geochemistry of calcium, strontium, barium and radium sulfates in some deep brines from the Palo Duro Basin, Texas, Geochimica et Cosmochimica Acta, 49(11), 2423-2432(1985).

[12] Posnjak, E., Deposition of calcium sulfate from sea water, American Journal of Science, 238, 559(1940).

[13] Partridge, E.P. and White, A.H., Solubility of calcium sulfate from 0°C to 200°C, Journal of American Chemical Society, 51, 360-370(1929).

[14] Hill, A.E., The transition temperature of gypsum to anhydrite, Journal of American Chemical Society, 59, 2242-2244(1937).

[15] Martynowicz, E.T.M.J., Witkamp, G.J. and van Rosmalen, G.M., The effect of aluminum fluoride on the formation of calcium sulfate hydrates, Hydrometallurgy, 41(2-3), 171-186(1996).

[16] Marshall, W.L. and Slusher, R., Aqueous systems at high temperature: Solubility to 200°C of calcium sulfate and its hydration in sea water and saline water concentrates, and temperature-concentration limits, Journal of Chemical and Engineering Data, 13(1), 83-93 (1968).

[17] OLI software, http://www.olisystems.com.

[18] Wehde, K.H. and Stichlmair, J., Solubility behavior of inorganic sulfates in sulfuric acids of various concentrations, Chem.-Ing.-Tech., 57(4), 348-349(1985) (in German).

[19] Kleinert, T. and Wurm, P., Solubilities in the aqueous system sulfuric acid-sodium-calcium sulfate, Monatsh., 83, 459-462(1952)(in German).

[20] Marshall, W.L. and Jones, E.V., Second dissociation constant of sulfuric acid from 25 to 350° evaluated from solubilities of calcium sulfate in sulfuric acid solutions, The Journal of Physical Chemistry, 70(12), 4028-4040(1966).

[21] Augustyn, W. and Fligier, M., Solubility of calcium sulfate in aqueous solutions of fluosilicic and sulfuric acids, Polish Journal of Chemistry, 55, 1947-1950(1981).

[22] Zdanovskii, A.B. and Vlasov, G.A., Solubility of various modifications of calcium sulfate in sulfuric acid solutions at 25°C, Zhurnal Neorganicheskoi Khimii, 13(10), 2747-2753(1968, a) (in Russian – English translation).

[23] Zdanovskii, A. B., Vlasov, G. A. and Sotnikova, L. I., Dehydration of gypsum in sulfuric acid solutions, Zhurnal Neorganicheskoi Khimii, 13(10), 2754-2757(1968, b) (in Russian – English translation).

[24] Zdanovskii, A. B. and Vlasov, G. A., Determination of the transformation limits of $CaSO_4 \cdot 2H_2O$ and γ-$CaSO_4$ in sulfuric acid solutions, Zhurnal Neorganicheskoi Khimii, 13(9), 2552-2554(1968, c) (in Russian – English translation).

[25] Zdanovskii, A. B. and Vlasov, G. A., Solubility of $CaSO_4 \cdot 2H_2O$ in sulfuric acid solutions at 25°C, Zhurnal Neorganicheskoi Khimii, 12(4), 1101-1102(1967) (in Russian – English translation).

[26] Zdanovskii, A. B. and Spiridonov, F. P., Solubilities of α- and β-modifications of $CaSO_4 \cdot 0.5H_2O$ and $CaSO_4 \cdot 2H_2O$, Zhurnal Neorganicheskoi Khimii, 11(1), 20-24(1966) (in Russian – English translation).

[27] Ostrovskii, S.V., Amirova, S.A. and Kalugina, M.K., Solubility of calcium sulfate in concentrated sulfuric acid, Zh. Neorg. Khim., 14(9), 2503-25-6(1969) (in Russian – English translation).

[28] Schaefer, W. and Hunger, E., Solubility of calcium sulfate in salt-containing, diluted sulfuric acid, German Z. Chem., 9(12), 462(1969) (in German).

[29] Beremzhanov, B.A. and Kruchenko, V.P., Solubility of calcium sulfate in the calcium sulfate – nitric-sulfuric acid – water system at 25 and 50°C, Zh. Neorg. Khim., 17(7), 1996-2000(1972) (in Russian).

[30] Beremzhanov, B.A. and Kruchenko, V.P., Solubility of calcium sulfate in the calcium sulfate – nitric-sulfuric acid – water system at 40°C, Zh. Neorg. Khim., 20(8), 2227-2230(1975) (in Russian).

[31] Beremzhanov, B.A. and Kruchenko, V.P., Solubility of calcium sulfate in the calcium sulfate – nitric-sulfuric acid – water system at 60°C, Zh. Neorg. Khim., 20(11), 3153-3156(1975) (in Russian).

[32] Zemelman, V.B., Identification of the solubility of calcium sulfate, Zh. Prikl. Khim., 48(8), 1666-1669(1975) (in Russian).

[33] Tsikaeva, D.V., Solubilities of calcium sulfate in concentrated solutions of sulfuric acid, Zh. Neorg. Khim., 25(11), 3073-3075(1980)(in Russian).

[34] Dvegubskii, N. S. and Shchiponilova, L.V., Solubility and phase transformation of calcium sulfate in concentrated sulfuric acid at 120-180°C, Zh. Prikl. Khim., 54(2), 234-239(1981) (in Russian).

[35] Khavskii, N.N., Lopatina, G.I. and Shcherbilin, V.B., Solubility of calcium sulfate dihydrate in weak solutions of sulfuric acid, Khim. Khim. Tekhnol., 28(8), 110-111(1985) (in Russian).

[36] Zhang, Y. and Muhammed, M., Solubility of calcium sulfate dihydrate in nitric acid solutions containing calcium nitrate and phosphoric acid, J. Chem. Eng. Data, 34(1), 121-124(1989).

[37] Huang, Y. and Luo, D., Solubilities and phase change of calcium sulfate in concentrated sulfuric acid from 10-200°C, Chengdu Keji Daxue Xuebao, 4, 83-86(1988) (in Chinese).

[38] Mutalala, B.K., Umetsu, Y. and Tozawa, K., Solubility of calcium sulfate in acidic zinc sulfate solutions over a temperature range of 25 to 60°C, Tohuko Daigalu Senko Seiren Kenkyusho Iho, 44(1), 57-68 (1988) (in Japanese).

[39] Kojima, Y., Shibano, K., Yasue, T., Ishii, S. and Arai, Y., Wet synthesis of α-gypsum hemihydrate from II-anhydrite under atmospheric pressure, Inorganic Materials, 255(2), 84-93(1995) (in Japanese).

[40] Calmanovici, C.E., Gabas, N. and Laguerie, C., Solubility measurements for calcium sulfate dihydrate in acid solutions at 20, 50 and 70°C, J. Chem. Eng. Data, 38(4), 534-536(1993).

[41] Martynowicz, E.T.M.J., Witkamp, G.J. and van Rosmalen, G.M., The effect of amuminum fluoride on the formation of calcium sulfate hydrates, Hydrometallurgy, 41(2-3), 171-186(1996).

[42] Dutrizac, J.E., Calcium sulfate solubilities in simulated zinc processing solutions, Hydrometallurgy, 65, 109-135 (2002).

[43] Yadav, S., Sharma, M.K., Siyag, S.R. and Pal, R., Predicting solubility of gypsum in aqueous salt solutions, Journal of the Indian Society of Soil Science, 43(2), 191-196(1995).

[44] Sullivan, J. M., Kohler, J.J. and Grinstead, J.H., Solubility of α-calcium sulfate hemihydrate in 40, 50, and 55% P_2O_5 phosphoric acid solutions at 80, 90, 100, and 110°C, J. Chem. Eng. Data, 33, 367-370 (1988).

[45] Klepetsanis, P.G., Dalas, E. and Koutsoukos, P.G., Role of temperature in the spontaneous precipitation of calcium sulfate dihydrate, Langmuir, 15(4), 1534-1540(1999).

[46] Marshall, W. L. and Jones, E. V., Determination of the solubility of calcium sulfate in sulfuric acid-water solutions at high temperature, U. S. Department Interior, Office of Saline Water Resource Development, Progress Report, No 302, 48-49 (1968).

Chapter 5

Transformation and Precipitation Reactions of Calcium Sulfate Hydrates

5.1 Introduction

As mentioned earlier, the major objective of this work was the development of and study of a method for direct preparation of α-hemihydrate by reaction of lime with sulfuric acid solutions. During the course of the early phase of this investigation, several interesting observations were made that required their systematic study. The first observation was that dihydrate formed during the early stage of the reaction subsequently converting to hemihydrate (refer to section 6.3 in chapter 6). Another observation was that the produced hemihydrate exhibited a needle-shaped morphology, even when the reaction system was seeded with brick-like hemihydrate crystals, suggesting that a dissolution and re-crystallization process was involved.

With the dual purpose on one hand to better design the experiments aimed at producing α-hemihydrate by reaction of H_2SO_4 and CaO and on the other to establish a basis for the interpretation of the obtained results (described in the subsequent chapters), the work described in this chapter was carried out. In particular the work undertaken involved first the transformation (both in terms of chemical structure and morphology) of calcium sulfate dihydrate or hemihydrate in aqueous solution with no acidity (de-ionized water) to high acidity. Then, a series of slow titration tests (for the purpose of controlling supersaturation at low levels) with sub-stoichiometric, stoichiometric or super-stoichiometric addition of H_2SO_4 into a slaked lime slurry were executed during which the evolution of the calcium sulfate hydrate product composition and morphology was monitored.

5.2 Transformation

5.2.1 Experimental

Most of the tests were done in the glass reactor described in section 3.3. The procedure involved preheating to 100°C aqueous H_2SO_4 solutions of varied acidity (from water of pH 6.5 and of pH 2.5, to 0.1M[1] H_2SO_4, 0.5M H_2SO_4, 1.0M H_2SO_4 and 1.5M H_2SO_4) and addition of excess[2] [1] amount of calcium sulfate dihydrate or hemihydrate. The hot slurry was agitated mildly (at about 300 rpm) for different times before subjected to filtration, washing and characterization. No higher than 1.5M H_2SO_4 concentration was tried because it was observed from the preliminary tests that hemihydrate was not stable enough above this H_2SO_4 concentration level to warrant an investigation (this is also supported by other investigators [2]). Finally, in order to check the possibility of instantaneous transformation of hemihydrate, some washing tests were done directly in the filtration/washing unit of the experimental set-up described in section 3.3. Hemihydrate was loaded in the preheated filter and subjected to washing with boiling water or preheated H_2SO_4 solution while samples were taken for characterization about every 5 minutes.

5.2.2 Transformation of calcium sulfate dihydrate

After more than 24 hours equilibration in boiling de-ionized water of pH 6.5 (see Figure 5.1), calcium sulfate dihydrate showed no change in its XRD pattern – i.e., dihydrate was

---

[1] Hereafter, **all H_2SO_4 concentrations reported in M** refer to the temperature of preparation of the solution, i.e. ~20°C, and not the temperature of reaction. Sometimes conversion from M (molarity, moles of solute per liter of solution) to m (molality, moles per 1000 grams solvent) or wt% (weight percentage) has also been used in order to compare with some other literature data.

[2] Here the term "excess" [1] means that, under all conditions tested, there were always "un-dissolved" crystals remaining.

metastable under these conditions. This is in agreement with the discussion presented in section 4.2 of chapter 4 according to which the transition temperature of dihydrate→hemihydrate is above 100°C (i.e., 106.68°C). However, when the pH was adjusted with H_2SO_4 to 2.5, evidence of hemihydrate formation was detected after 28 hours equilibration (see XRD pattern in Figure 5.2). With further increase in acidity to 0.1M H_2SO_4 (at 100°C always), hemihydrate formation was detected as early as after 20 minutes of equilibration (see Figure 5.3). However, the conversion process was slow and a mixture of dihydrate and hemihydrate was present (with dihydrate being the majority phase) even after 28 hours. The results of intermediate tests at 0.5M H_2SO_4 and 1.0M H_2SO_4 are shown in Figures 5.4 and 5.5. As the concentration of H_2SO_4 increased to 1.5M, dihydrate virtually disappeared after around 15 minutes (refer to Figure 5.6) suggesting almost complete conversion of dihydrate to hemihydrate (identified by DSC to be in the form of α-hemihydrate). It may be observed that the conversion of dihydrate to hemihydrate with increasing H_2SO_4 concentration is predicted by the phase diagram constructed in chapter 4 (Figure 4.5). The chemical transformation of dihydrate to hemihydrate was found to be associated with a drastic change of morphology as shown in Figure 5.7.

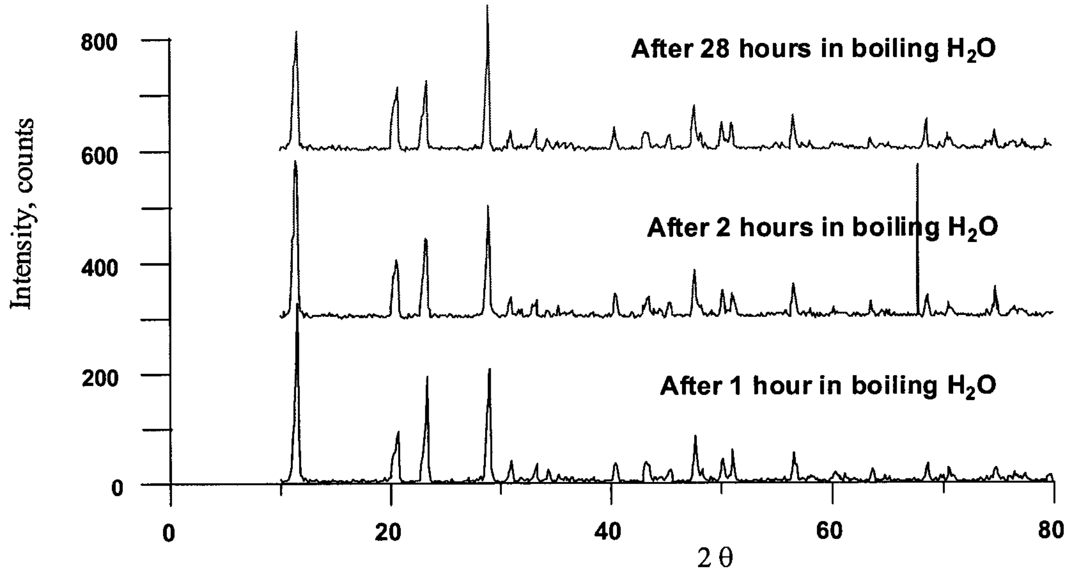

Figure 5.1: XRD monitoring of calcium sulfate dihydrate conversion in boiling water of pH 6.5

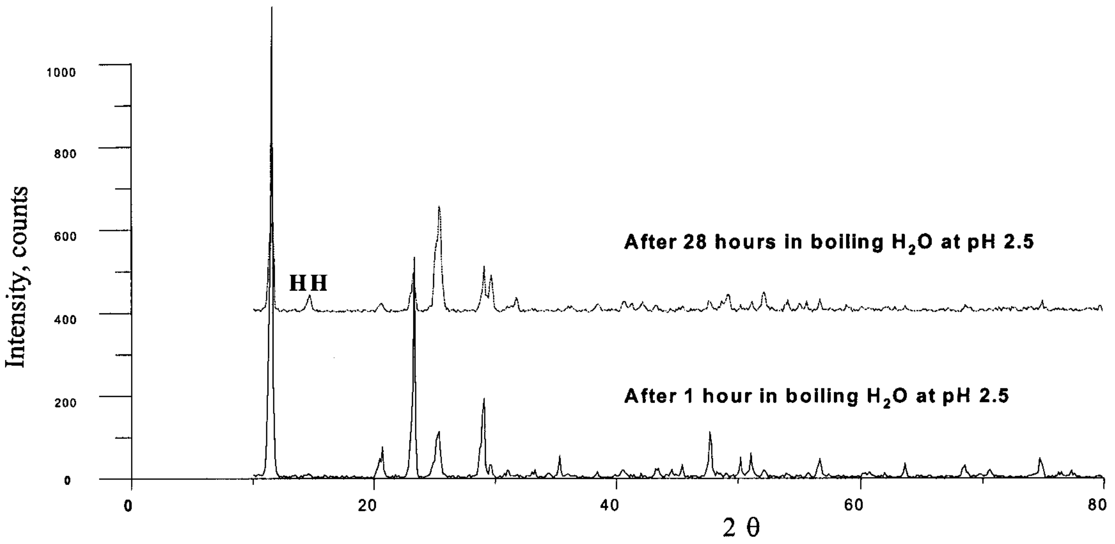

Figure 5.2: XRD monitoring of calcium sulfate dihydrate conversion in boiling water of pH 2.5

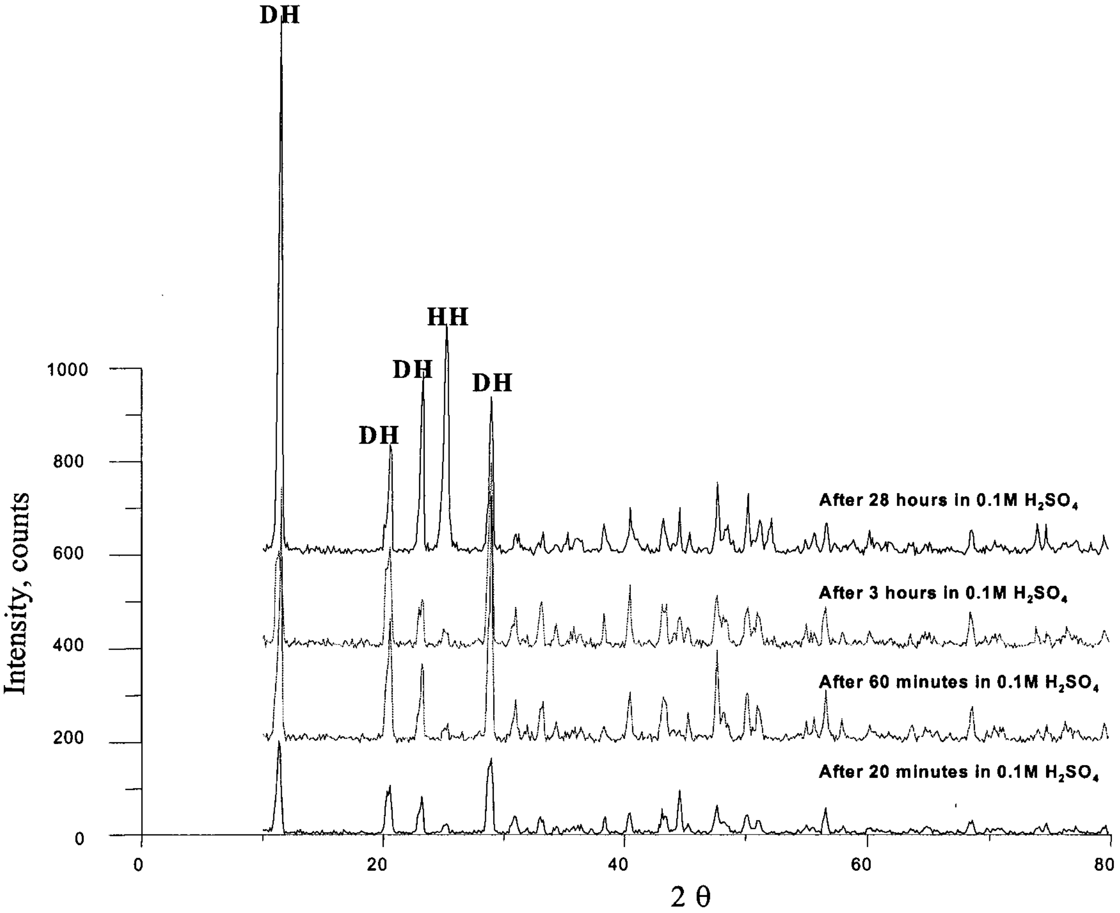

Figure 5.3: XRD monitoring of calcium sulfate dihydrate conversion in 0.1M H_2SO_4 at 100°C

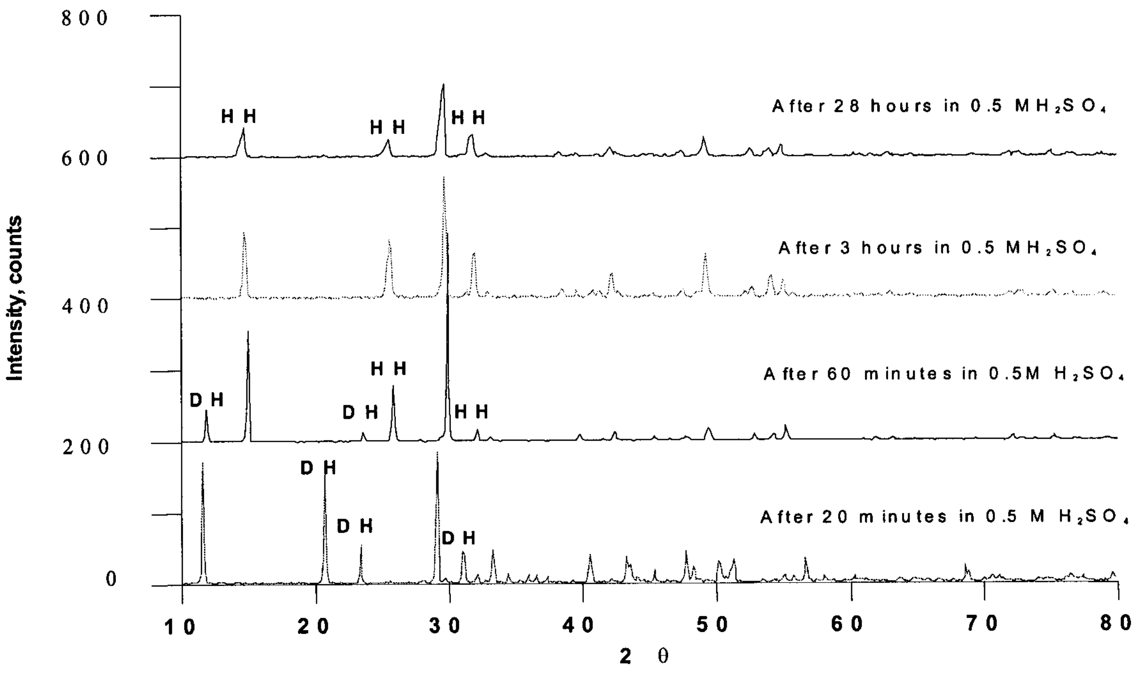

Figure 5.4: XRD monitoring of calcium sulfate dihydrate conversion in 0.5M H_2SO_4 at 100°C

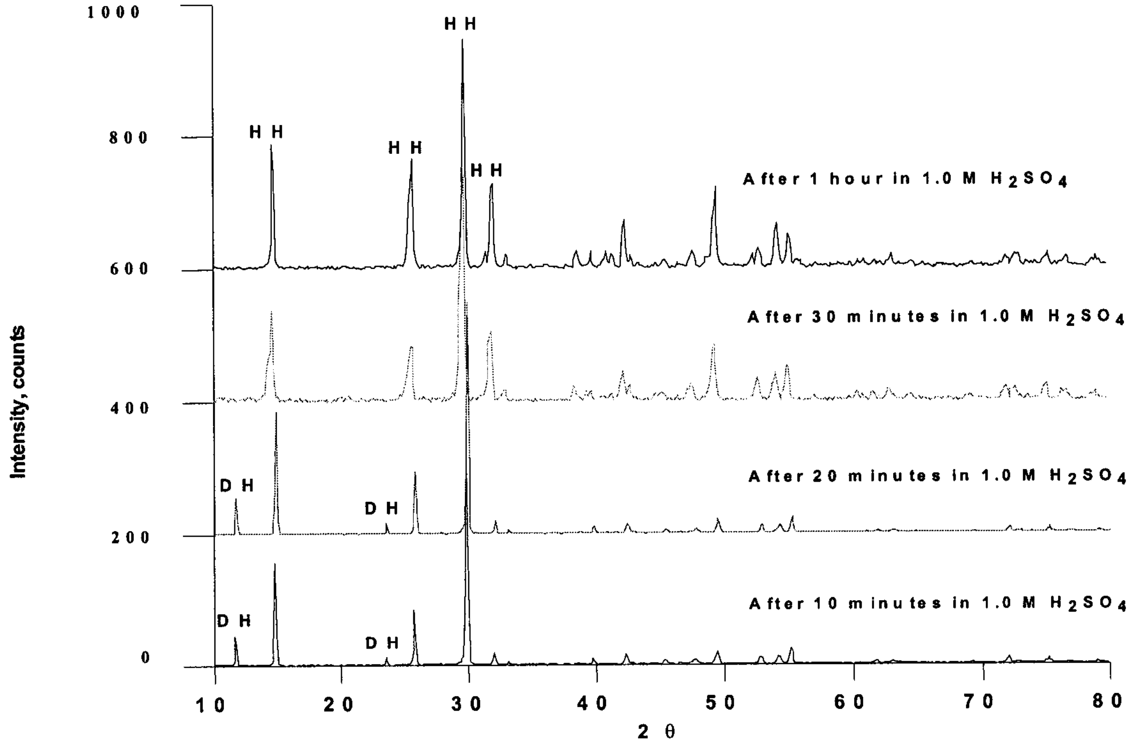

Figure 5.5: XRD monitoring of calcium sulfate dihydrate conversion in 1.0M H_2SO_4 at 100°C

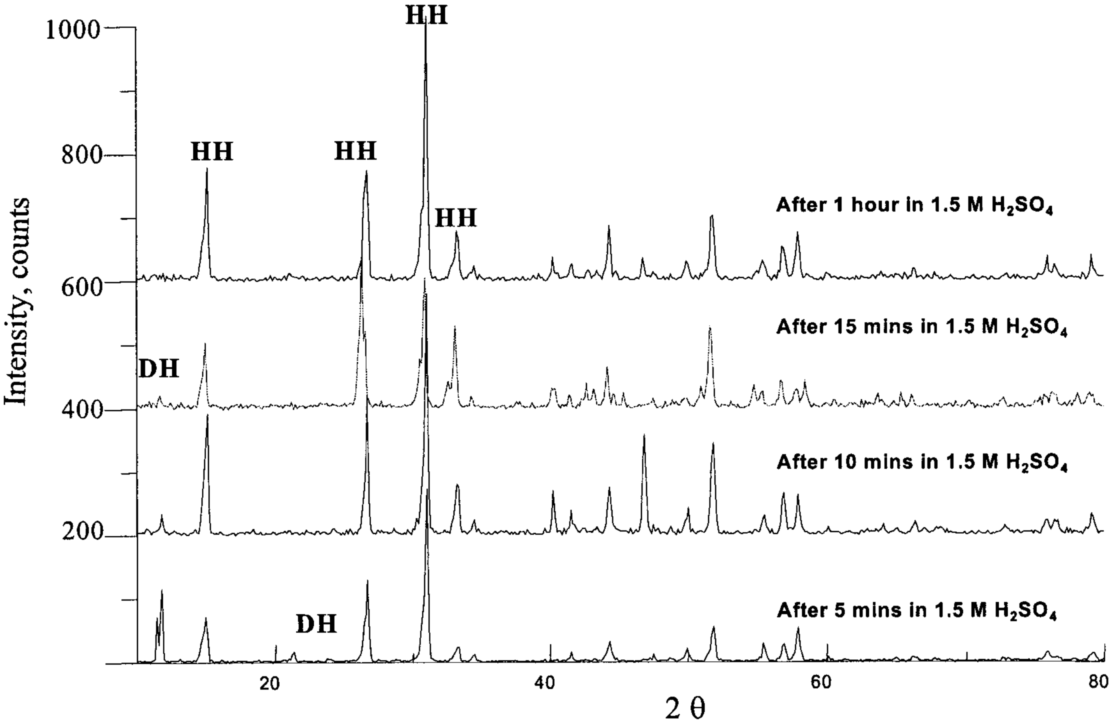

Figure 5.6: XRD monitoring of calcium sulfate dihydrate conversion in 1.5M H_2SO_4 at 100°C

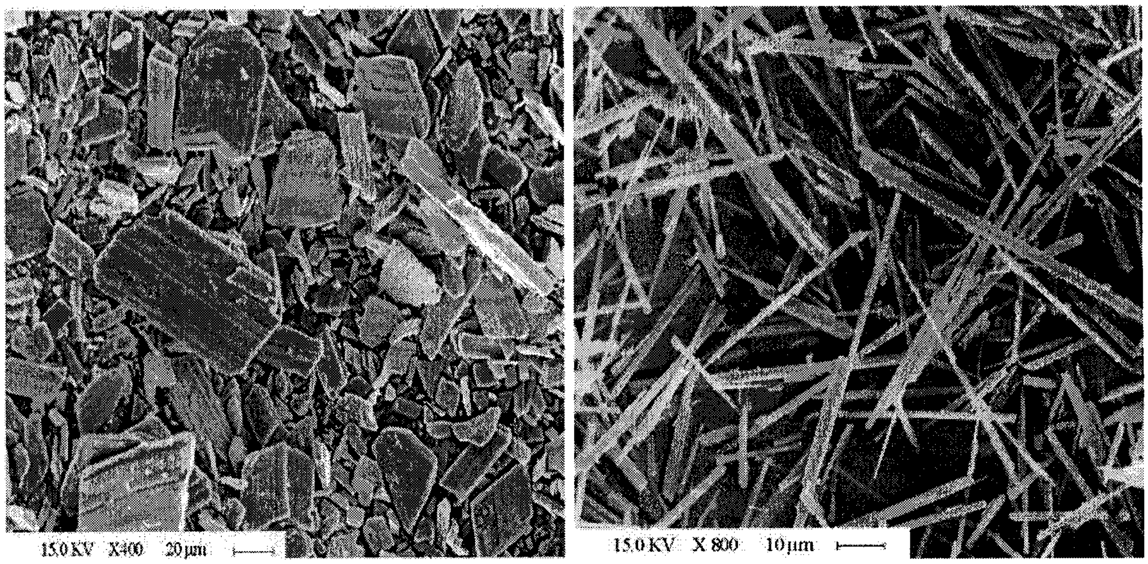

(a) Original shape of dihydrate (b) After 1 hour in 1.5M H_2SO_4 at 100°C

Figure 5.7: Morphological changes upon calcium sulfate dihydrate conversion to hemihydrate in 1.5M H_2SO_4 at 100°C

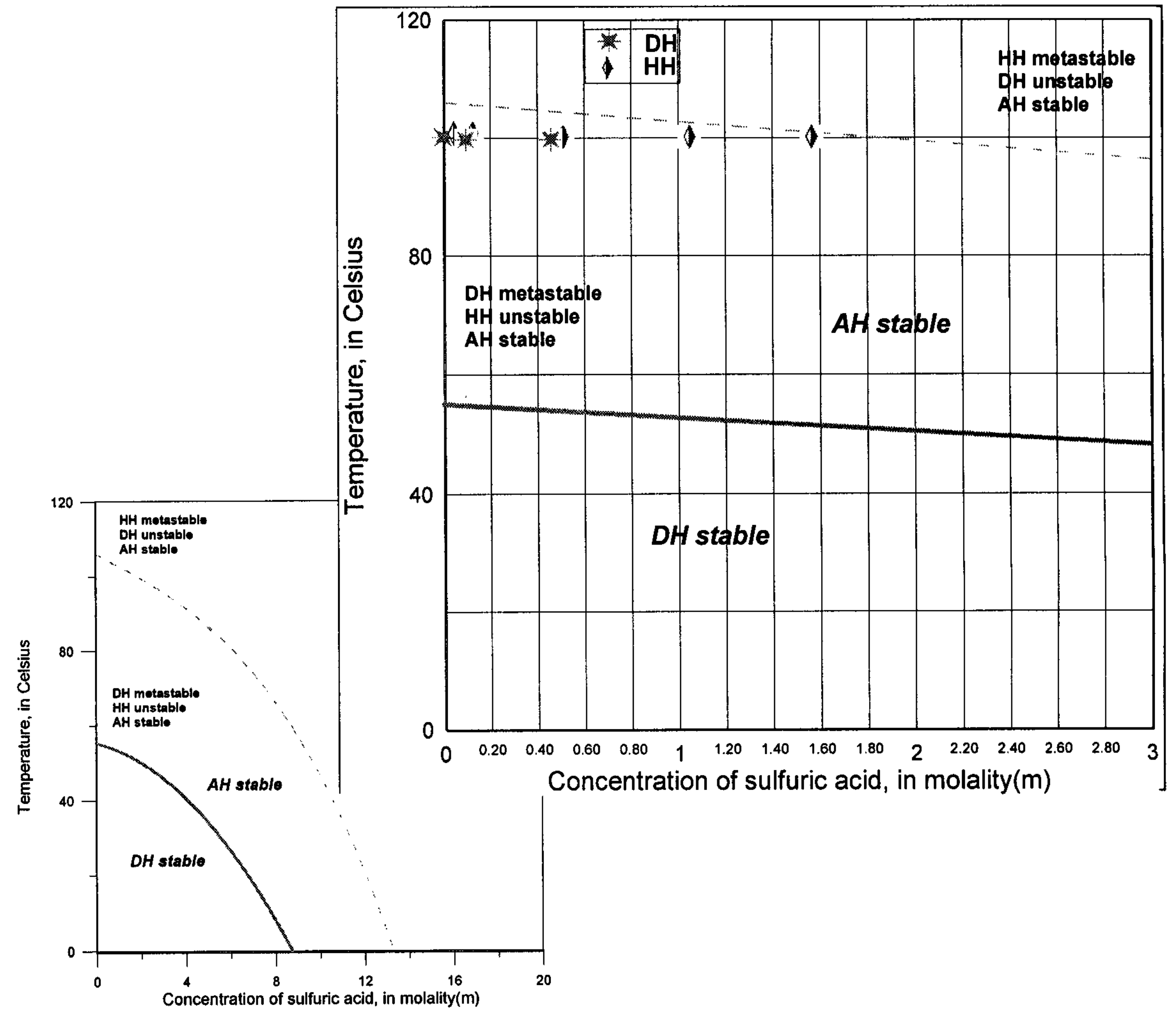

Figure 5.8: "Dihydrate transformation" on the predicted phase diagram

The corresponding points of dihydrate conversion are plotted on the calculated phase diagram (redrawn in Figure 5.8). The finding that dihydrate remains "metastable" in boiling water is in good agreement with the phase diagram prediction. But with the increase of acidity, from pH 2.5 to 0.1M, 0.5M, 1.0M H_2SO_4, hemihydrate was found to be metastable at slightly lower temperatures (by a few degrees) than those predicted by the phase diagram. Overall though there is satisfactory agreement between phase diagram prediction and experimental findings.

5.2.3 Transformation of calcium sulfate hemihydrate

Calcium sulfate hemihydrate was found to be stable for at least 28 hours when in contact with boiling de-ionized water (refer to Figure 5.9). At the same time, hemihydrate morphology remained intact as is evident with the images of Figure 5.10. Increasing the concentration of H_2SO_4 to 0.1M, 0.5M, 1.0M or 1.5M found not to bring a change to hemihydrate as for example can be noticed with the XRD pattern of Figure 5.11. However, in this case, significant change took place in terms of crystal morphology, especially at higher concentrations such as 1.0M and 1.5M (summarized in Table 5.1 at the end of this section). As an example, Figure 5.12 shows the acicular-shaped crystals[3] obtained upon equilibration of block-like hemihydrate crystals (Omega) in 1.5M H_2SO_4 at 100°C for 1 hour.

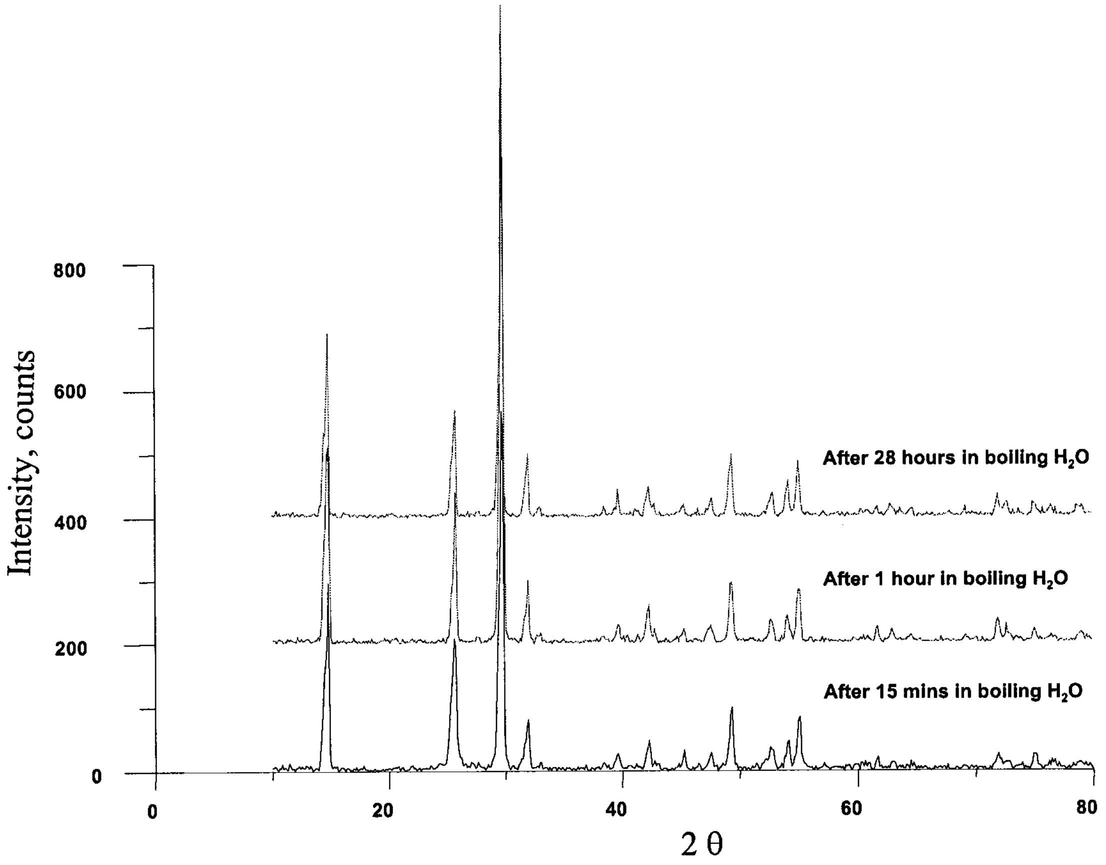

Figure 5.9: XRD monitoring of calcium sulfate hemihydrate in boiling water of pH 6.5

---

[3] These were also determined by DSC to be in the form of α-hemihydrate.

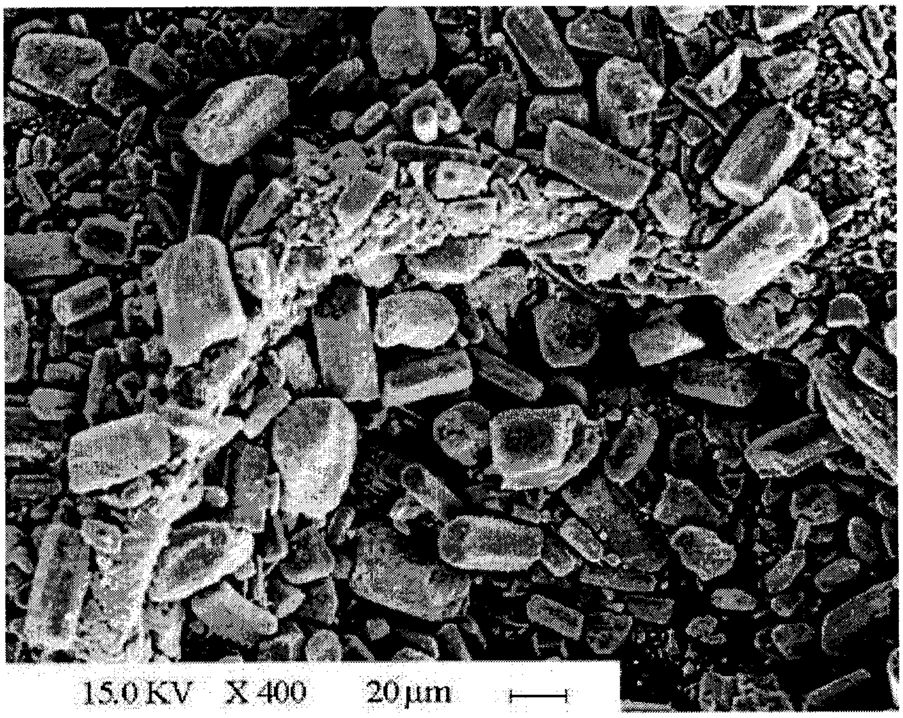

(a) Original hemihydrate (Omega)

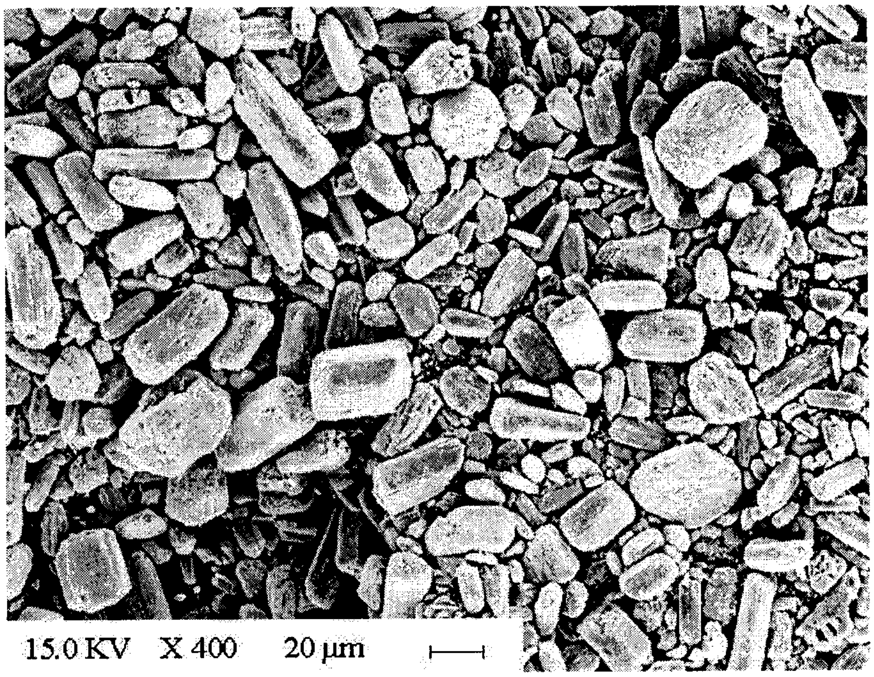

(b) After 28 hours in boiling water

Figure 5.10: SEM images of calcium sulfate hemihydrate (Omega material) equilibrated in boiling water

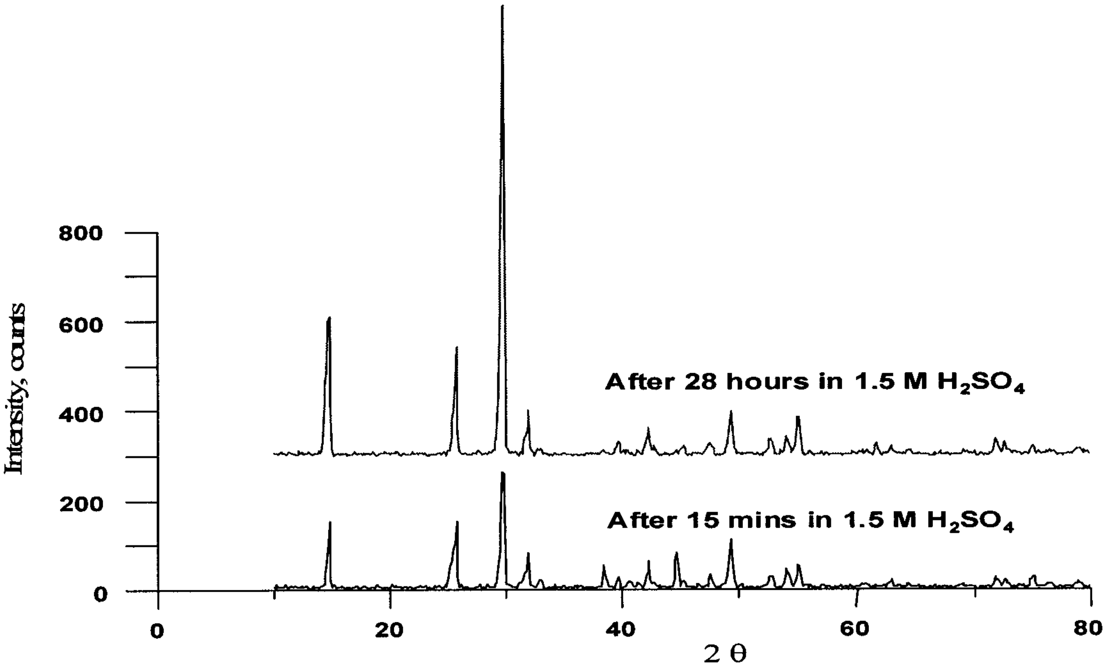

Figure 5.11: XRD monitoring of calcium sulfate hemihydrate in 1.5M H_2SO_4 at 100°C

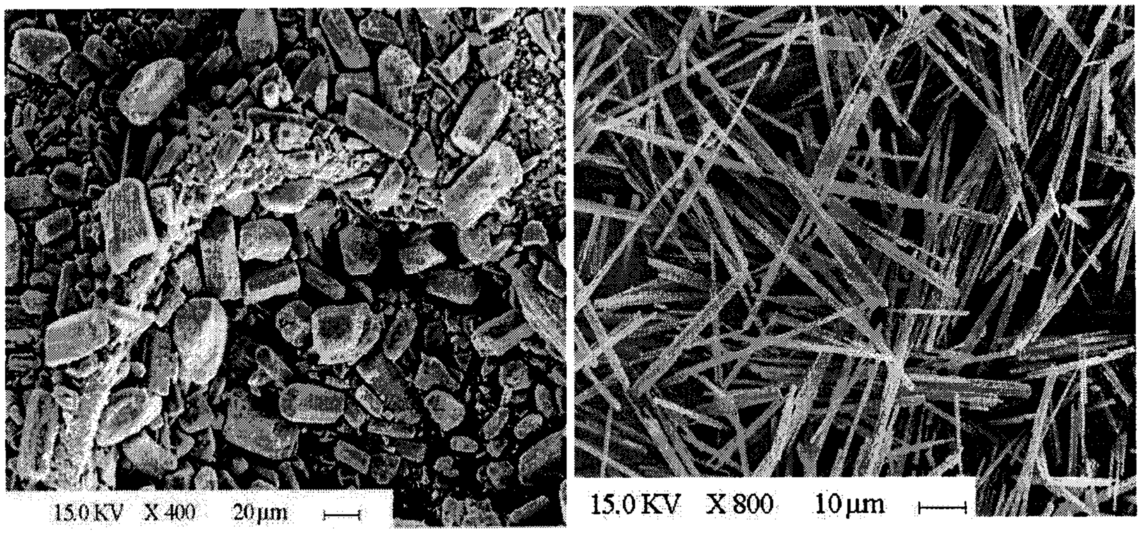

(a) Original α-hemihydrate (Omega) (b) After 1 hour in 1.5M H_2SO_4 at 100°C

Figure 5.12: Morphological change of calcium sulfate hemihydrate after equilibration for 1 hour in 1.5M H_2SO_4 at 100°C

Typically, as reported in the literature[2-8], there are three possible mechanisms via which phase transformation of calcium sulfate hemihydrates can occur in solutions, namely, liquid phase (or re-crystallization or "through-solution"), topochemical, and solid-phase conversion. In the first case, the new phase is nucleated out of solution; in the second case on the surface of the initial crystals; and in the third, within the body of the source phase. There has to date been no convincing experimental evidence for the solid-phase mechanism. Since in the first case, the new phase nucleates out of the solution, while in the other, on the surface of the original phase, they can also be classified in more general terms homogeneous crystallization and heterogeneous crystallization respectively. But clearly in the first case, dissolution (at least partially) of the original phase precedes nucleation-crystal growth of the new one.

It is obvious that recrystallization of hemihydrate particles was promoted as the H_2SO_4 concentration increased despite the fact that there was no change in the chemical structure of hemihydrate as supported by XRD characterization[4].

The hot washing tests also confirmed the abovementioned findings. Washing hemihydrate with boiling water resulted in no change of either its chemical structure or morphology. However washing hemihydrate with hot H_2SO_4 (1.5M, ~100°C) caused morphology to change as it can be witnessed with the SEM photos of Figure 5.13 (compare to SEM image of original material in Figure 5.12, a). In this case, though, the obtained morphology was not of acicular type. The reason could be ascribed to the fact that, in an environment of filter washing, the recrystallized nuclei have very slim chance to be well grown since the re-organizing constituents/units keep washed away, thus resulting in very fine particles as shown in Figure 5.13; while, in a relatively "abundant" aqueous environment as is the agitated hot H_2SO_4 solution, the nuclei have good opportunity to grow eventually assuring the most favorable, apparently under the conditions needle-shape morphology.

---

[4] They were also identified by DSC to be in the form of α-hemihydrate.

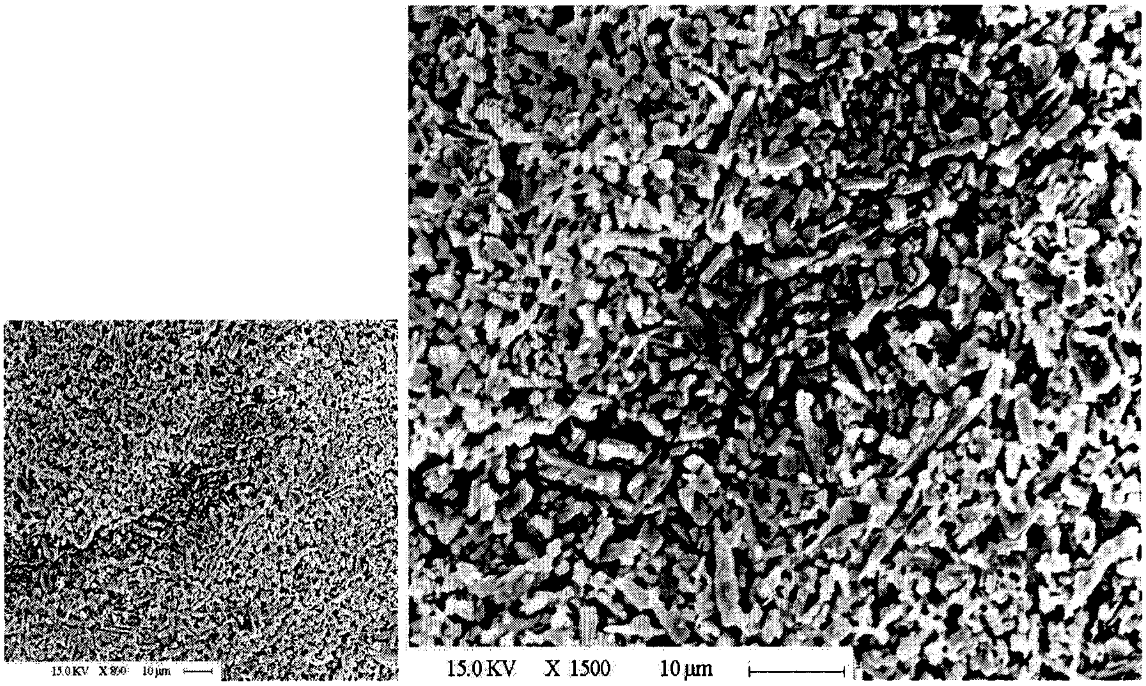

(a) 5 minutes washing (surface) (b) Higher magnification of image in (a)

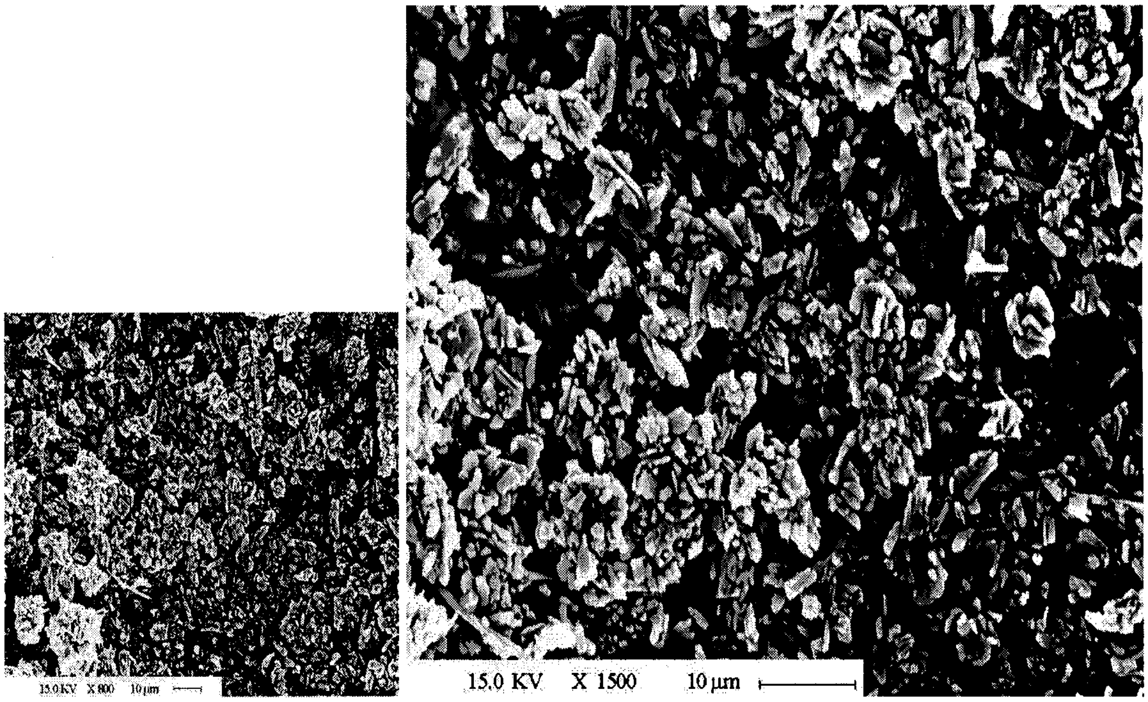

(c) 30 minutes washing (surface) (d) Higher magnification of image in (c)

Figure 5.13: SEM images of calcium sulfate hemihydrate (Omega material) washed with hot 1.5M H_2SO_4 (~100°C)

Table 5.1: Transformation of hemihydrate(Omega) in sulfuric acid solutions at 100°C

Original morphology of hemihydrate	Conditions	Morphology		XRD monitoring	
		After 1 hour	After 24 hours	After 1 hour	After 24 hours
Block-like (refer to Figures 5.10 and 5.12)	De-ionized boiling water (pH ~ 6.5)	Block-like	Block-like	HH	HH
	0.1M H_2SO_4	Block-like + needle-like	Needle-like	HH	HH
	0.5M H_2SO_4	Needle-like	Basically needle-like	HH	HH
	1.0M H_2SO_4	Needle-like	Fiber-like (refer to Figure 6.15)	HH	HH
	1.5M H_2SO_4	Needle-like		HH	HH

Note: the original morphology of Omega hemihydrate is shown in Figures 5.10 and 5.12

5.2.4 Summary

Here are the major findings of this part of the work:

(1) Both dihydrate and hemihydrate can stay intact in boiling water for at least 28 hours.

(2) In aqueous H_2SO_4 media (~100°C), as the acidity increases (from 0.1 to 1.5M as tested), dihydrate converts to hemihydrate with simultaneous re-crystallization, i.e., crystal morphology change occurs via apparently a dissolution–re-crystallization (or through-solution) mechanism. On the other hand, hemihydrate retains its chemical (XRD) structure even after 28 hours equilibration at 100°C in 1.5M H_2SO_4 solutions but its morphology changes to acicular (needle-shaped) crystals following apparently the dissolution - re-crystallization mechanism as well. The exact nature of the mechanism, i.e., homogeneous or heterogeneous (corresponding respectively to congruent or incongruent dissolution of the starting crystals) has not been identified.

5.3 Precipitation

5.3.1 Principles of supersaturation and crystallization

Crystallization of both readily and sparingly soluble substances consists of three stages: nucleation, growth and secondary changes such as agglomeration. According to the governing mechanism, nucleation is categorized [9-10] into: (i) primary nucleation, in which formation of the new solid phase is not influenced by the presence of the solid phase being formed. It is further classified into homogeneous and heterogeneous nucleation; and (ii) secondary nucleation, in which formation of the solid phase is initialized by the presence of solid phase of the crystallizing material itself. Nucleation and growth are critically dependent on the degree of supersaturation, which is defined as

$$S = \alpha / \alpha_0 \qquad (5.3.1)$$

where α, α_0 are the activities of the dissolved solute and of the pure solute in equilibrium with a macroscopic crystal respectively. Thus there is a critical supersaturation level that when reached signifies the onset of nucleation by a different mechanism [11]:

$$1 < S_{cr,\ secondary} < S_{cr,\ heterogeneous} < S_{cr,\ homogeneous} \qquad (5.3.2)$$

where $S_{cr,secondary}$, $S_{cr,heterogeneous}$, $S_{cr,homogeneous}$ represent respectively the critical supersaturation values for secondary nucleation, heterogeneous nucleation and homogeneous nucleation. Particularly, supersaturation level is defined as

$$S = {}^{Real\ concentration\ of\ CaSO_4} / {}_{solubility\ of\ CaSO_4\ in\ the\ solution} \qquad (5.3.3)$$

in this work.

Moreover, the nucleation rate is an exponential function of supersaturation but the growth rate is only (most of the cases) a linear function.

In an effort to shed light on the influence (during the early stages of crystallization) of the reaction conditions (between sulfuric acid and lime) on the production of α-hemihydrate, precipitation tests under low supersaturation environment were performed. The tests were designed in such a way that the supersaturation was kept extremely low by drop-wise titration (addition of H_2SO_4 into slaked lime). This work particularly sought to identify the changes (chemical and morphological) occurring upon reaction of sulfuric acid and slaked lime near the boiling temperature.

5.3.2 Experimental

The reactor setup described in section 3.3 equipped with burette for addition of solution (or titration) and reflux condenser for re-collecting the water vapor was used. Both the burette and condenser were tightly fitted to the reactor by hole-bored rubber stopper. The agitation was controlled at around 300 rpm. The titrant was 1.5M H_2SO_4 solution. The titrated suspension was slaked lime with fixed CaO weight 16.8g and solid/water weight ratio 1:6, which resulted in approximately 100 mL slurry of slaked lime. The slurry was preheated to 100°C before the titration actually started. The titration was controlled at a very slow speed (~50 mL/hour) such that when the cool titrant from the burette touched and mixed with the slurry, the influence on the temperature of the whole reaction system was negligible. Each run of titration was stopped at sub-stoichiometric, stoichiometric, or super-stoichiometric points with H_2SO_4/CaO molar ratio at 0.2, 0.8, 1.0, 1.2, 1.5, 2.0 and 2.5 respectively. Titration was immediately followed by 5-hour aging (in some cases, it was prolonged to around 24 hours) period during which temperature and agitation were maintained at the same levels as during titration. At certain time intervals, samples were taken for XRD and SEM analysis.

5.3.3 Results and discussion

SEM images of products obtained at different ratios of H_2SO_4 to CaO by titration and aging at 100°C are shown in Figure 5.14.

At sub-stoichiometric ratio, the crystals were mixtures of dihydrate and CaO/$Ca(OH)_2$ as confirmed with XRD; some of the dihydrate was found to have grown to very big plate-like crystals when the H_2SO_4/CaO ratio increased from 0.2 to 0.8. At stoichiometric or super-stoichiometric points, basically the crystals are hemihydrate; at lower H_2SO_4/CaO ratio, trace of dihydrate can be detected on XRD patterns. The material obtained at stoichiometric ratio (with the majority being hemihydrate) was very fine

(Figure 5.14, c) but that obtained at super-stoichiometric ratios (Figure 5.14, d) showed much larger crystals of about 20 μm in size.

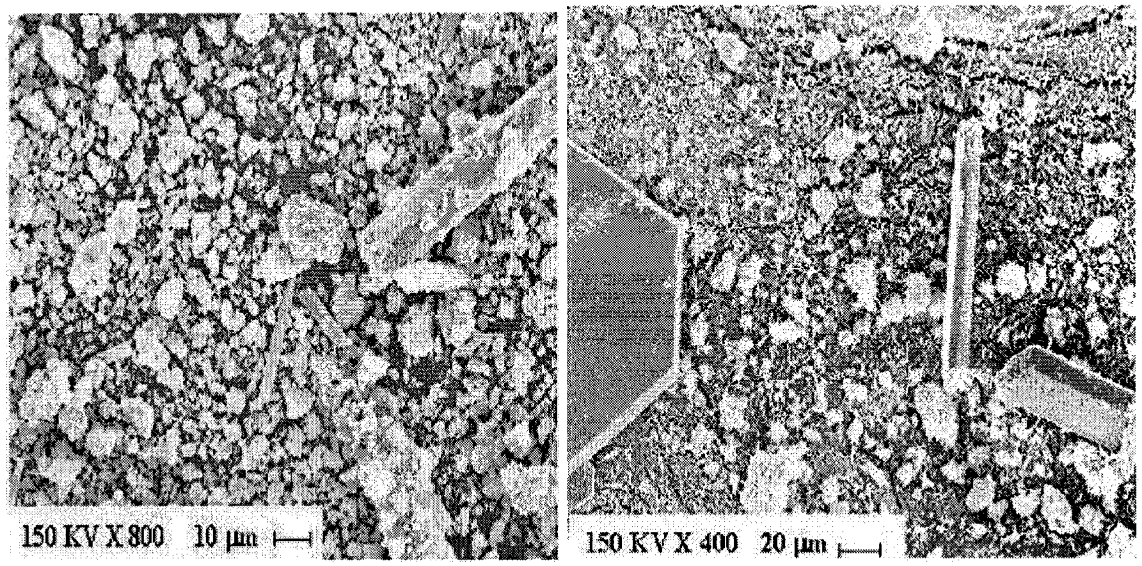

(a) at $H_2SO_4/CaO = 0.2$

XRD: DH+ $CaO/Ca(OH)_2$
(Titration Time: ~48 min)

(b) at $H_2SO_4/CaO = 0.8$

XRD: DH+ $CaO/Ca(OH)_2$
(Titration Time: ~192 min)

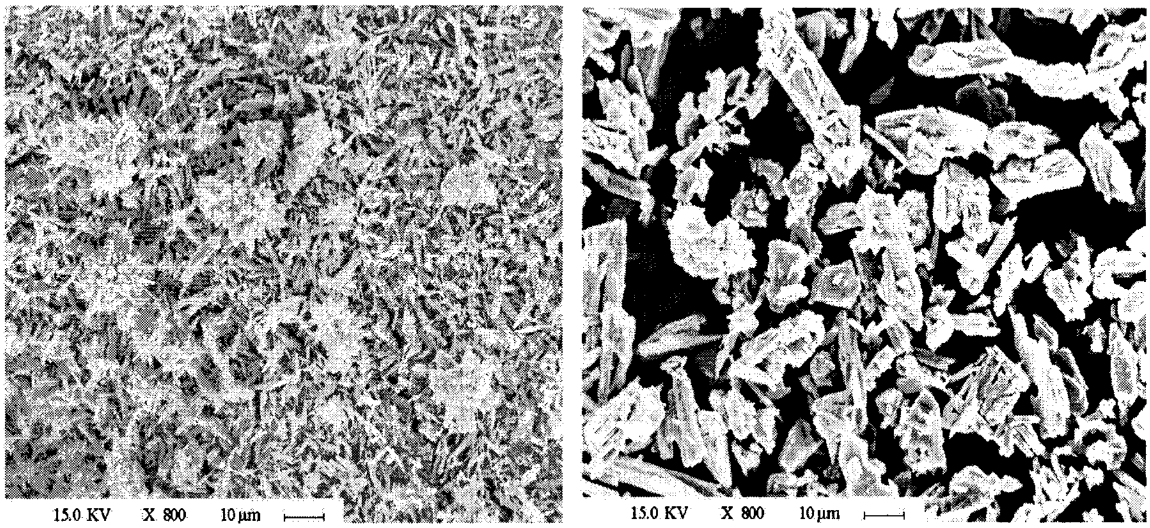

(c) at $H_2SO_4/CaO = 1.0$

XRD: Majority of HH + trace of DH

(Titration Time: ~240 min)

(d) at $H_2SO_4/CaO = 2.5$

XRD: basically HH

(Titration Time: ~600 min)

Figure 5.14: SEM images of crystals obtained by titration followed by 5-hour aging at different H_2SO_4/CaO ratios (Conditions: 1.5M H_2SO_4, 16.8g CaO, weight ratio of $CaO/H_2O=1:6$, 100°C)

By taking intermediate samples at super-stoichiometric ratios (with H_2SO_4/CaO ratio ≥ 1.0), it became clear that, dihydrate formed as intermediate product upon reaction of H_2SO_4 with CaO subsequently converting to "stable" hemihydrate. This can be seen with the aid of the SEM images of Figure 5.15. According to these figures (and XRD analysis – not shown), at the end of titration (stoichiometric ratio = 1.2) the product was well-grown plate-like dihydrate crystals, however, upon aging (Figure 5.15, b and c) re-crystallization occurred via which dihydrate converted to hemihydrate crystals (which appeared to be stacks of rod-like crystals).

In comparison with the phenomena observed during the transformation tests (see section 5.2.3), in which the phase transformation mechanism was found to be of dissolution and re-crystallization type, herein the conversion of the initially-formed dihydrate to hemihydrate appears to follow the solid-phase mechanism (refer to Figure 5.15 b, c, and d).

It is interesting to note that Sirota et al.[5] who studied the phase transformation of dihydrate into hemihydrate observed both mechanisms depending on the purity of the starting dihydrate material, i.e., via the re-crystallization mechanism in case of reagent-grade dihydrate and via the solid-phase mechanism in the case of commercial dihydrate. Although impurities may play a role – acting for example as nucleation sites, it is believed that, the differences observed between the transformation tests and titration tests in the present work are most likely reflection of differences in terms of supersaturation level. It is postulated in other words that, during the transformation tests that involved dissolution of dihydrate crystals a relatively high supersaturation was built-up. On the other hand, upon titration the supersaturation was kept low hence favoring heterogeneous nucleation (topotactic nucleation) and growth of hemihydrate crystals. Finally another difference between the two systems is the fact that in the latter case (titration tests) the conversion of dihydrate to hemihydrate occurs in a saturated system as opposed to former system that is under-saturated (at least initially).

The present work's finding that dihydrate forms as intermediate product during the crystallization of hemihydrate is in agreement with Stranski's rule or Ostwald's rule of stages which states that the least stable phase forms first [10, 12] in a initially-homogeneously nucleating system.

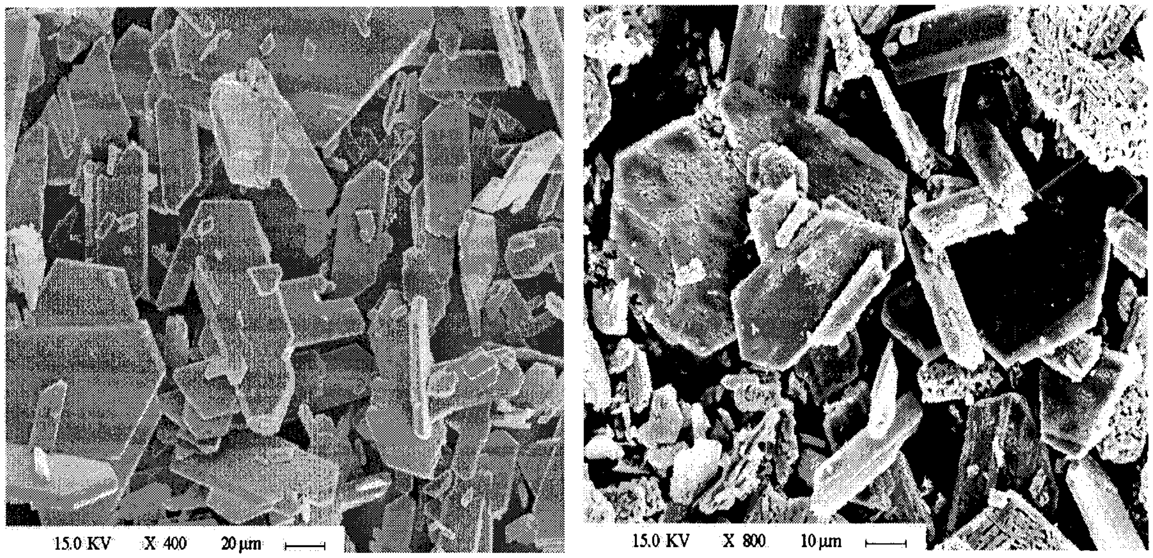

(a) 5 minutes aging

(XRD: basically DH)

(b) 0.5 hour aging

(XRD: DH + HH)

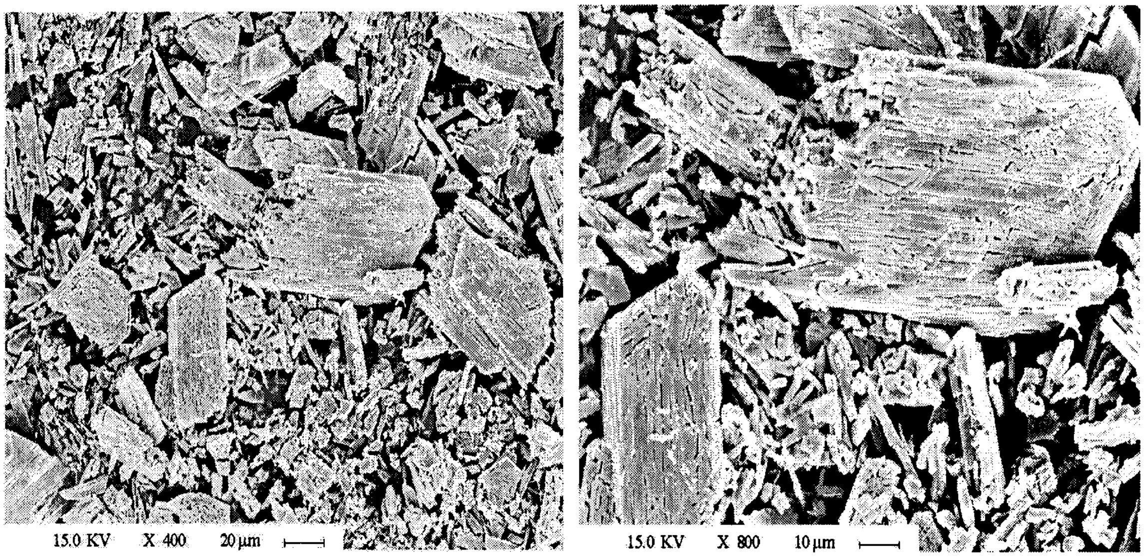

(c) 5-hour aging

(XRD: Majority of HH + trace of DH)

(d) higher magnification of image in (c)

(XRD: Majority of HH + trace of DH)

Figure 5.15: Morphological evolution of calcium sulfate product obtained with super-stoichiometric titration at $H_2SO_4/CaO = 1.2$ as a function of aging time (Conditions: 1.5M H_2SO_4, 16.8g CaO, weight ratio of $CaO/H_2O = 1:6$, 100°C Titration Time: ~280 min)

The production of α-hemihydrate at stoichiometric H_2SO_4/CaO ratio =1.0 is a very interesting one. Hence a large number of tests were preformed at this ratio by mixing the reagents at different ways. It was determined that, independent of whether the acid was added drop-wise (i.e. by titration) or all-at-once, the final product was always the same, i.e., mixture of dihydrate and hemihydrate with the majority being hemihydrate.

5.3.4 Summary

The main findings of this part of the work are summarized below:

(1) Sub-stoichiometric titration with H_2SO_4/CaO ratio < 1 always resulted in mixtures of dihydrate and $CaO/Ca(OH)_2$.

(2) Super-stoichiometric titration (with H_2SO_4/CaO ratio ≥ 1) yielded initially dominantly dihydrate crystals which upon aging converted to hemihydrate. The completeness or not of this conversion or effectively the speed of this conversion appears to relate to the amount of free acid remaining after the reaction.

(3) It has been established that dihydrate forms as intermediate product in the path towards hemihydrate. During the slow titration tests, the dihydrate material got the chance to grow into very big plate-like crystals, which, subsequently, slowly converted into hemihydrate crystals via an apparent solid-phase mechanism.

5.4 Concluding remarks

In hot aqueous H_2SO_4 media (~100°C), the starting solids of either dihydrate or hemihydrate undergo transformations via the dissolution – re-crystallization mechanism (liquid-phase or through-solution mechanism) resulting in significant morphological and chemical changes as the acidity increases in certain range (from 0 to 1.5M). Dihydrate converts to hemihydrate upon acid increase; no further conversion of hemihydrate was observed within the range of conditions tested (28 hours, 100°C, 1.5M H_2SO_4). The resultant morphology of hemihydrate is of needle-shape type. Calcium sulfate solids, either dihydrate or hemihydrate, can saturate the sulfuric acid solutions in only five minutes. Slow addition of sulfuric acid into slaked lime revealed that dihydrate forms initially as well-grown platelets which subsequently convert into hemihydrate by the solid-phase mechanism when excess H_2SO_4 is used ($H_2SO_4/CaO \geq 1$).

References

[1] Kontrec, J., Kralj, D. and Brecevic, L., Transformation of anhydrous calcium sulfate into calcium sulfate dihydrate in aqueous solutions, Journal of Crystal Growth, 240, 203-211 (2002).

[2] Zürz, A., Odler, I., Thiemann, F. and Berghöfer, K., Autoclave-free formation of α-$CaSO_4 \bullet 1/2H_2O$ gypsum, Journal of the American Ceramic Society, 74(5) 1117-1124 (1991).

[3] Bobrov, B.S., Romashkov, A.V. and Andreeva, E.P., Mechanism of the formation and growth of crystals of calcium sulfate hemihydrate, Izvestiya Akademii Nauk SSSR, Neorganicheskie Materialy, 23(3), 497-500(1987) (in Russian).

[4] Goto, M. and Ridge, M.J., Observations on the reaction calcium sulfate hemihydrate + water ⇔ gypsum, Australian Journal of Chemistry, 18, 769-776 (1965)

[5] Sirota, I. S., Dorozhkin, S. V., Kruchnina, M. V. and Melikhov, I. V., Phase transformation and dehydration of calcium sulfate dihydrate in solution studied by SEM, Scanning, 14, 269-275(1992).

[6] Melikhov, I.V., Rudin, V.N. and Vorob'eva, L.I., Non-diffusive topochemical transformation of calcium sulfate hemihydrate into the dihydrate, Mendeleev communications / Royal Society of Chemistry (London), [Akademiia Nauk SSSR], 1, 33-34(1991) (English translation).

[7] Melikhov, I.V., Saparin, G.V., Bozhevolnov, V.E., Obyden, S.K. and Kuleshova, O.V., Diagnostics for heterogeneous chemical reactions by cathodolumiscence, Scanning, 13, 358-362(1991).

[8] Gartner, E.M. and Gaidis, J.M., Hydration mechanisms, I, Materials Science of Concrete, 1, 95-125(1989).

[9] Söhnel, O. and Garside, J., Precipitation – Basic principles and industrial applications, Butterworth-Heinemann Ltd.: Oxford, UK, 41-272(1992).

[10] Mullin, J.W., Crystallization, 3rd ed., Butterworth-Heinemann Ltd.: Oxford, UK, 172-259 (1993).

[11] Dirksen, J.A. and Ring, T.A., Fundamentals of crystallization: Kinetic effects on particle size distribution and morphology, Chemical Engineering Science, 46(10), 2389-2427(1991).

[12] Blesa, M.E., and Mtijevic, E., Phase transformation of iron oxides, hydroxides, and hydrous oxides in aqueous media, Advances in Colloid and Interface Science, 29(3-4), 173-221(1989).

Chapter 6

Preparation of α-hemihydrate by Reaction of Sulfuric Acid with Lime

6.1 Introduction

The work involving the production of α-hemihydrate by reacting lime (dry or slaked) with sulfuric acid is described in this chapter. Some critical crystal growth control parameters, such as additives (including both organic and inorganic), seeding and recycling, which can possibly affect the morphology of the final crystals, are investigated in the following chapter.

Early on it was thought that the method by which the reaction between lime and sulfuric acid is initiated has consequences in terms of product composition and morphology. Hence, four procedures were tried, namely, (a) addition of dry lime to H_2SO_4; (b) addition of slaked lime to H_2SO_4; (c) addition of H_2SO_4 to dry lime and (d) addition of H_2SO_4 to slaked lime. The preliminary tests show that there was no much difference among the first three procedures, all three procedures produced α-hemihydrate of thin needle (acicular) shape; while procedure (d) resulted in different product morphology. Hence, procedure (a) addition of dry lime to H_2SO_4 and procedure (d) addition of H_2SO_4 to slaked lime were chosen as the main study focus.

6.2 Experimental

If not otherwise specified, all experiments discussed in this chapter were performed with the glass reactor described in section 3.3; the reaction slurry (or samples taken at different interval times) was hot-filtered and treated with method 3 described in section 3.5; the final dry samples were examined with XRD/DSC for phase identification and with SEM for morphology characterization.

Various types of experiments were carried out; most of them were based on procedure (a), i.e. addition of dry lime into hot sulfuric acid solution. These were: determination of the operating window, study of the reaction kinetics, evaluation of the influence of different preparation parameters such as CaO/H_2SO_4 ratio, acidity and retention time, slaking of lime etc. The experimental procedure for each type of experiments is outlined below.

6.2.1 Operating window experiments

Five hundred mL H_2SO_4 solution with concentration of 0.10M to 3.00M (at the interval of 0.05M), was preheated to 100°C, then certain amount of dry lime with CaO/H_2SO_4 ratio of 0.4 was added into the solution. From that point the reaction time was controlled at 1 hour and agitation speed 300 rpm. The same conditions but with different reaction temperatures from room temperature to boiling point of the slurry (20 to ~103°C) were also selectively examined.

6.2.2 CaO/H_2SO_4 ratio and agitation experiments

Five hundred mL 1.50M H_2SO_4 solution was preheated to 100°C, then lime was added to reach different CaO/H_2SO_4 ratios (from 0.2 to 1.2). The agitation rate was controlled at 300 rpm. The slurry was hot-filtered after 1 hour reaction. The final sample was collected and weighed, and examined by XRD/DSC and SEM; the filtrate was also collected for ICP analysis of calcium and sulfur abundance. As a variation, the reaction was also initiated by adding certain amount of lime into H_2SO_4 solutions at lower temperatures such as room temperature, and then the slurry was heated up to 100°C and retained at that point for 1 hour. In connection to this series of experiments the role of agitation was evaluated as well by applying different stirring speeds from no agitation at all to 900 rpm.

6.2.3 Acidity and retention time experiments

Five hundred mL H_2SO_4 solution with different acidity (from 0.10M to 1.50M) was preheated to 100°C, then certain amount of dry lime (with CaO/H_2SO_4 ratio of 0.4) was added. The agitation rate was controlled at 300 rpm. Samples were taken at different interval times.

6.2.4 Reaction kinetics experiments

The reaction kinetics was evaluated by two techniques. The first one involved monitoring of the concentration change of certain species such as H^+, Ca^{2+} or SO_4^{2-} in the solution with time while the second one involved monitoring conductivity of the reaction slurry. Five hundred mL H_2SO_4 solution with concentration of 1.25M/1.20M (0.5M, 1.50M or 1.80M) was preheated to 100°C, then lime with CaO/H_2SO_4 ratio of 0.4 (or 0.8) was added into the solution.

For the first technique of monitoring, once the reaction was initiated, (at certain interval times) samples were pipetted out and filtered while hot. The filtrates were sent for analysis of calcium and sulfur by ICP. The free acid or H^+ concentrations were determined by titration with 0.02N NaOH as described in section 3.7.

For the second technique of monitoring, conductivity was measured with a very robust conductivity sensor, model 228 Tefzel[1], coupled with 1054T analyzer from Rosemont Analytical Inc. [1]. The conductivity sensor was first calibrated with known-value standard solutions, and then, the conductivity values for sulfuric acid solutions were measured at different concentrations and different temperatures. The data were verified with values from literature [2-3] and with the aid of the OLI databank [4]. Figure 6.1, a shows the good agreement obtained. The specific conductivity was found to vary linearly with H_2SO_4 concentration up to 1.80M. The results are shown in Figure 6.1, b. In addition, conductivity measurements of sulfuric acid solutions saturated with calcium

---

[1] The sensor [1] is ideal for use in highly concentrated acids such as H_2SO_4, HNO_3,HF with working range 0-2000 *mS/cm,* temperature up to 200°C, and maximum pressure 200 psi (1345 kPa).

sulfate at 100°C and 25°C (after hot filtration-removal of finely-dispersed solids) were carried out as well and reported in Figure 6.1, b. Saturation of the solution with calcium sulfate was found not to influence the conductivity measurements. The following two empirical equations describe the variation of conductivity with H_2SO_4 concentration (range 0-1.80M):

$$\sigma_{25\,^{\circ}C}\ (\text{in mS/cm}) = 368.8450 \times [H_2SO_4]\ (\text{in M}) \qquad (6.2.1)$$

and

$$\sigma_{100\,^{\circ}C}\ (\text{in mS/cm}) = 574.5565 \times [H_2SO_4]\ (\text{in M}) \qquad (6.2.2)$$

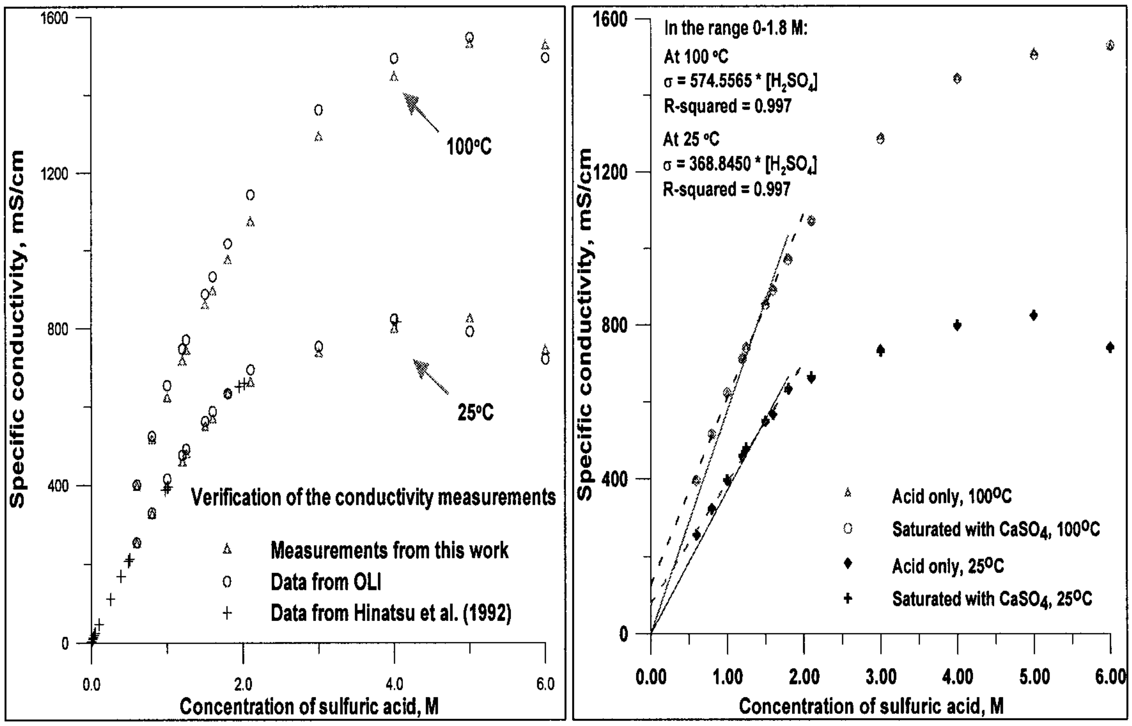

(a) Verification of the conductivity measurements

(b) Conductivity measurements of H_2SO_4 solution saturated with calcium sulfate

Figure 6.1: Specific conductivity of sulfuric acid solution as a function of H_2SO_4 concentration and temperature

Measurements of sulfuric acid solutions saturated with calcium sulfate at around 100°C and 25°C (after hot filtration-removal of finely-dispersed solids) were carried out before the "real" measurements: once the reaction was initiated, at certain interval times, the conductivity was recorded by immersing the sensor into the hot slurry.

6.2.5 Reverse procedure – addition of H_2SO_4 to slaked lime experiments

Slurry of slaked lime (the volume varied with the CaO/H_2O ratio) was prepared in the glass reactor by mixing certain amount (typically 16.8 g or 0.3 moles) of CaO with water at various CaO/H_2O ratios (1/1 to 1/20, typically 1/6). Initially experiments were run with the slurry having different temperature (20→100°C). As with the other procedure (discussed in section 6.3.2) the CaO/H_2O slurry was preheated to 75°C or higher for optimum results. Following the preheating of the slurry, the hot (100°C) H_2SO_4 solution (the actual volume also varied with the initial H_2SO_4 concentration and CaO/H_2SO_4 ratio used) was added to initiate the reaction. The CaO/H_2SO_4 ratio was 0.4 and the retention time was 1 hour with agitation speed of 300 rpm unless otherwise specified.

6.3 Results

6.3.1 Operating window

The purpose of this part of work was to determine the domain of conditions in terms of temperature and sulfuric acid concentration within which α-hemihydrate may be produced. It must be clarified that the determined range is not absolute but rather relatively a target area for detailed work.

The operating window is graphically presented in Figure 6.2, a and b. The first one is expressed in terms of initial H_2SO_4 concentration while the latter one in terms of final (pseudo-equilibrium or "steady-state") H_2SO_4 concentration.

According to the plotted data production of metastable α-hemihydrate is formed only at temperatures near the boiling point of the H_2SO_4 solution, i.e., 98~105°C (the upper temperature is the boiling point of the solution at 1 atmosphere). On the other hand the initial H_2SO_4 concentration was determined to be in the range of 1.0 to 1.8M or 0.6 to 1.1 M "equilibration" (or "steady-state") concentration.

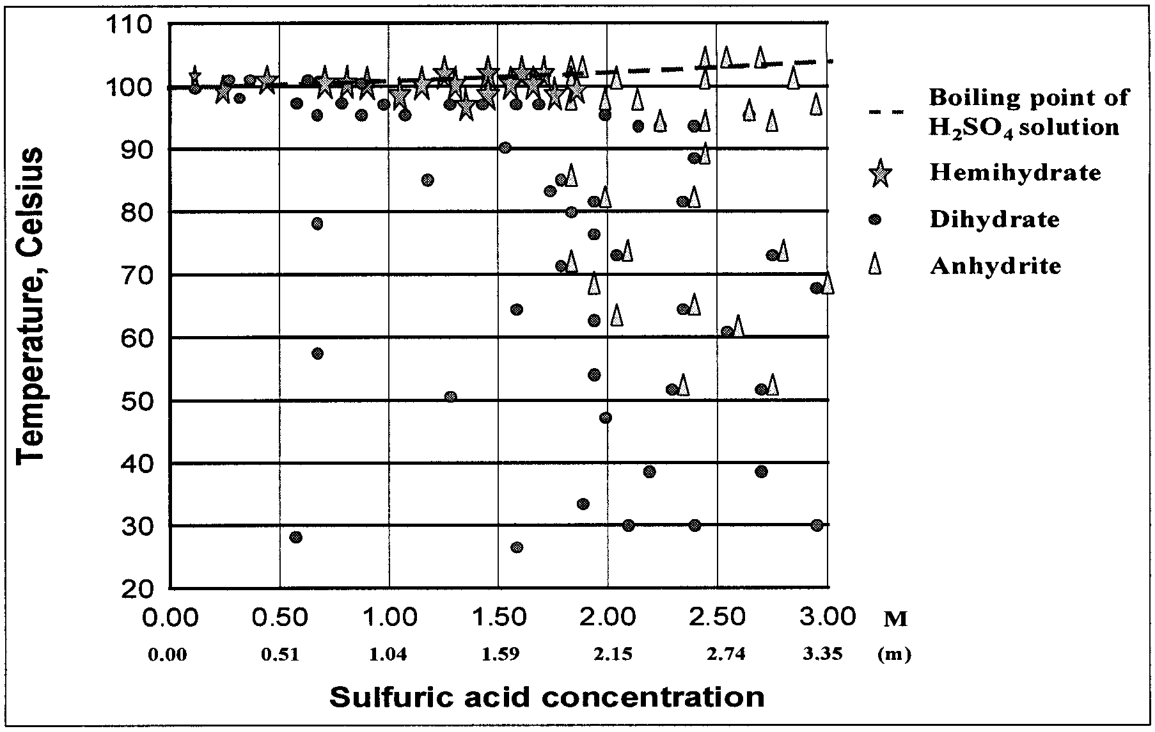

(a) In terms of initial H_2SO_4 concentration and temperature

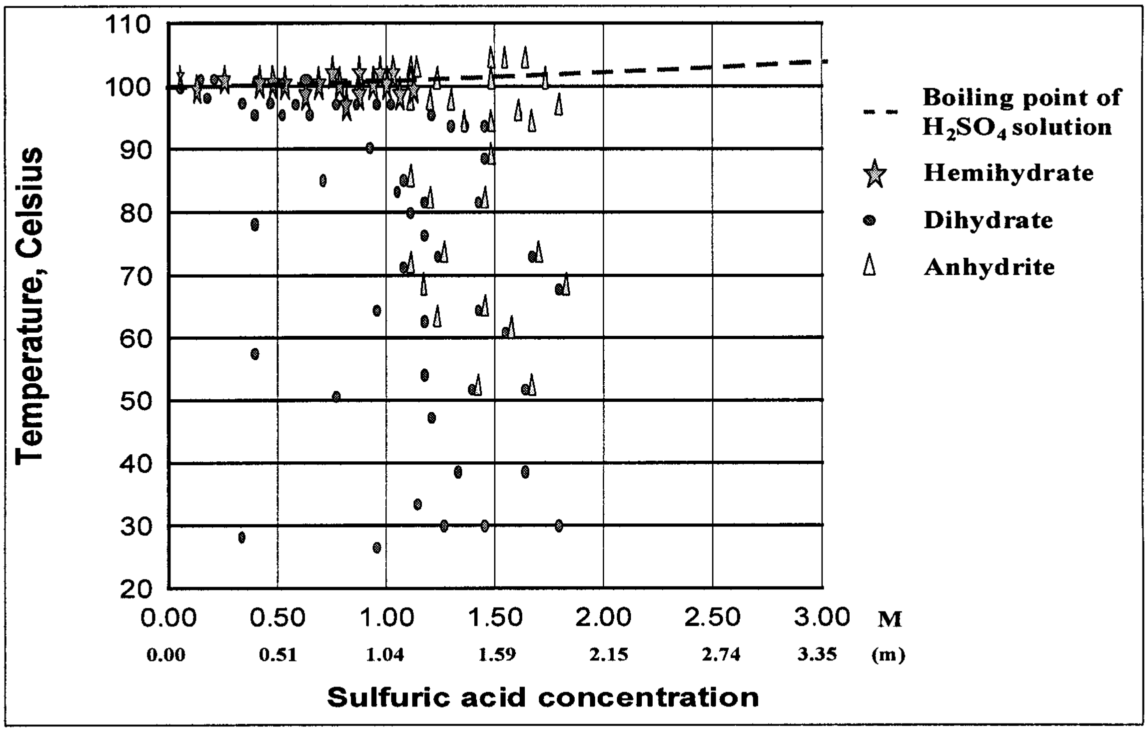

(b) In terms of final H_2SO_4 concentration and temperature

Figure 6.2: Operating window in terms of H_2SO_4 concentration and temperature for producing α-hemihydrate by reacting sulfuric acid with lime (1 hour retention time)

It should also be pointed out that α-hemihydrate was found to randomly report also outside this region but to be mixed with either dihydrate or anhydrite. Hence the region ("operating window") described above is the region where "clean" α-hemihydrate is produced. By "clean", it is meant that no sign of other calcium sulfate phase was detected by XRD. Furthermore, DSC confirmed the metastable hemihydrate to be the alpha form (see Figure 6.3).

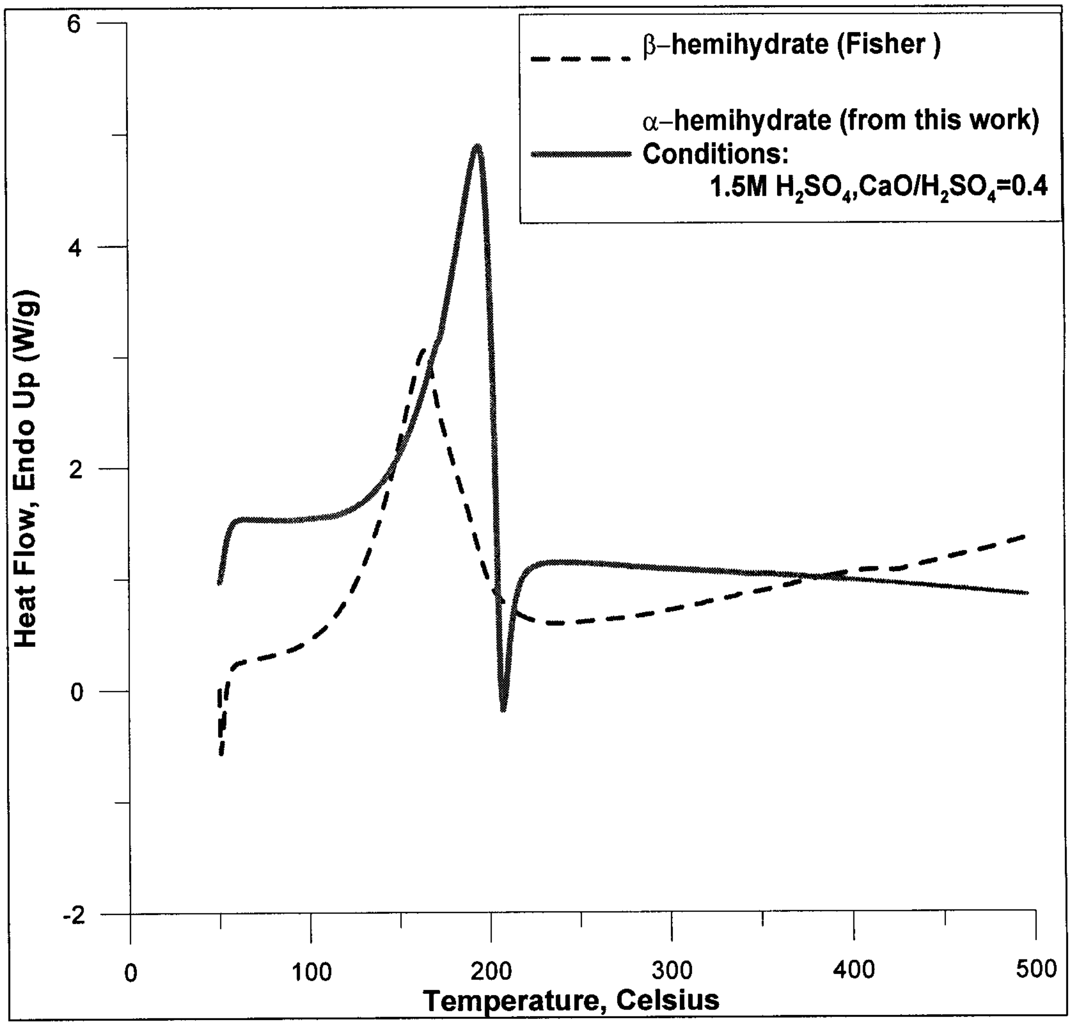

Figure 6.3: Typical DSC pattern of the α-hemihydrate material produced via the standard procedure of addition of dry lime to H_2SO_4 solution

It is interesting to place the "1-hour clean α-hemihydrate production region" in the context of the phase diagram determined in chapter 4. This is done in Figure 6.4. It is obvious that the determined operating window is very narrow and limited in comparison with the hemihydrate metastable region predicted by the phase diagram. This implies that the "metastability" of hemihydrate is not controlled solely by the activity of water as postulated in chapter 4. Apparently, other chemical properties of the system than water activity play a role in promoting or preventing the conversion of hemihydrate to anhydrite.

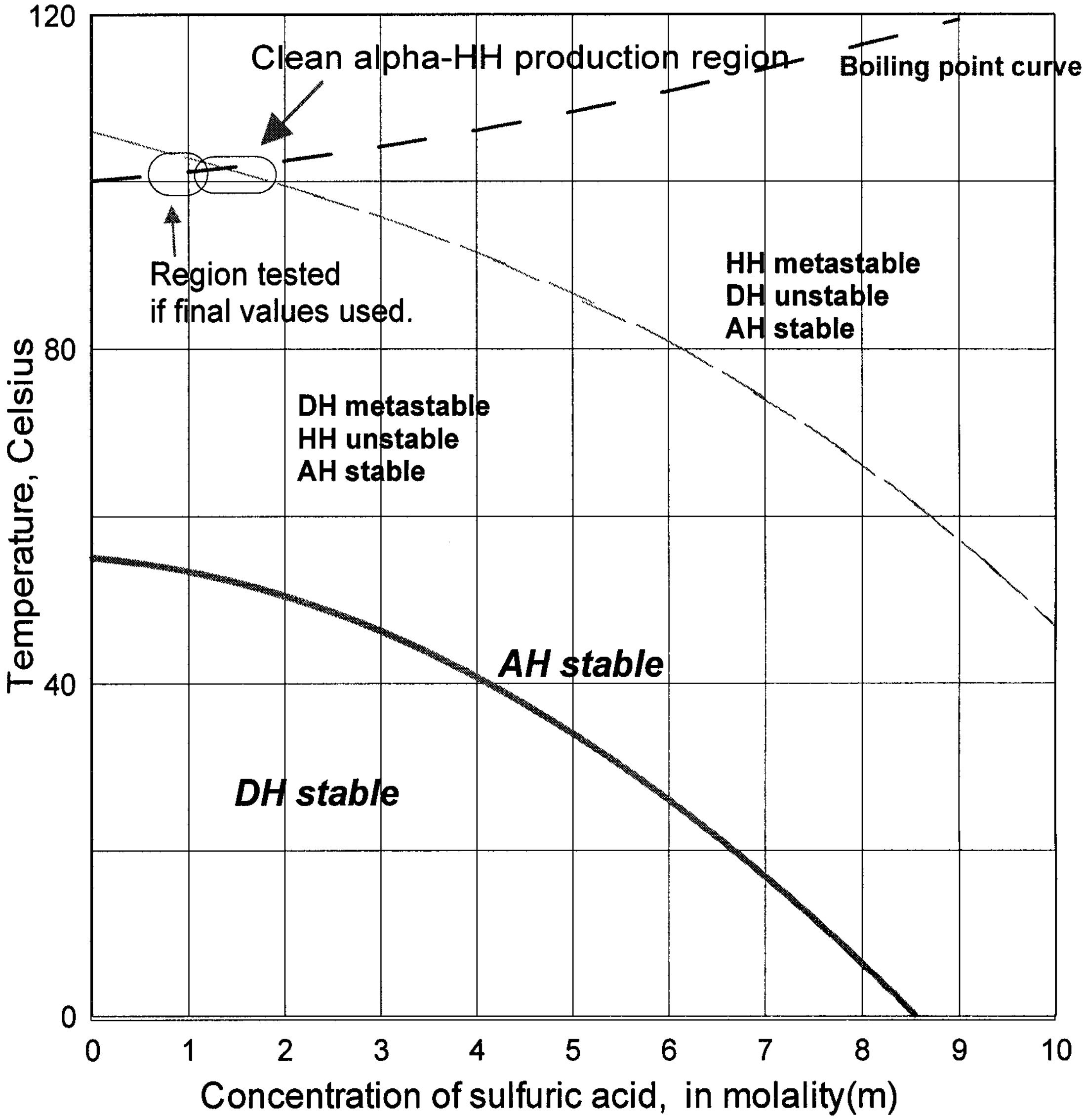

Figure 6.4: "clean α-hemihydrate production region" on the predicted phase diagram

6.3.2 Influence of CaO/H_2SO_4 ratio and mixing conditions

Figure 6.5 summarizes the results obtained at 100°C with various CaO/H_2SO_4 ratios in terms of yield of various products. Basically, hemihydrate was produced with all ratios tested but a fraction of calcium sulfate remains soluble (refer to solubility measurement section in chapter 4). However, when the ratio approached one, an "unknown" component was also present. This was determined to be unreacted $CaO/Ca(OH)_2$. Moreover, the viscosity of reaction slurry is too high at ratio near one making the process impractical.

Additional tests were done by adding lime to H_2SO_4 solution at lower temperatures and then raising the reaction slurry temperature to 100°C. The obtained results are depicted in Figure 6.6. It can be seen that a certain amount of unreacted lime persisted even at low CaO/H_2SO_4 ratios – clearly an undesirable outcome. The unreacted lime was in the form of "gravels" (Figure 6.7). XRD analysis determined these gravels to consist of mixture of dihydrate ($CaSO_4{\bullet}2H_2O$) and unreacted lime $CaO/Ca(OH)_2$. Chemical analysis gave the following composition: $CaSO_4{\bullet}2H_2O$ 40-70 wt% and CaO 20-33 wt%. This occurrence is consistent with overgrowth of dihydrate on unreacted lime that blocks further reaction of CaO with H_2SO_4. Similar observations have been made in case of calcite [5].

Thermodynamically, the stable form of lime in aqueous solution is calcium hydroxide [6-7]. It is postulated, therefore, that, in the present system the hydration of lime (or otherwise the slaking of lime) occurs prior to formation of calcium sulfate hydrate products. In other words, the following reaction sequence is assumed taking place:

$$CaO(s) + H_2O(l) \rightarrow Ca(OH)_2\ (aq/colloidal) \qquad (6.3.1)$$

$$Ca(OH)_2(aq/colloidal) + H_2\,SO_4(aq) \rightarrow HH\ or\ DH\ or\ AH \qquad (6.3.2)$$

As the slaking temperature approaches 100°C, the finer the particle size and greater the specific surface area of hydrated lime becomes [6, 8-9], hence resulting to 100% reaction. But from a practical point of view, addition of lime at a temperature just above 75°C would be most appropriate for optimum operation since lime hydration is associated with tense releases of heat facilitating the attainment of the target temperature of 100°C. Further work is required to optimize this particular aspect of the process.

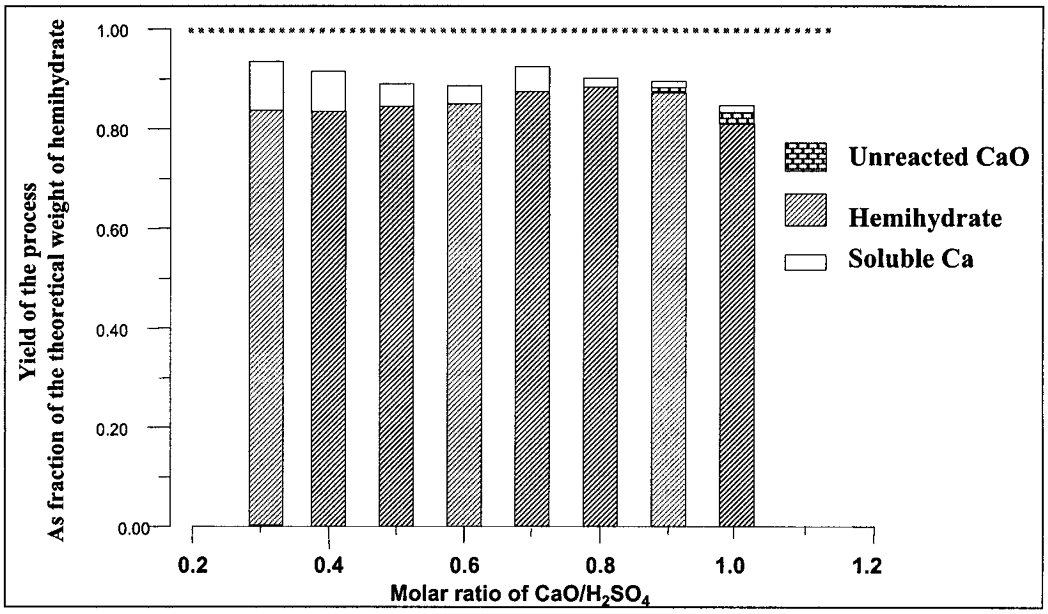

Figure 6.5: The effect of CaO/H_2SO_4 on hemihydrate yield

- reaction initiated by adding lime into sulfuric acid solution at 100°C

Conditions: 1.50M H_2SO_4

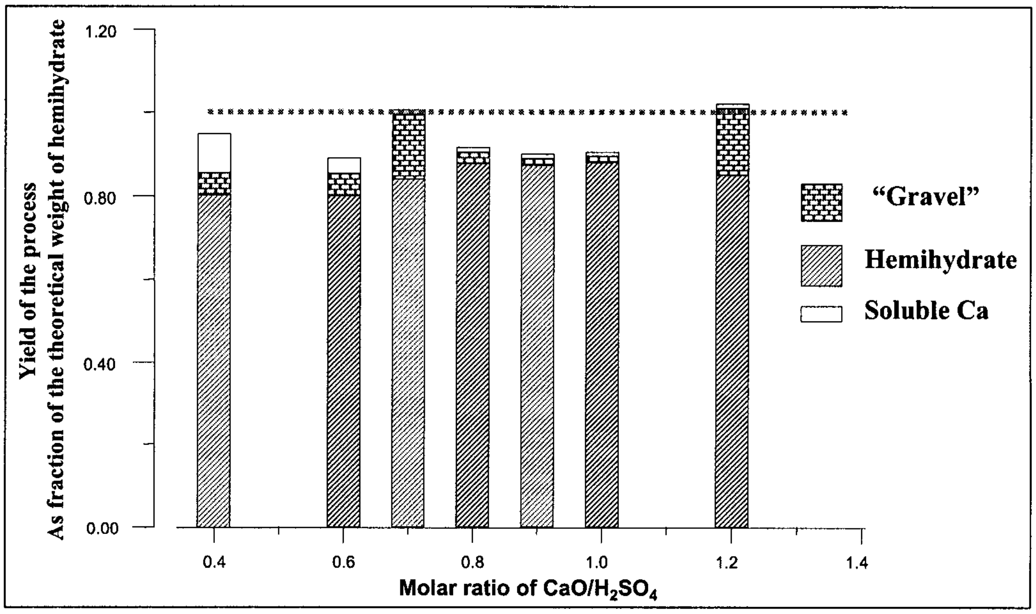

Figure 6.6: The effect of CaO/H_2SO_4 on hemihydrate yield

- reaction initiated by adding lime into sulfuric acid solution at room temperature

Conditions: 1.50M H_2SO_4, slurry heated up to 100°C

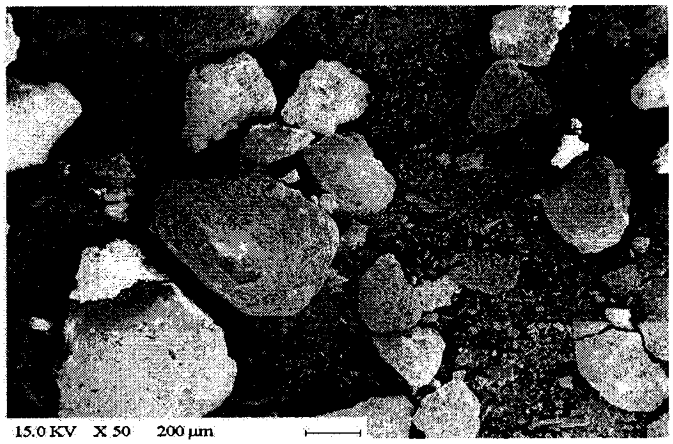

(a) At low magnification (X 50)

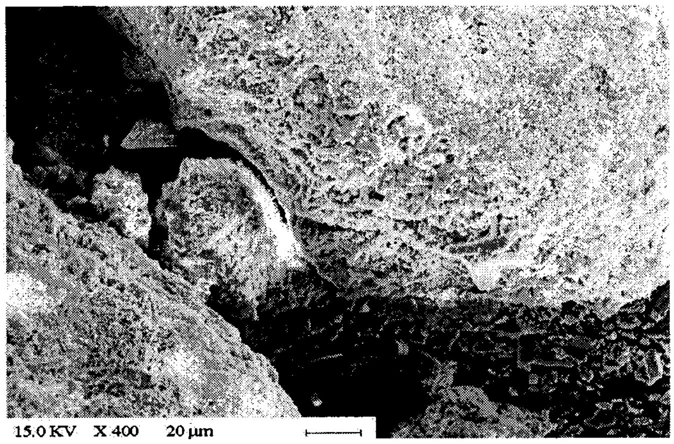

(b) At higher magnification (X 400)

Figure 6.7: Typical morphology of the “gravels” formed when slaking lime at low temperature (below 75°C)

Conditions: 1.50M H_2SO_4, CaO/H_2SO_4 ratio=0.4

(lime added to H_2SO_4 at room temperature and then slurry heated up to 100°C)

Having determined that slaking (addition of lime to H_2SO_4 solution) at high temperature (near 100°C) is required on one hand and a ratio of CaO/H_2SO_4 must be less than 1 on the other, a ratio equal to 0.4 was chosen for the next phase of the work. Another parameter at this point was the selection of appropriate agitation speed. The latter was found indeed not to be significant. Figure 6.8 compares the morphology of hemihydrate material produced with and without agitation. Given the absence of a significant effect a moderate agitation speed was selected (300 rpm) for all subsequent work.

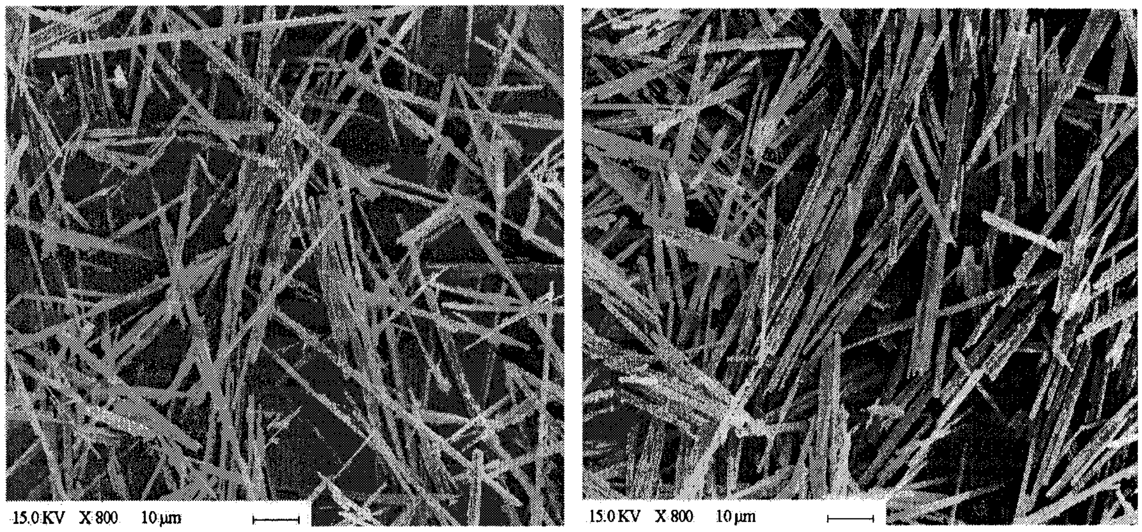

(a) No agitation (b) Strong agitation (900 rpm)

Figure 6.8: Influence of agitation on crystal morphology

Conditions: 1.25M H_2SO_4, CaO/H_2SO_4 ratio=0.4, 100°C

Procedure: addition of dry lime to H_2SO_4

(refer to Figure 6.13, a for the case of agitation at 300 rpm)

6.3.3 Influence of acidity and retention time

The effect of H_2SO_4 concentration and retention time on product evolution is shown in Figures 6.9 – 6.13. As it can be seen, dihydrate generally appears as intermediate product in the reaction between CaO and H_2SO_4; upon increase of acidity, the kinetics of dihydrate conversion to hemihydrate is strongly accelerated. Thus, while with 0.1M initial H_2SO_4 concentration there was still dihydrate present in the final product after 24 hours retention, no dihydrate was observed after 24 hours at 0.5M initial H_2SO_4 concentration. On the other hand, when the concentration of H_2SO_4 increased to 1.5M, conversion to hemihydrate was complete within 30 minutes (Figure 6.13). Hemihydrate apparently enjoys extensive metastability as it was detected always as the majority phase (if any conversion to anhydrite existed) after 24 hours retention time in the whole H_2SO_4 concentration range tested (0.1M-1.5M). Moreover, all hemihydrate materials produced were of α-form (refer to Figure 6.3).

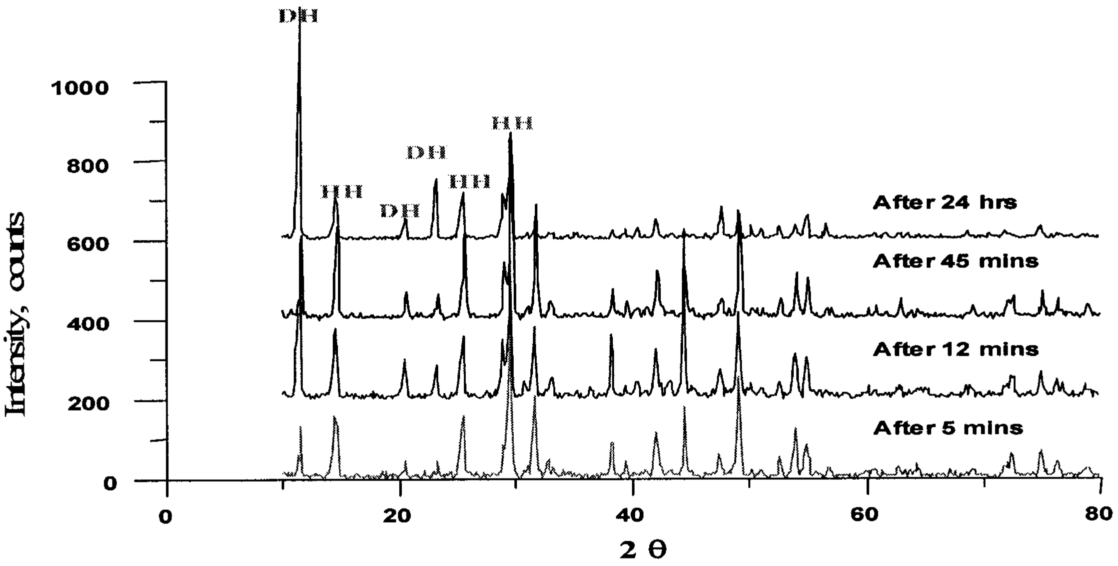

Figure 6.9: XRD monitoring of product as a function of retention time - dry lime added into 0.1M H_2SO_4 Conditions: CaO/H_2SO_4 ratio=0.4, 100°C

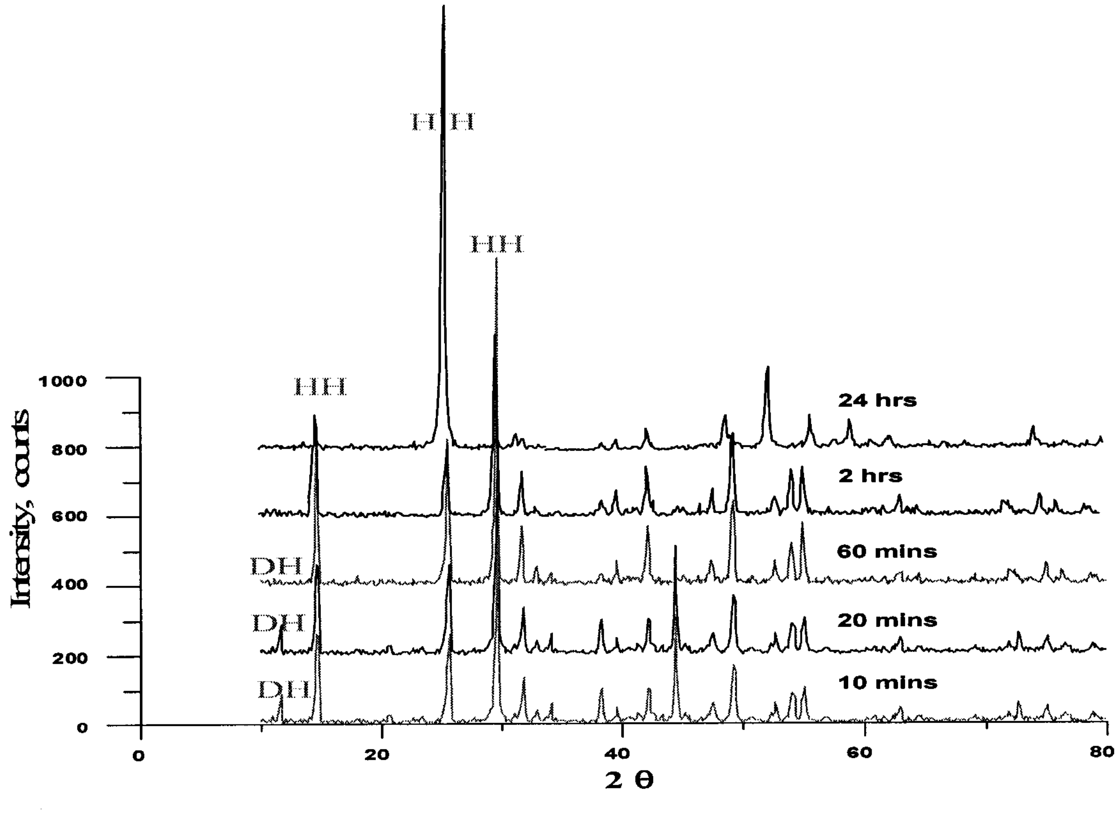

Figure 6.10: XRD monitoring of product as a function of retention time - dry lime added into 0.5M H_2SO_4 Conditions: CaO/H_2SO_4 ratio=0.4, 100°C

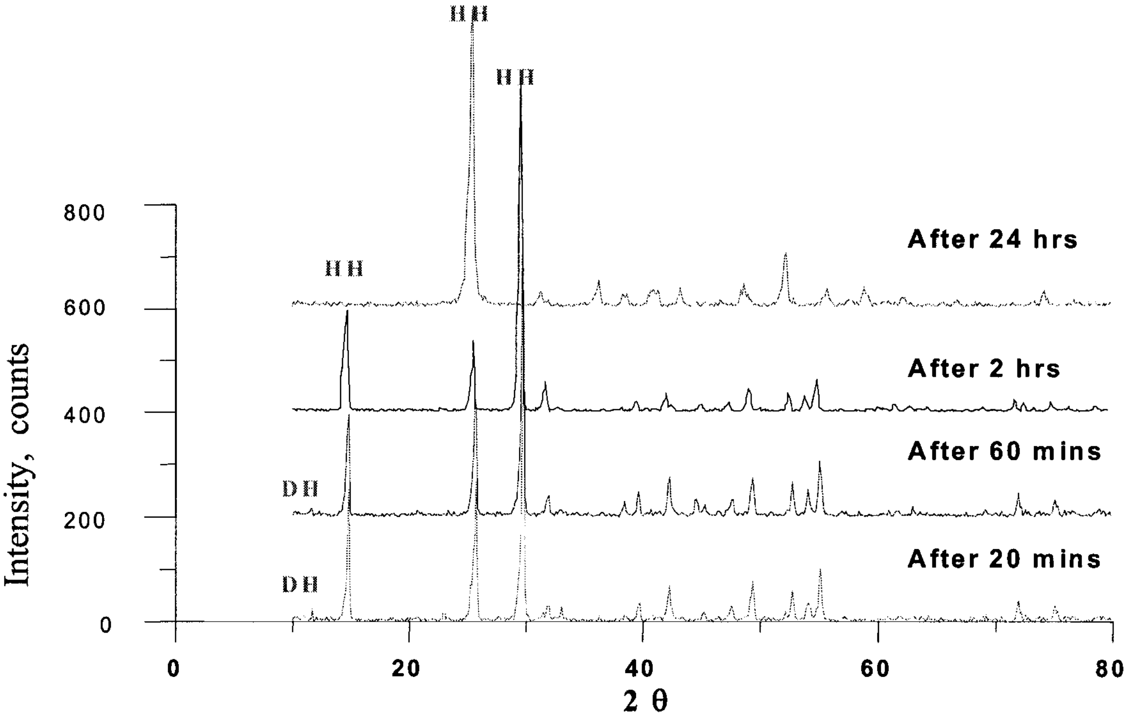

Figure 6.11: XRD monitoring of product as a function of retention time -dry lime added into 0.75M H_2SO_4
Conditions: CaO/H_2SO_4 ratio=0.4, 100°C

Prolonged retention time, however, was found to modify the morphology of hemihydrate from the characteristic needle-shaped crystals to fibrous crystals (Figure 6.14). Similar results were obtained when slaked lime (instead of dry) was added to H_2SO_4 (refer to Figure 6.15). Since anhydrite has similar morphology (in sulfuric acid), it is concluded that this fiber-like crystals are simply precursors to hemihydrate's conversion to anhydrite. This was further confirmed by detailed XRD examination[2] which revealed some subtle changes leading to conversion of hemihydrate to anhydrite. As discussed in chapter 7 the fibrous morphology is undesirable hence the crystallization process has to be appropriately controlled to avoid its appearance.

---

[2] Take for example the 24-hour XRD pattern of Figure 6.12 (dry lime added into 1.00M H_2SO_4), it can be seen that, some characteristic peaks drastically decreased (e.g., $2\theta \approx 14.7$) or virtually disappeared (e.g., $2\theta \approx 31.8$), whereas some small peaks (e.g., peak corresponding to $2\theta \approx 36.3$) characteristic of anhydrite (JCPDS card 37-1496) occurred.

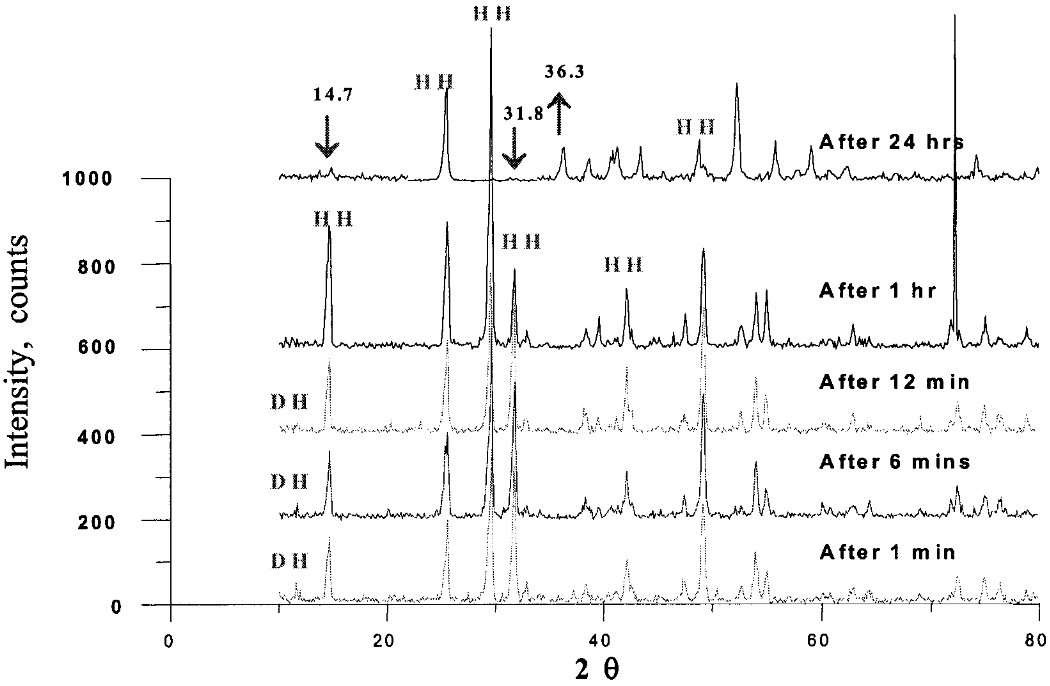

Figure 6.12: XRD monitoring of product as a function of retention time

- dry lime added into 1.0M H_2SO_4

Conditions: CaO/H_2SO_4 ratio=0.4, 100°C

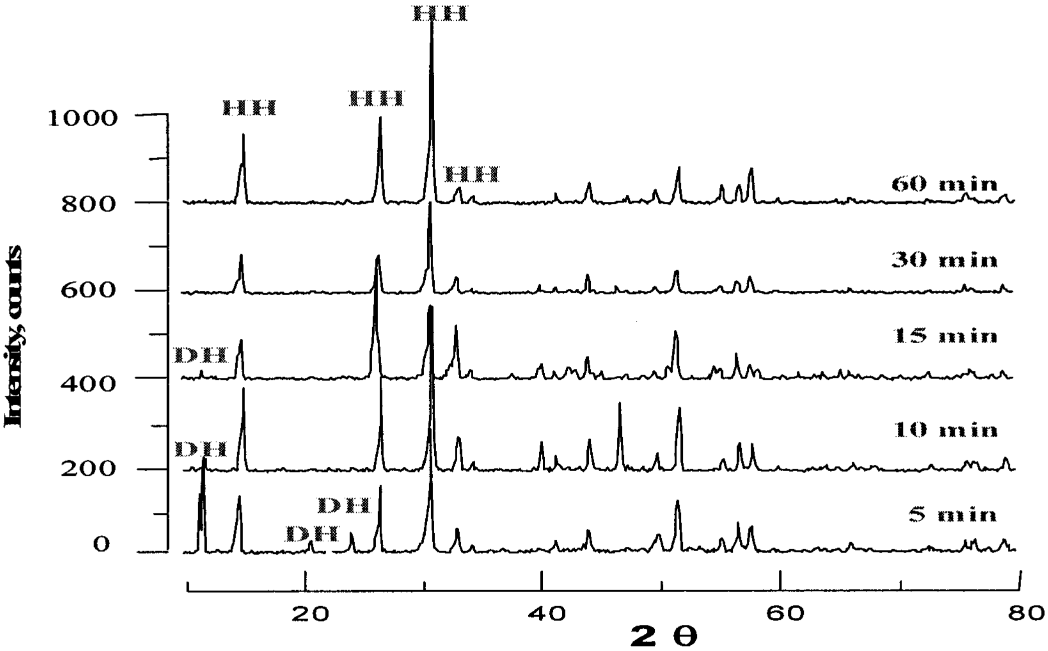

Figure 6.13: XRD monitoring of product as a function of retention time

- dry lime added into 1.5M H_2SO_4

Conditions: CaO/H_2SO_4 ratio=0.4, 100°C

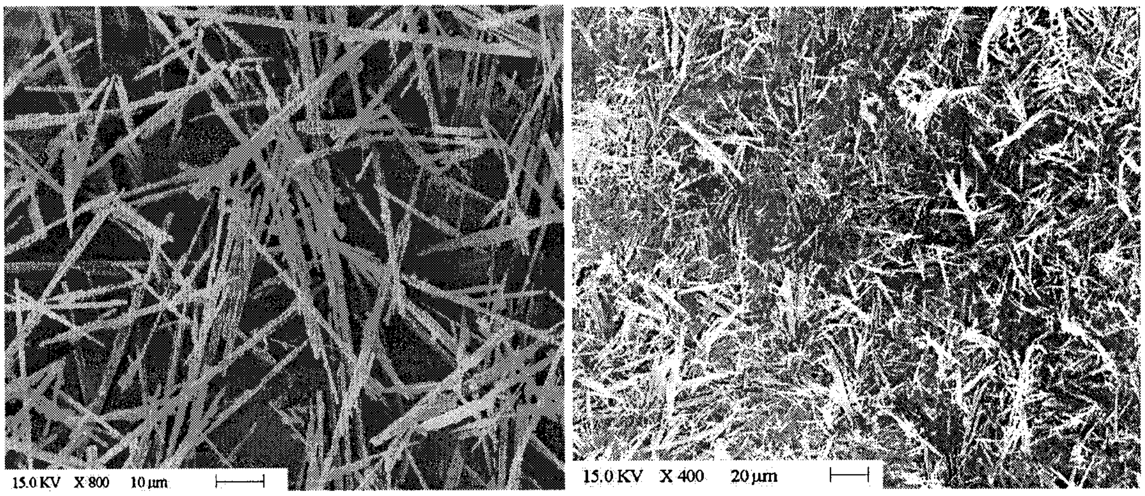

(a) After 1-hour retention time (b) After 24-hour retention time

Figure 6.14: Typical α-hemihydrate crystal morphology after different retention times - addition of dry lime to H_2SO_4

Conditions: 1.5M H_2SO_4, CaO/H_2SO_4 ratio=0.4, 100°C

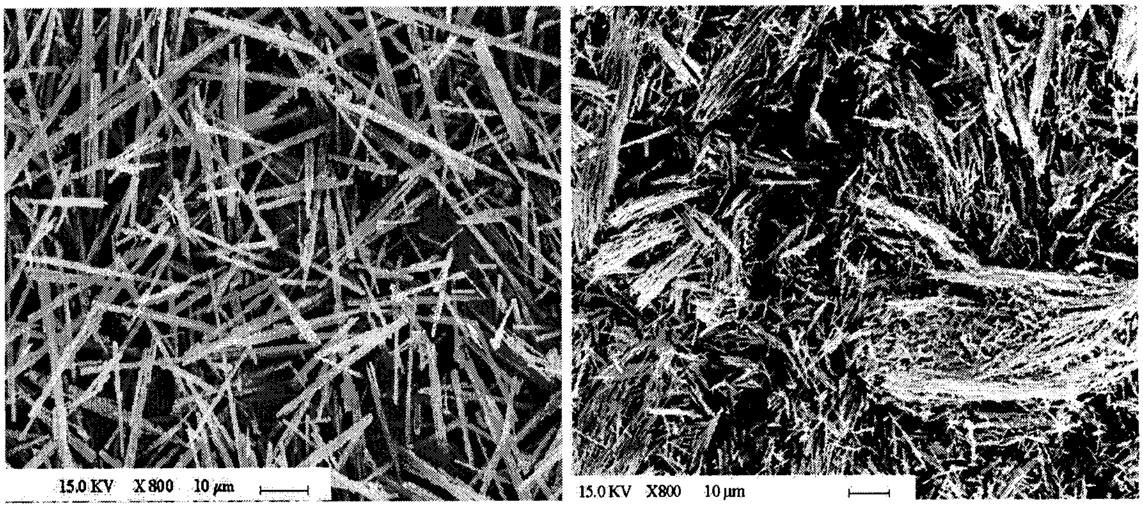

(a) After 1-hour retention (b) After 24-hour retention

Figure 6.15: Typical α-hemihydrate crystal morphology after different retention times - addition of slaked lime to H_2SO_4

Conditions: 1.50M H_2SO_4, CaO/H_2O=1/6, CaO/H_2SO_4 ratio=0.4, 100°C

6.3.4 Reaction kinetics

The reaction at 100°C between CaO/Ca(OH)$_2$ and H_2SO_4 is very fast proceeding almost to completion within 15 minutes. This is true independent of the initial H_2SO_4 concentration- compare Figure 6.16, a and b (1.25M H_2SO_4 vs. 0.5M H_2SO_4) or Figures 6. 16, c and d (CaO/ H_2SO_4 ratio 0.4 vs. 0.8). A quick analysis of the final concentration levels showed them to be in accordance with the stoichiometry of the process. Consider example Figure 6.16 that corresponds to 1.25M H_2SO_4 and CaO/H_2SO_4 = 0.4. The final ("steady-state") levels of H^+ and SO_4^{2-} correspond to the stoichiometric amounts:

$$(\sim 0.75M)\ [H_2SO_4]_{unreacted} = (1.25M)\ [H_2SO_4]_{initial} - (\sim 0.5M)[H_2SO_4]_{reacted} \quad (6.3.3)$$

This finding combined with the very low calcium content (~0.080M) explains why the conductivity depends only on H_2SO_4 concentration.

This fast reaction, however, does not yield necessarily the same calcium sulfate product. As discussed in section 6.3.3, the product varies from dihydrate to hemihydrate as the concentration increases. Take for example the product obtained after 20 minute reaction of CaO with 0.5M H_2SO_4 (CaO/H_2SO_4 = 0.4) was a mixture of dihydrate and hemihydrate (see Figure 6.10) but this was all hemihydrate when the initial H_2SO_4 concentration was 1.0 M (and all other concentrations the same). This reveals that the kinetics of phase transformation does not coincide with the kinetics of CaO/H_2SO_4 reaction.

Conductivity measurements were also done during the course of the reaction to monitor its kinetics. The conductivity change appears to be in good agreement with the concentration change (see Figure 6.17) suggesting that conductivity monitoring can be a good tool for process control purposes. Under such high-temperature, high-acidity and slurry environment, pH measurement is no longer reliable to monitor/control the reaction as normally; hence conductivity monitoring is a much better choice, especially from a practical operational perspective.

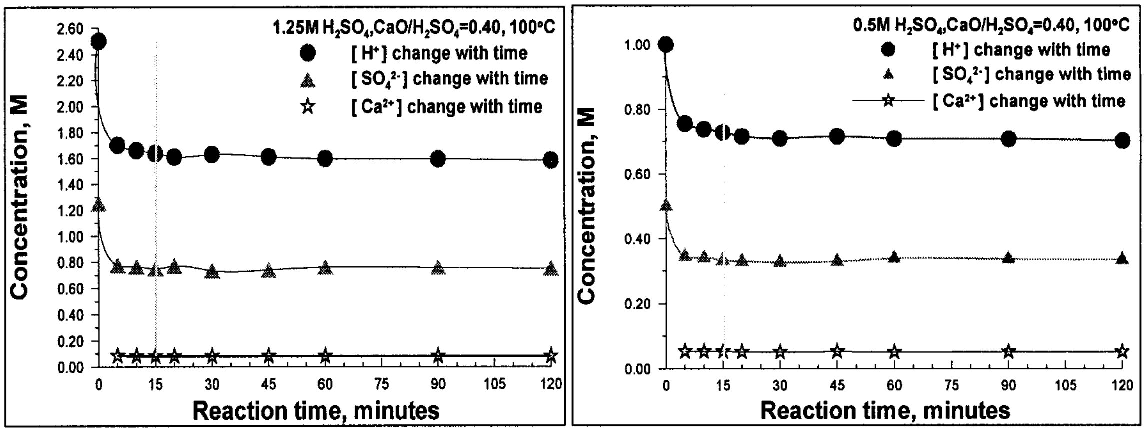

(a) 1.25M H_2SO_4, CaO/H_2SO_4 = 0.4 (b) 0.50M H_2SO_4, CaO/H_2SO_4 = 0.4

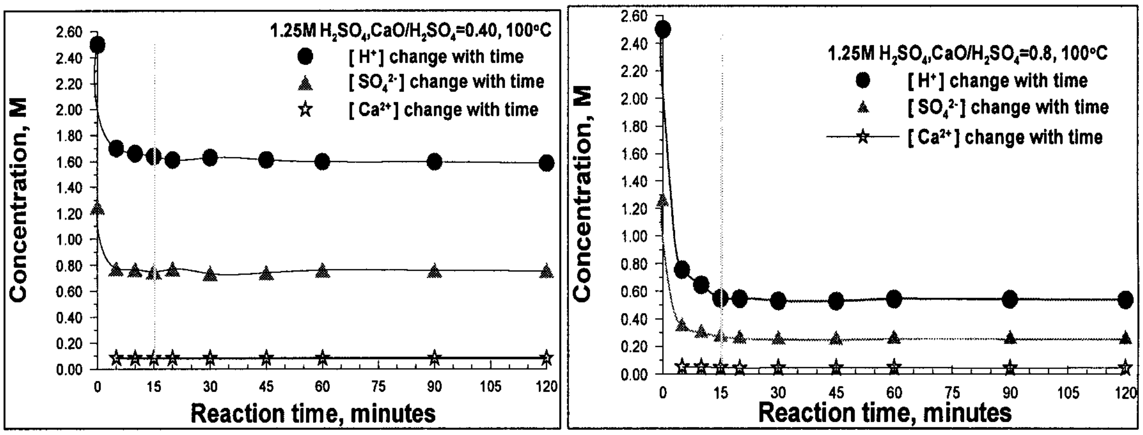

(c) 1.25M H_2SO_4, CaO/H_2SO_4 = 0.4 (d) 1.25M H_2SO_4, CaO/H_2SO_4 = 0.8

Figure 6.16: Monitoring the concentration[3] change of the reaction process

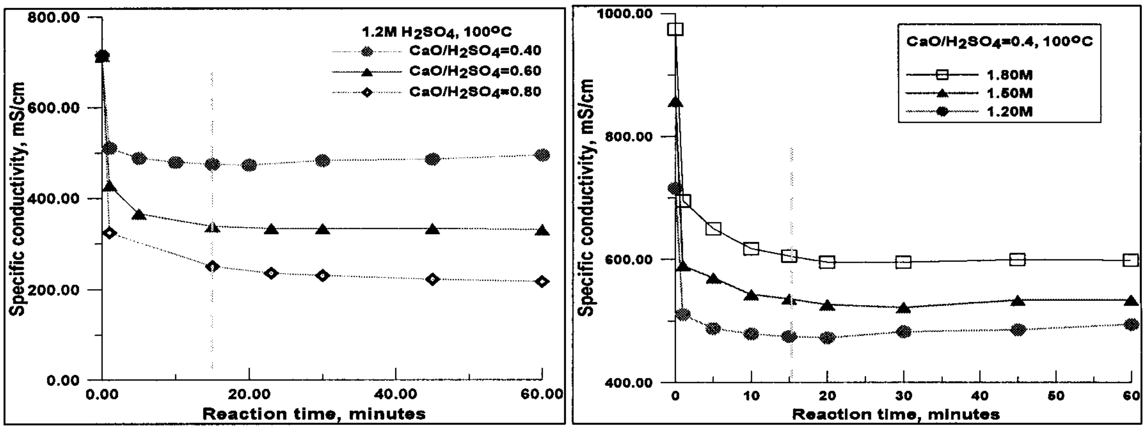

(a) varied CaO/H_2SO_4 ratios at 1.2MH_2SO_4 (b) varied [H_2SO_4] at CaO/H_2SO_4 ratio of 0.4

Figure 6.17: Monitoring conductivity change of the reaction process

---

[3] It should be clarified that, [SO_4^{2-}] is the equivalent SO_4^{2-} concentration that corresponds to total [S] in the reaction solution.

6.4 Reverse procedure – addition of H_2SO_4 to slaked lime

As mentioned at the opening of this chapter, the order of mixing of the two reactants, H_2SO_4 solution and lime, was found to impact significantly on the morphology of produced α-hemihydrate material. This is demonstrated when the SEM photos of Figure 6.18 are compared with the correspondent ones of Figure 6.15. In the latter case hemihydrate was produced by adding lime into H_2SO_4 solutions while the reverse procedure was used in the former case. The reverse procedure involved adding sulfuric acid solutions of various concentrations to slaked lime prepared with various CaO/H_2O ratios. The complete set of tests performed following the reverse procedure of mixing is summarized in Table 6.1. All these tests were run with 300 rpm agitation speed as agitation was found not to have an effect (see Figure 6.18 and refer to Figure 6.22, b for testing result at agitation speed of 300 rpm). Examination of the results of Table 6.1 does induce similar trends in terms of calcium sulfate species formation as with the standard method of mixing already discussed in the previous sections (refer to sections 6.3.1 and 6.3.3). In other words, it is seen that hemihydrate formation is favored in the "steady-state" H_2SO_4 concentration of 0.58 to 1.12M H_2SO_4 after 1 hour retention. Lower acid concentration was not adequate for complete conversion of the intermediately formed dihydrate. Meanwhile, higher acid concentrations or longer retention times favored conversion of hemihydrate to anhydrite.

From a practical point of view, a ratio CaO/H_2O of 1/3 or even lower (1/4 to 1/6) is preferred otherwise the slaked lime slurry dries up causing problems of agitation (lack of slurry fluidity). It is interesting to note that according to literature [10-11] for complete hydration of lime, in a static open-vessel, three times of the stoichiometric amount of water is needed as also observed here.

As for the slaking temperature of lime, it was found not to be so significant as opposed to that in the standard procedure of adding lime into H_2SO_4 solution. Dihydrate overgrowth was observed not to be a problem even at lower slaking temperature (e.g., room temperature), which was attributed to the colloidal nature of the slaked lime slurry. For optimum results, the slaking temperature of lime was controlled at around 75°C (or close to boiling point).

Table 6.1: Summary of reverse procedure results – procedure involved mixing 16.8g (0.3 moles) CaO at different slaking ratios with H_2SO_4 solutions of varied concentrations

Test No.	Initial H_2SO_4 Concentration (M)	Slaking ratio of lime to Water (by weight)	Estimated * H_2SO_4 Concentration after mixing with the slaking water	CaO / H_2SO_4 ratio	Phase composition (by XRD) after			Final H_2SO_4 Concentration (M)
					1 hour	3 hours	24 hours	
1	0.75	1/1	0.74	0.4	DH+ HH	HH	HH	0.44
2	1.0	1/1	0.98	0.4	HH	HH	HH	0.58
3	1.0	1/4	0.92	0.4	HH	HH	HH	0.55
4	1.0	1/8	0.85	0.4	DH+HH	HH	HH	0.50
5	1.5	1/2	1.41	0.4	HH	HH	HH**	0.84
6	1.5	1/6	1.25	0.4	HH	HH	HH**	0.74
7	1.5	1/8	1.18	0.4	HH	HH	HH	0.70
8	2.0	1/8	1.47	0.4	HH	HH	HH**	0.88
9	2.5	1/1	2.37	0.4	AH	AH	N/A	1.41
10	2.5	1/2	2.25	0.4	AH	AH	N/A	1.34
11	3.0	1/3	2.50	0.4	AH	AH	N/A	1.49
12	3.0	1/10	1.79	0.4	HH	HH+ AH	AH	1.07
13	6.0	1/18	1.75	0.4	HH	HH+ AH	AH	1.04
14	12.0	1/20	1.88	0.4	HH	HH+ AH	AH	1.12
The following tests were performed with different ratios of CaO/H_2SO_4								
15	1.5	1/6	1.30	0.3	HH	HH	HH**	0.90
16	1.5	1/6	1.15	0.6	HH	HH	HH	0.46
17	1.5	1/6	1.03	0.9	HH	HH	HH	0.10
18	1.5	1/6	1.00	1.0	HH+DH	HH+ DH	HH+DH	~0.00

* Estimated concentration of H_2SO_4 is defined as:

moles of initial H_2SO_4/(volume of initial H_2SO_4 + volume of slaking water)

which is a coarse estimation of the hypothetical H_2SO_4 concentration after dilution with the slaking water.

** Traces of anhydrite were observed among the majority of hemihydrate on the XRD pattern.

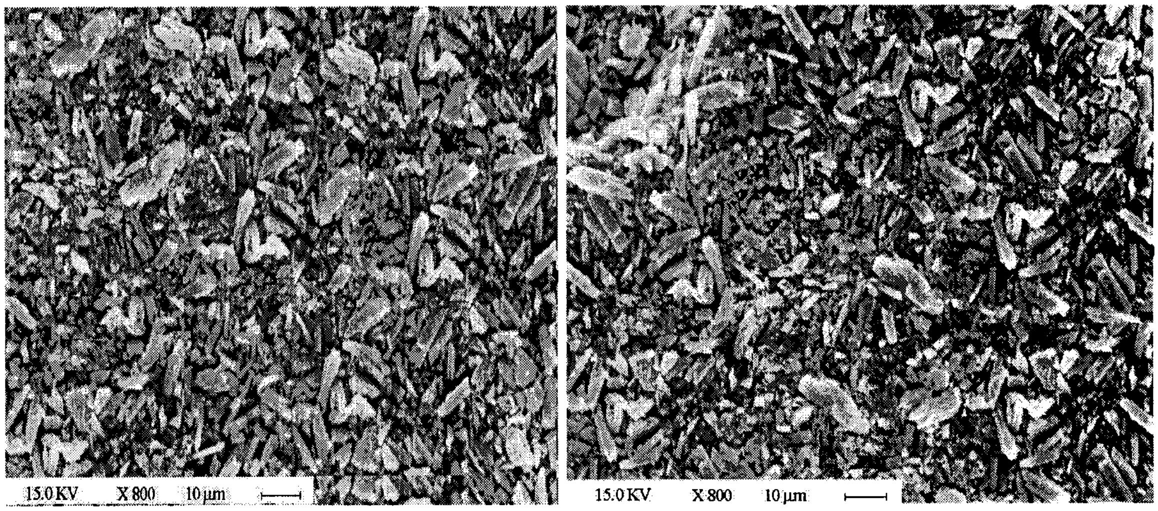

(a) No agitation (b) Strong agitation(900 rpm)

(refer to Figure 6.22, b for testing result at agitation speed of 300 rpm)

Figure 6.18: Reverse procedure - Influence of agitation on crystal morphology
Conditions: 1.50M H_2SO_4, $CaO/H_2O=1/6$, CaO/H_2SO_4 ratio=0.4, 100°C,
Reverse procedure: addition of H_2SO_4 to slaked lime; 1-hour retention time.

The production of α-hemihydrate (refer to Figure 6.19 for DSC verification of the produced material) via the reverse procedure was monitored by sampling and XRD analysis. Typical results are shown in Figure 6.20. It is informative to compare these data with those of the standard procedure involving addition of lime to H_2SO_4 (Figure 6.13). It can be seen that differences exist in the early stages of the reaction. Thus in the case of the reverse procedure, in addition to dihydrate, unreacted lime ($Ca(OH)_2$) can be seen to be present in the first 10 minutes of the reaction. There appears, in this case therefore, that conversion of the intermediately-formed dihydrate taking place before all hydrated lime has reacted, i.e., nucleation of hemihydrate occurs in an alkaline as opposed to acidic environment. The conversion of the intermediate products to hemihydrate was completed within 30 minutes[4].

---

[4] Similar to the observations made with the standard procedure (section 6.3.3) aging of the product (by prolongation of the retention time to 24 hours) started causing hemihydrate to fibrous anhydrite. Hence, one hour retention time was used for optimum yield of α-hemihydrate crystals as done with the standard procedure.

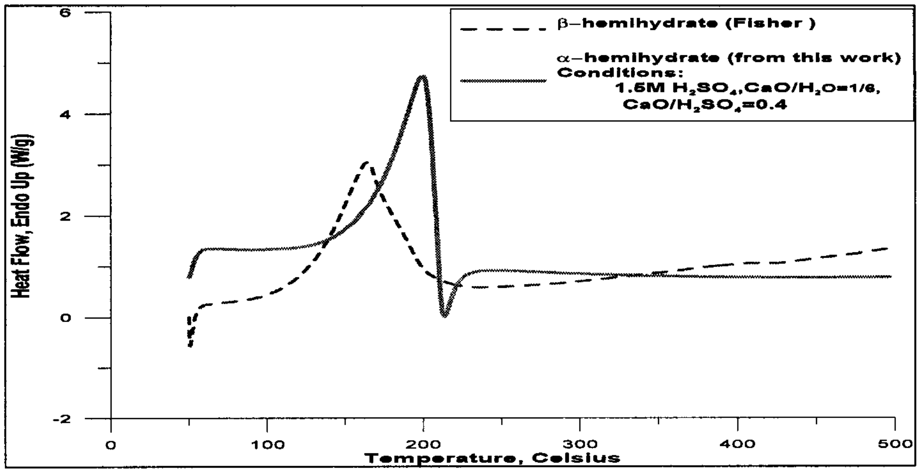

Figure 6.19: Typical DSC pattern of the α-hemihydrate material produced via the reverse procedure of addition of H_2SO_4 solution to slaked dry lime

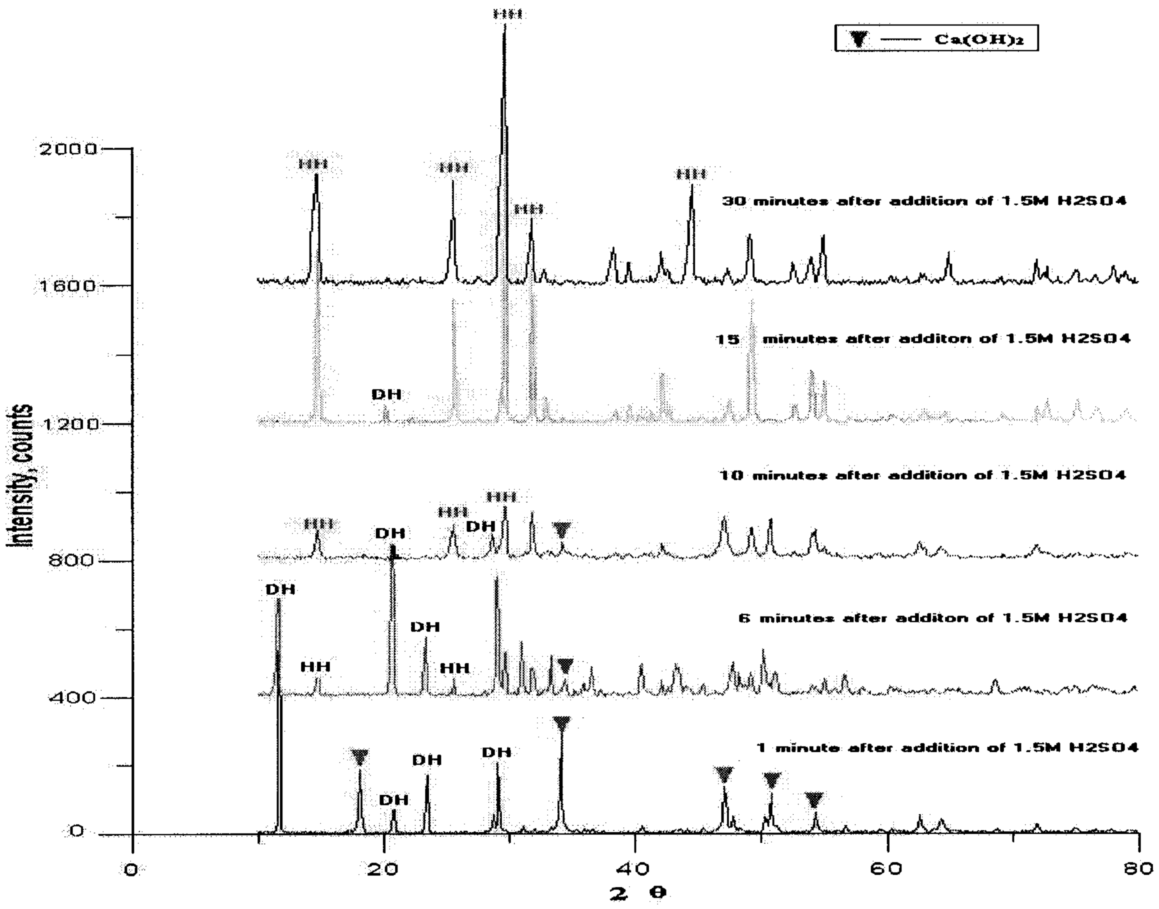

Figure 6.20: XRD monitoring of product obtained with reverse procedure involving addition of H_2SO_4 to slaked lime

Conditions: 1.50M H_2SO_4, CaO/H_2SO_4 ratio=0.4, CaO/H_2O=1/6, 100°C.

(Test No. 6 in Table 6.1)

The slurry of slaked lime has a relatively high pH value (around 12.40 as measured). Development of the hydration of lime results in large number of small primary crystallites of calcium hydroxide [12-13]. At higher temperatures, even higher number of smaller primary crystallites would form due to the reduced solubility of the calcium hydroxide [14-15], and hence more spontaneous/homogenous nucleation. Those fine crystallites of hydrated lime lead to a colloidal suspension [16]. This is evaluated with the SEM photos of Figure 6.21 demonstrating the influence of slaking on lime particle morphology. According to literature [12], the particle size of calcium hydroxide is in the range of 0.2-0.4μm. This may then be another factor, in addition to alkalinity, that causes the changes to hemihydrate morphology (from needle-shape of Figure 6.15, a to the morphology of Figure 6.18).

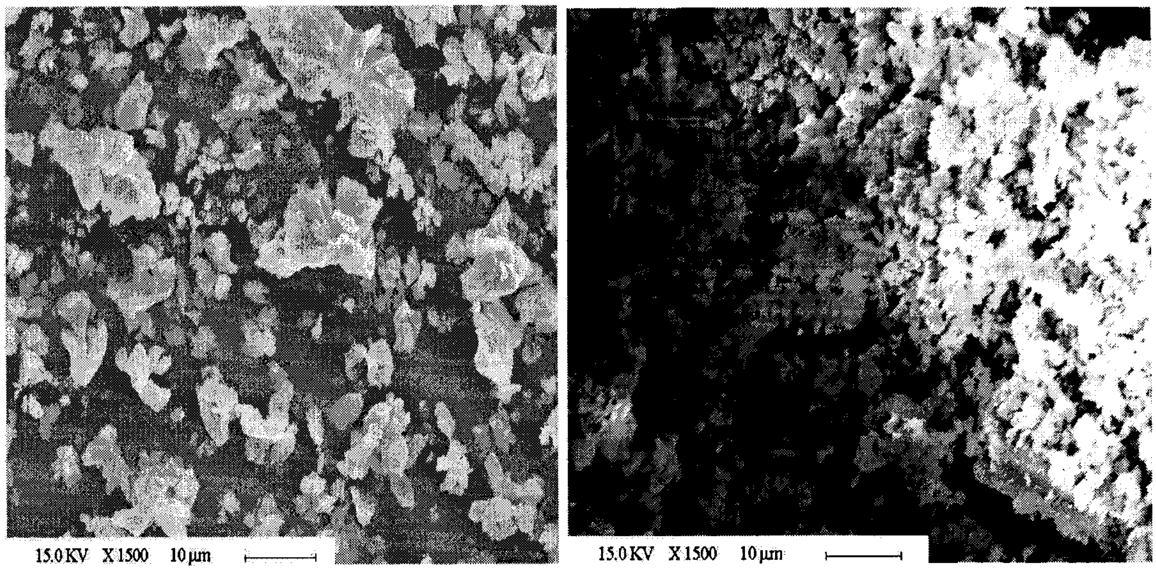

(a) Typical image of dry lime powder (b) Image of dried sample of slaked lime

Figure 6.21: SEM images of dry lime powder and slaked lime after drying

The morphology of hemihydrate was further improved when acid was added slowly to the slaked lime slurry rather than all-at-once. Compare the SEM photos in Figure 6.22, this improvement can be attributed to the relatively lower supersaturation level in case of slow addition, which in turn favors orderly crystal growth. It appears, after considering the results reported in section 5.3.3 (in particular Figure 5.14, d), that, when slow titration procedure is followed (i.e., slow addition of H_2SO_4 into the lime suspension), the dihydrate crystals that form initially convert to hemihydrate with minimum morphological changes, i.e., by mainly following a solid-state transformation (dehydration) mechanism as opposed to the dissolution-recrystallization (or through-solution) mechanism [17-19].

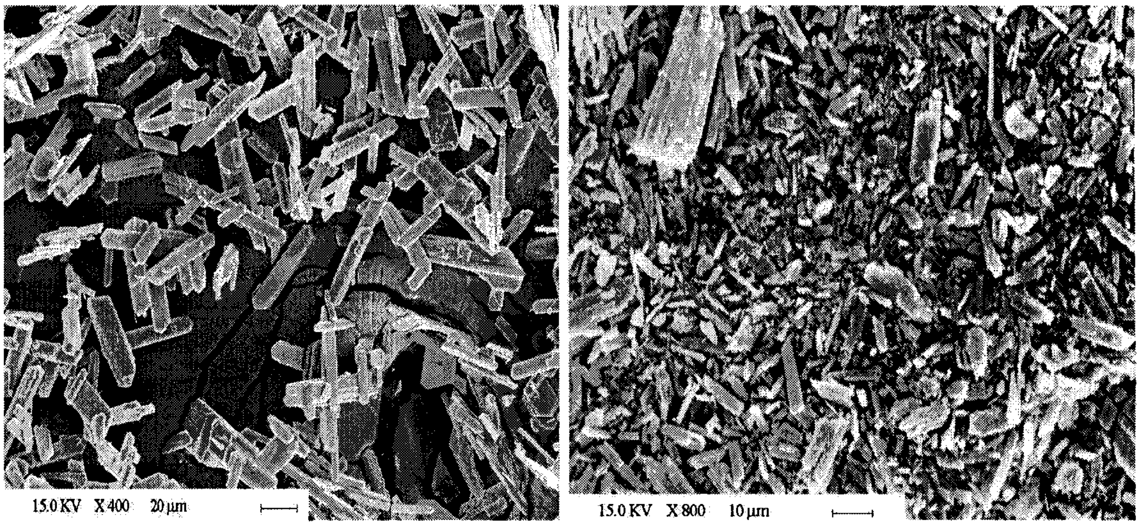

(a) Resultant image from slow addition of H_2SO_4 (in about 30 minutes)

(b) Resultant image from fast addition of H_2SO_4 (pour within 5 minutes)

Figure 6.22: Hemihydrate crystal morphology obtained by the reverse procedure involving addition of H_2SO_4 to slaked lime (1-hour retention time)
Conditions: 1.50M H_2SO_4, CaO/H_2SO_4 ratio=0.4, CaO/H_2O=1/6, 100°C

6.5 Conclusions

(1) An operating window has been determined in terms of H_2SO_4 concentration, temperature and time within which clean α-hemihydrate can be produced by reaction of lime with H_2SO_4. This window is defined as 0.6-1.1M H_2SO_4 (steady-state concentrations), 98-105°C and 1 hour retention time.

(2) The experimentally defined operating window is very narrow in comparison to metastable region of hemihydrate determined by thermodynamic calculations that consider the activity of water to control the phase equilibria: *dihydrate* $\rightleftarrows$ *hemihydrate* $\rightleftarrows$ *anhydrite*. This implies that, in the case of H_2SO_4, other factors (unknown) cause hemihydrate metastability to be drastically reduced.

(3) At lower steady-state acidities (<0.5M) hemihydrate is still produced but in co-existence with dihydrate, while at higher acidities (>1.1M) anhydrite formation dominates.

(4) Dihydrate forms as intermediate product quickly converting to hemihydrate. The kinetics of conversion depends on the acidity level. For example, at 0.06M (steady-state) H_2SO_4 dihydrate conversion to hemihydrate is not complete even after 24 hours while the conversion is complete after 1 hour at 0.6M (steady state).

(5) The typical morphology of α-hemihydrate crystals is needle-shape with 50-100 μm length and 1-3 μm thickness.

(6) Upon prolonged equilibration (typically 24 hours or longer) in their acid-preparation solutions hemihydrate needle-shaped crystals become fibrous and eventually convert to anhydrite.

(7) The ratio CaO/H_2SO_4 should be kept at or below 0.8 to avoid high viscosity conditions on one hand and promote the conversion of dihydrate to hemihydrate on the other. Optimum results in this work were obtained with CaO/H_2SO_4 ratio equal to 0.4.

(8) Due to the exothermic nature of the process, the reaction may be initiated at lower than 100°C temperature, however temperature below 75°C was found to result in "gravel-like" dihydrate overgrowth around unreacted $CaO/Ca(OH)_2$ that hinders further acid attack, hence temperatures above 75°C should be used.

(9) Addition of dry or slaked lime to H_2SO_4 yields the same results in terms of product quality (XRD and SEM characterization).

(10) Agitation speed was found not to have any significant effect on crystal morphology apparently due to conducting the system at a temperature near the boiling point.

(11) The reaction between CaO and H_2SO_4 is very fast at 100°C reaching completion in less than 20 minutes. It has been determined that it is feasible to monitor the reaction by in-situ conductivity measurements.

(12) Slow addition of H_2SO_4 solution to slaked lime – reverse procedure – (preferred CaO/H_2O range 1/4-1/6) was found to favor the production of α-hemihydrate with column-shaped as opposed to needle-shaped crystal morphology within otherwise the same operating window, 0.6-1.1M H_2SO_4.

(13) The slaking of lime that produces a colloidal suspension of hydrated $Ca(OH)_2$ particles and/or the alkaline environment dominating during the nucleation process of α-hemihydrate were thought as possible reasons for causing the different hemihydrate crystallization behavior when the reverse procedure was used.

References

[1] http://www.mersonprocess.com/RAIhome/liquid/products/Model_228.asp.

[2] Hinatsu, J. T., Tran, V. D. and Foulkes, F. R., Electrical conductivities of aqueous zinc sulfate-sulfuric acid solutions, Journal of Applied Electrochemistry, 22(3), 215-223(1992).

[3] Baghalha, M. and Papangelakis, V. G., High-temperature conductivity measurements for industrial applications. 1. A new cell, Industrial & Engineering Chemistry Research, 39(10), 3640-3645(2000).

[4] http://www.olisystems.com.

[5] Booth, J., Hong, Q., Compton, R.G., Prout, K. and Payne, R. M., Gypsum overgrowths passivate calcite to acid attack, Journal of Colloid and Interface Science, 192, 207-214(1997).

[6] Hassibi, M., An overview of lime slaking and factors that affect the process, http://www.chemcoequipment.com/Overview_of_Lime_Slaking.PDF.

[7] Manufacture and uses of lime, http://www.gcsechemistry.com/rk19.htm.

[8] Tolonen, J., Tolonen, O. and Puhakka, J., Optimization of the causticising process, http://www.tappsa.co.za/html/optimisation.htm.

[9] Technical Advice Note - The Maturity of Lime Putty, http://www.rose-of-jericho.demon.co.uk/support/rjtan_01.htm.

[10] Couturier, M.F., Marquis, D.L., Steward, F.R. and Volmerange, Y., Reactivation of partially sulphated limestone particles from a CFB combustor by hydration, Canadian J. Chemical Engineering, 72(1), 91-97(1994).

[11] Khan, T., Kuivalainen, R. and Lee, Y.Y., Improving limestone utilization in circulating fluidized bed combustors through the reactivation and recycle of partially utilized limestone in the ash, Proceedings of 13th International Conference on Fluidized Bed Combustion, Orlando, May 7-10, The American Society of Mechanical Engineers: New York, NY, USA, 2, 831-840(1995).

[12] Glasson, D.R., Reactivity of lime and related oxides. V. Crystal changes in hydrated lime at different temperatures, J. Applied Chemistry, 11(1), 24-27(1961).

[13] Gill, A.F. and Way, T.H., The treatment of hydrated lime with aluminum sulphate, Canadian J. Research, 12, 253-260(1935).

[14] Bassett, H., Notes on the system lime-water, and on the determination of calcium, J. Chemical Society, 1270-1275(1934).

[15] Glasson, D.R., Reactivity of lime and related oxides. XIII. Sulphating of hydrated lime, J. Applied Chemistry, 15(8), 378-383(1965).

[16] Ray, K. W. and Mathers, F. C., The colloidal behavior of lime, Industrial & Engineering Chemistry, 20, 475-477(1928).

[17] Gartner, E.M. and Gaidis, J.M., Hydration mechanisms, I, Materials Science of Concrete, 1, 95-125(1989).

[18] Zürz, A., Odler, I., Thiemann, F. and Berghöfer, K., Autoclave-free formation of α-hemihydrate gypsum, Journal of the American Ceramics Society, 74(5), 1117-1124(1991).

[19] Bobrov, B.S., Romashkov, A.V. and Andreeva, E.P., Mechanism of the formation and growth of crystals of calcium sulfate hemihydrate, Izvestiya Akademii Nauk SSSR, Neorganicheskie Materialy, 23(3), 497-500(1987) (in Russian).

Chapter 7

Crystal Modification and Property Evaluation

7.1 Introduction

This chapter is divided into two parts: Part I, crystal modification; and Part II, property evaluation.

Part I focuses on the role of additives (comprising organic and inorganic) and seeding-recycling on the morphology of the α-hemihydrate crystals. The study involved both preparation procedures described in chapter 6, i.e., addition of dry lime to H_2SO_4 solution (the standard procedure) and addition of H_2SO_4 to slaked lime (reverse procedure).

Testing of additives is an exhausting and time-consuming (and sometimes fruitless) job. Given the vast variety of chemicals, testing of additives can only be done selectively. Choosing/screening of additives was made mainly on the basis of information derived from literature [1-8]. Inorganic salts, weak organic acids and their salts with strong bases, alcohols, amines and their derivatives, some long chain polymers as well as combinations of organic and inorganic chemicals have been tried.

Seeding and recycling are similar techniques that are commonly used to favor crystal growth. Both techniques were tested here. Moreover, seeding was done after the solution was saturated with calcium sulfate in order to avoid the dissolution of the seed material.

Property evaluation of α-hemihydrate products is reported in Part II. Alpha-hemihydrates were tested physically so as to assess their use as plaster materials. In this regard, properties such as normal consistency (water/solid ratio), setting time and compressive strength were evaluated. Measurement of these properties was made following ASTM standard procedures (ASTM C472-93).

Part I: Crystal Modification – Additives, Seeding and Recycling

7.2 Experimental

If not otherwise specified, all experiments were carried out with the glass reactor described in section 3.3; the agitation rate was controlled at 300rpm, the reaction slurry was hot-filtered after 1 hour retention and treated with method 3 as described in section 3.5; the final dry samples were examined with XRD/DSC for phase identification and with SEM for morphology evaluation.

7.2.1 Testing of additives

The additives tested are listed below:

Inorganic chemicals:[1] salts of K^+, Na^+, NH_4^+, Fe^{2+}, Zn^{2+}, Mg^{2+}, Cu^{2+}, Ni^{2+}, Fe^{3+}, Al^{3+}, Sr^{2+} etc. combined with either Cl^-, NO_3^- or SO_4^{2-};

Organic chemicals[2]: Most of these were acids such as gluconic acid, phthalic acid, succinic acid, pyruvic acid, tartaric acid, malic acid, glutamic acid, malonic acid, tricarballylic acid, fumaric acid, mellitic acid, salicylic acid, mandelic acid, benzoic acid, and citric acid; some salts were also tested such as sodium citrate, sodium succinate; finally a variety of other organic chemicals such as sorbitol, lignosol, amines and their derivatives, and some long-chain polymers such as polyethylene glycol (mw~10,000), polyvinyl alcohol (mw~22,000), polyvinyl acetate (mw~50,000), polythethylene glycol succinate (mw~5000), etc., were also selected for testing.

The selected additives were tested at various dosages, for example, 10wt%, 5wt% and 1wt% [3] (with reference to the weight of CaO added) in the case of inorganic

---

[1] Inorganic chemicals are mainly from A&C American Chemicals.

[2] Organic chemicals are mainly from Alfa Aesar.

[3] Theoretically speaking, mol% should be better than wt%, since it is not unusual that commercial chemicals (either inorganic or organic) come in the form of hydrates (with hydrated water). However, wt% is dominantly used in the literature and in practice [1-8], even in the ASTM standard C472-93 for hemihydrate testing. Hence, wt% is employed in this work.

chemicals; or 10wt% and 1wt% in the case of organic chemicals. The most promising of the additives were subjected to further testing in order to optimize their performance.

7.2.1.1 Testing of additives with the standard procedure

In 500 mL 1.25M (1.20M or 1.50M in some cases) H_2SO_4 solution preheated to 100°C, specific amount of the additive(s) was added while stirring for around 2-3 minutes prior to the addition of lime. The CaO/H_2SO_4 ratio was 0.4. Some tests were also run with CaO/H_2SO_4 ratio equal to 1.0.

7.2.1.2 Testing of additives with the reverse procedure

As specific amount of additive(s) was first added into certain amount of de-ionized water while stirring for around 5 minutes, then dry lime (typically 16.8g or 0.3 moles) at certain CaO/H_2O ratio (typically 1/6) was added to form slurry of slaked lime. The slaking temperature was controlled as desired (above 75°C). Finally, 500 mL 1.50M H_2SO_4 solution preheated to 100°C was poured into the glass reactor to reach CaO/H_2SO_4 ratio of 0.4. Some tests were run at CaO/H_2SO_4 ratio at 1.0 as well.

7.2.2 Seeding experiments

7.2.2.1 Seeding experiments with the standard procedure

In all tests, 500 mL 1.50M (1.20M or 1.25M in some cases) H_2SO_4 solution was preheated to 100°C. Then, seed was added in one of the following ways: (i) excess hemihydrate, say, 15g, was added all at once into the solution; or (ii) the sulfuric acid was first saturated with calcium sulfate, and then, followed by the addition of extra, say, 10g hemihydrate material into the slurry. In both cases, the addition of seed was followed by the addition of lime to give CaO/H_2SO_4 ratio of 0.4 (or 1.0 in some tests).

7.2.2.2 Seeding experiments with the reverse procedure

Slurry of slaked lime with specific CaO/H_2O ratio (typically 1/6) was prepared and heated to 100°C [4], then, excess hemihydrate (refer to section 7.2.2.1) was introduced into the slurry while stirring the slurry for 5 minutes, reaction was initiated by adding 500 mL 1.50M H_2SO_4 solution (also pre-heated to 100°C) into the slaked lime slurry to reach a CaO/H_2SO_4 ratio of 0.4 (or 1.0 in some tests).

7.2.3 Recycling experiments

7.2.3.1 Recycling experiments with the standard procedure

The first run involved adding lime into 500 mL 1.50M H_2SO_4 solution preheated to 100°C to reach CaO/H_2SO_4 ratio of 0.4 and agitating the slurry for 1 hour; the slurry of run one was hot-filtered and a faction of the cake (1/4 to 1/2), was recycled to act as seed for the next run; in general, the procedure was repeated for 3 runs, or in some cases, up to 6 or 7 runs were carried out.

7.2.3.2 Recycling experiments with the reverse procedure

The first run involved adding 500 mL 1.50M H_2SO_4 solution (pre-heated to 100°C) to slurry of slaked lime (typically with CaO/H_2O ratio 1/6 and in some cases mixed with additives following the procedure described in section 7.2.1.2) to give a CaO/H_2SO_4 ratio of 0.4 (1.0 in some tests) and agitating for 1 hour. Then the resultant slurry of run one was hot-filtered with a slice (1/4 to 1/2) of the cake used as seed in the next run; generally, the procedure was repeated for 3 runs, or in some cases, up to 6 or 7 runs.

---

[4] Temperature at such level is necessary for preventing the seeded hemihydrate from possible phase transformation.

7.3 Influence of additives

7.3.1 Standard procedure of dry lime addition to H_2SO_4 solution

The hemihydrate is generally believed to have structure with channels where water molecules may be situated as illustrated in Figure 7.1 (refer for details to section 2.2 in chapter 2). A very interesting finding is that, as discussed in the previous chapter, the morphology of the α-hemihydrate crystals produced by reacting lime with sulfuric acid is exclusively acicular (refer for example to 6.15, a). 6.15, a is reproduced in this chapter for quick reference. Similarly, acicular shape α-hemihydrate morphology has been reported to be obtained in the absence of crystallization modifier(s) under a variety of preparation conditions [3, 5-6]. It may thus be deduced that, α-hemihydrate grows preferentially in the **c** axis direction (on the plane (001)) much more rapidly than in other directions ending in the form of fine needle-shaped crystals.

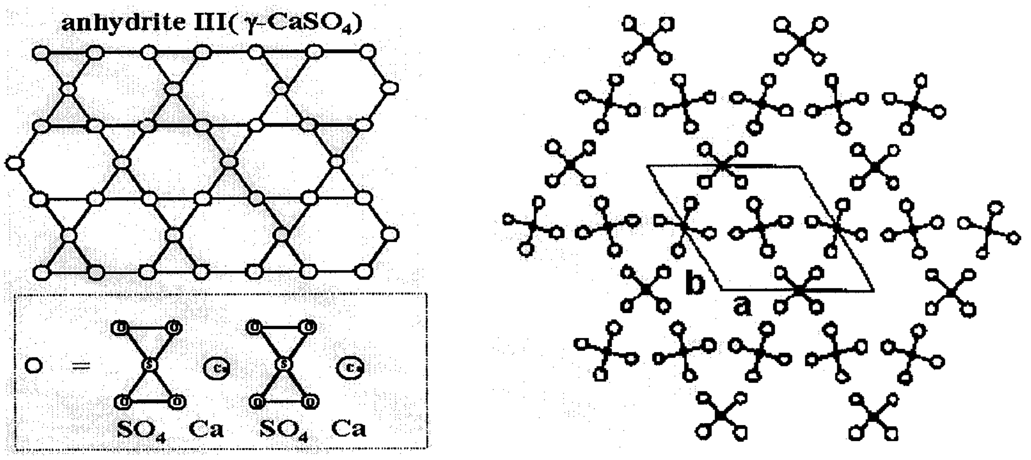

(a) Structure of anhydrite III(γ-$CaSO_4$); a chain of alternating Ca^{2+} and SO_4^{2-} perpendicular to plane of paper is represented by a small circle (after Abriel et al. [9]).

(b) [001] projection of anhydrite III structure illustrating the channels developed parallel to **c** axis - perpendicular to plane of paper (after Lager et al.[10]).

Figure 7.1: Schematic illustration of the hemihydrate structure with water molecules situated in the channels of the above Ca-SO_4 frame

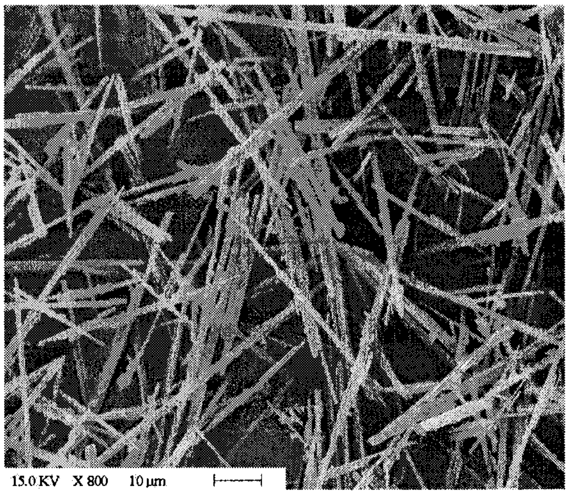

Figure 7.2: Typical acicular α-hemihydrate crystal morphology yielded by the standard procedure (refer to Figure 6.15, a)
Conditions: 1.50M H_2SO_4, CaO/H_2SO_4 ratio=0.4, 100°C

The effect of monovalent or divalent cation salts (with Cl^-, NO_3^- or SO_4^{2-}) on product morphology is shown in Figure 7.3. It is clear that none of these caused changes to the standard acicular morphology (Figure 7.2). According to reports divalent sulfate salts are supposed to be more effective [11-12] than the equivalent chloride or nitrate salts; however, no such trend was observed here. This perhaps reflects the fact that the system under investigation is predominantly sulfate any way (especially at the early stage of the reaction). Similar to anions, no obvious effect from monovalent and divalent cations was observed. However, with trivalent cation salts as additives a drastic alteration in morphology was observed (Figure 7.4). Basically, the product became "cotton-like" with individual crystals becoming extremely thin and small. The effect of the trivalent cation salts gradually disappeared as the additive's dose decreased below 1wt% (see Figure 7.5). Eventually, $Al_2(SO_4)_3$ at 3wt% dose was chosen (refer to Figure 7.6) as representing the most interesting additive system in producing hemihydrate morphology distinctly different from the typical acicular type (Figure 7.2).

Monovalent Cations Divalent Cations

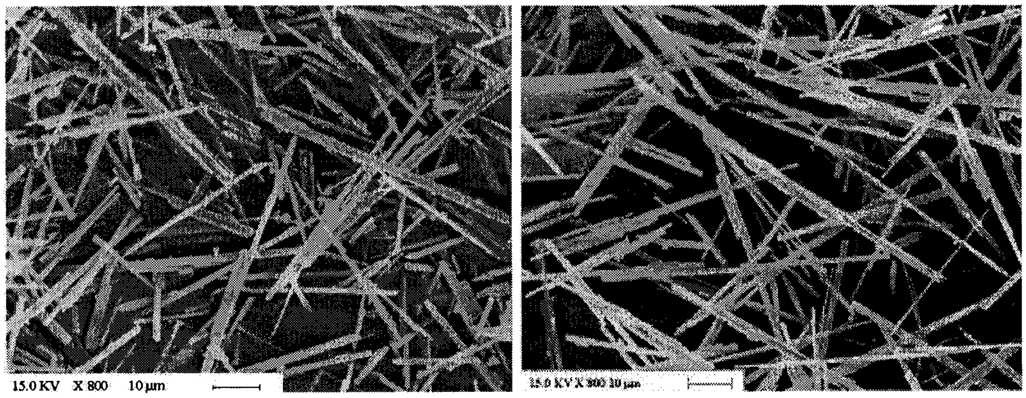

(a) 10wt% KCl (d) 10wt% $Mg(NO_3)_2$

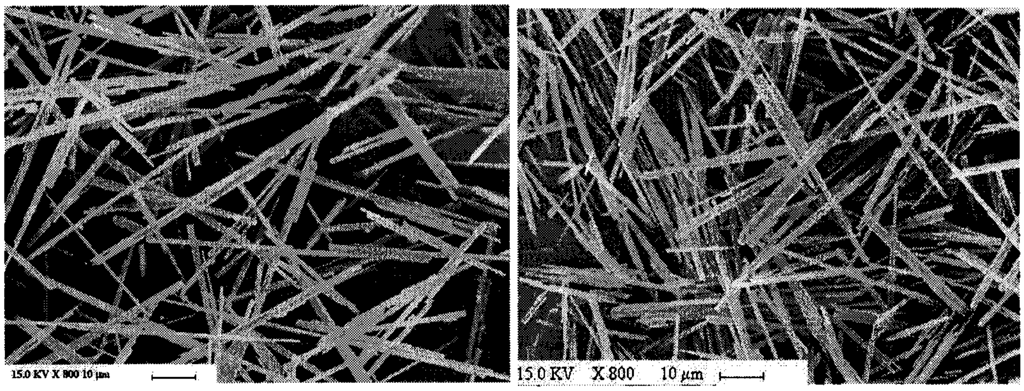

(b) 10wt% $NaNO_3$ (e) 10wt% $MgSO_4$

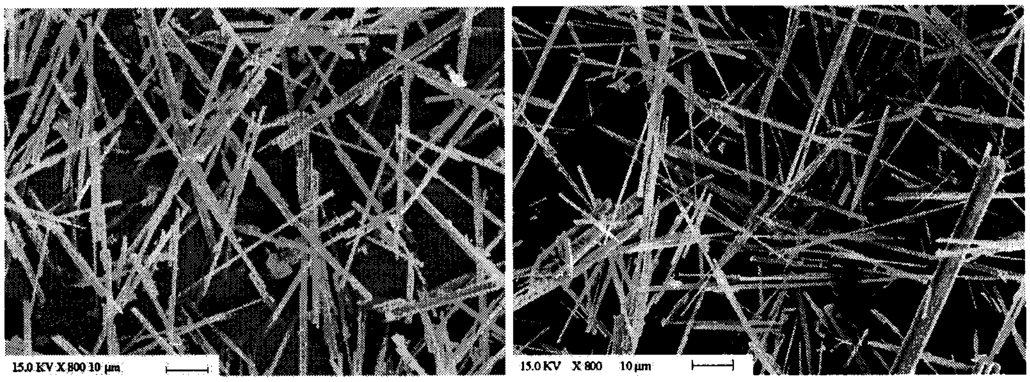

(c) 10wt% NaCl (f) 10wt% $NiCl_2$

Figure 7.3: Influence of monovalent and divalent inorganic salts on morphology of α-hemihydrate

Conditions: 1.25M H_2SO_4, CaO/H_2SO_4 ratio=0.4, 100°C

Standard procedure: addition of dry lime to H_2SO_4

Trivalent Cations

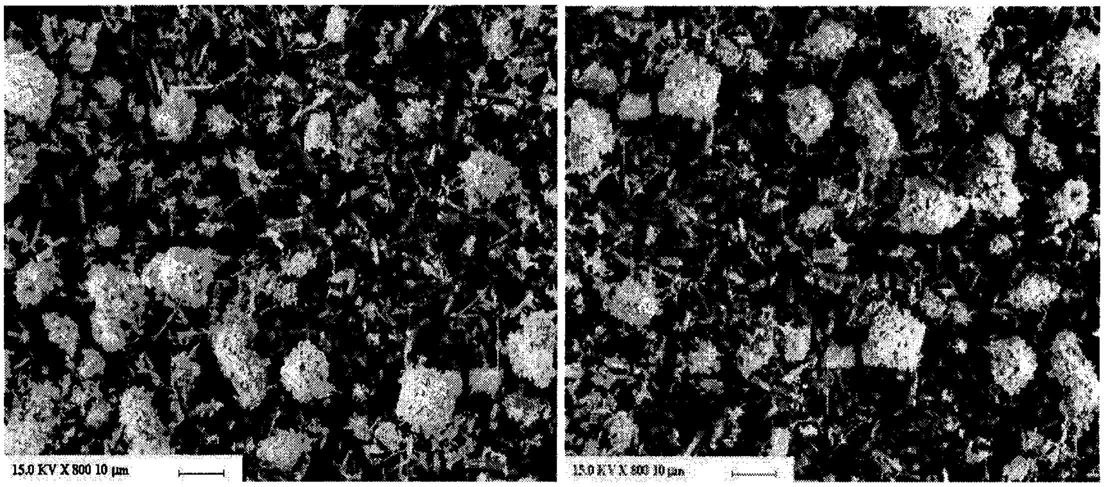

(a) 10 wt% $Fe_2(SO_4)_3$ (b) 10 wt% $Fe(NO_3)_3$

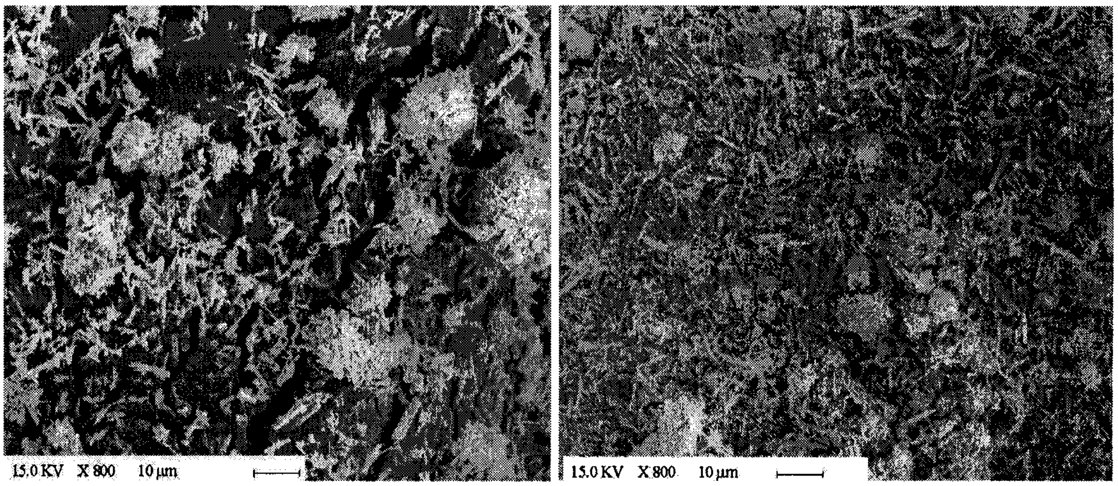

(c) 10 wt% $AlCl_3$ (d) 5 wt% $Al_2(SO_4)_3$

Figure 7.4: Influence of trivalent inorganic salts on morphology of α-hemihydrate

Conditions: 1.25M H_2SO_4, CaO/H_2SO_4 ratio=0.4, 100°C

Standard procedure: addition of dry lime to H_2SO_4

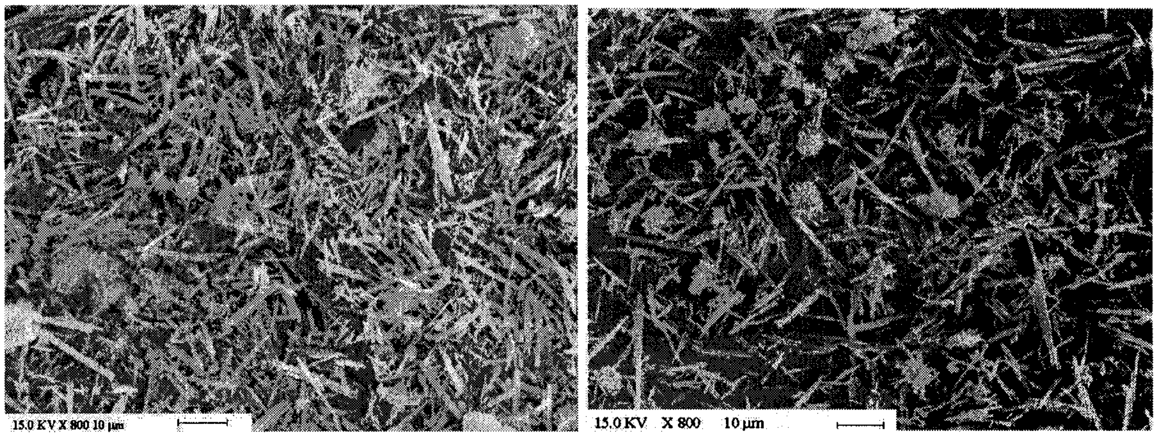

(e) 1wt% $Fe_2(SO_4)_3$ (f) 1wt% $Al_2(SO_4)_3$

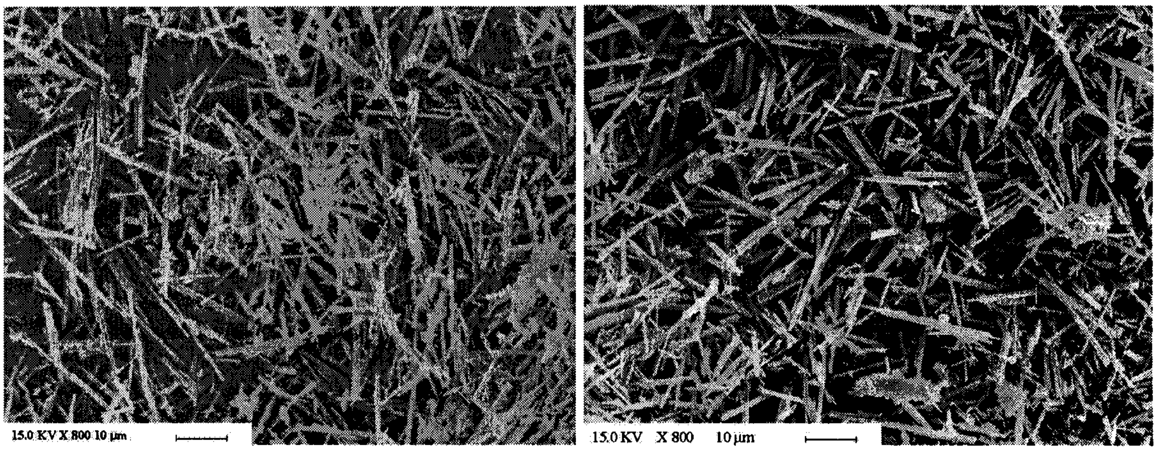

(c) 0.5wt% $Fe_2(SO_4)_3$ (d) 0.5wt% $Al_2(SO_4)_3$

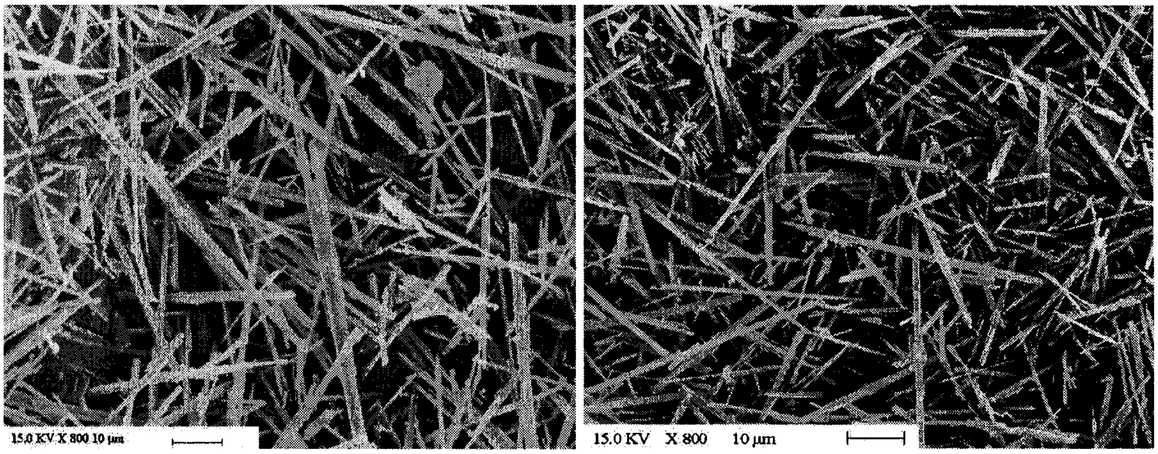

(c) 0.1wt% $Fe_2(SO_4)_3$ (d) 0.1wt% $Al_2(SO_4)_3$

Figure 7.5: Influence of decreasing dose of trivalent inorganic salts on morphology of α-hemihydrate

Conditions: 1.25M H_2SO_4, CaO/H_2SO_4 ratio=0.4, 100°C

Standard procedure: addition of dry lime to H_2SO_4

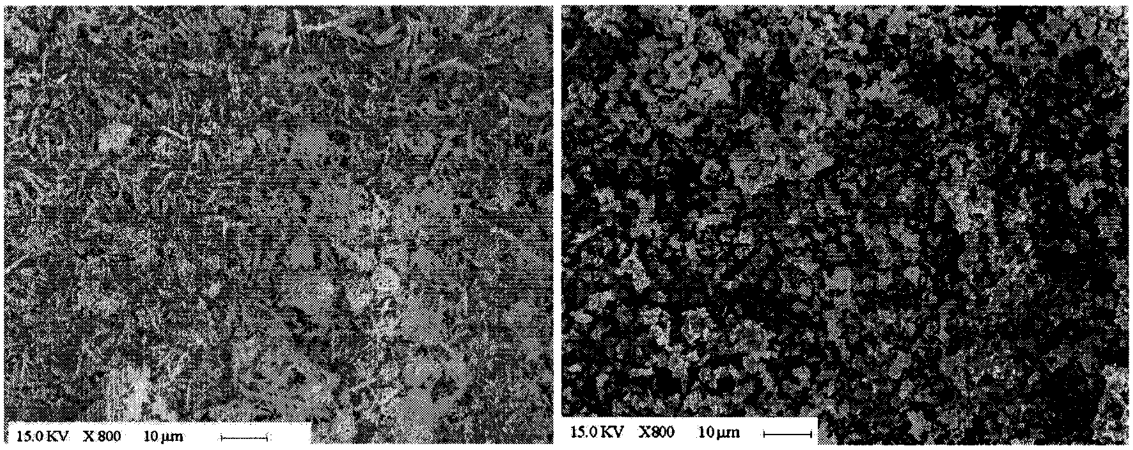

(a) 5wt% $Al_2(SO_4)_3$ (b) 3wt% $Al_2(SO_4)_3$

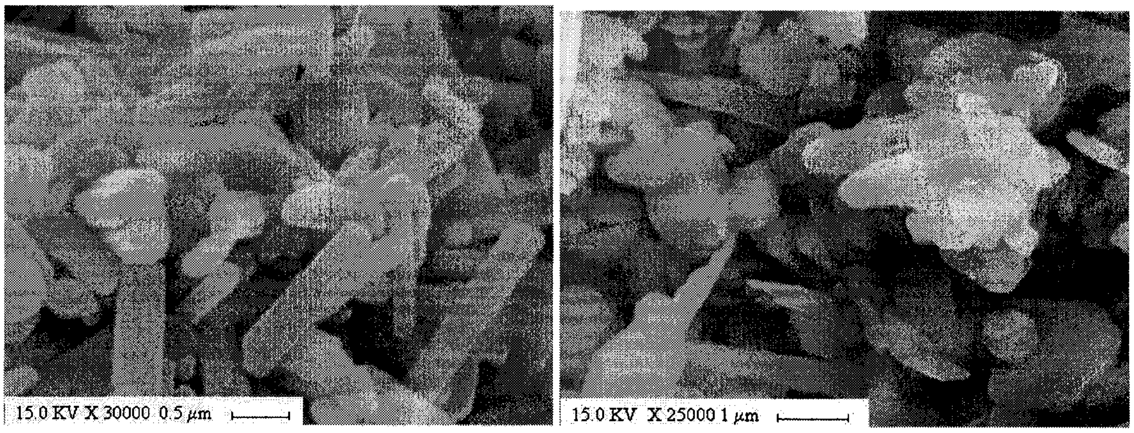

(c) Higher magnification of image in (a) (d) Higher magnification of image in (b)

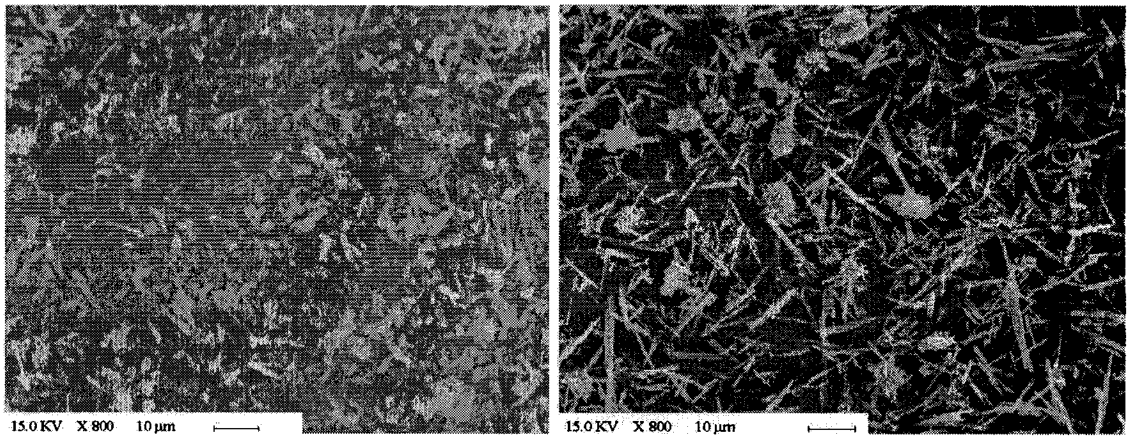

(e) 2wt% $Al_2(SO_4)_3$ (f) 1wt% $Al_2(SO_4)_3$

Figure 7.6: Influence of decreasing amount of $Al_2(SO_4)_3$ additive on α-hemihydrate morphology

Conditions: 1.25M H_2SO_4, CaO/H_2SO_4 ratio=0.4, 100°C

Standard procedure: addition of dry lime to H_2SO_4

Murat et al. [13] correlated the effectiveness of the cations to the ratio of Ψ/r, where Ψ is the charge and r is the radius of the ion corresponding to the solid state[5] instead of the hydrated form in the solution. It was proposed that cations with a Ψ/r ratio less than that of Ca^{2+} tended to accelerate growth (of dihydrate), while others with higher Ψ/r ratio tended to retard growth (of dihydrate) if present at equal concentrations. The corresponding Ψ/r ratio for K^+, Na^+, Mg^{2+}, Ni^{2+}, Fe^{3+} and Al^{3+}, etc., along with that of Ca^{2+} are listed in Table 7.1. As it can be seen the Ψ/r ratio for Fe^{3+} and Al^{3+} is considerably higher than that of Ca^{2+} (while the ratios for other divalent cations such as Mg^{2+}, Ni^{2+} and Zn^{2+} etc. are very close to that of Ca^{2+}). On the basis of this observation it can be postulated that, the effectiveness of Fe^{3+} and Al^{3+} is owed to their capability to lower the surface free energy of charged hemihydrate nuclei, and hence increase their rate of homogeneous nucleation[6]. Alternatively, it may be thought that the role of Fe^{3+} and Al^{3+} is manifested by blocking the growth of hemihydrate crystals. In the latter case for the blocking mechanism to be true, the adsorption of foreign species (herein Fe^{3+} and Al^{3+}) on the active growth sites will have to occur until new surface nuclei can be formed; in this case, it also implies that more nuclei would be indirectly resulted. X-ray microprobe analysis was performed to determine the location of Al with reference to single α-hemihydrate crystal. According to Figure 7.7, no preferential accumulation of Al on the perimeter of the crystal is evident. This may then be interpreted as support for the mechanism of directly accelerated homogeneous nucleation.

Table 7.1: Corresponding Ψ/r ratio for cations tested in this work

Cation	Charge of the cation, Ψ	Ionic radii, r (10^{-9} m)	Ψ/r ratio
K^+	1	0.133	7.519
Na^+	1	0.098	10.204
Sr^{2+}	2	0.127	15.748
Ca^{2+}	**2**	**0.106**	**18.868**
Zn^{2+}	2	0.083	24.096
Fe^{2+}	2	0.082	24.390
Mg^{2+}	2	0.078	25.641
Ni^{2+}	2	0.078	25.641
Fe^{3+}	3	0.067	44.776
Al^{3+}	3	0.057	52.632

---

[5] Data for radii of cations can be retrieved online [14].

[6] The propensity of these cations to form strong sulfato-complexes [15-19] may be another factor contributing to their influence as additives in this regard but the exact mechanism is not clear.

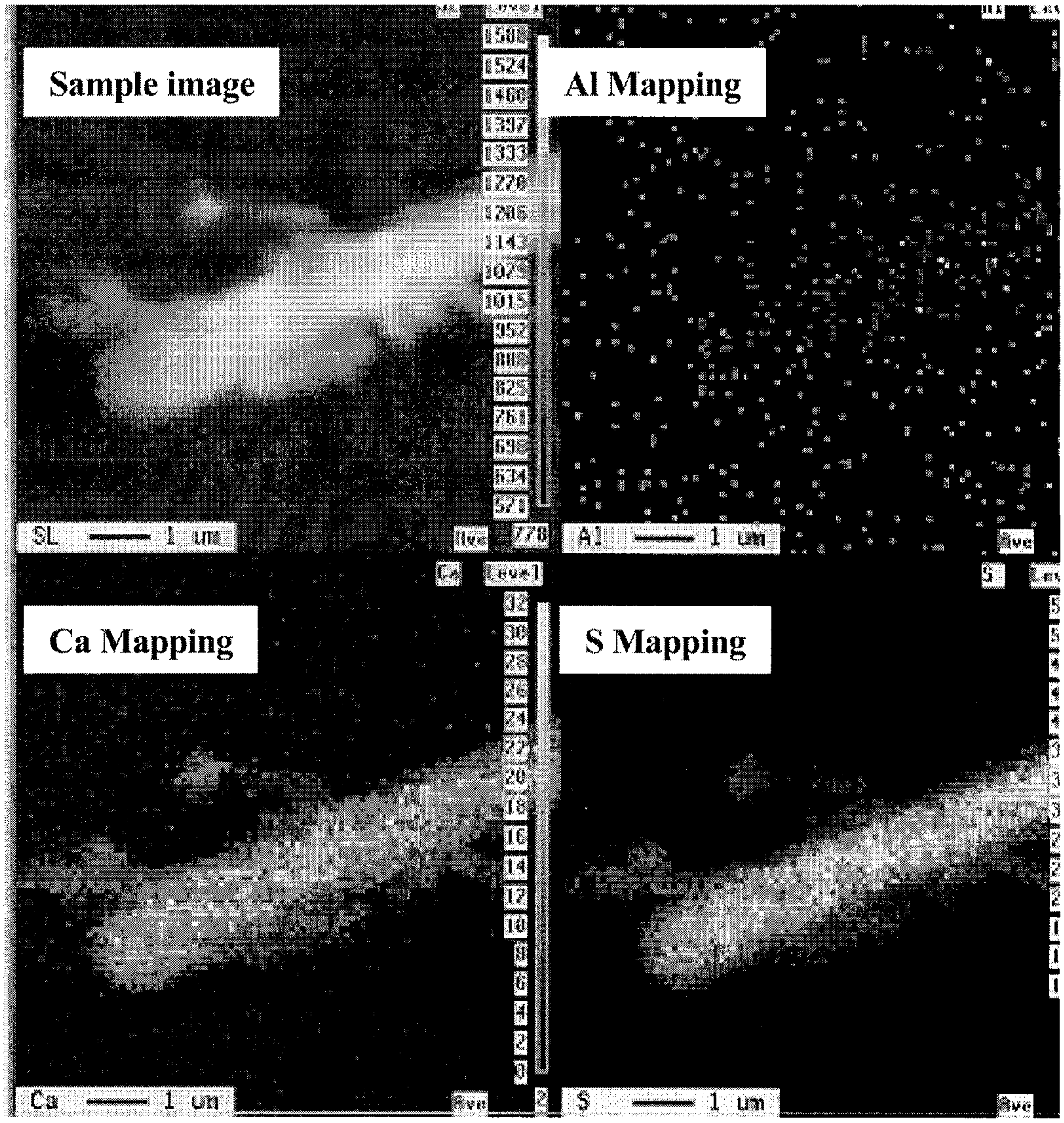

Figure 7.7: X-ray electron microprobe mappings of α-hemihydrate crystal after modification with $Al_2(SO_4)_3$ additive

Condition: 1.25M H_2SO_4, CaO/H_2SO_4 ratio=0.4, 3wt% $Al_2(SO_4)_3$, 100°C

Standard procedure: addition of dry lime to H_2SO_4

Organic additives were found not to exert significant effect on modifying the morphology of the product. SEM images of products obtained with some of the organic additives are shown in Figure 7.8. Similar results were obtained with all other additives tested but not shown for space economy.

Organic additives are known to be effective in salt solutions [2, 6] but in the present system proved ineffective. One possible reason for this ineffectiveness may be that the additives decomposed in the strongly acidic and hot (100°C) environment employed in this study. Another possible cause for the ineffectiveness of the organic additives may be related to the mechanism of calcium sulfate hemihydrate growth. It is known from literature [11,20] that the uptake of sulfate is the rate-limiting step in the dihydrate nucleation/growth process, according to these studies, excess SO_4^{2-} accelerates dihydrate growth whereas excess Ca^{2+} does not. In extrapolation, if assumed that hemihydrate crystallization process is similar to the dihydrate crystallization process [12], then, the uptake of SO_4^{2-} instead of Ca^{2+} would be as well the rate-determining step. Since the present system involves excess sulfuric acid, this implies that an abundance of SO_4^{2-} is always surrounding the hemihydrate nuclei, hence, not leaving much room for the organic additive(s) to act.

On the other hand, some modest effects from some organic additives (as can be seen in Figure 7.8) may be related to their adsorption or formation of calcium complexes on the crystal surfaces [21-25], more work is required to investigate the exact mechanism in the presence of organic additives.

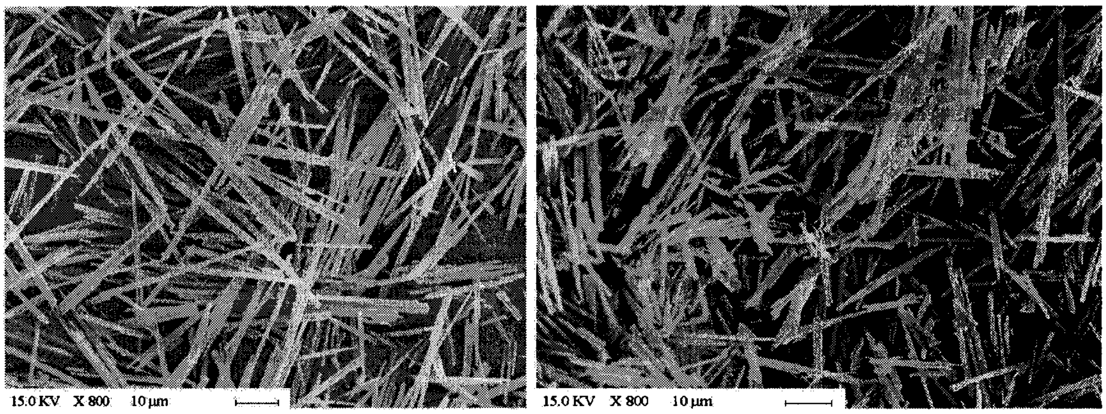

(a) 10wt% polyvinyl acetate(mw~50000) (b) 10wt% polyvinyl alcohol(mw~22000)

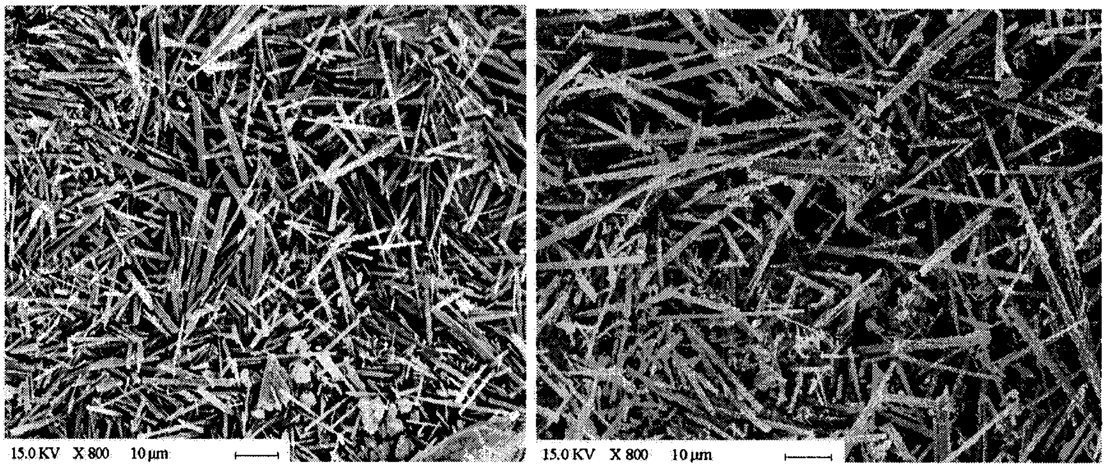

(c) 1wt% lignosol (d) 0.5wt% citric acid

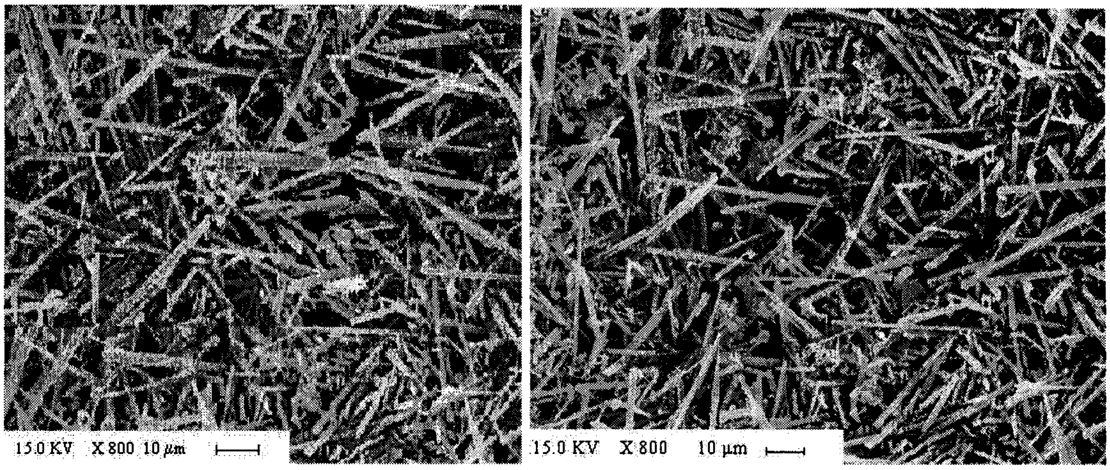

(e) 0.5wt% sodium citrate (f) 3 wt% sodium citrate

Figure 7.8: Influence of organic additives on morphology of α-hemihydrate

Conditions: 1.25M H_2SO_4, CaO/H_2SO_4 ratio=0.4, 100°C

Standard procedure: addition of dry lime to H_2SO_4

7.3.2 Reverse procedure of H_2SO_4 addition to slaked lime

The effect of additives on the morphology of α-hemihydrate is illustrated with the SEM images of Figure 7.9. It can be clearly seen (compare Figures 7.9, a and f) that $Al_2(SO_4)_3$ (at 1mol% dose or equivalently ~6.11wt% dose) resulted in promoting the production of large ("pebble-like") crystals. In contrast, addition of $Fe_2(SO_4)_3$ resulted in the crystals that appeared to be very easily fragmented to smaller pieces.

The mechanism by which $Al_2(SO_4)_3$ acts on crystal growth is not clear. As compared to the case of a typical H_2SO_4-excess environment in which the growth of α-hemihydrate crystals along the **c**-axis direction is much more rapidly than in other directions ending in the form of fine needle crystals (refer to Figures 7.1 and 7.2), it can be observed that, with presence of small amount of $Al_2(SO_4)_3$ the growth in directions other than **c**-axis was greatly improved whereas the growth along **c**-axis was not inhibited at all and still overran the growth in other directions resulting in pillar-shaped crystals (compare Figures 7.11, a and 7.2). It has been speculated that $Al(OH)_3$ [26-28], which forms as result of hydrolysis of $Al_2(SO_4)_3$ due to the initial alkaline environment presenting in this procedure, may be responsible for allowing the resultant crystal morphology. Particularly, appreciable improvement of the rheological properties of the slurry in the presence of small amount of $Al_2(SO_4)_3$ (3-6wt%) may play a role given that it may greatly facilitate the "through-solution" (or "dissolution-recrystallization") mechanism [20-22] of α-hemihydrate crystallization (refer to section 5.2 and section 7.4). Detailed characterization studies are required to elucidate the true mechanism.

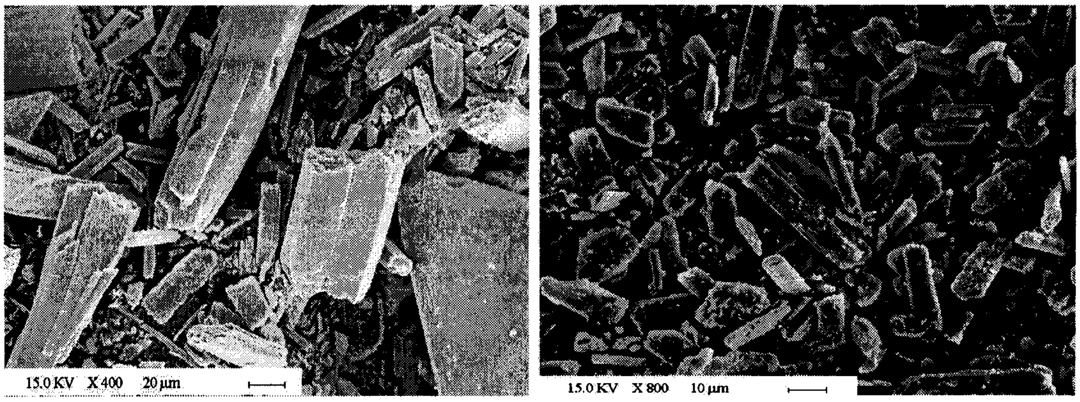

(a) 6.11 wt% (1 mol%) $Al_2(SO_4)_3$ (b) 3 wt% $Al_2(SO_4)_3$

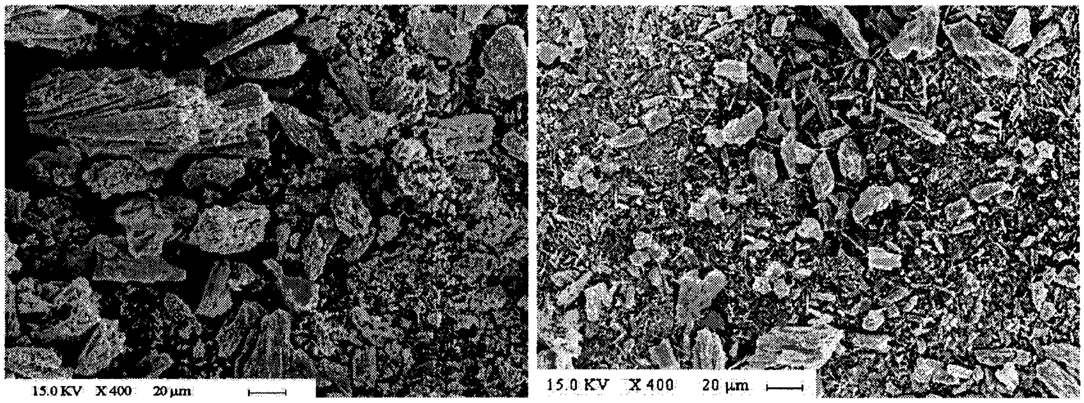

(e) 7.14 wt% (1 mol%) $Fe_2(SO_4)_3$ (c) 0.5wt% sodium citrate

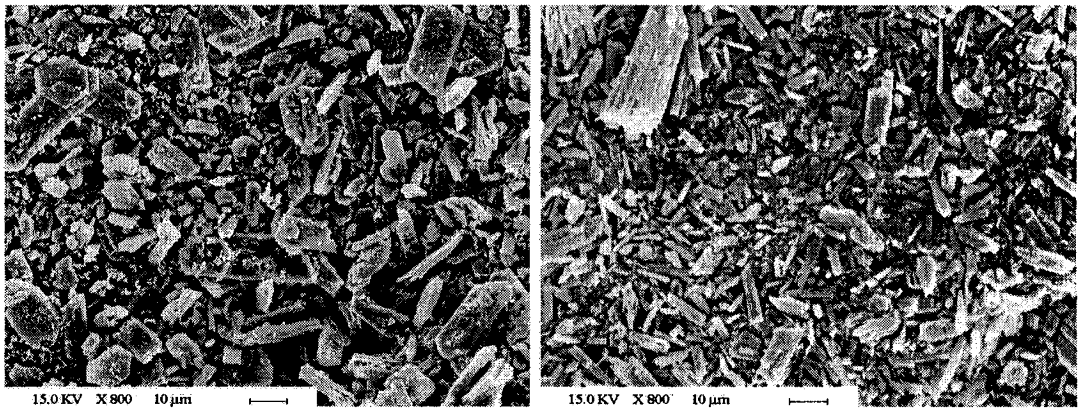

(d) 3wt%$Al_2(SO_4)_3$+0.5wt% sodium citrate (f) Reference image (without additive) (refer to Figure 6.22, b)

Figure 7.9: Influence of additives on morphology of α-hemihydrate
Conditions: 1.5M H_2SO_4, $CaO/H_2O=1/6$, CaO/H_2SO_4 ratio=0.4, 100°C
Reverse procedure: addition of H_2SO_4 to slaked lime

In addition to the standard H_2SO_4/CaO ratio of 0.4, some tests at ratio equal to one with additives were performed as well. Of interest in connection with these tests is the finding that, when sodium citrate is present the conversion of dihydrate to hemihydrate is "catalyzed". Thus, in the absence of sodium citrate, the final product was always a mixture of dihydrate and hemihydrate with the majority being hemihydrate. However, with addition of around 0.5wt% of sodium citrate (with reference to the weight of CaO), the dihydrate peak was significantly reduced indicating virtually complete conversion to hemihydrate (as shown in Figure 7.10). It is known from literature [29] that sodium citrate significantly inhibits the growth of dihydrate, i.e., it is a gypsum growth retarder, apparently, in this case, by suppressing the growth of dihydrate and allowing for its faster conversion to hemihydrate. Images of the product morphology at a ratio $H_2SO_4/CaO = 1$ in the presence of sodium citrate (with or without $Al_2(SO_4)_3$ as additive) are shown in Figure 7.11.

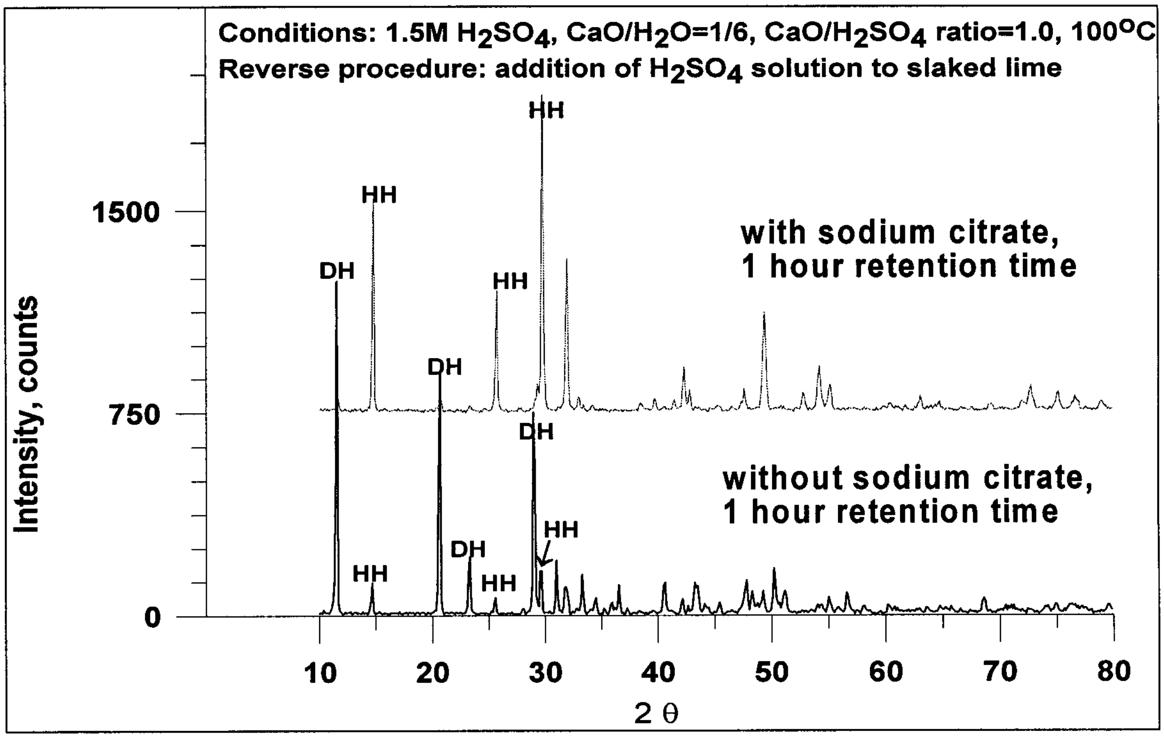

Figure 7.10: Influence of sodium citrate on the final product at CaO/H_2SO_4 =1.0 Reverse procedure: addition of H_2SO_4 to slaked lime.

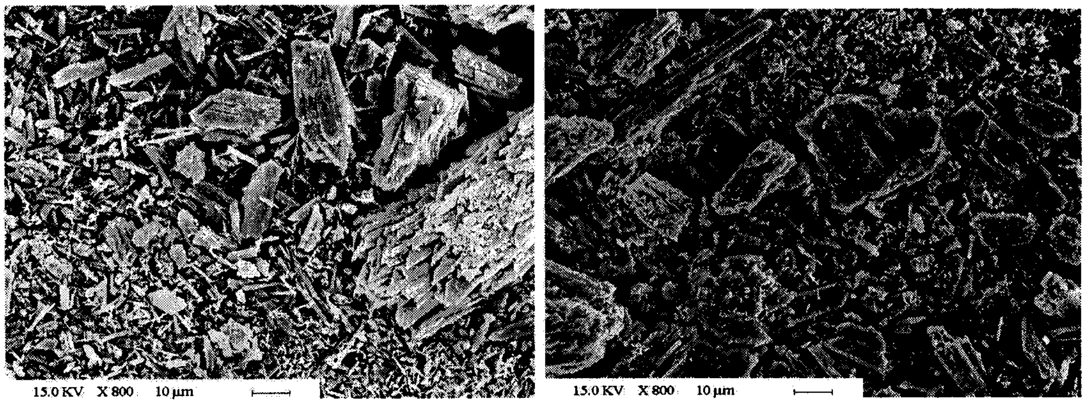

(a) 0.5 wt% sodium citrate (b) 3wt%$Al_2(SO_4)_3$+0.5wt% sodium citrate

Figure 7.11: Influence of sodium citrate on α-hemihydrate morphology at $CaO/H_2SO_4 = 1.0$

Reverse procedure: addition of H_2SO_4 to slaked lime.

7.4 Influence of seeding/recycling

7.4.1 Standard procedure of dry lime addition to H_2SO_4 solution

Conventionally, seeding and recycling play important roles in the crystal growth. But in this context, clearly limitations were encountered in employment of these methods. As exposed earlier in section 4.2, addition of hemihydrate particles in hot sulfuric acid solution resulted in their re-organization (by "dissolution-recrystallization" mechanism or "through solution" mechanism) to acicular shape crystals. Similar phenomena were observed in this part of work.

It was thought that if the H_2SO_4 solution is pre-saturated with calcium sulfate the re-crystallization of the seed material via dissolution would be stopped hence allowing for its effective use as growth promoter. This can be further understood by considering Figure 7.12. On this diagram 3 zones are involved: Zone 1 (below the solubility curve, $S=1$) is the dissolution zone; Zone 2 (between the equilibrium curve, $S=1$, and critical supersaturation curve, $S_{cr,\ homo}$ is the heterogeneous (=growth) zone; and Zone 3 (above the $S_{cr,homo}$) is the homogeneous zone. The critical supersaturation curve was determined by adding various amount (following a titration protocol) of 1.0M $Ca(NO_3)_2$ solution into a hot (100°C) 1.2M H_2SO_4 solution and observing the appearance of cloud (signifying the onset of homogeneous nucleation). The results are summarized in Table 7.2. It is obvious from these data that $S_{cr,\ homo}$ is a function of time, alternatively different induction times exist depending on $S_{cr,\ homo}$. Subsequent to determination of $S_{cr,homo}$, the 1.2M H_2SO_4 solution was saturated with the addition of 1.0M $Ca(NO_3)_2$ solution (yielding 0.1-0.11M Ca^{2+} concentration, corresponding to 13.6-15.0 g $CaSO_4$/L) into which seed material (0.05M or 7.5 g/L) was added followed by the addition of CaO, CaO was added "little-by-little") (illustrated with the zig-zag line in Figure 7.12) with the intent of controlling supersaturation within Zone 2 hence favoring surface nucleation and growth.

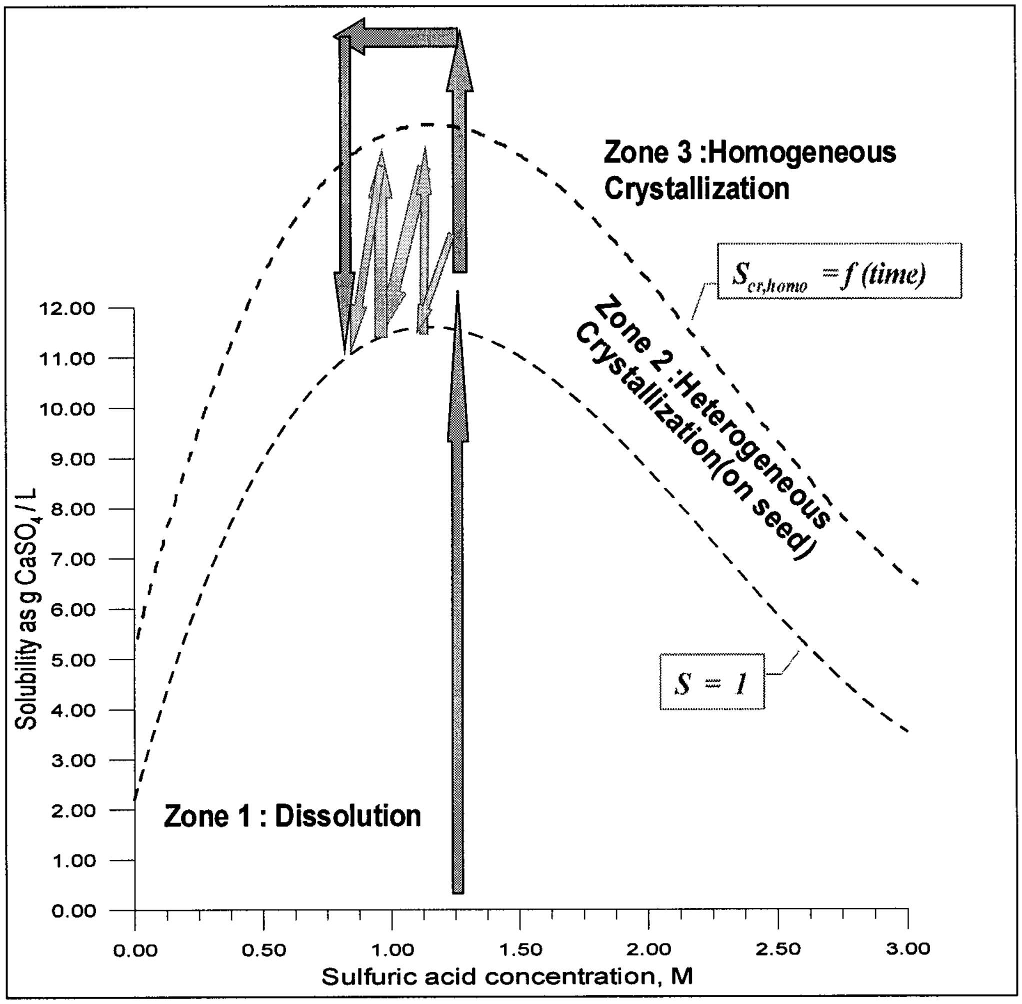

Figure 7.12: Illustration of crystallization control by adjusting supersaturation level

Table 7.2: Relationship between supersaturation level and induction time determined by addition of 1.0M$Ca(NO_3)_2$ to 1.2M H_2SO_4 at 100°C

Induction time	**Supersaturation* Level ($S_{cr,homo}$)**
Immediately	1.99 [7]
$3'30'' \sim 4'30''$	1.61
$22' \sim 24'$	1.42
$27' \sim 29'$	1.36
$90'$ Nothing happened	1.17

* Supersaturation level (refer to equation 5.3.3) defined by:

$$[CaSO_4] / [CaSO_4]_{eq} \qquad (7.4.1)$$

The obtained crystal morphologies in this series of tests are represented with the SEM images of Figure 7.13. As it can be seen, the pebble-like morphology of the starting materials converted to needle-shaped crystals in all cases[8], i.e., the same morphology was obtained as when no seed was used (refer for example to Figure 7.13, f). Then, in other words, the crystals changed morphology but no chemical identity, i.e., they remained α-hemihydrate as it was detected by XRD and DSC analysis (refer to Figure 7.14 for the XRD and DSC verification).

---

[7] Given that, addition of $Ca(NO_3)_2$ results in generation of small amount of HNO_3 acid and there is lack of solubility data for calcium sulfate in mixture of H_2SO_4 and HNO_3 (Kojima et al. [5] reported some data but at relatively high HNO_3 concentration), only a simplified semi-quantitative analysis of the supersaturation level was carried out:

Say, (1) 100 mL 1.0M $Ca(NO_3)_2$ solution was added into 500 mL 1.2M H_2SO_4;
(2) Assuming the total volume was 600 mL: $[H_2SO_4] \Rightarrow$ 1.0M, $[Ca^{2+}]=1/6\approx0.167$M;
(3) Ignoring the influence of HNO_3 on solubility of calcium sulfate, the solubility value of calcium sulfate hemihydrate corresponding to 1.0M H_2SO_4, namely, 11.41 g $CaSO_4$/L or $[Ca^{2+}]_{eq}=0.0839$M was used;
(4) Supersaturation level was calculated as:

$$S_{cr,\,homo} = [Ca^{2+}] / [Ca^{2+}]_{eq} = 0.167/0.839 = 1.99.$$

[8] The somewhat larger size crystal morphology in the case of the ProMineral seed material is attributed to the presence of additives found in this commercial product. The author could clearly observe the release of an "oily" substance upon the addition of the ProMineral material into the hot H_2SO_4 solution.

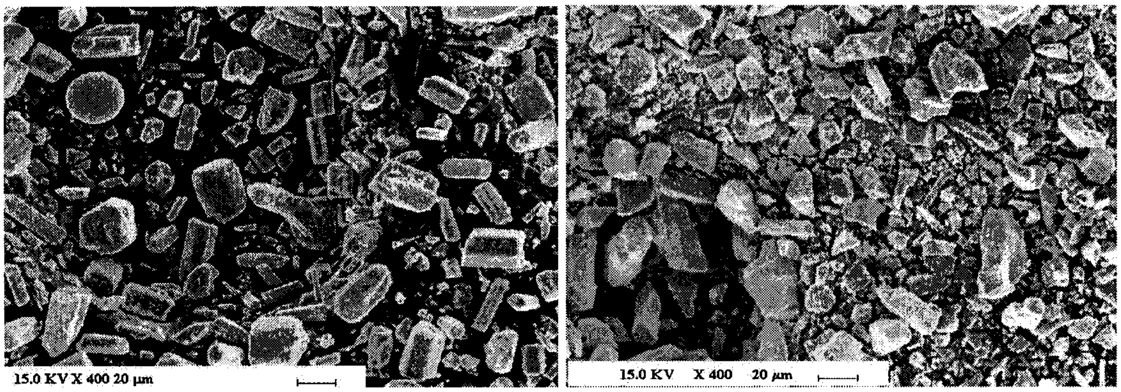

(a) Seed 1 - Omega material (α-HH)

(b) Seed 2 - ProMineral material (α-HH)

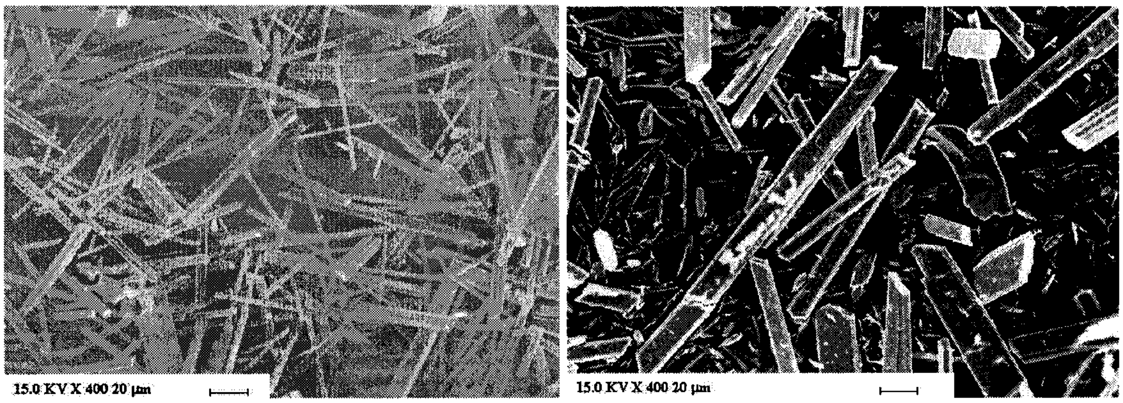

(c) Product after seeding with Omega

(d) Product of seeding with ProMineral

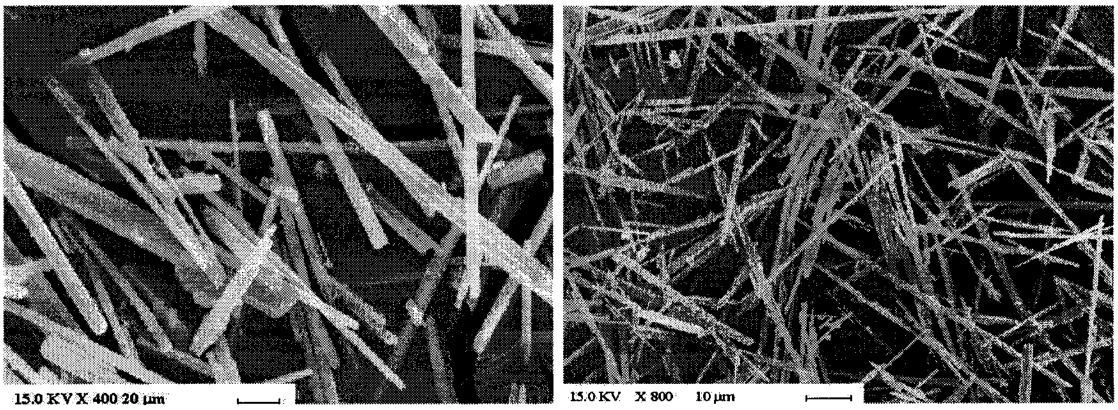

(e) Recycling product (after 3rd recycle)
(with Omega as the original seed)

(f) Reference image (Figure 6.15, a)
(without seeding and recycling)

Figure 7.13: Influence of seeding and recycling on α-hemihydrate crystal morphology
Conditions: 1.25M H_2SO_4, CaO/H_2SO_4 ratio=0.4, 100°C
Standard procedure: addition of dry lime to H_2SO_4

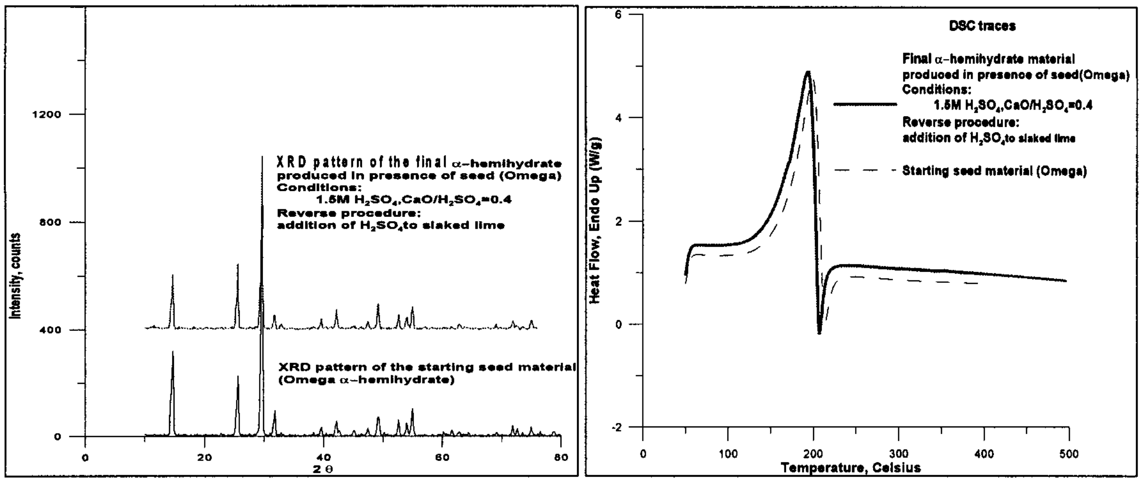

(a) XRD patterns (b) DSC patterns

Figure 7.14: XRD and DSC analyses of starting seed material and the final product (corresponding to materials of Figure 7.13, a and c)

This finding suggests that the dominant (stable) crystal morphology of α-hemihydrate in hot H_2SO_4 solution (at least in the concentration range employed in this work, from 0.6 - 1.1 M H_2SO_4 "steady-state") is long-needle shaped because of the preferential growth along the crystallographic **c** axis. On the other hand, the α-hemihydrate morphology of the OMEGA and ProMineral products is stable in slightly acidic environment (pH ~6.5). As also shown in the present work, the morphology of the product was not any more of needle-shape when the reverse procedure of preparation was employed (refer to sections 6.4, 7.3.2 and 7.4.2).

7.4.2 Reverse procedure of H_2SO_4 addition to slaked lime

Figure 7.15 presents SEM images of α-hemihydrate material subjected to several recycles using the reverse procedure of production, i.e., addition of H_2SO_4 to slaked lime. It must be noted that the CaO/H_2SO_4 ratio was kept at 1.0 for the purpose of increasing the yield of the reaction. By comparing these images to that of Figure 7.11, a, it can be seen that there was significant growth occurring upon recycling but apparently the crystals were quite fragile generating a lot of "dusty" particles.

Similarly, some growth can also be observed in case of seeding (refer to Figure 7.16).

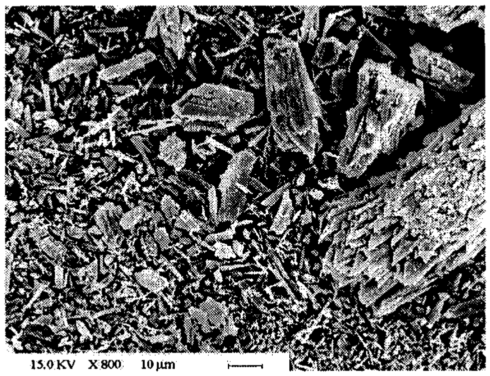

(a) Reference image (Figure 7.11, a)

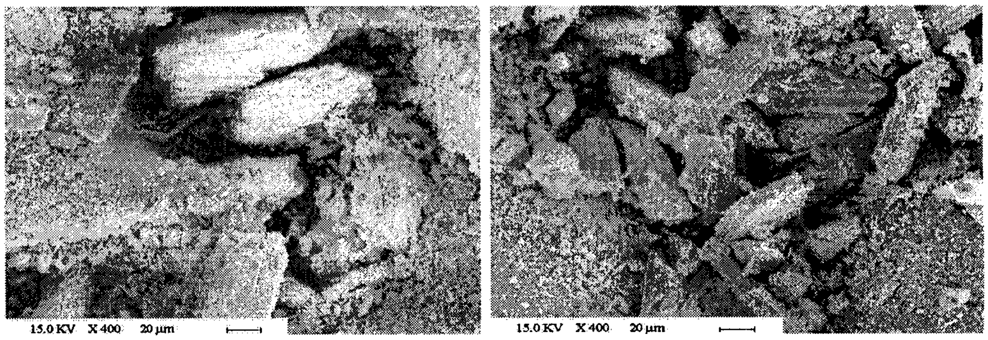

(b) After 1st recycle (c) After 3rd recycle

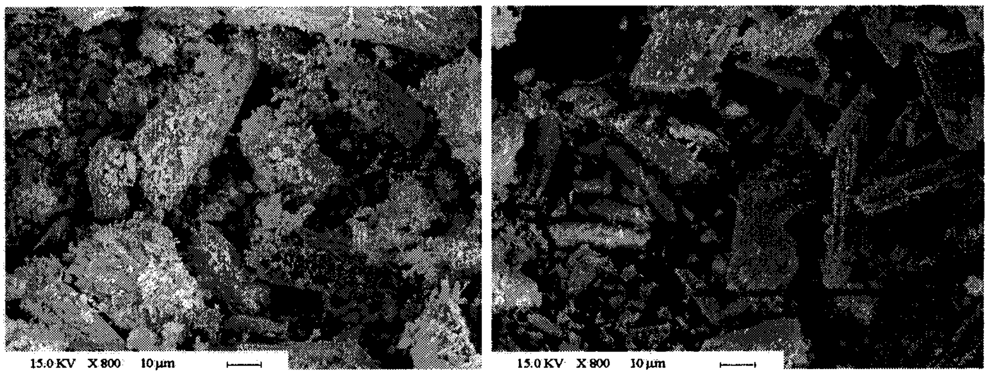

(d) After 5th recycle (e) After 7th recycle

Figure 7.15: Influence of recycling on crystal morphology[9]

Conditions: 1.5M H_2SO_4, CaO/H_2SO_4 ratio=1.0, CaO/H_2O=1/6, 100°C, 0.5wt% sodium citrate

Reverse procedure: addition of H_2SO_4 to slaked lime

---

[9] The author apologizes for the "dusty" images. All samples in this project were cleaned by "Dust Off" Aerosol Spray before the carbon or gold coating. However, it happened that during the treatment of this batch of samples, there was no enough air in the "dust-off" spray. Many fine particles resulting from friction/abrasion in the sample handling still remained adhered to substrate or surfaces of bigger particles hence creating the "dusty" appearance.

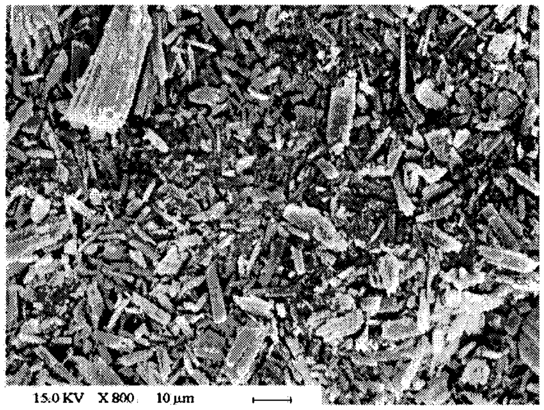

(a) Reference image (without additive)

(refer to Figure 6.22, b)

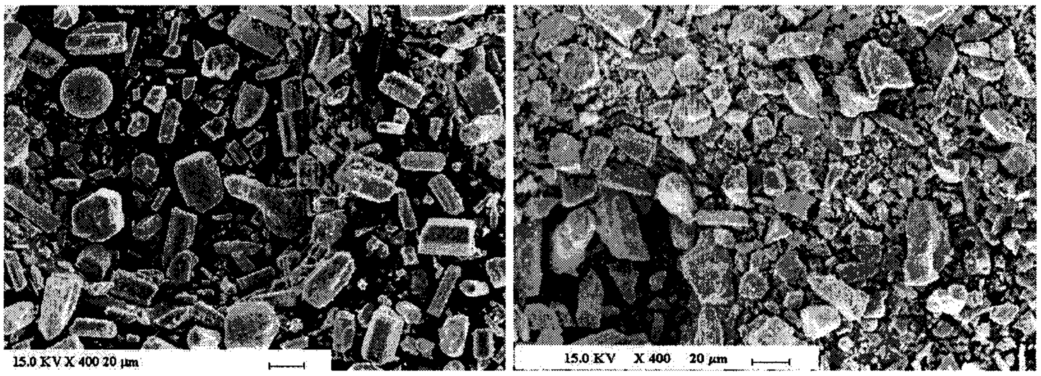

(b) Seed 1 - Omega material (c) Seed 2 - ProMineral material

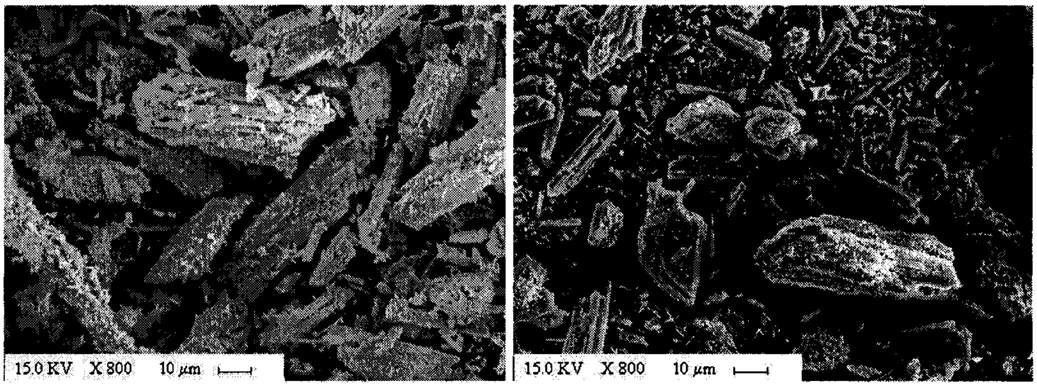

(d) Product after seeding with Omega (e) Product of seeding with ProMineral

Figure 7.16: Influence of seeding on crystal morphology

Conditions: 1.5M H_2SO_4, CaO/H_2SO_4 ratio=0.4, $CaO/H_2O=1/6$, 100°C,

Reverse procedure: addition of H_2SO_4 to slaked lime

Part II: Property Evaluation of the α-hemihydrate Materials

7.5 Experimental

A limited number of α-hemihydrate materials throughout this work were selected to be subjected to physical property measurement. A list of laboratory products tested along with their preparation conditions is given in Table 7.3. Tests under the same conditions were repeated several times until enough amount of sample was obtained. Typically 3-5 kg of material was required for each round of measurements and since each test could produce only 0.25 kg over 10 repeats had to be done. The samples were hot-filtered, washed with boiling water and dried at 100°C for 12 hours. The dry samples were ground with pestle and mortar before subjected to ASTM testing (standard C472-93).

Table 7.3: Preparation conditions for laboratory hemihydrate products

Experiment No.	Procedure (with 1.5MH_2SO_4)	CaO/H_2SO_4 ratio	CaO/H_2O (if applicable)	Additive(s)	Note
PT1	Standard*	0.4		None	
PT2	Standard	0.4		3 wt% $Al_2(SO_4)_3$	
PT3	Reverse**	0.4	1/6	None	
PT4	Reverse	0.4	1/6	3 wt% $Al_2(SO_4)_3$	
PT5	Reverse	1.0	1/6	0.5wt% sodium citrate	7th recycle

* Standard procedure involved the addition of dry lime to hot H_2SO_4 solution.

** Reverse procedure involved the addition of hot H_2SO_4 to slaked lime.

The ASTM standard apparatus used for the determination of normal consistency[10], setting time and compressive strength is shown in Figure 7.17.

---

[10] One particular problem arising with these testing procedures is the determination of the normal consistency of the material. According to the procedure, the material "*shall be considered of normal consistency when a penetration of 30 ± 2 mm is obtained*". The distance 30 ± 2 *mm*, is where subjectivity lies in. Different values for normal consistency may result, which, in turn, could lead to varied values for setting time and, particularly, compressive strength which are directly based on the measured value of normal consistency. Hence it takes a lot of repeats and training in obtaining reliable measurements out of the consistency technique.

For each type of sample, say PT1, a series of tests with various water/solid ratios were performed in order to determine first the normal consistency of the material. Then, based on the measured normal consistency, the setting time was determined. And paste was prepared at the measured normal consistency and cast into specimen molds; after removed from the molds, the cube specimens were placed in moisture chamber (≥ 90% RH) for 24 hours; after 7 x 24 hours drying[11] at around 37°C, the cubes were finally subjected to compressive strength tests on Sintech 30/G from MTS Systems Corp (the work was done in the Materials Laboratory of the Department of Civil Engineering and Applied Mechanics), the testing itself was controlled with the self-integrated software.

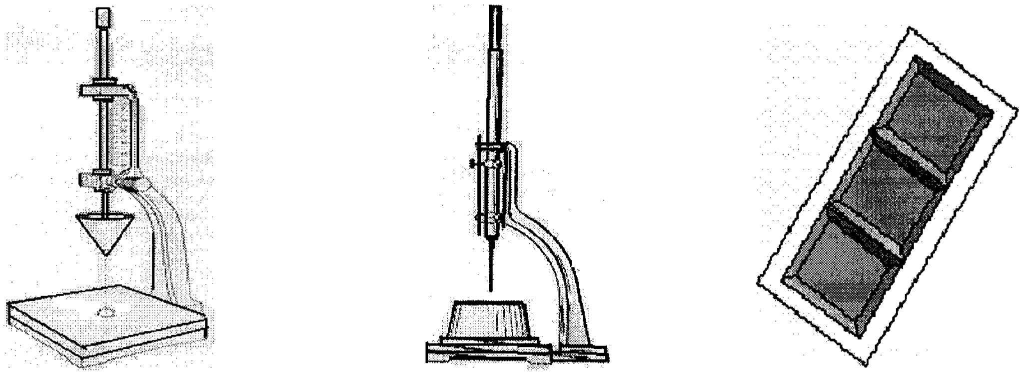

(a) (b) (c)

Figure 7.17: ASTM standard apparatus (C472-93) for physical testing of gypsum plasters

(a) Vicat apparatus with conical plunger for determination of normal consistency

(b) Vicat apparatus with needle for determination of setting time

(c) Specimen molds with three 2-inch cube compartments for making cube specimen used for determination of compressive strength

7.6 Results

Before the actual measurements on the laboratory products were made, the author performed measurements on a commercial gypsum plaster product of known

---

[11] 24 or 2 x 24 hours drying are also commonly adopted (because of its convenience and economy) in literature and in industry.

specifications. The product in question with trade name "Laboratory Plaster" from WhipMix [30] is a dental material of proprietary composition. The manufacturer specifications as well as the tested values are listed in Table 7.4. As can be seen, the strength value in manufacture specification is ~20% lower than the tested value. Given that, the former was obtained after 2 x 24 hours drying while the latter after 7 x 24 hours drying on one hand; and on the other, as high as 15% deviation is allowed in the ASTM standard testing procedure for the same batch of specimens, the tested value is deemed reasonable, hence, the measurement procedure was validated.

Table 7.4: Validation tests using as control gypsum plaster material from WhipMix

Commercial gypsum plaster product: **Laboratory Plaster**	Normal consistency (mL H_2O per 100g sample)	Setting time (minute)	Compressive strength	
			(psi)	(MPa)
Manufacture specification	45	14	1500[12]	10.342
			3300[13]	22.752
Tested values	45	15	4174	28.778

The influence of morphology (refer to Figure 7.18) on the final strength is quite intuitive: typical long needle-shaped particles yield strength values lower than particles with column-shaped or some other more-compact forms, in other words, hemihydrate crystals with higher aspect ratios (ratio of width or diameter/length) result in higher strength [3, 5].

The testing results for laboratory hemihydrate products are given in Table 7.5. Some data from the literature are also mentioned here for comparison purposes. It should be noted that, according to standard ASTM C472-93, the tested value of the specimen cube for each type of material should not vary more than 15% [14], the reported strength value for each type of material is the average compressive strength of 6 specimen cubes.

---

[12] Value obtained after 1 hour

[13] Value obtained after 2 x 24 hours.

[14] In that case (deviation >15%), the cube should be discarded or the test be repeated.

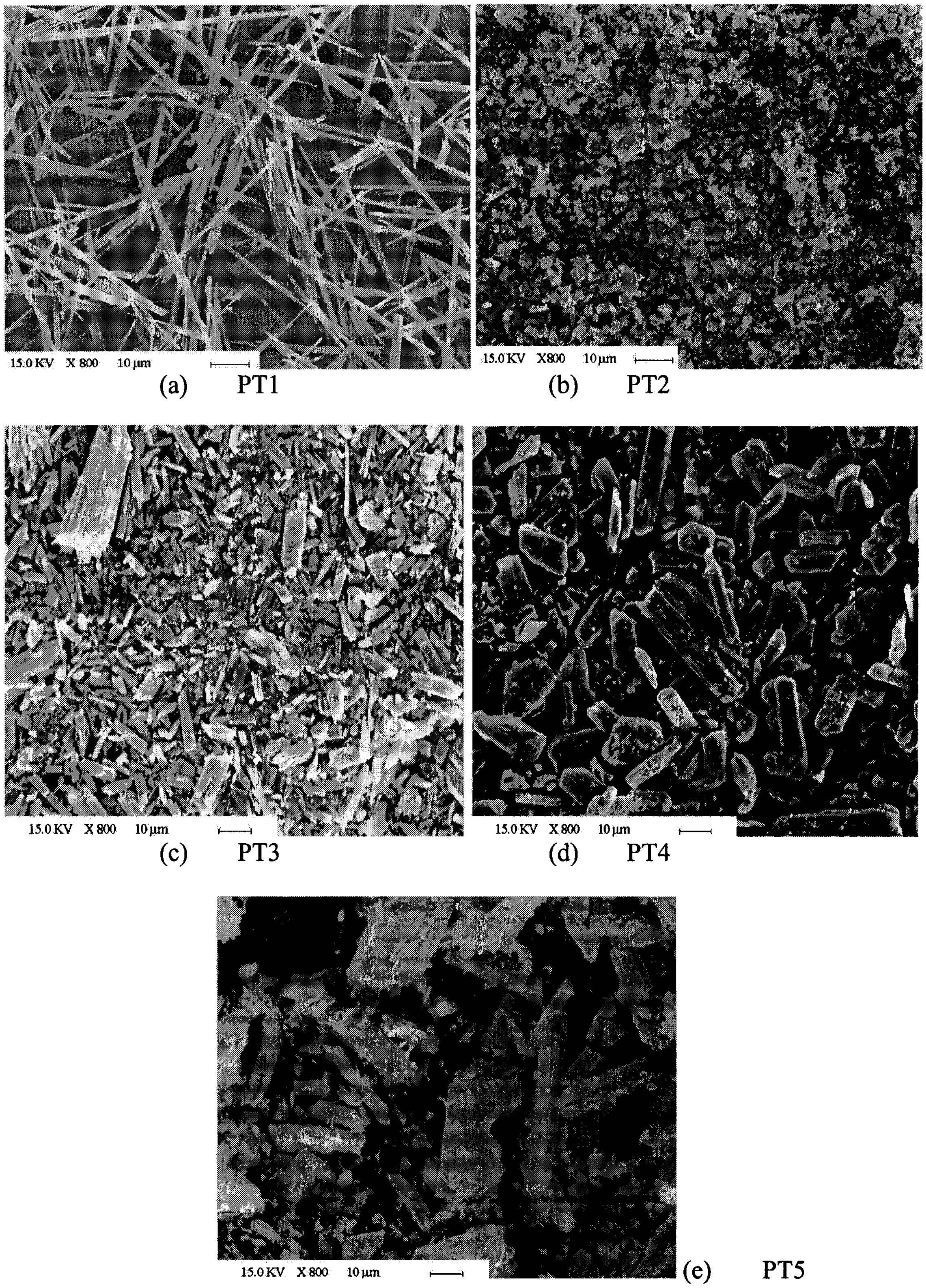

(a) PT1

(b) PT2

(c) PT3

(d) PT4

(e) PT5

Figure 7.18: Morphology of the laboratory-made hemihydrate products subjected to ASTM testing

Table 7.5: ASTM testing results for laboratory hemihydrate products

Exp. No.	Procedure (with $1.5MH_2SO_4$)	Additive(s)	Normal consistency (mL H_2O per 100g sample)	Setting time (min)	Compressive strength	
					(psi)	(MPa)
PT1	Standard	None	70	12	2415	16.7
PT2	Standard	3 wt% $Al_2(SO_4)_3$	52	16	3045	21.0
PT3	Reverse	None	58	12	2854	19.7
PT4	Reverse	3 wt% $Al_2(SO_4)_3$	60	12	2740	18.9
PT5	Reverse	0.5wt% sodium citrate after 7th recycle	61	15	2674	18.4
Reference Materials						
Laboratory Plaster	(from WhipMix [30])	Tested values	45	15	4174	28.8
β-HH	reagent grade, data source: [31]		61	12	1938	13.4
Omega	from Eastroc plant of BPB, date source:[31]		41	15	6461	44.5
BPB	from Westroc plant of BPB, data source:[32]		50		3745	26
α-HH-1	Autoclave-made, data source:[2]		49	11	3118±450	21.5±3.1
α-HH-2	from 42% $Mg(NO_3)_2$,data source:[2]		60	9	3031±508	20.9±3.5
α-HH	From concentrated salt solutions, data source:[32]				2900 - 4351	20 - 30

Similar to the findings of German investigators Zürz et al.[2], the laboratory products were found to have relatively high water requirement (in the range of 50 to 70). During preliminary measurements, it was found that, without grinding, the measured normal consistency could go as high as 100 with compressive strength only around 8-10MPa. Hence grinding was tried. First, machine grinding using pulverizer or ball mill was tried. Unfortunately, the material was stuck on the surfaces of the machines resulting in loss of a significant portion of those "very precious" laboratory products. Finally, hand grinding using a pestle and mortar was applied. With relatively large amount of samples, hand grinding is a demanding job and can hardly achieve uniform particle size[15]. Eventually, the measured normal consistency of the present work's products was determined to be comparable to that from Zürz et al.[2] [16] (refer to Table 7.5). In terms of

---

[15] It should be noted that hand grinding in this work did not cause too much difference on morphology of individual crystals; hand grinding is rather a crushing/breaking-down of the agglomerates formed as result of sample handling during filtration and drying.

[16] The specimens in their strength testing [2] were in the dimensions of *10mm X 10mm X 60mm* instead of ASTM standard size, 2-inch cube.

compressive strength, the best value measured in this work was around 3000 psi or 20MPa. This compares favorably with the values reported by Zürz et al.[2] but is lower than values obtained from the commercial Omega product. It is postulated that the latter contains some proprietary additive(s) and not pure α-hemihydrate per say. Hina and Nancollas in their recent patent [32], in which they describe the production of α-hemihydrate materials by the conversion of dihydrate in concentrated salt solutions, report strength for their products in the order of 20 MPa to 30 MPa [17]. The same authors observed that, simply by hand grinding, the compressive strength can be improved from 12 MPa to 27 MPa, which further confirmed the similar finding from Zürz et al.[2] that, an improved water solid/ratio can be obtained if the size distribution was optimized by briefly grinding the product. The above-observed facts and the testing results in this work indicate that, particle size distribution, besides the morphology of the particles (another important factor), has very significant influence [33] on the final strength of α-hemihydrate products.

The author, beyond the topic of ASTM testing, has to point out that, the impact of grinding on compressive strength indirectly confirms the earlier observation made in chapter 2 that, α-hemihydrate cannot be merely considered as well-crystallized β-hemihydrate. If so, grinding should have resulted in lower values of compressive strength instead of the other way around. The reason that, α-hemihydrate products, even with relatively high values of normal consistency, can still give good high-strength properties, may be "*due to a more favorable texture of the hydrated material formed*" from α-hemihydrate as suggested by Zürz et al.[2].

Given that, on the one hand, grinding can have such significant impact on strength, on the other that the lab-made α-hemihydrate products were only poorly ground here, the author is quite confident that, there is plenty of room for improvement of final strength of the α-hemihydrate materials by preparation method elaborated in this thesis.

In this regard, physical testing of the laboratory-made α-hemihydrate products is far from being considered complete. More work needs to be done to further clarify the

---

[17] Those values are much lower than the tested values (around 44 MPa [27]) for Omega from Eastroc plant of BPB. Also, they [28] evaluated some other α-hemihydrate products from Westroc plant of BPB and reported strength values around 26MPa (also lower than the values for Omega).

effects of particle size distribution and impact the method of preparation (standard vs. reverse procedure) and type/amount of additives have on product properties. Furthermore, the production of α-hemihydrate of sulfuric acid should, preferably, be done at larger scale, so as to produce a more representative sample and also to lead to accurate assessment of the method of production itself.

7.7 Conclusions

1. With reference to the standard procedure of α-hemihydrate production (involving addition of dry lime to H_2SO_4 solution) the following conclusions can be drawn:

(a) Monovalent or divalent salts (tested up to 10wt% ratio to CaO used) were found not to exert any influence on crystal morphology independent of the accompanying anion.

(b) Trivalent cations such as Fe^{3+} and Al^{3+}, on the other hand, were found to modify crystal morphology from needle-shape to small "grain" type morphology. Their role, relating to the ratio of Ψ/r (where Ψ is the charge and r is the radius of the ion), was thought to be in lowering the surface free energy of charged hemihydrate nuclei thus resulting higher homogeneous nucleation values. Alternatively, their role may be in blocking crystal growth.

(c) $Al_2(SO_4)_3$ at 3 wt% (with reference to CaO mass) proved the most effective of the additives tested.

(d) Organic additives proved ineffective in modifying hemihydrate morphology. Their ineffectiveness is attributed either to their degradation in the strong hot acid environment employed in this procedure or to the SO_4^{2-}-rich environment assuming in the latter case uptake of SO_4^{2-} (as opposed to Ca^{2+}) to be the rate-determining step of the growth process.

2. With reference to the testing of additives with the reverse procedure of α-hemihydrate preparation (involving addition of H_2SO_4 to slaked lime) the following remarks can be made:

(a) Addition of small amount (3–6 wt% with reference to CaO mass) of $Al_2(SO_4)_3$ to slurry of hydrated lime was found to appreciably improve the rheological properties of the slurry and result in relatively "large" pillar-shaped crystals.

(b) Sodium citrate (or citric acid) was found to inhibit growth of dihydrate and catalyze its conversion to hemihydrate when CaO/H_2SO_4 ratio of 1.0 was used.

3. No significant improvement on morphology of the resultant α-hemihydrate has been achieved by either seeding or recycling tests. However, some modest growth was evident.

4. When the standard procedure of preparation was used, the morphology of seed material was found to change from pebble-like to acicular type despite that the acid solution was pre-saturated with calcium sulfate. This implies that the stable morphology of α-hemihydrate in H_2SO_4 environment is that of acicular type. Resultant α-hemihydrate crystals are independent of the original shape of seed particles, which further confirm the "dissolution-recrystallization" (or "through-solution") mechanism for α-hemihydrate crystallization/precipitation.

5. Preliminary assessment of the properties of the α-hemihydrate materials synthesized in this work showed them to compare satisfactorily with other materials produced by conversion of dihydrate to hemihydrate. Hemihydrate particles with higher aspect ratios (ratio of width or diameter/length), namely, more-compact forms, produced by the standard procedure in the presence of $Al_2(SO_4)_3$ as additive or by the reverse procedure, were found to possess the best properties as plaster materials.

6. In addition to morphology, particle size distribution was found to have a significant influence on the final strength of α-hemihydrate products.

References

[1] Ng, T.W., Modification of FGD gypsum crystal habit by metal ions, FGD and Other Synthetic Gypsum, 4th International Conference, Toronto, May 17-18, [Proceedings], Process Research ORTECH Inc.: Mississauga, Ontario, Canada, 18,1-17 (1995).

[2] Zürz, A., Odler, I., Thiemann, F. and Berghöfer, K., Autoclave-free formation of α-hemihydrate gypsum, Journal of American Ceramics Society, 74(5), 1117-1124(1991).

[3] Tang, X. and Shi, C., Effect of crystallization modifiers on morphologies and properties of α-hemihydrate from phosphogypsum, FGD and Other Synthetic Gypsum, 4th International Conference, Toronto, May 17-18, [Proceedings], Process Research ORTECH Inc.: Mississauga, Ontario, Canada, 15, 1-11(1995).

[4] Yue, W. and Wang, Z., Investigation on the mechanism of crystal shape modifying agent of α-hemihydrate, Wuhan Gongye Daxue Xuebao, 18(2), 1-4 (1996) (in Chinese).

[5] Kojima, Y., Shibano, K., Yasue, T., Ishii, S. and Arai, Y., Wet synthesis of α-gypsum hemihydrate from II-anhydrite under atmospheric pressure, Inorganic Materials, 255(2), 84-93(1995) (in Japanese).

[6] Moisset, J., Plaster setting modifiers, Proceeding of 16th Eurogypsum Congress, Association of European Gypsum Industries: Brussels, Belgium, 1-27(1985).

[7] Genin, C., Yvon, J., Bouzat, G. and Blazy, P., Modifiers of crystal growth of α-calcium sulfate hemihydrate, Bulletin de Mineralogie, 108(3-4), 341-352 (1985)(in French).

[8] College, J.W., Sulfur dioxide removal from sulfur dioxide-containing hot gaseous streams under formation of α-hemihydrate gypsum, USA Patent, US 5,312,609 (1994).

[9] Abriel, W., Reisdorf, K. and Pannetier, J., Dehydration reaction of gypsum: A neutron and X-ray diffraction study, J. Solid State Chem., 85, 23-30(1990).

[10] Lager, G.A., Armbruster, T., Rorella, F.J., Jorgensen, J.D. and Hinks, D.G., A crystallographic study of the low-temperature dehydration products of gypsum,

$CaSO_4 \cdot 2H_2O$, hemihydrate $CaSO_4 \cdot 0.5H_2O$, and γ-$CaSO_4$, American Mineralogist, 69(9-10), 910-919(1984).

[11] Ridge, M.J., Surkevicius, H. and Lardner, K.I., Hydration of calcium sulfate hemihydrate—II. Acceleration by neutral salts, Journal of Applied Chemistry, 12, 246-252(1962).

[12] Gartner, E.M. and Gaidis, J.M., Hydration mechanisms, I, Materials Science of Concrete, 1, 95-125(1989).

[13] Murat, M., Hajjouji, A. E. and Comel, C., Investigation on some factors affecting the reactivity of synthetic orthorhombic anhydrite with water, I. Role of foreign cations in solutions, Cement and Concrete Research, 17, 633-639(1987).

[14] Online data for radii of cations, http://www.warwick.ac.uk/fac/sci/Chemistry/thermochemistry/thermo10.htm.

[15] Filippou, D., Demopoulos, G. P., Papangelakis, V. G., Hydrogen ion activities and species distribution in mixed metal sulfate aqueous systems, AIChE Journal , 41(1), 171-184(1995).

[16] Fedorov, V. A., Chernikova, G. E., Kuznechikhina, M. A., and Mironov, V. E, Effect of the ionic medium and temperature on the formation of sulphato-complexes of zinc and cadmium and calculations of their thermodynamic stability constants, Russian J. of inorganic Chemistry, 18(3), 645-50(1973).

[17] Magini, M., Solute structuring in aqueous iron(III) sulphate solutions: evidence for the formation of iron(III)-sulphate complexes, J. of Chem. Phys., 7091), 317-324(1979).

[18] Lister, M. W. and D. E. Rivington, Ferric sulphate complexes, and ternary complexes with thiocyanate ions, Canadian J. of Chemistry, 33, 1591-1602 (1955).

[19] Rudolph, W.W. and Mason,R., Spectroscopic studies of sulfato-complex formation in aqueous $Al_2(SO_4)_3$ solutions and the formation of hydronium alunite, GAC/MAC Annual Meeting, 50th Anniversary Celebration, Ottawa 1997, May 19 - 21, abstract (A 128) (1997).

[20] Liu, S.T. and Nancollas, G.H., The kinetics of crystal growth of calcium sulfate dihydrate, Journal of Crystal Growth, 6, 281-289(1970).

[21] Stability constants of metal-ion complexes, Special publication No 17, The Chemical Society: London, U.K.(1964).

[22] Solberg, C. and Hansen, S., Dissolution of $CaSO_4 \cdot 1/2H_2O$ and precipitation of $CaSO_4 \cdot 2H_2O$ - A kinetic study by synchrotron X-ray powder diffraction, Cement and Concrete Research, 31(4), 641-646(2001).

[23] Thomas, N.L. and Double, D.D., The hydration of Portland cement, C_3S and C_2S in the presence of calcium complexing admixtures(EDTA), Cement and Concrete Research, 13, 391-400(1983).

[24] Thomas, N.L. and Birchall, J.D., The retarding action of sugars on cement, Cement and Concrete Research, 13, 830-842(1983).

[25] Deslouis, C., Lefaucheux, F., Robert, M.C., and Rinaudo, C., Effect of added polymer traces on crystal growth: electrochemical simulation, Journal of Applied Electrochemistry, 23, 141-150(1993).

[26] Gill, A.F. and Way, T.H., The treatment of hydrated lime with aluminum sulphate, Canadian J. Research, 12, 253-260(1935).

[27] Glasson, D.R. and O'Neill, P., Reactivity of lime and related oxides. XVII. Sulphating of lime with magnesium and aluminum sulphates, J. Applied Chemistry, 17(4), 96-101(1967).

[28] Kraus, C.E., Building cement or plaster, USA Patent, US 1,747,551(1930).

[29] Koslowski, T. and Ludwig, U., Retardation of gypsum plasters with citric acid: mechanism and properties, The Chemistry and Technology of Gypsum, ASTM STP 861, Kuntze, R.A., Ed., American Society for Testing and Materials: Philadelphia, PA, 97-104(1984).

[30] WhipMix gypsum products physical properties comparison, http://www.whipmix.com/2gypsum/phyprop.html.

[31] Ling, Y., Demopoulos, G. P., Giove, A. and Filippou, D., Technical evaluation and characterization of alpha calcium sulfate materials, Gypsum and Fly Ash 2002, 7th International Science and Technology Conference and Short Course, Toronto, June 2-4, [Proceeding], Process Research ORTECH Inc. :Mississauga, Ontario, Canada, 6, 1-14 (2002).

[32] Hina, A. and Nancollas, G.H., Alpha calcium sulfate hemihydrate and a method of making alpha calcium sulfate hemihydrate, International Patent, WO 0,179,116(2001).

[33] Luckevich, L.M. and Kuntze, R.A., The relationship between water demand and particle size distribution of stucco, The Chemistry and Technology of Gypsum, ASTM STP 861, Kuntze, R.A., Ed., American Society for Testing and Materials: Philadelphia, PA, 84-96(1984).

Chapter 8

Synopsis

8.1 Introduction

In this chapter global conclusions are first summarized and then various aspects of the work that are considered as original contributions to knowledge are listed. Finally, suggestions for further research work are made.

8.2 Global conclusions

With the ultimate goal of developing a novel, direct and cost-effective method for preparation of α-hemihydrate from sulfuric acid under atmospheric pressure as opposed to elevated pressure conditions, the crystallization of α-hemihydrate in sulfuric acid medium and the correlation between its properties and preparation conditions have been thoroughly investigated. The major findings of this study are summarized below:

(1) Through a systematic study, the detection limits for XRD to distinguish between dihydrate and hemihydrate phases, and DSC to distinguish between α- and β-hemihydrates, were determined to be respectively 1 wt% and 5 wt%.

(2) Proper post-reaction treatment was essential for preservation and accurate identification of possible co-existing dihydrate and hemihydrate resulting from the reaction between lime and sulfuric acid. Particularly, hot filtration followed by washing with a hydrophilic organic such as 2-propanol and drying at around 59-60°C has been proved to be effective.

(3) Thermodynamic calculations with the aid of FactSage determined that, in pure water, below 55.7°C, dihydrate is more stable than anhydrite; and above 55.7°C, anhydrite is the stable phase. Dihydrate and hemihydrate can exist metastably, and dihydrate is more stable than hemihydrate up to 106.6°C, whereas hemihydrate is more stable than dihydrate above 106.6°C; the phase transition temperatures, between dihydrate and anhydrite and between dihydrate and hemihydrate, in the aqueous solution are exclusively determined by the water activity. By further correlating the water activity (estimated with the aid of OLI software) to the concentration of sulfuric acid, a phase diagram for the $CaSO_4$–H_2SO_4–H_2O system was quantitatively established. The stable zones for dihydrate and anhydrite were well defined. The metastable zones for dihydrate and hemihydrate were also clearly delineated.

(4) The solubility of calcium sulfate hemihydrate in H_2SO_4 solution up to 3.0M concentration at 100°C was quantitatively determined to be given by the following equations:

$$Sol_{CaSO4,\ g/L} = 1.59597M^3 - 10.8168M^2 + 18.5334M + 2.19264$$

$$Sol_{CaSO4,\ wt\%} = 0.000224189wt\%^3 - 0.0137187wt\%^2 + 0.206176wt\% + 0.217479$$

$$Sol_{CaSO4,\ m} = 0.00984176m^3 - 0.072212m^2 + 0.135638m + 0.0176073.$$

(5) From a series of phase transformation experiments it was determined that dihydrate or hemihydrate crystals upon equilibration in hot aqueous H_2SO_4 solution (~100°C) undergo transformation via the dissolution – recrystallization mechanism (liquid-phase or through-solution mechanism) resulting in significant morphological and chemical changes as the acidity increases in certain range (from 0 to 1.5M). Dihydrate converts to hemihydrate upon acid increase; no further conversion of hemihydrate was observed within the range of conditions tested (28 hours, 100°C, 1.5M H_2SO_4). The resultant morphology of hemihydrate is of needle-shape type. Calcium sulfate solids, either dihydrate or hemihydrate, can saturate the sulfuric acid solutions in only five minutes. Slow addition of

sulfuric acid into slaked lime revealed that dihydrate forms initially as well-grown platelets which subsequently convert into hemihydrate by the solid-phase mechanism when excess H_2SO_4 is used ($H_2SO_4/CaO \geq 1$).

(6) An operating window has been determined in terms of H_2SO_4 concentration, temperature and time within which clean α-hemihydrate can be produced by reaction of lime with H_2SO_4. This window is defined as 0.6-1.1M H_2SO_4 (steady-state concentrations), 98-105°C and 1 hour retention time. The experimentally defined operating window is very narrow in comparison to metastable region of hemihydrate determined by thermodynamic calculations that consider the activity of water to control the phase equilibria: *dihydrate* $\rightleftarrows$ *hemihydrate* $\rightleftarrows$ *anhydrite*. This implies that, in the case of H_2SO_4, other factors (unknown) cause hemihydrate metastability to be drastically reduced.

(7) Dihydrate forms as intermediate product quickly converting to hemihydrate. The kinetics of conversion depends on the acidity level. For example, at 0.06M (steady-state) H_2SO_4 dihydrate conversion to hemihydrate is not complete even after 24 hours while the conversion is complete after 1 hour at 0.6M (steady state).

(8) The typical morphology of α-hemihydrate crystals is needle-shape with 50-100 μm length and 1-3 μm thickness. Upon prolonged equilibration (typically 24 hours or longer) in their acid preparation solutions hemihydrate needle-shaped crystals become fibrous and eventually convert to anhydrite.

(9) The ratio CaO/H_2SO_4 should be kept at or below 0.8 to avoid high viscosity conditions on one hand and promote the conversion of dihydrate to hemihydrate on the other. Addition of dry or slaked lime to H_2SO_4 yields the same results in terms of product quality (XRD and SEM characterization). Due to the exothermic nature of the process, the reaction may be initiated at lower than 100°C temperature; however, temperatures below 75°C were found to result in "gravel-

like" dihydrate overgrowth around unreacted $CaO/Ca(OH)_2$ that hinders further acid attack, hence temperatures above 75°C should be used. The reaction between CaO and H_2SO_4 is very fast at 100°C reaching completion in less than 20 minutes. It has been determined that it is feasible to monitor the reaction by in-situ conductivity measurements.

(10) Slow addition of H_2SO_4 solution to slaked lime – reverse procedure – (preferred CaO/H_2O ratio 1/4-1/6) was found to favor the production of α-hemihydrate with column-shaped as opposed to needle-shaped crystal morphology within otherwise the same operating window, 0.6-1.1M H_2SO_4. The slaking of lime that produces a colloidal suspension of hydrated $Ca(OH)_2$ particles and/or the alkaline environment dominating during the nucleation process of α-hemihydrate were thought as possible reasons for causing the different hemihydrate crystallization behavior when the reverse procedure was used.

(11) For the standard procedure of adding lime into hot sulfuric acid, α-hemihydrate grows in the **c**-axis direction (on the plane (001)) much more rapidly than in other directions ending in the form of fine needle crystals. Also, independent of the shape of the seed particles, the resultant crystals of hemihydrate are needle-shaped, which further suggests a "dissolution-recrystallization" mechanism.

(12) It is believed that uptake of SO_4^{2-} instead of Ca^{2+} is the rate-determining step in the hemihydrate crystallization process. A SO_4^{2-}-rich environment makes most of the additives ineffective as confirmed experimentally. $Al_2(SO_4)_3$ proved effective to alter the morphology yielding grain-type as opposed to needle-type crystal when the standard procedure of α-hemihydrate production (involving addition of dry lime to H_2SO_4 solution) was used. On the other hand, use of $Al_2(SO_4)_3$ in the reverse procedure of α-hemihydrate production (involving addition of H_2SO_4 to slaked lime) was found to appreciably improve the rheological properties of the slurry and result in relatively "large" pillar-shaped crystals.

(13) No significant improvement on morphology of the resultant α-hemihydrate has been achieved by either seeding or recycling tests. However, some modest growth was evident.

(14) Preliminary assessment of the properties of the α-hemihydrate materials synthesized in this work showed them to compare satisfactorily with other materials produced by conversion of dihydrate to hemihydrate. Hemihydrate particles with higher aspect ratios (ratio of width or diameter/length), namely, more-compact forms, produced by the standard procedure in the presence of $Al_2(SO_4)_3$ as additive or by the reverse procedure, were found to possess the best properties as plaster materials.

8.3 Claims of originality

(1) It is the first time that, the detection limits of most-commonly used characterization methods, XRD and DSC, have been carefully evaluated for distinguishing between dihydrate and hemihydrate, and distinguishing between α- and β-hemihydrates respectively.

(2) It is the first time dihydrate or hemihydrate crystals equilibrated in hot H_2SO_4 solutions (~100°C) have been proved to experience re-organization by "dissolution–recrystallization" (or "through solution") mechanism accompanied with change in morphology in certain range of acidity (0-1.5M).

(3) The solubility of calcium sulfate in H_2SO_4 solution (concentration range 0-3.0M) at 100°C has been determined for the first time.

(4) It is the first time that the phase diagram for the $CaSO_4$–H_2SO_4–H_2O system has been quantitatively established based on thermodynamic calculations.

(5) It is the first time to observe that, under extremely low supersaturation level (controlled by slow addition of H_2SO_4 into slaked lime), calcium sulfate dihydrate that forms as intermediate product, gets the chance to grow into large plate-like crystals which subsequently convert into hemihydrate by the solid-phase mechanism contrary to the conclusions drawn by Sirota et al [1].

(6) Equally novel is the definition of the operating window for the production of α-hemihydrate in $CaO-H_2SO_4-H_2O$ system.

(7) It is the first time to demonstrate that, morphology of the resultant hemihydrate from the reaction between CaO and H_2SO_4 is independent of the shape of the seed particles, which leads to the conclusion that formation of hemihydrate is also by "dissolution-recrystallization" mechanism.

(8) The procedural impact of mixing sulfuric acid and lime on the morphology of resultant hemihydrate has been successfully identified for the first time.

8.4 Suggestions for future work

Some ideas that may help for better understanding and, hence, improvements of the technology of hemihydrate production out of sulfuric acid media are proposed below:

(1) More crystallographic work is needed to unveil the structural nature of the resultant hemihydrate crystals out of sulfuric acid, which has never been done previously in the literature. Crystals may be grown to about 1-2 *mm* for the purpose of determination of the symmetry, unit cell parameters as well as unit formula.

(2) More work is required on the role of additives and seeding/recycling in conjunction with the reverse procedure of α-hemihydrate preparation.

(3) More work should be done to determine the influence of morphology and, more importantly, the particle size distribution on the final strength of the hemihydrate product.

(4) The use of $CaCO_3$ in lieu of CaO should be tested.

(5) It is proposed that, the two procedures developed in this work to produce hemihydrate out of sulfuric acid to be tested on a mini pilot-plant scale to verify the viability of this technology.

References

[1] Sirota, I. S., Dorozhkin, S. V., Kruchnina, M. V. and Melikhov, I. V., Phase transformation and dehydration of calcium sulfate dihydrate in solution studied by SEM, Scanning, 14, 269-275(1992).

Appendix A:

Conversion Chart among Concentration Units Molarity(M), Molality(m) and Weight Percentage(wt%) and Density Data for Sulfuric Acid Solutions

Table A.1: Conversion chart among concentration units molarity(M), molality(m) and weight percentage(wt%) and density data for sulfuric acid solutions

H_2SO_4 in molarity (M)	Temp (°C)	Density, Aqueous (g/mL)	Molality (m)	Weight percentage (wt%)
0.00	20	0.9981	0.00	0.00
0.05	20	1.0016	0.05	0.49
0.10	20	1.0049	0.10	0.98
0.15	20	1.0082	0.15	1.46
0.20	20	1.0114	0.20	1.94
0.25	20	1.0147	0.25	2.41
0.30	20	1.0179	0.30	2.89
0.35	20	1.0210	0.35	3.36
0.40	20	1.0242	0.41	3.83
0.45	20	1.0274	0.46	4.29
0.50	20	1.0305	0.51	4.75
0.55	20	1.0337	0.56	5.21
0.60	20	1.0368	0.61	5.67
0.65	20	1.0400	0.67	6.13
0.70	20	1.0431	0.72	6.58
0.75	20	1.0463	0.77	7.02
0.80	20	1.0494	0.82	7.47
0.85	20	1.0525	0.88	7.91
0.90	20	1.0556	0.93	8.36
0.95	20	1.0588	0.98	8.79
1.00	20	1.0619	1.04	9.23
1.05	20	1.0650	1.09	9.66
1.10	20	1.0681	1.15	10.09
1.15	20	1.0713	1.20	10.52
1.20	20	1.0744	1.25	10.95

H_2SO_4 in molarity (M)	Temp (°C)	Density, Aqueous (g/mL)	Molality (m)	Weight percentage (wt%)
1.25	20	1.0775	1.31	11.37
1.30	20	1.0806	1.36	11.79
1.35	20	1.0837	1.42	12.21
1.40	20	1.0869	1.47	12.62
1.45	20	1.0900	1.53	13.04
1.50	20	1.0931	1.59	13.45
1.55	20	1.0962	1.64	13.86
1.60	20	1.0994	1.70	14.26
1.65	20	1.1025	1.75	14.67
1.70	20	1.1056	1.81	15.07
1.75	20	1.1088	1.87	15.47
1.80	20	1.1119	1.92	15.86
1.85	20	1.1151	1.98	16.26
1.90	20	1.1182	2.04	16.65
1.95	20	1.1214	2.10	17.04
2.00	20	1.1246	2.15	17.43
2.05	20	1.1278	2.21	17.81
2.10	20	1.1309	2.27	18.20
2.15	20	1.1342	2.33	18.58
2.20	20	1.1374	2.39	18.96
2.25	20	1.1406	2.45	19.33
2.30	20	1.1438	2.50	19.71
2.35	20	1.1471	2.56	20.08
2.40	20	1.1504	2.62	20.45
2.45	20	1.1536	2.68	20.81
2.50	20	1.1570	2.74	21.18
2.55	20	1.1603	2.80	21.54
2.60	20	1.1636	2.86	21.90
2.65	20	1.1669	2.92	22.26
2.70	20	1.1703	2.98	22.61
2.75	20	1.1736	3.04	22.96
2.80	20	1.1769	3.10	23.32
2.85	20	1.1803	3.16	23.66
2.90	20	1.1836	3.22	24.01
2.95	20	1.1869	3.29	24.36
3.00	20	1.1902	3.35	24.70
3.05	20	1.1934	3.41	25.05
3.10	20	1.1967	3.47	25.39
3.15	20	1.1999	3.53	25.73
3.20	20	1.2031	3.60	26.07
3.25	20	1.2063	3.66	26.40
3.30	20	1.2094	3.72	26.74
3.35	20	1.2125	3.79	27.08
3.40	20	1.2156	3.85	27.41

H_2SO_4 in molarity (M)	Temp (°C)	Density, Aqueous (g/mL)	Molality (m)	Weight percentage (wt%)
3.45	20	1.2187	3.92	27.74
3.50	20	1.2217	3.98	28.08
3.55	20	1.2248	4.05	28.40
3.60	20	1.2278	4.11	28.73
3.65	20	1.2308	4.18	29.06
3.70	20	1.2337	4.25	29.39
3.75	20	1.2367	4.31	29.72
3.80	20	1.2396	4.38	30.04
3.85	20	1.2425	4.45	30.37
3.90	20	1.2454	4.52	30.69
3.95	20	1.2483	4.59	31.01
4.00	20	1.2512	4.66	31.33
4.05	20	1.2540	4.73	31.65
4.10	20	1.2568	4.80	31.97
4.15	20	1.2597	4.87	32.29
4.20	20	1.2625	4.94	32.60
4.25	20	1.2652	5.01	32.92
4.30	20	1.2680	5.08	33.23
4.35	20	1.2708	5.15	33.55
4.40	20	1.2735	5.22	33.86
4.45	20	1.2763	5.30	34.17
4.50	20	1.2790	5.37	34.48
4.55	20	1.2817	5.44	34.79
4.60	20	1.2844	5.52	35.10
4.65	20	1.2871	5.59	35.41
4.70	20	1.2897	5.67	35.71
4.75	20	1.2924	5.74	36.02
4.80	20	1.2951	5.82	36.32
4.85	20	1.2977	5.90	36.63
4.90	20	1.3003	5.97	36.93
4.95	20	1.3030	6.05	37.23
5.00	20	1.3056	6.13	37.53
5.05	20	1.3082	6.21	37.83
5.10	20	1.3108	6.29	38.13
5.15	20	1.3134	6.37	38.43
5.20	20	1.3160	6.45	38.72
5.25	20	1.3185	6.53	39.02
5.30	20	1.3211	6.61	39.32
5.35	20	1.3237	6.69	39.61
5.40	20	1.3262	6.78	39.90
5.45	20	1.3288	6.86	40.19
5.50	20	1.3314	6.94	40.48
5.55	20	1.3339	7.03	40.78
5.60	20	1.3364	7.11	41.07

H_2SO_4 in molarity (M)	Temp (°C)	Density, Aqueous (g/mL)	Molality (m)	Weight percentage (wt%)
5.65	20	1.3390	7.19	41.35
5.70	20	1.3415	7.28	41.64
5.75	20	1.3440	7.37	41.93
5.80	20	1.3466	7.45	42.21
5.85	20	1.3491	7.54	42.49
5.90	20	1.3516	7.63	42.78
5.95	20	1.3541	7.72	43.06
6.00	20	1.3566	7.81	43.34
0.00	25	0.9969	0.00	0.00
0.05	25	1.0003	0.05	0.49
0.10	25	1.0036	0.10	0.98
0.15	25	1.0068	0.15	1.46
0.20	25	1.0100	0.20	1.94
0.25	25	1.0132	0.25	2.42
0.30	25	1.0163	0.30	2.89
0.35	25	1.0195	0.36	3.36
0.40	25	1.0226	0.41	3.83
0.45	25	1.0257	0.46	4.30
0.50	25	1.0288	0.51	4.76
0.55	25	1.0319	0.56	5.22
0.60	25	1.0350	0.61	5.68
0.65	25	1.0381	0.67	6.14
0.70	25	1.0412	0.72	6.59
0.75	25	1.0443	0.77	7.04
0.80	25	1.0474	0.83	7.49
0.85	25	1.0504	0.88	7.93
0.90	25	1.0535	0.93	8.37
0.95	25	1.0566	0.99	8.81
1.00	25	1.0596	1.04	9.25
1.05	25	1.0627	1.09	9.68
1.10	25	1.0657	1.15	10.12
1.15	25	1.0688	1.20	10.54
1.20	25	1.0719	1.26	10.97
1.25	25	1.0749	1.31	11.40
1.30	25	1.0779	1.37	11.82
1.35	25	1.0810	1.42	12.24
1.40	25	1.0840	1.48	12.66
1.45	25	1.0871	1.53	13.07
1.50	25	1.0901	1.59	13.49
1.55	25	1.0932	1.65	13.89
1.60	25	1.0962	1.70	14.30
1.65	25	1.0992	1.76	14.71
1.70	25	1.1023	1.82	15.11
1.75	25	1.1053	1.87	15.52

H_2SO_4 in molarity (M)	Temp (°C)	Density, Aqueous (g/mL)	Molality (m)	Weight percentage (wt%)
1.80	25	1.1084	1.93	15.91
1.85	25	1.1114	1.99	16.31
1.90	25	1.1144	2.05	16.71
1.95	25	1.1175	2.10	17.10
2.00	25	1.1205	2.16	17.49
2.05	25	1.1236	2.22	17.88
2.10	25	1.1266	2.28	18.27
2.15	25	1.1296	2.34	18.65
2.20	25	1.1327	2.40	19.03
2.25	25	1.1357	2.46	19.42
2.30	25	1.1388	2.52	19.79
2.35	25	1.1418	2.58	20.17
2.40	25	1.1449	2.64	20.54
2.45	25	1.1479	2.70	20.92
2.50	25	1.1510	2.76	21.29
2.55	25	1.1541	2.82	21.65
2.60	25	1.1571	2.88	22.02
2.65	25	1.1602	2.94	22.38
2.70	25	1.1633	3.00	22.75
2.75	25	1.1663	3.07	23.11
2.80	25	1.1694	3.13	23.47
2.85	25	1.1725	3.19	23.82
2.90	25	1.1756	3.25	24.17
2.95	25	1.1787	3.32	24.53
3.00	25	1.1818	3.38	24.88
3.05	25	1.1848	3.44	25.23
3.10	25	1.1879	3.51	25.57
3.15	25	1.1910	3.57	25.92
3.20	25	1.1941	3.63	26.26
3.25	25	1.1972	3.70	26.60
3.30	25	1.2003	3.76	26.94
3.35	25	1.2033	3.83	27.28
3.40	25	1.2064	3.89	27.62
3.45	25	1.2095	3.96	27.95
3.50	25	1.2125	4.03	28.29
3.55	25	1.2155	4.09	28.62
3.60	25	1.2185	4.16	28.95
3.65	25	1.2215	4.23	29.28
3.70	25	1.2245	4.29	29.61
3.75	25	1.2274	4.36	29.94
3.80	25	1.2303	4.43	30.27
3.85	25	1.2332	4.50	30.60
3.90	25	1.2361	4.57	30.92
3.95	25	1.2390	4.64	31.24

H_2SO_4 in molarity (M)	Temp (°C)	Density, Aqueous (g/mL)	Molality (m)	Weight percentage (wt%)
4.00	25	1.2419	4.71	31.56
4.05	25	1.2447	4.78	31.89
4.10	25	1.2475	4.85	32.21
4.15	25	1.2503	4.92	32.53
4.20	25	1.2531	4.99	32.85
4.25	25	1.2559	5.06	33.16
4.30	25	1.2586	5.14	33.48
4.35	25	1.2614	5.21	33.80
4.40	25	1.2641	5.28	34.11
4.45	25	1.2668	5.36	34.43
4.50	25	1.2695	5.43	34.74
4.55	25	1.2722	5.51	35.05
4.60	25	1.2749	5.58	35.36
4.65	25	1.2776	5.66	35.67
4.70	25	1.2802	5.73	35.98
4.75	25	1.2829	5.81	36.28
4.80	25	1.2855	5.89	36.59
4.85	25	1.2882	5.97	36.90
4.90	25	1.2908	6.04	37.20
4.95	25	1.2934	6.12	37.51
5.00	25	1.2960	6.20	37.81
5.05	25	1.2986	6.28	38.11
5.10	25	1.3012	6.36	38.41
5.15	25	1.3038	6.44	38.71
5.20	25	1.3064	6.53	39.01
5.25	25	1.3090	6.61	39.30
5.30	25	1.3116	6.69	39.60
5.35	25	1.3142	6.77	39.89
5.40	25	1.3167	6.86	40.19
5.45	25	1.3193	6.94	40.48
5.50	25	1.3219	7.03	40.77
5.55	25	1.3244	7.11	41.07
5.60	25	1.3270	7.20	41.36
5.65	25	1.3295	7.28	41.65
5.70	25	1.3321	7.37	41.93
5.75	25	1.3347	7.46	42.22
5.80	25	1.3372	7.54	42.51
5.85	25	1.3398	7.63	42.79
5.90	25	1.3423	7.72	43.08
5.95	25	1.3449	7.81	43.36
6.00	25	1.3474	7.90	43.64

Appendix B:

Calculated Results of Water Activities in Sulfuric Acid Corresponding to Different Concentrations (0-6m) and Temperatures (20-100°C) with the Aid of OLI StreamAnalyser

Table B.1: Calculated Results of Water Activities in Sulfuric Acid Corresponding to Different Concentrations (0-6m) and Temperatures (20-100°C) with the Aid of OLI StreamAnalyser

H_2SO_4 (m)	20°C	25°C	30°C	35°C	40°C	45°C	50°C	55°C	60°C	65°C
0.00	1.0000	1.0000	1.0000	1.0000	1.0000	1.0000	1.0000	1.0000	1.0000	1.0000
0.10	0.9965	0.9965	0.9966	0.9966	0.9966	0.9966	0.9966	0.9966	0.9966	0.9966
0.20	0.9931	0.9931	0.9932	0.9932	0.9932	0.9932	0.9932	0.9932	0.9932	0.9932
0.30	0.9896	0.9897	0.9897	0.9897	0.9897	0.9897	0.9897	0.9898	0.9898	0.9898
0.40	0.9861	0.9861	0.9861	0.9861	0.9861	0.9861	0.9862	0.9862	0.9862	0.9862
0.50	0.9824	0.9824	0.9824	0.9824	0.9824	0.9825	0.9825	0.9825	0.9825	0.9826
0.60	0.9786	0.9786	0.9786	0.9786	0.9787	0.9787	0.9787	0.9787	0.9788	0.9788
0.70	0.9747	0.9747	0.9747	0.9747	0.9748	0.9748	0.9748	0.9749	0.9749	0.9750
0.80	0.9707	0.9707	0.9707	0.9707	0.9707	0.9708	0.9708	0.9709	0.9710	0.9710
0.90	0.9666	0.9666	0.9666	0.9666	0.9666	0.9667	0.9667	0.9668	0.9669	0.9670
1.00	0.9624	0.9623	0.9623	0.9623	0.9624	0.9624	0.9625	0.9626	0.9627	0.9628
1.10	0.9581	0.9580	0.9580	0.9580	0.9580	0.9581	0.9582	0.9583	0.9584	0.9586
1.20	0.9536	0.9535	0.9535	0.9535	0.9536	0.9536	0.9538	0.9539	0.9540	0.9542
1.30	0.9491	0.9490	0.9489	0.9489	0.9490	0.9491	0.9492	0.9494	0.9495	0.9497
1.40	0.9445	0.9443	0.9442	0.9442	0.9443	0.9444	0.9446	0.9447	0.9449	0.9452
1.50	0.9398	0.9396	0.9395	0.9395	0.9395	0.9396	0.9398	0.9400	0.9402	0.9405
1.60	0.9351	0.9347	0.9346	0.9346	0.9346	0.9348	0.9350	0.9352	0.9354	0.9357
1.70	0.9302	0.9298	0.9296	0.9296	0.9296	0.9298	0.9300	0.9303	0.9305	0.9309
1.80	0.9253	0.9248	0.9245	0.9245	0.9245	0.9247	0.9249	0.9252	0.9256	0.9259
1.90	0.9204	0.9197	0.9193	0.9193	0.9194	0.9195	0.9198	0.9201	0.9205	0.9209
2.00	0.9154	0.9145	0.9141	0.9140	0.9141	0.9143	0.9146	0.9149	0.9153	0.9157
2.10	0.9104	0.9092	0.9088	0.9086	0.9087	0.9089	0.9092	0.9096	0.9100	0.9105
2.20	0.9054	0.9039	0.9033	0.9032	0.9032	0.9035	0.9038	0.9042	0.9047	0.9052
2.30	0.9004	0.8986	0.8978	0.8976	0.8977	0.8979	0.8983	0.8987	0.8993	0.8998
2.40	0.8955	0.8932	0.8923	0.8920	0.8921	0.8923	0.8927	0.8932	0.8937	0.8943
2.50	0.8906	0.8877	0.8866	0.8863	0.8863	0.8866	0.8870	0.8876	0.8882	0.8888
2.60	0.8858	0.8822	0.8809	0.8805	0.8805	0.8808	0.8813	0.8819	0.8825	0.8832
2.70	0.8811	0.8767	0.8752	0.8747	0.8747	0.8750	0.8755	0.8761	0.8768	0.8775
2.80	0.8765	0.8712	0.8693	0.8687	0.8687	0.8691	0.8696	0.8702	0.8710	0.8717
2.90	0.8720	0.8656	0.8634	0.8628	0.8627	0.8631	0.8636	0.8643	0.8651	0.8659
3.00	0.8677	0.8601	0.8575	0.8567	0.8567	0.8570	0.8576	0.8583	0.8591	0.8600

H_2SO_4 (m)	20°C	25 °C	30 °C	35 °C	40 °C	45 °C	50 °C	55 °C	60 °C	65 °C
3.10	0.8634	0.8545	0.8515	0.8506	0.8505	0.8509	0.8515	0.8523	0.8531	0.8541
3.20	0.8592	0.8490	0.8455	0.8444	0.8443	0.8447	0.8453	0.8462	0.8471	0.8481
3.30	0.8549	0.8435	0.8394	0.8382	0.8381	0.8385	0.8391	0.8400	0.8410	0.8420
3.40	0.8504	0.8380	0.8333	0.8319	0.8318	0.8322	0.8329	0.8338	0.8348	0.8359
3.50	0.8458	0.8325	0.8271	0.8256	0.8254	0.8258	0.8266	0.8275	0.8286	0.8298
3.60	0.8410	0.8271	0.8209	0.8192	0.8190	0.8194	0.8202	0.8212	0.8223	0.8236
3.70	0.8361	0.8216	0.8147	0.8128	0.8125	0.8130	0.8138	0.8148	0.8160	0.8173
3.80	0.8308	0.8161	0.8084	0.8063	0.8060	0.8065	0.8073	0.8084	0.8097	0.8110
3.90	0.8254	0.8105	0.8021	0.7998	0.7995	0.7999	0.8008	0.8020	0.8033	0.8047
4.00	0.8197	0.8049	0.7958	0.7932	0.7929	0.7933	0.7943	0.7955	0.7969	0.7983
4.10	0.8138	0.7992	0.7894	0.7867	0.7862	0.7867	0.7877	0.7890	0.7904	0.7919
4.20	0.8078	0.7934	0.7830	0.7800	0.7796	0.7801	0.7811	0.7824	0.7839	0.7855
4.30	0.8015	0.7875	0.7765	0.7734	0.7729	0.7734	0.7744	0.7758	0.7774	0.7791
4.40	0.7950	0.7814	0.7700	0.7667	0.7661	0.7667	0.7678	0.7692	0.7708	0.7726
4.50	0.7883	0.7752	0.7635	0.7599	0.7594	0.7599	0.7611	0.7626	0.7642	0.7660
4.60	0.7815	0.7688	0.7569	0.7532	0.7526	0.7532	0.7544	0.7559	0.7576	0.7595
4.70	0.7745	0.7623	0.7503	0.7464	0.7458	0.7464	0.7476	0.7492	0.7510	0.7530
4.80	0.7674	0.7557	0.7437	0.7396	0.7389	0.7396	0.7409	0.7425	0.7444	0.7464
4.90	0.7602	0.7490	0.7370	0.7327	0.7321	0.7327	0.7341	0.7358	0.7377	0.7398
5.00	0.7528	0.7421	0.7302	0.7259	0.7252	0.7259	0.7273	0.7290	0.7310	0.7332
5.10	0.7453	0.7352	0.7234	0.7190	0.7183	0.7190	0.7205	0.7223	0.7244	0.7266
5.20	0.7377	0.7281	0.7166	0.7121	0.7114	0.7122	0.7136	0.7155	0.7177	0.7200
5.30	0.7301	0.7210	0.7098	0.7051	0.7045	0.7053	0.7068	0.7088	0.7110	0.7133
5.40	0.7224	0.7138	0.7028	0.6982	0.6975	0.6984	0.7000	0.7020	0.7043	0.7067
5.50	0.7146	0.7065	0.6959	0.6913	0.6906	0.6915	0.6932	0.6952	0.6976	0.7001
5.60	0.7067	0.6992	0.6889	0.6843	0.6837	0.6846	0.6863	0.6885	0.6909	0.6934
5.70	0.6989	0.6918	0.6819	0.6773	0.6767	0.6777	0.6795	0.6817	0.6841	0.6868
5.80	0.6910	0.6844	0.6749	0.6703	0.6698	0.6708	0.6726	0.6749	0.6774	0.6801
5.90	0.6830	0.6770	0.6678	0.6634	0.6628	0.6639	0.6658	0.6681	0.6707	0.6735
6.00	0.6751	0.6695	0.6607	0.6564	0.6559	0.6570	0.6590	0.6614	0.6640	0.6669

(Table B.1 continued)

H_2SO_4 (m)	65 °C	70 °C	75 °C	80 °C	85 °C	90 °C	95 °C	100 °C
0.00	1.0000	1.0000	1.0000	1.0000	1.0000	1.0000	1.0000	1.0000
0.10	0.9966	0.9966	0.9966	0.9966	0.9967	0.9928	0.9927	0.9927
0.20	0.9932	0.9933	0.9933	0.9933	0.9933	0.9854	0.9853	0.9853
0.30	0.9898	0.9898	0.9898	0.9898	0.9898	0.9781	0.9780	0.9779
0.40	0.9862	0.9862	0.9863	0.9863	0.9863	0.9708	0.9707	0.9706
0.50	0.9826	0.9826	0.9826	0.9827	0.9827	0.9635	0.9634	0.9633
0.60	0.9788	0.9789	0.9789	0.9790	0.9790	0.9563	0.9562	0.9561
0.70	0.9750	0.9750	0.9751	0.9752	0.9753	0.9492	0.9491	0.9490
0.80	0.9710	0.9711	0.9712	0.9713	0.9714	0.9421	0.9420	0.9418
0.90	0.9670	0.9671	0.9672	0.9673	0.9674	0.9350	0.9349	0.9348
1.00	0.9628	0.9629	0.9631	0.9632	0.9633	0.9280	0.9279	0.9277

H_2SO_4 (m)	65 °C	70 °C	75 °C	80 °C	85 °C	90 °C	95 °C	100 °C
1.10	0.9586	0.9587	0.9589	0.9590	0.9592	0.9211	0.9209	0.9208
1.20	0.9542	0.9544	0.9545	0.9547	0.9549	0.9142	0.9140	0.9139
1.30	0.9497	0.9499	0.9501	0.9504	0.9506	0.9074	0.9072	0.9070
1.40	0.9452	0.9454	0.9456	0.9459	0.9461	0.9006	0.9004	0.9002
1.50	0.9405	0.9407	0.9410	0.9413	0.9416	0.8938	0.8936	0.8934
1.60	0.9357	0.9360	0.9363	0.9367	0.9370	0.8871	0.8869	0.8867
1.70	0.9309	0.9312	0.9315	0.9319	0.9323	0.8805	0.8802	0.8800
1.80	0.9259	0.9263	0.9267	0.9271	0.9275	0.8739	0.8736	0.8734
1.90	0.9209	0.9213	0.9217	0.9221	0.9226	0.8673	0.8671	0.8669
2.00	0.9157	0.9162	0.9166	0.9171	0.9176	0.8608	0.8605	0.8603
2.10	0.9105	0.9110	0.9115	0.9120	0.9126	0.8543	0.8541	0.8539
2.20	0.9052	0.9057	0.9063	0.9069	0.9075	0.8479	0.8476	0.8474
2.30	0.8998	0.9004	0.9010	0.9016	0.9023	0.8415	0.8413	0.8411
2.40	0.8943	0.8950	0.8956	0.8963	0.8970	0.8352	0.8349	0.8347
2.50	0.8888	0.8895	0.8902	0.8909	0.8916	0.8289	0.8287	0.8284
2.60	0.8832	0.8839	0.8847	0.8854	0.8862	0.8227	0.8224	0.8222
2.70	0.8775	0.8783	0.8791	0.8799	0.8808	0.8165	0.8162	0.8160
2.80	0.8717	0.8726	0.8734	0.8743	0.8752	0.8104	0.8101	0.8099
2.90	0.8659	0.8668	0.8677	0.8687	0.8696	0.8043	0.8040	0.8038
3.00	0.8600	0.8610	0.8620	0.8630	0.8640	0.7983	0.7979	0.7977
3.10	0.8541	0.8551	0.8561	0.8572	0.8582	0.7922	0.7919	0.7917
3.20	0.8481	0.8492	0.8503	0.8514	0.8525	0.7863	0.7860	0.7857
3.30	0.8420	0.8432	0.8443	0.8455	0.8467	0.7804	0.7800	0.7798
3.40	0.8359	0.8371	0.8383	0.8396	0.8408	0.7745	0.7742	0.7739
3.50	0.8298	0.8310	0.8323	0.8336	0.8349	0.7687	0.7683	0.7681
3.60	0.8236	0.8249	0.8262	0.8276	0.8289	0.7629	0.7625	0.7623
3.70	0.8173	0.8187	0.8201	0.8215	0.8229	0.7571	0.7568	0.7565
3.80	0.8110	0.8125	0.8139	0.8154	0.8169	0.7514	0.7511	0.7508
3.90	0.8047	0.8062	0.8077	0.8093	0.8108	0.7458	0.7454	0.7452
4.00	0.7983	0.7999	0.8015	0.8031	0.8047	0.7401	0.7398	0.7395
4.10	0.7919	0.7936	0.7952	0.7969	0.7986	0.7346	0.7342	0.7340
4.20	0.7855	0.7872	0.7889	0.7907	0.7924	0.7290	0.7287	0.7284
4.30	0.7791	0.7808	0.7826	0.7844	0.7862	0.7235	0.7232	0.7229
4.40	0.7726	0.7744	0.7762	0.7781	0.7800	0.7181	0.7177	0.7175
4.50	0.7660	0.7679	0.7699	0.7718	0.7738	0.7127	0.7123	0.7120
4.60	0.7595	0.7615	0.7635	0.7655	0.7675	0.7073	0.7069	0.7067
4.70	0.7530	0.7550	0.7570	0.7591	0.7612	0.7019	0.7016	0.7013
4.80	0.7464	0.7485	0.7506	0.7528	0.7549	0.6966	0.6963	0.6960
4.90	0.7398	0.7420	0.7442	0.7464	0.7486	0.6914	0.6910	0.6908
5.00	0.7332	0.7354	0.7377	0.7400	0.7423	0.6862	0.6858	0.6856
5.10	0.7266	0.7289	0.7312	0.7336	0.7359	0.6810	0.6806	0.6804
5.20	0.7200	0.7223	0.7247	0.7272	0.7296	0.6758	0.6755	0.6753
5.30	0.7133	0.7158	0.7182	0.7207	0.7232	0.6707	0.6704	0.6702
5.40	0.7067	0.7092	0.7118	0.7143	0.7169	0.6657	0.6653	0.6651
5.50	0.7001	0.7026	0.7053	0.7079	0.7105	0.6606	0.6603	0.6601
5.60	0.6934	0.6961	0.6988	0.7015	0.7041	0.6557	0.6553	0.6551

H_2SO_4 (m)	65 °C	70 °C	75 °C	80 °C	85 °C	90 °C	95 °C	100 °C
5.70	0.6868	0.6895	0.6923	0.6950	0.6978	0.6507	0.6504	0.6501
5.80	0.6801	0.6829	0.6858	0.6886	0.6914	0.6458	0.6455	0.6452
5.90	0.6735	0.6764	0.6793	0.6822	0.6851	0.6409	0.6406	0.6403
6.00	0.6669	0.6698	0.6728	0.6757	0.6787	0.6361	0.6357	0.6355